

RICHARD JAMES HAYES
DEPARTMENT OF GEOGRAPHY
UNIVERSITY OF SHEFFIELD

**MOUNTAIN GLACIER HEALTH SIGNATURES
STORED IN THEIR THREE-DIMENSIONAL ICE
SURFACE GEOMETRY**

PHD THESIS
SUBMITTED IN ACCORDANCE WITH THE REQUIREMENTS
FOR THE DEGREE OF DOCTOR OF PHILOSOPHY

DECEMBER 2014

Abstract

Mountain glaciers are amongst the fastest responding components of the cryosphere to climatic perturbations and are thus an essential parameter in climate system monitoring. However, despite advances in remote sensing approaches to glacier observation, there remains a dearth of information pertaining to how glaciers in many of the world's regions are faring in today's climate. Accordingly, this thesis investigates whether observations of three-dimensional ice surface geometry can be used to gain information concerning glacier state and climate forcing.

The thesis commences with a thorough review and assessment of the physical mechanisms that cause mountain glaciers to tend towards a common surface geometry in response to climate forcing. The theorised relationship between climate forcing and three-dimensional ice surface geometry is then tested using empirical observations by comparing ice surface information, obtained through remote sensing, with well-established glacier-climate indices such as ELA and mass balance.

Our understanding of the relationship between climate forcing and three-dimensional ice surface geometry is then further developed through a number of experiments whereby glacier fluctuations are driven by various mass balance forcing mechanisms using the iSOSIA glacier-flow model developed by David Egholm (Egholm et al., 2011). Using the knowledge gained from the empirical observations and the modelling experiments, remotely sensed observations of ice surface geometry are then used to assess the dynamic state of 2409 glaciers spanning the entirety of the Hindu-Kush-Karakoram-Himalaya (HKKH) region.

The results suggest that the distinct ice surface geometries that characterise mountain glaciers are the manifestation of the complex interactions that ensue between climate forcing, glacier flow, and topography as glaciers strive to achieve equilibrium with their physical and climatic surroundings. As a result, observations of ice surface characteristics can be applied to global scale samples in order to identify regions characterised by dynamically unbalanced glaciers and thus can inform us of those areas that are most likely to display the greatest rates of glacier thinning and retreat in the future.

Acknowledgements

Firstly I would like to extend my gratitude to my supervisor Chris Clark for his expert guidance, encouragement and continued enthusiasm throughout this PhD. I would always leave our meetings feeling enthused, enlightened and generally more positive about my research.

Thank you also to David Egholm for being so generous with his time and expertise and for conducting the modelling that provides the basis for chapter six.

I also acknowledge the financial support of the Natural Environmental Research Council for providing the studentship that has funded this research.

I owe a great deal of gratitude to my friends and colleagues in the department. The trips to the pub and football on a Wednesday night have often been the highlight of my week. I'm also indebted to my parents who have provided encouragement and financial support throughout my time as a student.

Lastly, I say thank you to my fiancé Emma. You have been a constant source of encouragement and inspiration and words can never truly express how grateful I am for your patience and support. Without you this thesis would never have been achievable.

Table of Contents

Abstract	I
Acknowledgements	III
Table of Contents.....	V
Tables and Figures	IX
List of Acronyms	XII
Chapter 1 Introduction and review	1
1.1 Aim	1
1.2 Background	1
1.3 Objectives	15
1.4 Thesis structure.....	16
Chapter 2 Understanding the Hess Altitude	19
2.1 Origins and Observations	19
2.2 The flow-field and idealised glacier geometry	24
2.2.1 Balance velocity.....	24
2.2.2 Extending and compressing flow	25
2.2.3 Submergence and emergence velocities	27
2.3 Hess Altitude as a measure of glacier health	31
2.3.1 Suitability of Hess altitude for estimating ELA.....	31
2.4 Monitoring PCT location and evolution	33
2.4.1 PCT Elevation.....	33
2.4.2 Monitoring PCT change through time.....	35
2.4.3 Advance and retreat scenarios.....	37
2.5 PCT as an indicator of glacier / climate synchronicity.....	46
2.5.1 Insights from temporal changes in PCT_p	46
2.5.2 Insights from PCT_p for a single time slice.....	49
Chapter 3 Planform Curvature Transition and Existing Glacier Health and Climate Measures	54
3.1 Previous Work	54
3.2 Methodology	56
3.2.1 Approach.....	56
3.2.2 Data Sources	56
3.2.3 Digitized glacier outlines and attributes	64
3.2.4 PCT_a extraction.....	64
3.2.5 AAR and Proxy ELA calculations	66
3.3 Results.....	67
3.3.1 PCT_a vs ELA	68
3.3.2 PCT Derived AAR vs AAR0 (WGMS).....	75
3.3.3 PCT vs proxy ELA	76
3.4 Discussion.....	78

3.5	Implications for glacier/climate synchronicity assessment	83
3.6	Summary of outcomes.....	85
Chapter 4 Monitoring and Understanding PCT change over time		86
4.1	Methodology.....	87
4.1.1	Approach	87
4.1.2	Data Sources	87
4.2	Results.....	93
4.2.1	PCT Change and Mass Balance	93
4.2.2	PCT Change in Longyearbyen.....	103
4.3	Discussion	111
4.3.1	Supporting evidence for the PCT as a glacier health measure	111
4.3.2	Insights Provided by the PCT.....	115
4.4	Summary of outcomes.....	123
Chapter 5 Guidelines for PCT Assessments.....		125
5.1.1	Observations of PCT _a	126
5.1.2	Proportional PCT elevation (PCT _p).....	127
Chapter 6 Computational Ice Flow Simulations		131
6.1	Methodology.....	131
6.1.1	iSOSIA	131
6.1.2	Study area	132
6.1.3	Model runs	133
6.1.4	PCT and glacier attribute extraction.....	138
6.2	Results.....	139
6.2.1	ELA variation	139
6.2.2	Variable retreat forcing mechanisms.....	150
6.2.3	Assessing confounding factors.....	157
6.2.4	Synthesis of Results.....	159
6.3	Discussion	161
6.4	Summary of outcomes.....	173
Chapter 7 PCT Observations in the Hindu Kush-Karakoram-Himalayas		176
7.1	The Current State of HKKH Glaciation.....	176
7.2	Methodology.....	179
7.2.1	Study Area	179
7.2.2	Sample Glacier Characteristics	181
7.2.3	Data Sources	184
7.2.4	Extraction of PCT and Inventory Data	185
7.3	Results.....	185
7.3.1	PCT elevation	185
7.3.2	PCT _p	188
7.4	Discussion	191
7.5	PCT derived insights for the HKKH.....	198
7.6	Summary of outcomes.....	200
Chapter 8 The PCT: What have we learned?		202

8.1 The PCT, a function of climate?	202
8.2 So what is the PCT?	204
8.3 What does the PCT tell us?	208
8.4 Proposed applications for the PCT?	213
8.5 Limitations and practicality considerations.	217
Chapter 9 Conclusions.....	224
References.....	230
Appendix	i
Appendix A.....	ii
Appendix B	iii
Appendix C.....	vi

Tables and Figures

Tables

Table 3-1 Glaciers observed in Sample I	63
Table 3-2 - ELA and PCT measurements from sample I.....	69
Table 3-3 Summary statistics for PCT and AAR derived ELA	78
Table 4-1 Summary results of PCT change on Hintereisferner	93
Table 4-2 Summary results of PCT change on Kesselwandferner	97
Table 4-3 Summary results of PCT change on Blue glacier.....	99
Table 4-4- PCT change in Svalbard	104
Table 6-1 - Steady state advance summary results.....	139
Table 6-2 Summary results for abrupt advance experiment.....	145
Table 6-3 summary results from abrupt retreat experiment.....	147
Table 6-4 Summary results from accumulation driven retreat experiment.....	151
Table 6-5 – Summary results from ablation driven retreat experiment	155
Table 7-1 - Summary results of PCT characteristics across HKKH and sub regions.....	185

Figures

Figure 2.1 – Changing characteristics of the contour transition from ice free valley to glacier surface	20
Figure 2.2 - Idealised three-dimensional ice surface geometry	21
Figure 2.3 Contour curvature transition I.....	22
Figure 2.4 Contour curvature transition II.....	23
Figure 2.5 - Longitudinal flow	25
Figure 2.6 – Laterally Constrained vs Unconstrained mountain glaciers.....	26
Figure 2.7 - Flow planes.....	28
Figure 2.8 – Mechanism governing the ablation profile	29
Figure 2.9 - Mechanism governing the accumulation profile	30
Figure 2.10 - Observed 3D flow field.....	31
Figure 2.11 - Proportional PCT calculation.....	34
Figure 2.12 - ELA variation	36
Figure 2.13 - PCT change scenarios.....	38
Figure 2.14 – Scenario 1	39
Figure 2.15 - Scenario 2	40
Figure 2.16 - Scenario 3	41
Figure 2.17 – Scenario 2/3 stages	42
Figure 2.18 – Scenario 4	42
Figure 2.19 – Scenario 5	43
Figure 2.20 – Scenario 6	44
Figure 2.21 – Scenario 7	44
Figure 2.22 – Scenario 6/7	45
Figure 2.23 – Scenario 8	46
Figure 2.24 - Potential variation in PCT_p over time	48
Figure 2.25 - Hypothetical distribution of PCT_p observations.....	51
Figure 3.1 - Kinematic ELA vs Climatic ELA	55
Figure 3.2 ELA_0 calculation for Hinereisferner	60

Figure 3.3 - Valley glacier classification.....	61
Figure 3.4 – Surface complexity due to icefalls.....	62
Figure 3.5 - PCT mapping and extraction.....	66
Figure 3.6 - ELA compared with PCT _a	70
Figure 3.7 - Normalised PCT compared to Normalised ELA.....	71
Figure 3.8 - Normalised PCT vs ELA Normalised using Max Glacier Elevation.....	73
Figure 3.9 ELA/AAR vs MB on Karabatkak and Kintereisferner.....	75
Figure 3.10 - PCT derived AAR vs WGMS derived AAR.....	76
Figure 3.11 - PCT vs AAR derived ELA in the Hindu Kush – Karakorum.....	77
Figure 3.12 - PCT vs ELA offset (percentage).....	84
Figure 4.1- Tirol LiDAR.....	88
Figure 4.2 - – PCT change on Hintereisferner.....	95
Figure 4.3 - PCT change compared to Mass Balance and ELA on Hintereisferner.....	96
Figure 4.4 – PCT change on Kesselwandferner.....	98
Figure 4.5 - PCT change vs MB and ELA on Kesselwandferner.....	99
Figure 4.6 – PCT change on Blue glacier.....	101
Figure 4.7 - PCT change vs Mass Balance and ELA on Blue Glacier.....	102
Figure 4.8 – Map showing the 47 glaciers observed between 1936 and 1995 in Longyearbyen, Svalbard.....	103
Figure 4.9 – ΔPCT_x compared with Δ Glacier length.....	105
Figure 4.10 - PCT location change in Longyearbyen, 1936 – 1995.....	106
Figure 4.11 – PCT change across the study region.....	110
Figure 4.12 – Hintereisferner Mass Balance.....	117
Figure 5.1 - PCT _p values.....	127
Figure 6.1 – Modelling study area.....	132
Figure 6.2 – Steady state mass balance forcing.....	134
Figure 6.3 – Ablation forced change.....	136
Figure 6.4 – Accumulation forced change.....	136
Figure 6.5 – Potential topographic controls on PCT formation.....	138
Figure 6.6 PCT migration under long-term steady state advance.....	140
Figure 6.7 - PCT change over time.....	141
Figure 6.8 - Advance scenarios.....	142
Figure 6.9 - PCT vs ELA.....	143
Figure 6.10 - PCT _p variation.....	144
Figure 6.11 – PCT _a and PCT _x planar changes.....	145
Figure 6.12 - - PCT _p variation during abrupt glacier advance.....	146
Figure 6.13 - PCT elevation and planar change retreat.....	148
Figure 6.14 - PCT _p variation during abrupt glacier retreat.....	149
Figure 6.15 - Accumulation driven PCT evolution.....	150
Figure 6.16 - Accumulation-driven PCT change.....	151
Figure 6.17 - PCT _p variation driven by accumulation change.....	152
Figure 6.18 – Ablation-Driven PCT Evolution.....	154
Figure 6.19 - Ablation driven PCT change.....	155
Figure 6.20 - PCT _p variation driven by ablation change.....	156
Figure 6.21 - PCT location under different sliding regimes.....	157
Figure 6.22 - Ice confluences and PCT location.....	158
Figure 6.23 - PCT vs ELA on all glaciers.....	160
Figure 6.24 – Modelled PCT _p values.....	160
Figure 6.25 - PCT _p values from “real world Glacier” observations.....	162
Figure 6.26 - Ice surface thinning.....	168
Figure 6.27 – Synchronised retreat and thinning.....	169

Figure 7.1 – HKKH study area	180
Figure 7.2 – Glacier types across the HKKH	183
Figure 7.3 – Complex glacier surface.....	184
Figure 7.4 - PCT Elevation.....	186
Figure 7.5 - PCT vs Topography map.....	187
Figure 7.6 – PCT _a compared to the maximum topographic elevation recorded in each 25 km ² cell	188
Figure 7.7 - PCT _p Values across HKKH.....	189
Figure 7.8 - PCT _p Across the HKKH.....	190
Figure 7.9 - Aggregated PCT _p values across HKKH	190
Figure 7.10 – Schematic of passive retreat	194
Figure 8.1 - PCT _p for all glaciers in the study	203
Figure 8.2 - PCT _p boundary issues	215
Figure 8.3 – Glacier Flow-state identification.....	217
Figure 8.4 – Simple PCT deliniation	220
Figure 8.5 – Complex PCT deliniation.....	221

List of Acronyms

ASTER – Advanced Spaceborne Thermal Emission and Reflection Radiometer

B_n – Net Mass Balance (glacier wide, over the mass-balance year. metres water equivalent)

b_n – Net Mass Balance (point, over the mass-balance year. metres water equivalent)

DEM – Digital Elevation Model

ELA – Equilibrium Line Altitude

ETM+ - Environmental Thematic Mapper Plus

EWT – Equivalent Water Thickness

FOG – Fluctuation of Glaciers

GDEM – Global Digital Elevation Model

GIS – Geographical Information System

GLIMS – Global Land Ice Measurements From Space

GLOF – Glacier Lake Outbursts Flood

GMBB – Glacier Mass Balance Bulletin

GTN-G – Global Terrestrial Network for Glaciers

IPCC – Inter-Governmental Panel on Climate Change

iSOSIA – integrated Second Order Shallow Ice Approximation

LiDAR – Light Detection And Ranging

m.a.s.l – Metres above sea-level

MB – Mass Balance

NSIDC – National Snow Ice Data Centre

PCT – Planform Curvature Transition

PCT_a – Planform Curvature Transition Altitude

PCT_p – Planform Curvature Transition Altitude (by proportion of glacier elevation range)

PSFG - Permanent Service on Fluctuations of Glaciers

RS – Remote Sensing

SIA – Shallow Ice Approximation

SOSIA – Second Order Shallow Ice Approximation

SRTM – Shuttle Radar Topographic Mission

THAR – Terminus-to-Headwall-Altitude-Ratio

WGMS – World Glacier Monitoring Service

Chapter 1 Introduction and review

1.1 Aim

The aim of this thesis is to utilise empirical observations from remotely sensed data alongside results from computational ice flow simulations in order to assess how climate signals are manifested in the three dimensional surface geometry of mountain glaciers and to ascertain how these observations can be used as a tool for monitoring and assessing glacier state.

1.2 Background

Since 1990, the Intergovernmental Panel on Climate Change has recognised the importance of glaciers as a global climate indicator by including glacier fluctuations in all of their assessments. Mountain glaciers and ice caps provide clear evidence of the effects of climate perturbations and are, therefore, key in the early detection strategies which are devised to combat the current hypothesised trend of planetary warming. The continued recession of many of the world's mountain glaciers (Dyurgerov and Meier, 2005; Meier et al., 2003; WGMS, 2012; Zemp and van Woerden, 2008) has widespread implications. At the time of study, Meier et al. (2007) identified that ice loss to the sea, extrapolated from direct measurements of glacier mass balance, accounted for virtually all sea-level rise that was not attributable to ocean warming between 1996 and 2006. A more recent study supported this notion when it was observed that between 2003 and 2009, the global glacier mass budget was -259 ± 28 gigatons per year (Gardner et al., 2013). This was equivalent to the ice loss from both major ice sheets during the study period and accounted for $29 \pm 13\%$ of observed sea level rise during the study period. Furthermore calculations of glacier volume and ice thickness distributions have identified that the global population of glaciers, outside of the two ice sheets, have the potential to raise sea level by a further 0.43 ± 0.06 m (Huss and Farinotti, 2012).

Mountain glaciers also play a crucial role in the lives of billions of people in the world's glaciated and surrounding regions. According to Barnett et al. (2005) over one sixth of the world's population rely upon glaciers for their water supply. This is particularly true in High Mountain Asia where glacier melt

water accounts for more than half of all stream flow in the region's main rivers. Furthermore, aspects of glacier retreat can pose a serious threat to life whereby glacier melt and retreat can contribute to potential glacier lake outburst floods (GLOFs) and the creation of jökulhlaups (Armstrong, 2010).

In response to the suggested rapid disintegration of the globe's mountain glaciers (Meier et al., 2007), it is clear that mountain glacier monitoring should play an integral role in climate change science. Accordingly it is apparent that scientists concerned with the interactions between mountain glaciers and climate change require ways of measuring and assessing the "health" of the world's glacier population. This is vital if we are to understand how they are currently responding to the proposed anthropogenically enhanced warming and how they will react in the future to further perturbations in global climate.

However, before discussing the many approaches utilised in glacier monitoring efforts, it is first necessary to define the term "health" in a glacial context. Whilst avoiding anthropomorphising glacier behaviour, the term "glacier health" in the context of this work describes the state of the glacier relative to its environmental setting. Thus the term encompasses not only whether the glacier has a negative, positive or balanced mass budget, it also considers whether glacier flow dynamics are capable of maintaining the glacier's current extent and three-dimensional mass distribution, or more generally whether flow dynamics are synchronised with current climate forcing. Thus the term "glacier health" takes a more generalised approach to assessing the state of a glacier, where glaciers that are dynamically balanced, advancing and displaying evidence of a regular flow regime are considered to be healthy; and *vice versa*.

One of the cornerstone approaches for monitoring glacier change is through the acquisition of annual mass balance data. The direct, or glaciological, method of measuring mass balance involves repeated point measurements upon the glacier surface to ascertain rates of accumulation and ablation through the employment of stakes and snow pits (Hubbard and Glasser, 2005). Since the initiation of long-term mass balance monitoring in 1945 upon Storglaciären, Sweden (Holmlund et al., 2005), many monitoring programs have been set up and countless studies have utilised continuous records of annual mass balance in order to assess glacier health and climate forcing on an individual and

regional scale (e.g. Cogley and Adams, 1998; Fischer, 2010; Fountain and Vecchia, 1999; Pu et al., 2008; Vuille et al., 2008).

However, the records produced through direct mass balance measurements can contain quite large errors due to the fact that measurements are often made under difficult site conditions and that the reality of glacier dynamics is much more complex than simply gains and losses at the glacier surface (Braithwaite 2009). Furthermore, problems can arise when considering the fact that the method struggles to take into account crevasses, debris covered zones (Nakawo and Rana, 1999), calving and internal accumulation (Rabus and Echelmeyer, 1998). There is also the potential for sampling error to bias the results by excluding localised regions of extremely high mass exchange, whether that is positive (accumulation) or negative (ablation). As a result, if the number of point mass balance observations is insufficient in accounting for the potential spatial heterogeneity of surface mass balance, the extrapolated mean annual mass balance may deviate significantly from the true mean annual mass balance (Fountain and Vecchia, 1999).

Nevertheless, mass balance provides evidence of the direct response of glaciers to atmospheric conditions and despite methodological constraints it remains an essential tool in glacier monitoring (Zemp et al., 2009). This is reflected by the fact that today, annual mass balance is recorded each year on over 100 glaciers as part of Global Terrestrial Network for Glaciers' (GTNG) integrated monitoring strategy. Mass balance data have been collated and published by the World Glacier Monitoring service (WGMS) in the form of the "Glacier Mass Balance Bulletins" and the "Fluctuation of Glaciers" series (Kasser, 1967; PSFG, 1973, 1977, 1985; WGMS, 1988, 1993, 1998, 2005, 2008, 2012) and have been used by scientists to produce estimates of mountain glacier mass change on a global scale (e.g. Meier et al. 2007; Meier et al., 2003; Dyurgerov, 2005; Dyurgerov and Meier, 2005; Dyurgerov et al., 2002). These studies are all in agreement that the global population of glaciers are experiencing negative mass balance and have been shrinking at an accelerating rate. Such observations have led to estimations and projections of global sea-level rise. For example, by calculating global glacier volumes through volume-area scaling, Meier et al. (2007) and Raper and Braithwaite (2006) estimated future sea-level rises of 0.25 m and

0.097 m by 2100 respectively, based upon extrapolation of the current “global” sample of mass balance observations. However, a key concern here is the representativeness of the global mass balance observations upon which the estimates were based. For example, for the period between 1990 and 2004, Dyurgerov and Meier (2005) estimated that the melting of glaciers and ice caps contributed 0.77 ± 0.22 mm yr⁻¹ to global sea level rise. However, the results of this study were based upon observations from only 163 glaciers, of which only 101 provided records for more than 5 years. This is particularly concerning when one considers the fact that this estimate is based on data from <0.1% of the global glacier population yet the results from this study were utilised in the IPCC’s 2007 report (Lemke et al., 2007). In the same report, data from only 11 glaciers found in Hindu-Kush Karakorum Himalayan region were utilised despite the area representing the largest concentrations of glaciated terrain outside the poles. Although great efforts have been made to perform mass balance studies using large samples of glaciers, spanning vast geographical ranges, the results may tell us relatively little about the state of the world’s collective mountain glacier population due to the fact that the data used are simply not representative.

The majority of the studies that claim to assess global trends in glacier health are based on information provided in the databases operated by the WGMS (World Glacier Monitoring Service). This is problematic as the data collections contain very few long series of uninterrupted records. Gaps in the data make comparisons between different regions, and thus the identification of global trends through time, very difficult. Ultimately, there is not enough data available to allow results to be representative. For example Braithwaite (2002) identified that less than 2% of the global land area covered by mountain glaciers has been measured in terms of mass balance for a minimum duration of one year. This shortcoming is exacerbated by the fact that there is extreme bias in the geographical derivation of what little data are available. Zemp et al. (2009) observed that 90% of mass balance data come from the Northern Hemisphere and 40% of that are from the European Alps. Furthermore, the measured glaciers are not representative of the “average” mountain glacier as they are skewed towards maritime conditions. These “wetter” glaciers have a higher sensitivity to climate change than those in cold, dry continental locations such

as those located in the Himalayas (Braithwaite and Zhang, 2000). Consequently, estimates of global mass balance may be erroneous due to the limited observational data that form the basis of the global calculations.

The limited availability of mass balance measurements and the bias apparent in the data that are available can be attributed to logistical constraints. The need to gain physical access to the ice surface in order to utilise the direct or glaciological approach means that current records are limited to those glaciers that are easily accessible. Furthermore, in some instances gaining access to the glacier surface is virtually impossible due to the remoteness and often very dangerous conditions associated with glaciated environments. Geopolitical issues can also provide logistical barriers, particularly in High Mountain Asia where glaciated regions cross national boundaries. Mass balance monitoring programs are also a costly commitment. Accordingly, scientists have explored alternative approaches to glacier monitoring that utilise the ever-improving availability and quality of remotely sensed data, thus negating the requirement of costly field seasons.

Variations in glacier terminus position have long been studied and are considered by many as one of most recognisable indicators of glacier health and thus climate change (Haeberli, 2004; Houghton et al., 2001). There has been a recognizable retreat (>2 km) of many large valley glaciers on a global scale in response to a temperature increase of only 1 K since 1850, which would have been unnoticeable without climate records (Paul et al., 2007). This observation supports the idea therefore that glacier length fluctuation measurements are an invaluable tool in glacier health monitoring.

Historically, glacier terminus fluctuations in Europe and the USA have been well-documented and interpreted using paintings, photographs and field surveys due to a relative ease of access. Terminus variation monitoring then became more systematic with the implementation of the length measurement network setup by Forel in 1893 (Haeberli and Beniston., 1998). Today, terminus fluctuation measurements for a global sample of 605 glaciers can be found in the latest instalment of the Fluctuation of Glaciers series (WGMS, 2008). Work by Jóhannesson et al. (1989) and Hoelzle et al. (2003) highlights the importance of long term cumulative length change data, such as those used in Andreassen

et al. (2005), as a tool for calculating secular mass balance trends using a continuity approach over time periods corresponding to the dynamic response time of individual glaciers. Oerlemans (2005) took his work a step further and reconstructed temperature histories ranging back to the Little Ice Age for differing global regions using glacier terminus fluctuations alone. Oerlemans' global temperature reconstruction exhibited good agreement with other temperature reconstructions and his reconstruction for more recent decades agreed well with instrumental records, evidencing global warming at rapid rates. His reconstruction was based on the assumption that variable precipitation over the reconstruction period had negligible impact on terminus variations (WGMS, 2008).

Armstrong (2010) suggests that it is important to acknowledge that variations in glacier terminus position cannot provide a comprehensive assessment of the glacier's state or health. This is because the terminus can fluctuate in response to the governing glacier dynamics that are disconnected from the current climatic conditions (Raper and Braithwaite, 2009). For example, the retreat of a glacier's snout suggests that ice at the terminus is melting at a faster rate than at which it can be replaced by the flow of ice from further up glacier. However, this is not to say that the mass budget for the entire glacier is negative, as some terminus-based studies would suggest (Stokes et al., 2006). There is the possibility that the glacier is actually gaining mass at higher elevations through precipitation, input from avalanche and so on at a rate greater than that of ablation at the snout despite terminus retreat. Similarly, the terminus may advance during unchanging climatic conditions or even during periods of negative mass balance due to changes in flow velocities associated with surges and melt water routing perturbations (Hewitt 2007; Jiskoot et al. 2000; Quincey et al. 2011; Sund et al. 2009). The issue is further complicated when one takes into account the fact that a large proportion of glaciers in many of the world's most densely glaciated mountain regions have their snouts mantled by thick debris layers (Scherler et al., 2011b). This is because the presence of a thick debris mantle insulates the covered snout from incoming radiation, decreasing melt rates and potentially enabling snouts to survive at lower (warmer) altitudes (Anderson, 2000; Mihalcea et al., 2006; Nakawo and Rana, 1999). This was highlighted by Bolch et al. (2008) who identified that debris mantled snouts

remained “remarkably stable” on glaciers that were shrinking and thinning in the Khumbu Himal, Nepal. However, if a glacier has displayed continued cumulative advance or retreat, it is fair to assume that the glacier is not in balance with the current climate.

With the recent and rapid increase of freely accessible remotely sensed data in the form of satellite images and digital elevation models, glaciologists moved from glacier terminus studies and steered their attention towards assessing fluctuations in glacier coverage or area. Remote Sensing (RS) data has enabled glacier area, amongst other glaciological variables, to be calculated on an extremely large scale and so by digitizing the outlines of glaciers using RS data from a range of dates, it is possible to identify variations in glacier extent through time (Beedle et al., 2008; Kargel et al., 2005; Racoviteanu et al., 2010).

The very low reflectance of ice and snow in middle-infrared wavelengths has widely been used for glacier classification, for example using threshold ratio images from Landsat ETM+ bands 4 and 5 (Paul et al., 2004). This has enabled many scientists to perform automated extraction of glacier outlines from a variety of optical RS data and quickly build up large databases of digitised glacier outlines complete with glacier area data. A number of researchers have used such automated glacier extraction as well as manual glacier boundary delineation to assess changes in glacier area calculated from two or more satellite images acquired at different dates (e.g. Bhambri et al., 2011; Bolch, 2007; Liu et al., 2006; Nuth et al., 2007; Paul et al., 2004). The results of these studies support the view that glaciers in the majority of the world’s glaciated regions are and have been retreating and losing mass for the past three to four decades. Although these studies can provide quantitative estimates of glacier area fluctuations, they do suffer with some key drawbacks.

Firstly, over a short-term basis, fluctuations in glacier area may be due to glacier dynamics that are out of sync with the glacier’s current “health” or mass balance regime. Similar to the problems that are associated with terminus change studies, area change assessments must take into account that fluctuations may be due to surges. Further problems can arise when considering that moraine dammed lakes can be observed abutting the glacier fronts in many regions (Kääb, 2005). Therefore, glaciers that ablate by calving

into proglacial lakes as well as through surface melting will display asynchronous and possibly enhanced areal reduction compared to nearby non-calving glaciers.

There are also some important methodological issues to consider. For example, when using threshold band ratios as discussed by Paul et al. (2002), the band ratios are sufficient in automatically extracting areas of clean ice and snow. However, when a glacier is mantled by debris, automated extraction of the glacier boundary becomes error strewn, as the spectral signature of supra-glacial debris is very similar to that of the surrounding ice-free topography. As a result such band ratios are unable to delineate the margins of glaciers where supra-glacial debris mantles the ice surface to the edge at the valley walls. One possible solution to circumvent this issue is to manually digitise glacier outlines, as performed by Stokes et al. (2006). However, this is not particularly appropriate when mapping glacier outlines on an extremely large scale due to the sheer amount of time that manual digitising consumes. Even manually digitising glacier outlines on small samples can be difficult if the optical imagery is not of a high enough resolution or if the debris mantle is extremely uniform and large in extent such as in the Khumbu Himal (Bolch et al., 2008). Another important consideration when measuring glacier advance/retreat as evidence of glacier health is lag times. Because glacier flow occurs at such a slow pace, a significant time lag exists between changes in climatic conditions and the responding advance or retreat (Armstrong, 2010). As a result, fluctuations in glacier length and area over short periods of time may be the result of a climatic perturbation that occurred decades, or more, ago. This is further complicated by the fact that the lag time is believed to scale with glacier size, slope and thermal regime amongst other factors. For example, small, warm based glaciers on steep terrain will respond to climate forcing much faster than large, cold based glaciers with relatively shallow surface slopes. Thus length and area changes of such large glaciers, particularly if debris covered, cannot be considered direct indicators of recent climate change (Raper and Braithwaite, 2009).

Perhaps the underlining issue with assessing glacier health and climate signals based on length and area change is that it does not take into account volume

change due to thinning. Bolch et al. (2008) identified that supra-glacial melt water ponds and surface thinning provided clear evidence that glaciers in the Khumbu-Predash were shrinking and losing mass despite the fact that they had displayed no variation in length or area over a substantial amount of time. This was likely due to the fact that the glaciers concerned were mantled with an extensive debris cover, which can become stagnant and in some cases almost separated dynamically from the rest of the glacier (Scherler et al., 2011b). Paul et al. (2007) identified that surface lowering in the European Alps could be identified by observing the increasing exposure of rock outcrops from beneath glacier ice in satellite images from different dates. However this can only provide a mostly qualitative estimate of glacier thinning. It has been identified that over the last ten years or so the acceleration of increasingly negative mass balance has led to greater disequilibria in glaciers of the European Alps. As a result they are down-wasting and disintegrating rather than retreating (Haeberli et al., 2007; Paul et al., 2007), making length and area change studies inappropriate as a stand alone measure of glacier health.

In response to observations of increased glacier thinning, scientists are turning to approaches that can take volumetric changes into account. Geodetic mass balance studies assess glacier health by observing fluctuations, not in terms of length or areal reduction and expansion, but in terms of volumetric changes that can then be converted into water equivalents. The method is based upon the ability to measure changes in ice surface elevation using topographic data from two different acquisition dates. The change in surface elevation (glacier thickening or thinning) is assessed for the entire glacier area. Coupled with knowledge of ice density, this information is used to calculate mass loss in metres water equivalent, thus producing a mass balance estimate for the studied glacier(s) between the two dates of data acquisition. In the past decade, geodetic mass balance studies have featured in the glaciological literature with increasing frequency. This is due to the increasing availability of high quality DEM sources and elevation data, such as the freely available SRTM (Rabus et al., 2003) and ASTER GDEM (Frey and Paul, 2011) as well as satellite laser altimetry collected by sensors on board NASA's ICESat earth observation system (Moholdt et al., 2010) and airborne LiDAR (Rees and Arnold, 2007). Furthermore, digital elevation models can be generated, using photogrammetry

software, from overlapping high-resolution optical imagery from airborne and satellite sensors. It is worth noting that, technically, gravimetry is also a geodetic method (Moholdt, 2013) however this technique will be discussed separately from volume changes derived from repeated elevation measurements.

Geodetic methods utilising repeat ice surface elevation measurements have been used to provide evidence of regional glacier volume changes in the European Alps (Paul, 2008), Canada and Alaska (e.g. Berthier and Toutin, 2008; Larsen et al., 2007; Schiefer et al., 2007), Patagonia (e.g. Rivera and Casassa, 2004), Svalbard (e.g. James et al., 2012; Kohler et al., 2007; Nuth et al., 2007; Nuth et al., 2010) and in High Mountain Asia (e.g. Berthier et al., 2007; Bolch et al., 2008; Bolch et al., 2011; Fujita and Nuimura, 2011; Gardelle et al., 2012b; Gardelle et al., 2013; Kääb et al., 2012; Surazakov and Aizen, 2006). Gardner et al. (2013) went so far as to produce a global glacier mass budget estimate of $-259 \pm 28\text{Gt yr}^{-1}$ between 2003 and 2009 based, in part, upon single-track ICESat elevation footprints. One of the key advantages of using the geodetic approach to glacier monitoring is that, unlike the glaciological mass balance method, physical access to the glacier is not necessary. This is particularly true as geolocators upon sensors continually improve and reduce the need for ground control points (Berthier et al., 2007). Accordingly, where suitable DEMs or optical imagery are available, DEM differencing can be utilised to assess glacier volume changes in extremely remote regions. Furthermore, the existence of historic maps and aerial photographs means that changes in glacier volume can also be studied retrospectively. Although geodetic techniques have the potential to inform us of glacier change in remote regions and for relatively large geographical extents (Cogley, 2009), retrieving geodetic mass balance estimates can be considerably taxing as there are a number of considerations that need to be accounted for before DEM differencing can ensue.

For example, when estimating elevation changes based upon DEM differencing, it is imperative that the two DEMs in use are accurately co-registered. It is vital that the pixels of each DEM represent the same location and area on the Earth surface because even sub-pixel horizontal misalignment between DEMs can cause large bias in elevation change estimates (Nuth and Kääb, 2011; Paul et al.,

2013). According to Nuth and Kääb (2011), the magnitude of the bias induced by failing to co-register the two DEMs is directly related to the direction and magnitude of the shift between them with the direction and slope of the glacier surface. Accordingly, upon flat glaciers the required correction would be relatively small. However, upon steep glaciers such as those in mountainous regions, elevation differences resulting from DEM misalignment may exceed the change in elevation that has occurred upon the glacier surface. Furthermore, multiple DEMs may have different spatial resolutions, which may require the resampling of one or both of the DEMs to a common resolution (Paul et al., 2013). However, this produces data differing from that measured initially and thus may produce artefacts when differencing the newly resampled DEMs (Gardelle et al., 2012a; Paul, 2008). There are also biases and uncertainties associated with the source DEMs that may need to be corrected, such as the variable C-band penetration into snow and ice of the SRTM DEM (Berthier et al., 2006; Gardelle et al., 2012a), sensor-specific rotational corrections (Berthier et al., 2007) and along-track satellite attitude pointing biases in ASTER DEMs related to satellite “jitter” (Nuth and Kääb, 2011).

Once temporal changes in glacier surface elevations are recorded using sufficiently co-registered DEMs, the volume change calculations are then converted into mass loss estimates. These mass estimates are based upon assumptions concerning the mass density. However, this has proven to be problematic as glacier mass density is by no means constant in space or time (Huss, 2013; Kääb et al., 2012;). Although geodetic methods based upon DEM differencing are undoubtedly an important tool for assessing changes in glacier volume, mass and thus health in remote regions, the recognised uncertainties and the measures required to overcome sensor biases and co-registration issues mean that this approach can be difficult to apply to very large geographical extents and samples.

One method that can assess glacier changes on a very large spatial scale however, is gravimetry. Since its launch in 2002, the Gravity Recovery and Climate Experiment (GRACE) satellite has recorded monthly variations in the globe’s gravitational field and enabled scientists to calculate mass variations on the Earth’s surface (Wahr, 2004). These gravity solutions have been used to

identify changes in the Earth's glaciated regions and have evidenced large losses of ice mass in Alaska (e.g. Arendt et al., 2008; Arendt et al., 2013; Chen et al., 2006; Luthcke et al., 2008; Tamisiea, 2005), Canada (e.g. Gardner et al., 2011), Patagonia (e.g. Chen et al., 2007) and High Mountain Asia (e.g. Matsuo and Heki, 2010). GRACE data have even been used to calculate a global glacier and ice cap (glaciers and ice caps, not including glaciers peripheral to Greenland ice sheet and Antarctica) mass budget of $-148 \pm 30 \text{ Gt yr}^{-1}$ between January 2003 and December 2010 (Jacob et al., 2012). Thus, unlike geodetic and glaciological approaches to assessing changes in glacier state, gravimetry is suited to assessing changes in glacier state on a very large geographical scale.

However there are a number of limitations and uncertainties associated with estimating glacier mass loss using gravimetry data. Before estimating glacier mass change from variations in the earth's gravity field, the influence of glacial isostatic adjustments must be accounted for and removed from final mass estimations (Zhang et al., 2013). Similarly, mass balance estimates may also be affected due to deficiencies in the model used to correct atmospheric interference in GRACE products (Duan et al., 2012). Spurious jumps identified in the atmospheric and ocean de-aliasing product, used in post-processing of GRACE data, have the potential to falsely account for 7 cm of equivalent water thickness (EWT) change for glaciated regions in the Qinghai-Tibetan Plateau and South America (Duan et al., 2012). Terrestrial water stores can also complicate interpretations of glacier mass loss. For example groundwater recharge by glacier melt water, if occurring close to the source of the melt water, would result in little variation in the gravitational mass of the region (Jacob et al., 2012). This may help to explain why gravimetric estimations of mass balance are consistently less negative than local estimates obtained using the direct/glaciological method as well as ice surface elevations differencing (Gardelle et al., 2013). The gravimetric approach also produces a great deal of uncertainty when trying to distinguish between variations in ground water storage and glacier ice mass (Gardner et al., 2011; Zhang et al., 2013). For example, gravimetric data have been used as evidence of the depletion of ground water stores in northern India over the past decade (Rodell et al., 2009; Tiwari et al., 2009). However, this is particularly problematic for gravimetric based assessments of glacier mass change in the Himalayas as the region of

rapid ground water depletion is located within a few hundred kilometres from Himalaya. Furthermore, the low spatial resolution of GRACE data means that it is impossible to separate changes in northern Indian groundwater from glacial signals in this region (Matsuo and Heki, 2010). However, perhaps the key limitation to using GRACE data to assess glacier health is that the gravimetric method has a coarse spatial resolution (typically ~ 400 km), meaning that individual glaciers and small hydrological basins cannot be resolved from the wider signal (Gardner et al., 2013).

These issues pertaining to the resolution and scale, to which the methods discussed thus far can be applied, provide the crux of the problem concerning how global estimates of glacier health and thus climate change are observed and produced. Using wide covering, low resolution gravimetry or extrapolating global signals of glacier health and climate change from a relatively small number of direct / geodetic observations would be sufficient if the world's glacier population was responding to climate forcing homogeneously. However, recent observations demonstrate that this is simply not the case.

For example, global glacier ice mass loss calculated using GRACE data produced much lower estimates than those achieved by direct / glaciological mass balance measurements (Gardner et al., 2013). To account for these variations, Gardner et al. (2013) used ICESat elevation data to assess ice surface elevation changes within 100 km of each glaciological measurement in the five main glaciated regions on the globe where both datasets existed. The results revealed that "neighbourhoods" of the glaciological measurements were thinning at a significantly higher rate than their regional means. Gardner et al. attributed this variation to sampling bias where glaciological measurements tend to be located in sub regions where mass loss is greater than in their region as a whole. Nevertheless, the results highlight the spatial heterogeneity with which glaciers respond to climate forcing and the inability of GRACE estimates to measure such complexity.

Similarly, recent observations from across the Hindu-Kush-Karakoram-Himalaya (HKKH) have identified significant variation in the way that the region's glaciers are responding to climate perturbations (Gardelle et al., 2013; Käab et al., 2012). Rapid glacier retreat, stagnation and thinning has been identified in

the Eastern, Central and Western Himalaya (Berthier et al. 2007; Bolch et al. 2012; Fujita and Nuimura, 2011; Kääb, 2005) whilst glacier equilibrium and even thickening and advance has been proposed for the Karakorum (Gardelle et al., 2012b; Gardelle et al. 2013; Hewitt 2005; Kääb et al., 2012) and the Pamirs (Gardelle et al., 2013). These regional variations in glacier behaviour in recent decades have been attributed to spatially heterogeneous climate forcing (Gardelle et al., 2013; Rasmussen, 2013; Shekhar et al., 2010; Wiltshire, 2013) or the role of varying degrees of supra-glacial debris coverage (Scherler et al., 2011b).

Heterogeneous glacier behaviour has also been observed on sub-regional scales. For example, glacier behaviour, in terms of area variations, has been observed to vary markedly in the Tien Shan between 1970 and 2000 due to differences in basin climate (Narama et al., 2010). Similarly, Paul and Haeberli (2008) identified significant variability in glacier thinning rates across the Swiss Alps. They identified that mean thickness changes of individual glaciers could be correlated to their size, elevation, and exposure to insolation. As a result, mass loss upon large glaciers can be underestimated if inferred from direct mass balance measurements from smaller glaciers. These observations were supported by Braithwaite et al. (2013), who identified that temperature sensitivities varied significantly between individual glaciers across the Alps. Accordingly, they concluded that the Alps could not be regarded as a single region of homogenous glacier mass balance variations.

With these studies in mind, it is clear that extrapolating global estimates of glacier state from a small number of directly measured mass balance observations is inappropriate. Variations in hypsometry (Raper and Braithwaite, 2009), debris cover (Nakawo and Rana 1999; Scherler et al., 2011a), local climate (Braithwaite et al., 2013), aspect (Paul and Haeberli, 2008), thermal regime and surging (Hewitt, 2007) and bed slope (Kääb, 2005) can result in heterogeneous glacier response to a uniform climatic forcing. Therefore if we are to truly understand how mountain glaciers are faring in the current climate, it is imperative that we are able to identify changes in glacier health at a higher spatial resolution. Unfortunately, GRACE estimates lack the spatial resolution to fully capture the complexity of the glacier-climate interactions being

observed across the Earth's mountain ranges, and geodetic methods, although vitally important, remain too taxing to enable analysis to extend to the global glacier populous. Thus, given the complex, spatially and temporally variable responses that glaciers have displayed to current climate perturbations, it is clear that a glacier health measure is required that can be replicated with ease and efficiency upon each individual glacier on a global scale. Furthermore, necessity states that the metric be a function of the complex relationship between climate forcing, flow dynamics and ultimately glacier extent and thus must extend beyond realm of basic Glacier Elevation Indices, such as mid-range glacier elevation or the terminus-to-headwall altitude ratio (THAR) metric (Benn and Lehmkuhl, 2000).

1.3 Objectives

The main aim of this work will be achieved through the completion of the following objectives.

- I. Develop our understanding of steady state glacier surface geometries by linking observations to physical processes, namely ice flow mechanics.
- II. Assess the degree to which ice surface Planform Curvature Transition presence and position is a function of the interaction between climate forcing and glacier dynamics by comparing ice surface geometry to other well established measures of glacier health (ELA, mass balance and AAR).
- III. Develop guidelines as to how three-dimensional ice surface geometry, and changes thereof, should be measured and how observations can be related to climate forcing and glacier health.
- IV. Conduct modelling experiments to assess how ice surface geometry is affected by various climate forcing mechanisms and topographic settings.
- V. Compile a database of ice surface geometry characteristics for a large sample of glaciers in the Hindu Kush-Karakorum-Himalaya (HKKH).
- VI. Use the compiled data to infer the state of glaciers across the region and identify climate-forcing mechanisms that may have resulted in such observations.
- VII. Evaluate the use of three-dimensional ice surface geometry observations as a tool for glacier health and climate monitoring, by drawing

interpretations and conclusions from the empirical observations and modelling results.

1.4 Thesis structure

The following thesis can be divided into two distinct approaches: the first part focuses upon developing our understanding of how surface geometry of mountain glaciers is related to climate forcing and how observations of this phenomenon can inform us of how glaciers are faring in the current climate. The second part of the thesis then utilises this newly developed knowledge and applies this understanding to the task of assessing the health state of a large sample of glaciers that, hitherto, have not been studied at such a scale and in such detail. These insights will then be used to infer climate changes for the region.

This process is initiated in chapter two where the origin of the idea that three-dimensional surface geometry characteristics can be used to infer information about glacier state, will be discussed. The chapter then goes on to thoroughly review and assess the physical mechanisms that cause mountain glaciers to tend towards an idealised surface geometry. The chapter will then provide new insights by theoretically exploring how ice surface geometry may evolve over time and discussing how such observations may be linked to climate forcing. The chapter will conclude with a discussion concerning how it is believed that ice surface geometry observations may be used to gain information pertaining to glacier health.

The subsequent two chapters then extend the theoretical understanding developed in chapter two by comparing ice surface geometry observations with other glacier-climate metrics. Relying upon empirical observations from remotely sensed data as well as utilising archive data from the WGMS, chapter three will focus upon how characteristics of ice surface geometry relate to ELA records across a globally distributed sample of glaciers. The fourth chapter then investigates how changes in ice surface geometry over time can be related to glacier mass balance forcing and other indicators of glacier fluctuation. This is achieved through the use of both remotely sensed data as well as historical topographic datasets.

Chapter five then takes stock of the observations made and knowledge gained by highlighting how the theoretical understanding of the ice surface geometry developed in chapter two combined with the observations from chapters three and four can be used to develop a new approach for monitoring glacier health and climate forcing. The interpretations and recommendations proposed in this chapter are then tested in chapter six through a number of experiments where glacier fluctuations are driven by various mass balance forcing mechanisms using the iSOSIA glacier flow model developed by David Egholm (Egholm et al., 2011).

In chapter seven the framework for assessing glacier health developed in chapter five and tested in chapter six is used to gain insight into how wide regions of unstudied glaciers in High Mountain Asia are responding to contemporary climate forcing.

Chapter eight then assimilates the observations made and knowledge gained to that point in order to ascertain whether collecting ice surface geometry information provides a suitable tool for monitoring glacier health and climate signals. The chapter goes on to discuss the limitations and practical considerations associated with using ice surface characteristics to infer glacier health. Subsequently, chapter nine concludes the thesis by highlighting the key findings of the work, discussing how these findings contribute to the wider field of glaciology and finally by proposing how the work can be built upon through future research.

Chapter 2 Understanding the Hess Altitude

This chapter introduces the concept of the Hess Altitude and begins with a discussion of the initial observations and the subsequent development of the idea that the Hess Altitude represents a measure of the relationship between mass balance and flow dynamics. The chapter will then move forward and consider the physical processes that govern the formation and location of the Hess Altitude upon a glacier's surface. The chapter then theorises in detail how observations of ice surface geometry could potentially be used as a metric of glacier health and provide the scientific community with new forms of climate information.

2.1 Origins and Observations

Hess (1904) observed that glacier surfaces tend towards an idealised geometry (figure 2.1) where the accumulation and ablation areas display distinctly different transverse surface profiles to one another.

He proposed that observations of the three-dimensional form of the ice surface could be used to identify the position of the long-term equilibrium line altitude (ELA). By focussing his observations upon the appearance of contours on topographic maps, he identified that the contours in the accumulation area were distinctly different in characteristic to those in the ablation area. He proposed that the accumulation area could be identified where the contours pass without a sharp change of direction from the ice surface onto the bedrock area. Conversely, the ablation area could then be identified where the contours pass from the ice-surface onto the ice-free valley sides with a sharp change of direction (figure 2.1). He thus believed that a glacier's ELA could be located upon an accurate topographic map by locating the point at which this transfer of the contour from ice surface to ice free topography changed from smooth to sharp change of direction. The elevation at which this change in contour characteristic occurred was labelled the **Hess Altitude**.

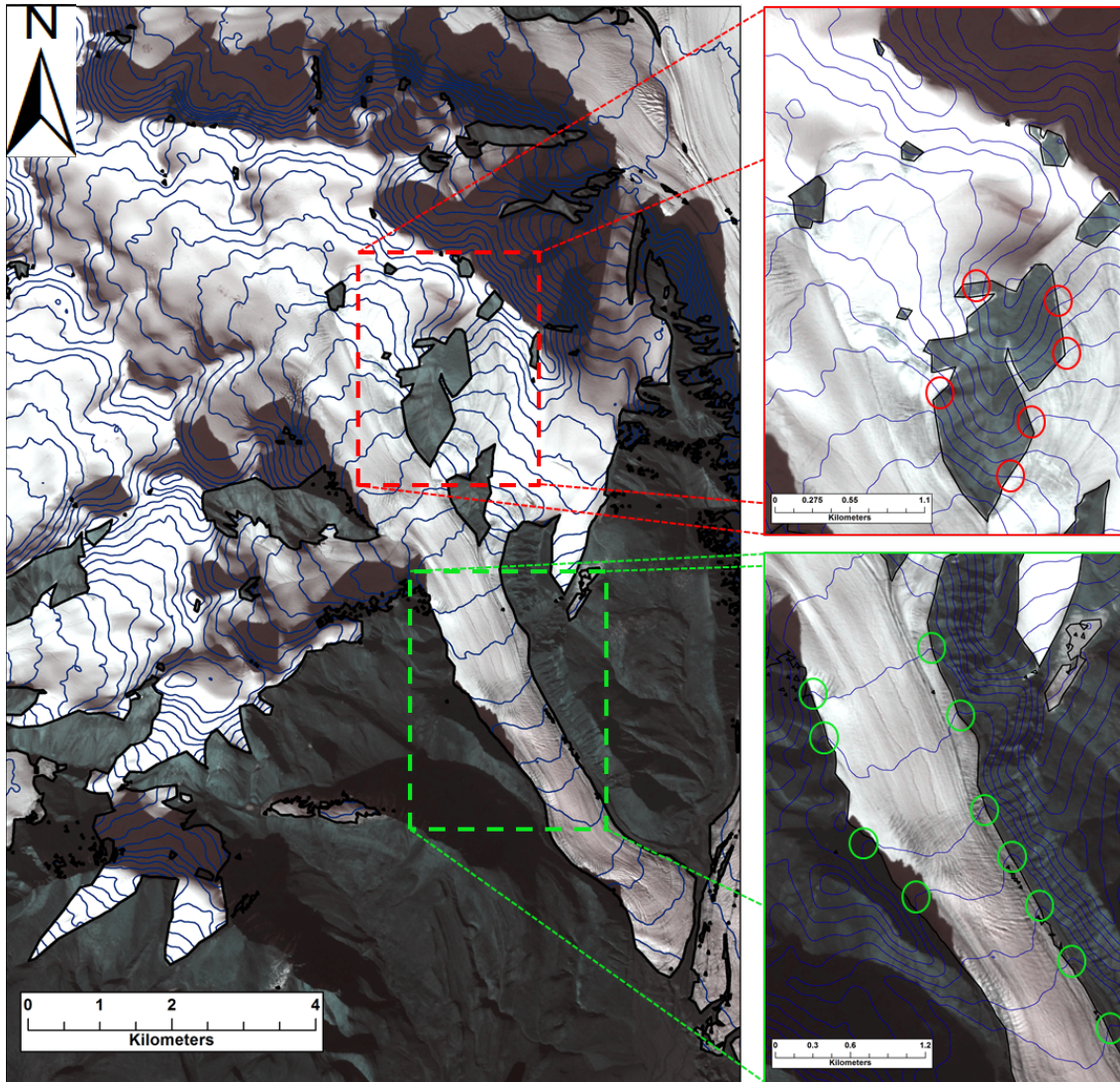


FIGURE 2.1 – CHANGING CHARACTERISTICS OF THE CONTOUR TRANSITION FROM ICE FREE VALLEY TO GLACIER SURFACE
Surface contours generated from ASTER GDEM data overlain upon a SPOT5 image of White Glacier, Axel Heigberg Island. Note the smooth transition in the accumulation area (red circles) compared to the sharp / abrupt transition in the ablation area (green circles)

Hess' aim was to contrast the sharp inflection at the glacier margin in the ablation area with the smooth transition between ice and adjacent topography in the accumulation area. However, more recent work has focussed upon the contrasting curvature characteristics that contour lines display across the entire transverse profile of the accumulation and ablation areas. Østrem (1966) developed Hess' observations by suggesting that the boundary between the accumulation and ablation area could be delineated by locating the elevation at which concave contours in the accumulation changed to convex contours in the ablation area. He concluded that the long-term ELA of a glacier could be identified by locating the contour line upon the ice surface that was most straight (the straight contour line marking the transition between the

accumulation area (concave contours) and the ablation area (convex contours) (figures 2.2, 2.3 and 2.4).

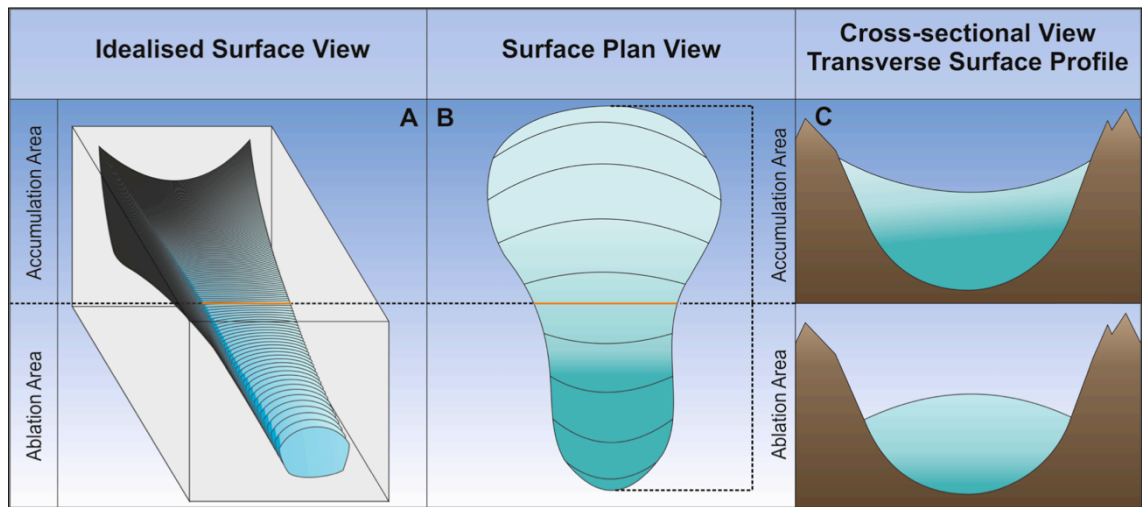


FIGURE 2.2 - IDEALISED THREE-DIMENSIONAL ICE SURFACE GEOMETRY

A simplified representation of the three dimensional shape that ice surfaces have been observed to tend towards

More recent use of the term “Hess Altitude” has incorporated the observations made by Østrem concerning the transverse surface profile of mountain glaciers rather than focussing upon the characteristics of contour lines at the ice margin only. Accordingly, from this point onwards the term Hess Altitude will be used in reference to the elevation contour that is most straight upon the ice surface as has been done in the most recent literature (Leonard and Fountain, 2003 and Cogley and McIntyre, 2003).



FIGURE 2.3 CONTOUR CURVATURE TRANSITION I
The change in transverse surface profile from the accumulation area (concave) to the ablation area (convex) on White Glacier (A), Hellstugubreen (B) and Hintereisferner (C). The red box highlights the transition zone. Topographic maps taken from the WGMS GMBB 12 (WGMS, 2013)

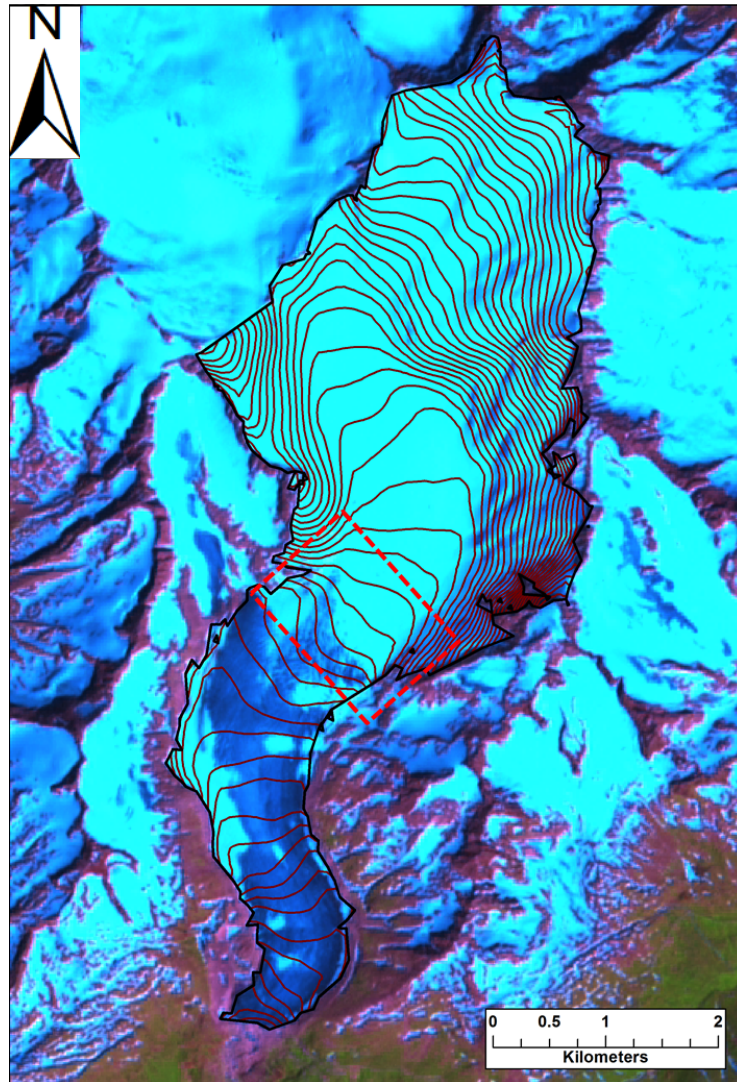


FIGURE 2.4 CONTOUR CURVATURE TRANSITION II
The change in transverse surface profile from the accumulation area (concave) to the ablation area (Convex) on Rhone Glacier, Switzerland. The red box highlights the transition zone. Contours generated from SRTM data overlain upon a Landsat false colour composite image.

With the increasing availability of high resolution, freely available digital elevation models (DEMs) and the continued improvements in photogrammetry techniques, there is now a wealth of data that enable one to assess the use of the Hess altitude. While previous studies that focussed upon glacier geometry were restricted to the availability of accurately drawn topographic maps, modern day assessments can be conducted on a global scale using data that are collected through remote sensing. Thus, if the surface form of a mountain glacier does indeed reveal key information concerning its long-term mass balance and response to climate change, there is the potential to utilise global-spanning DEM datasets in order to measure the 'Hess Altitude' upon every mountain glacier in the world. This could yield a global assessment of glacier health and

the production of a wide spanning climate signal. However, before discussing how the Hess altitude can be developed as a tool for extracting climate signals, it is important to examine the physical principles that govern glacier flow and demonstrate why a glacier's surface naturally tends towards the idealised form described by Hess and Østrem.

2.2 The flow-field and idealised glacier geometry

In order to maintain equilibrium, glaciers must transport material from higher elevations where net mass balance is positive as a result of accumulation through snow precipitation, avalanche and windblown snow, to lower elevations where net mass balance is negative as a result of melting, calving and sublimation. Therefore to achieve equilibrium, annual ice flux in a cross section at any point along the glacier must equal the integral of accumulation minus ablation over the entire area of the glacier above that cross section. Glacier flow occurs by two mechanisms: Ice creep, where ice deformation occurs as a result of movement between individual ice crystals, and basal sliding, where slip occurs between the base of the ice and the bed. This is aided by the presence of liquid water in linked cavity systems and/or a layer of dilated, deformable sediment that acts as a lubricant to reduce traction at the ice-bed interface (Raymond, 1969; Schoof, 2005). Existing literature currently focuses upon the role of ice creep in causing glaciers to tend towards the idealised surface geometry displayed in figure 2.1. Accordingly, sections 2.2.1 through to 2.2.3 will maintain the same focus.

2.2.1 Balance velocity

Assuming an idealized glacier in steady state, velocity vectors within a flow path are determined by the net budget. The mean horizontal velocity averaged over the depth of the ice at distance x from the headwall is then

$$\bar{u} = \frac{1}{h(x)} \int_0^x b_n(x) dx \quad \text{EQ 1}$$

where $h(x)$ is the glacier thickness and b_n is net mass balance (point) over the mass-balance year. This equation describes the "balance velocity", \bar{u} , (Hooke, 2005) and is an expression of the principle of the conservation of mass for an

incompressible medium, wherein as much mass that is added to a control volume or cross section (including accumulation on the surface) must be removed by flow. Consider, then, the case for a typical mountain glacier where the surface can be divided into two distinct zones: the upper accumulation zone where $b_n > 0$ and a lower ablation zone where $b_n < 0$. The annual flux that passes through a transverse cross section in the accumulation area must equal the total annual mass balance upstream. Correspondingly, the flux through a transverse cross section in the ablation area must equal the mass of ice lost by net ablation downstream of the cross section. It is therefore apparent that in order to conserve mass (EQ 1), longitudinal balance velocity, \bar{u} , and thus flux must increase steadily from the head of the glacier to the equilibrium line, and then decrease towards the terminus (Cuffey and Paterson, 2010). This variation in longitudinal flow gives rise to extending and compressing flows (figure 2.5).

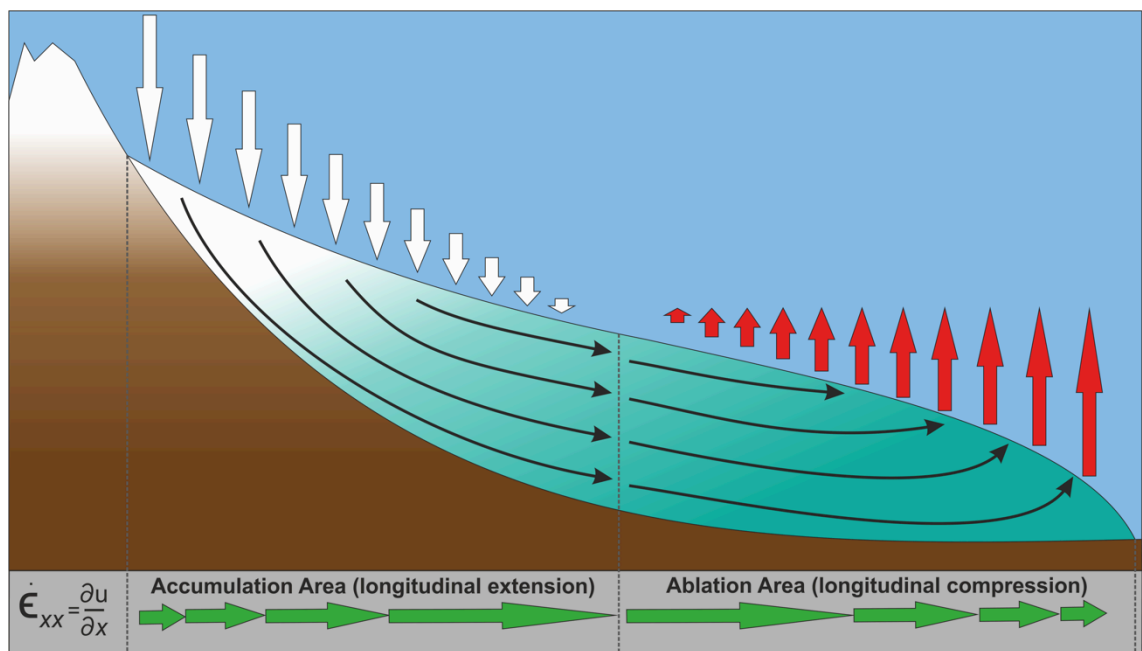


FIGURE 2.5 - LONGITUDINAL FLOW
 Longitudinal extension from headwall to ELA switches to longitudinal compression from ELA to terminus. The white and red arrows signify rates of accumulation and ablation respectively.

2.2.2 Extending and compressing flow

As flux increases along the accumulation zone toward the equilibrium line, the longitudinal strain rate, $\dot{\epsilon}_{xx} = \partial u / \partial x$, is positive and thus extending and in the ablation zone $\dot{\epsilon}_{xx}$ is negative and compressing. This is an important consideration when discussing glacier flow as it is the variation in extending and compressing flow along-glacier that largely determines the vertical velocity

component of flow (w). Owing to the fact that ice is nearly incompressible, extension in the x -direction (along-glacier) must be accompanied by corresponding shortening in the z (vertical) direction. This allows steady-state glaciers to maintain a constant ice thickness in their upper regions despite the addition of mass through accumulation. Similarly, longitudinal compression in the ablation zone results in vertical stretching. However it is important to note that this process applies strictly to valley glaciers where valley walls prevent the lateral expansion of the ablation area (figure 2.6).

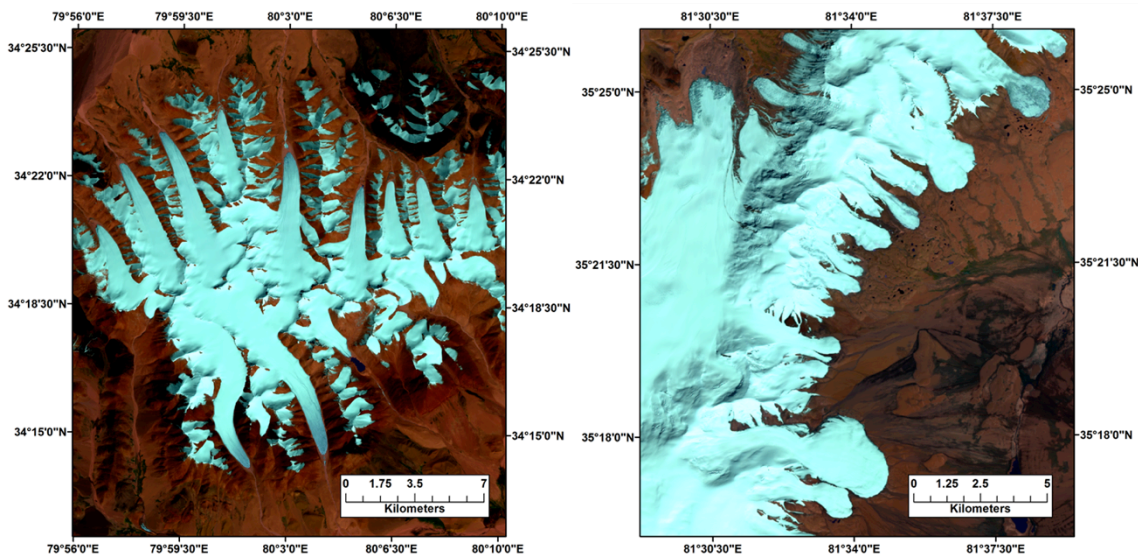


FIGURE 2.6 – LATERALLY CONSTRAINED VS UNCONSTRAINED MOUNTAIN GLACIERS
 Left) Glaciers in the Kunlun Shan constrained by the wider topography. Right) Glaciers in the Kunlun Shan where ice is not confined to by valley walls. Under such conditions, transverse ice flow compression is drastically reduced.

Given that the vertical component of flow (w) is governed by the horizontal velocity components (u and v , see figure 2.7), w at a depth (z) in a column of ice can be calculated as follows:

$$w(z) = w_b - \int_B^z \left[\frac{\partial u}{\partial x} + \frac{\partial v}{\partial y} \right] dz, \quad \text{EQ 2}$$

where w_b is the vertical velocity at the base (B) (often negligible when rapid basal sliding is not occurring). Ice therefore tends to flow down towards the bed in zones of horizontal extension and upwards to the surface in zones of horizontal compression (figure 2.5) (Cuffey and Paterson, 2010). It can thus be stated that downward flow vectors or “submergence velocities” are commonly

associated with the accumulation area and upward flow vectors or “emergence velocities” with the ablation area.

2.2.3 Submergence and emergence velocities

Having identified the importance of longitudinal flow in maintaining equilibrium (see Eq. 1) it is now important to consider the significance of vertical velocities in mass conservation. Hooke (2005) discussed the role of the vertical component of glacier flow at the ice surface in some detail, highlighting the importance of emergence and submergence velocities in maintaining equilibrium. He states that in steady-state conditions, the ice surface at any point in the accumulation area must sink at a rate that balances accumulation at locally. Consequently, ice beneath the surface in the ablation area must be rise at a rate that counters mass lost at the surface by melting and sublimation. It follows that the vertical velocity at a glacier’s surface is closely related to the net balance, b_n (point), over the mass-balance year. Keeping in mind that any point on the glacier surface is moving with a longitudinal velocity u_s and that the surface has a slope α , the relationship is:

$$b_n = -w_s + u_s \tan \alpha$$

EQ 3

In the accumulation area, w_s (the vertical velocity component at the ice surface) is negative (due to positive $\dot{\epsilon}_{xx}$) and owing to the fact that surface slope α is negative, the right hand side of the equation is positive, reflecting the positive mass balance, b_n , in the accumulation area. In the ablation area, the right hand side of EQ 3 is the submergence velocity. Conversely, in the ablation area, w_s is positive (due to negative $\dot{\epsilon}_{xx}$) thus the terms on the right hand side of the equation take on negative values, reflecting the negative b_n in the ablation area. Accordingly, the right hand side of the equation in the ablation area is termed the emergence velocity. In the context of this thesis it is the lateral variation in emergence and submergence velocities that define the distinctive upwardly concave and upwardly convex transverse surface profiles that are associated with the accumulation and ablation areas respectively.

In order for a glacier to achieve equilibrium w_s cannot be 0 along the margins, as accumulation or ablation is still taking place. However, because ice thickness reaches 0 at the ice margins, ice must be drawn away from the valley sides

towards the centre in the accumulation area in order to produce longitudinal extension and thus a downward (w_s) component to flow. Conversely, ice in the ablation area must be drawn away from the centre line towards the valley sides in order to produce longitudinal compression and an upward (w_s) flow component. Transverse slopes towards the centre of the glacier in the accumulation and away from the centre in the ablation area are required to generate the forcing for this flow and allow the glacier surface to reach equilibrium.

Firstly consider the ablation area. Down-glacier longitudinal surface velocity, u_s , diminishes away from the centreline towards the margins due to the increasing effect of drag as flow nears the valley walls whilst in the majority of cases, the longitudinal slope, α , will remain constant across the glacier. The ablation rate will also be approximately uniform across the glacier if not slightly enhanced at the margins due to heat radiated from darker rocks on the valley sides. Thus, if EQ 3 is to be balanced, w_s must be higher nearer to the margins than to the centreline. Thus, a transverse surface slope towards the margins in the ablation area is required to provide the horizontal compression (v) in the “Y” direction (figure 2.7). This in turn drives the large emergence velocities needed at the ice margins. Figure 2.8 shows a hypothetical example of how such a transverse profile is formed in order to maintain the required transverse flow component in the ablation area.

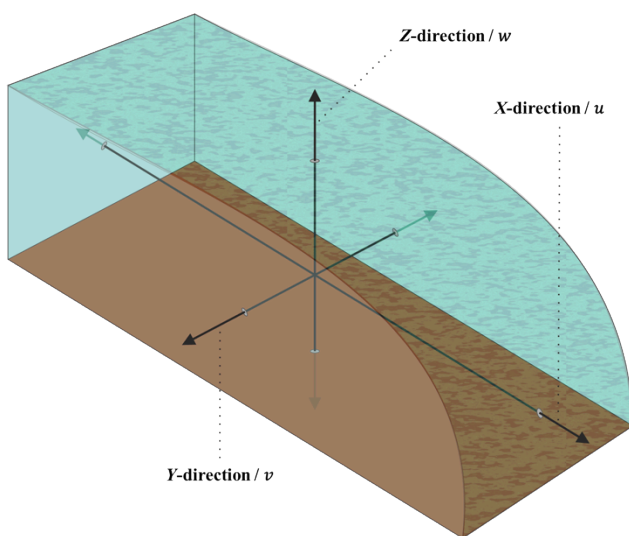


FIGURE 2.7 - FLOW PLANES
Definition of velocity components in 3D in a valley glacier

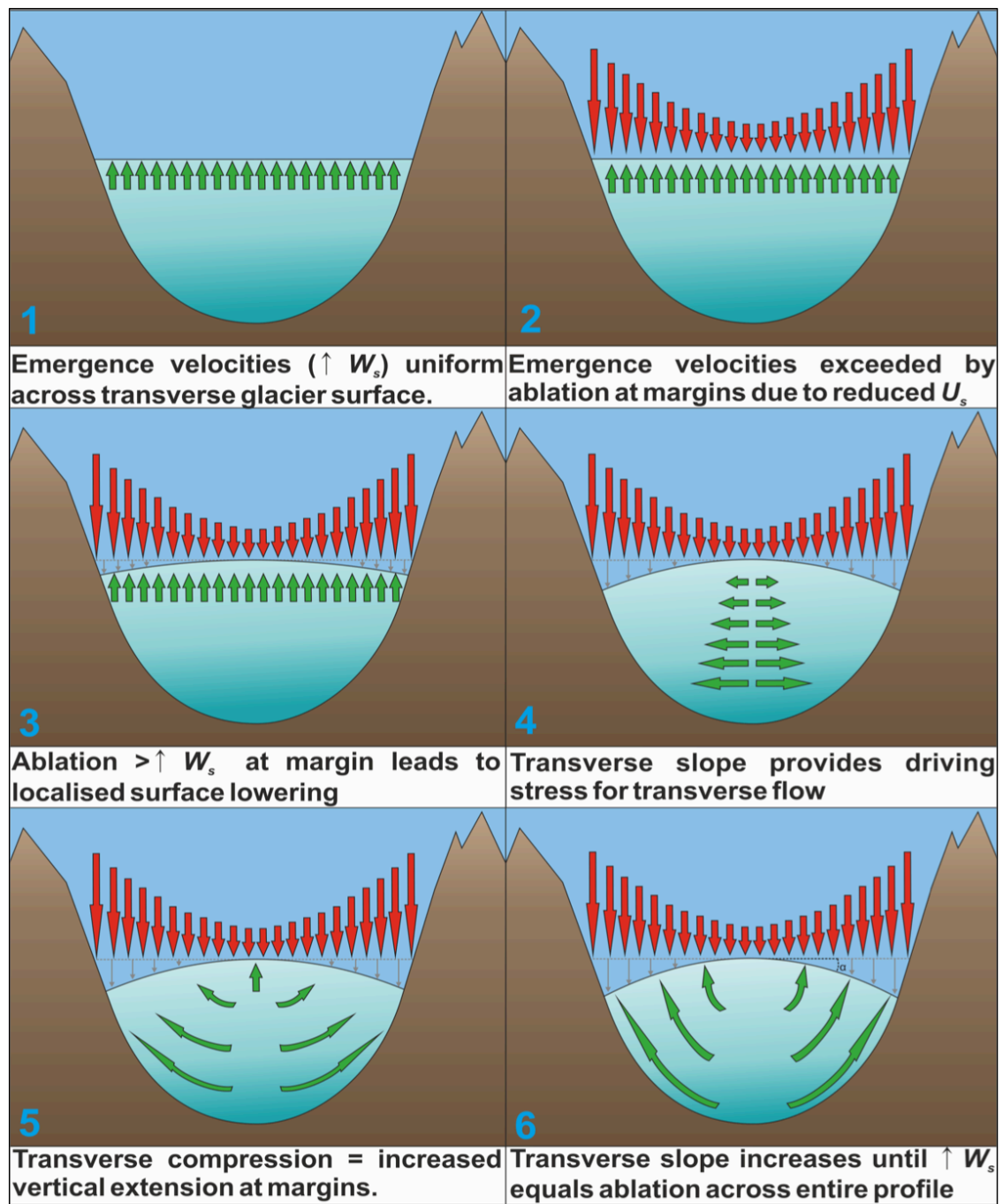


FIGURE 2.8 – MECHANISM GOVERNING THE ABLATION PROFILE
 Hypothetical scenario that describes the evolution through time of the convex transverse surface profiles that characterise ablation areas

In the accumulation area, as with the ablation area, u_s is lowest near the margin whilst the longitudinal slope, α , will remain constant across the glacier. However, it can also be stated that accumulation is preferential at the margins due to avalanche and snowdrift. As ice thins rapidly towards the margins, u_s and the longitudinal stretching rates at the glacier edges are too small to produce the required downward w_s . As a result w_s must be higher at the

margins in order to balance the accumulation and satisfy EQ 3. Therefore, a transverse slope towards the centre in the accumulation area is required in order to produce a transverse component of flow from the margins to the centre of the glacier. As glacier thickness usually increases rapidly away from the margins, stretching rates along flow-lines that creep towards the centre from the margin are very high. As a result, the transverse stretching away from the margins, driven by the concave upward transverse profile in the accumulation area, provides the more negative w_s required at the margins (Eq.2) (figure 2.9).

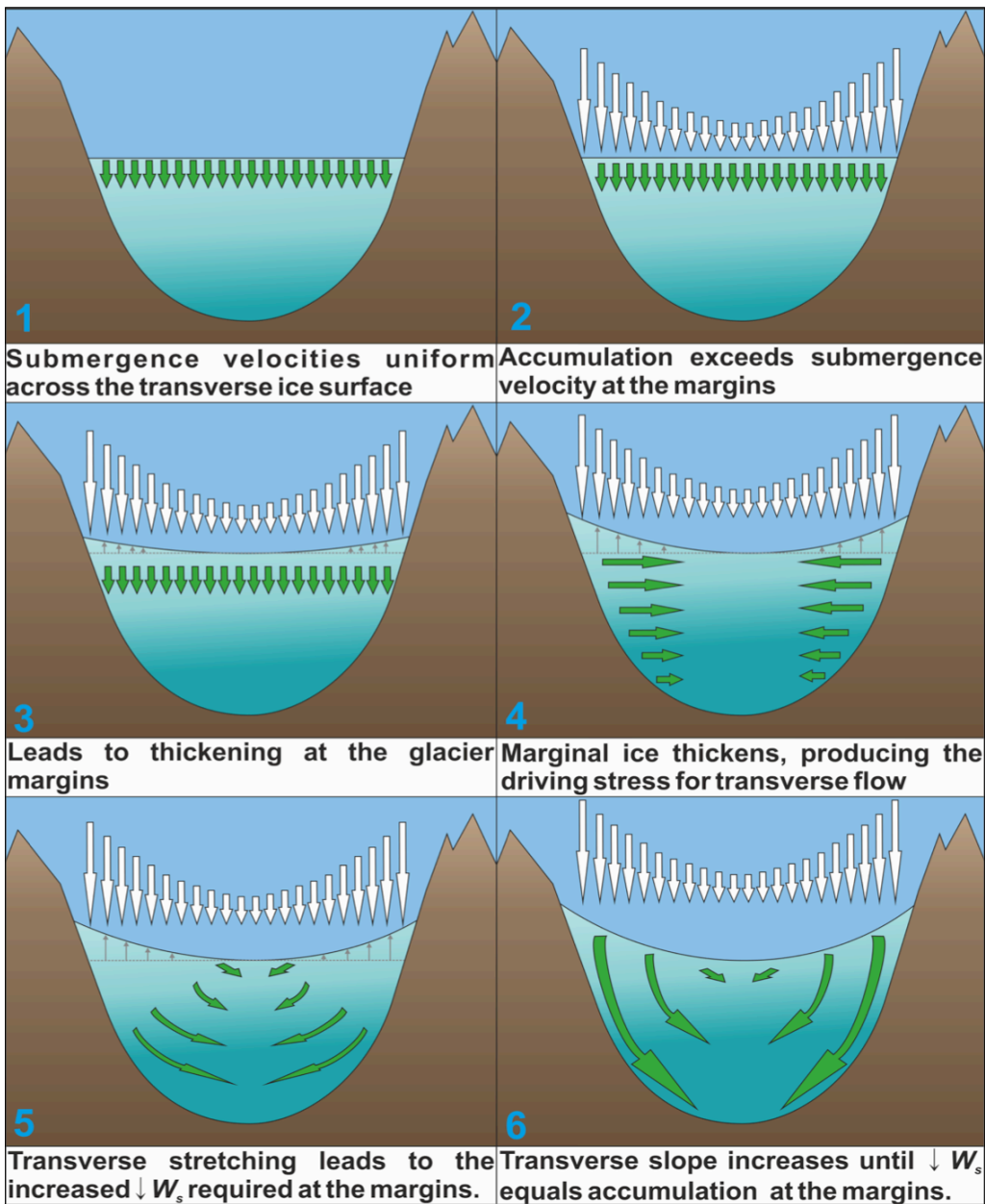


FIGURE 2.9 - MECHANISM GOVERNING THE ACCUMULATION PROFILE
 Hypothetical scenario that describes the evolution through time of the concave transverse surface profiles that characterise accumulation areas.

Relatively little observational work has been conducted into providing real world data to support the above reasoning. However, one study by Raymond (1969) conducted flow measurements using 8 boreholes in the ablation area of Athabasca Glacier, Alaska. The results demonstrated that the convex surface form in the ablation area was the driving force that enabled transverse horizontal flow and the large values of w_s that were required at the margins to counter ablation (figure 2.10).

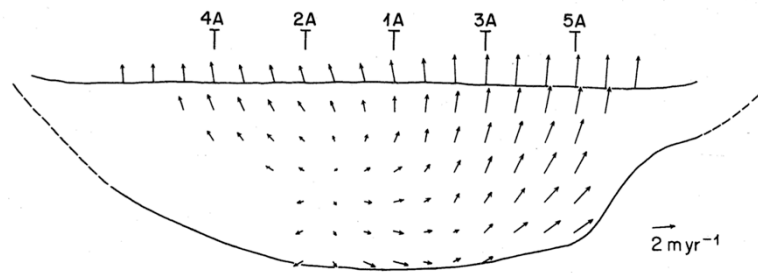


FIGURE 2.10 - OBSERVED 3D FLOW FIELD
The observed 3D flow-field in the ablation area of Athabasca Glacier, Alaska. (extracted from Raymond, 1969)

2.3 Hess Altitude as a measure of glacier health

2.3.1 Suitability of Hess altitude for estimating ELA

Section 2.2 provides a sound argument as to why valley glaciers conform to a commonly recognised three-dimensional geometry and develop the surface forms observed by Hess (1904) and Østrem (1966). However it is important at this point to highlight the fact that Hess's idea; that the straight or "smooth" contour demarked the "firn-line" (ELA), is not entirely accurate. This notion is supported by the fact that in the only two studies that have empirically tested the relationship between Hess Altitude and ELA (see Section 3.1), the Hess altitude consistently underestimates ELA by some distance. This discrepancy between the Hess Altitude and climatic ELA may arise due to the fact that the straight contour does not indicate the location of the climatic ELA. When considering EQ 3, it is clear that the ELA cannot be located at the same position as the smooth/straight contour transition. This is because when $b_n = 0$, w_s must be negative and therefore ice must be flowing downward into the glacier in order to balance both sides of the equation owing to the negative longitudinal

ice surface slope. As a result, the mass balance derived ELA must then be located across a concaved section of the glacier surface.

It is important to consider the fact that the dominant control upon glacier flow and evolution of the glacier's surface form is mass balance (EQ 1). Therefore the position of the straightest contour that demarcates the divide between the negative w_s (concave) and the positive w_s (convex) delimits the locality at which horizontal flow vectors deviate in response to a change from one balance regime to another. Put plainly, the Hess Altitude represents the region upon the glacier where ice flow vectors change as they flow from an area of positive mass balance to an area of negative mass balance. As the organisation of the glacier flow-field decides upon the location of the Hess Altitude and that these flow vectors are in turn controlled by mass balance, it could be suggested that the Hess Altitude marks the locality of dynamical change in the glacier's behaviour. Whereas the climatic ELA, which is the set of points on the surface of the glacier where the climatic mass balance is zero, is not directly controlled by glacier flow, the Hess altitude differs, as it is the direct result of glacier flow. The Hess Altitude could therefore be considered to symbolise a "**Dynamic ELA**". The dynamic ELA differs to the climatic ELA, which only accounts for year on year surficial gains and losses, due to the fact that it represents dynamic behaviour that glaciers display as flow adjusts to changes in climate within the constraints of the containing topography. Accordingly, the Hess altitude is the manifestation of the complex relationship between climate forcing, flow dynamics and the characteristics of the constraining topography, that evolve as glaciers tend towards equilibrium.

In this light, the Hess Altitude should no longer be considered as a direct indicator of climatic ELA as Hess (1904) and Østrem (1966) saw it. For the remainder of this study the Hess Altitude will be considered to be a completely different measure, one that represents a zone of dynamic change in glacier flow controlled by climate. In response to this altered definition and to avoid confusion, the straight contour that marks the boundary between the concave and convex ice surface areas will, from this point onwards, be referred to as the "Planform Curvature Transition" or "**PCT**".

2.4 Monitoring PCT location and evolution

2.4.1 PCT Elevation

It is clear that the PCT cannot be used as a precise measure for climatic ELA. Nevertheless the studies discussed later in Section 3.1 and the results in section 3.3 suggest that they are closely related and are to an extent governed by the same external controls. It therefore seems logical that the PCT is recorded and documented in a similar way to climatic ELA. The “fluctuations of glaciers” (FOG) series has been compiled by the WGMS since 1959 and continues to be the most comprehensive source of glacier health information such as ELA and mass balance to date (WGMS, 1967, 1973, 1977, 1985, 1988, 1993, 1998, 2005, 2008, 2012). In this series, climatic ELA is simply recorded and displayed by the altitude (metres above sea level) at which it is observed, irrespective of whether the data came from firn-line estimation studies (e.g. Benn and Lehmkuhl, 2000; Benn et al. 2005; Braithwaite and Raper, 2010; Osmaston, 2005; Carrivick and Brewer, 2004; Rea, 2009) or through direct glaciological mass balance methods (e.g. Cogley and Adams, 1998; Fischer, 2010; Fountain and Vecchia, 1999; Pu et al., 2008; Vuille et al., 2008). The PCT is well suited to this method of documentation and therefore the altitude (in metres above sea level) at which the PCT is located upon a glacier surface will be recorded and displayed as the PCT_a (planform curvature transition altitude). By recording PCT_a, it not only allows for a simple and rapid comparison between PCT_a on different glaciers, it also facilitates comparison between PCT_a and ELA as well as other glacial morphological indices such as mean, median, and mid range glacier elevations and maximum and minimum ice elevations.

Owing to the dynamic nature of the PCT, it is hypothesised here that knowledge of its proportional elevation upon an individual glacier can provide insight into whether current flow characteristics are capable of maintaining the glaciers hypsometry and extent. The most straightforward way of assessing this proportional elevation is to calculate PCT_a relative to the maximum and minimum ice elevation for each glacier. Similar to the process for calculating the toe-head-wall ratio (THAR) (Benn and Lehmkuhl, 2000; Benn et al., 2005; Kayastha and Harrison, 2008; Torsnes et al., 1993), the PCT is attributed a value

between 0 and 1 which marks its elevation within the total elevation range that the glacier spans (figure 2.11).

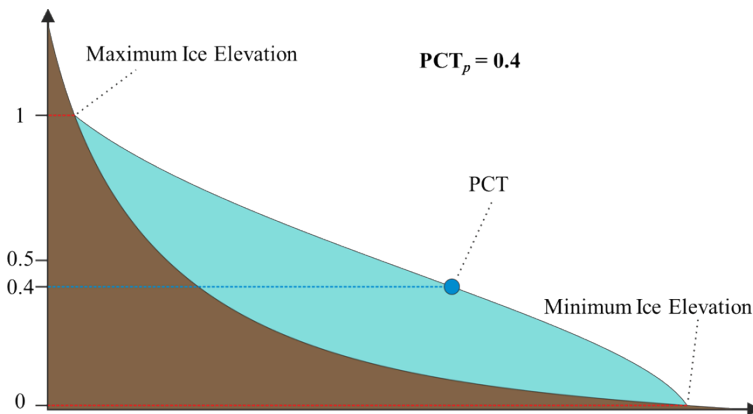


FIGURE 2.11 - PROPORTIONAL PCT CALCULATION

This elevation ratio would be calculated as follows:

$$PCT_p = \frac{PCT_a - z_0}{z_m - z_0} \quad \text{EQ 4}$$

where PCT_p is the proportional PCT elevation value, z_0 is the minimum ice elevation (at the snout) and z_m is the maximum ice elevation (at the headwall). Knowledge of PCT_p is important as it enables one to assess the relationship between glacier dynamics, the surrounding topography and climate controls in greater detail. By comparing PCT_p to those on other glaciers in that locality, assuming climate is relatively uniform across that region, disparities between PCT_p could be attributable to other non-climatic controls. For example, it would enable one to assess the degree to which variables such as longitudinal ice surface slope, aspect and basin geometry control the behaviour of the PCT (Carrivick and Brewer, 2004). Similarly it would enable the identification of large-scale trends when comparing PCT_p values across a global dataset. One could test whether PCT_p values show distinct variations across large geographical regions. For instance, are PCTs located at proportionally lower elevations on glaciers in maritime Scandinavia than they are in continental High Mountain Asia? Thus knowledge of PCT_p would enable one to explore the degree to which glaciological characteristics such as balance gradient (Braithwaite et al., 2013; Oerlemans, 2005; Oerlemans and Fortuin, 1992; Raper and Braithwaite, 2006) and thermal regime (Fowler et al., 2001; Robinson, 1984;

Scherler et al., 2011a) interacts with the glacier dynamic – climate relationship and how these interactions manifest themselves upon the glacier’s ice surface geometry. Records of the PCT_p may even have the potential to provide clues concerning how certain aspects of the climate system are forcing glacier variation (this will be discussed in greater detail in section 2.5).

Another key component to glacier monitoring is the ability to track changes over time and the necessity to relate these changes to climate forcing and glacier mass balance. It is envisaged that if PCT_a is measured and documented, the result will be the creation of a long-term data set of absolute PCT altitudes. As has been done with historical ELA records, this record will facilitate the analysis of how glacier dynamics respond to and reflect the changing climate. Furthermore, by regularly maintaining records of PCT_p data for each individual glacier, we are provided with greater insight into their response to climate forcing. For example a detailed record of variation in PCT_p will aid the glaciological community in assessing the degree to which the dynamics of individual glaciers respond heterogeneously to relatively uniform climate forcing (on a local scale).

An advantage of monitoring the PCT for the purpose of glacier health monitoring is that it can be executed retrospectively. There are data sources in the form of historical topographic maps, DEMs from previous dates and old aerial photographs of glacier surfaces that can be used to generate DEMs through photogrammetry. This is important because not only does this allow one to compare historical PCT data with those from today, it enables one to assess how PCTs vary and evolve over time upon glaciers that have accurately documented mass balance histories. Ideally, such an insight would also provide empirical evidence that would enable one to investigate the occurrence and extent of lag times between the onset of climatic perturbation and the resulting response of glacier flow dynamics.

2.4.2 Monitoring PCT change through time

The ELA displays an almost immediate response to climate forcing and as a result, the ELA of a glacier can vary drastically between consecutive years, reflecting the degree to which the ELA is controlled by each year’s weather

(figure 2.12). This can make the process of identifying long-term climate singles using ELA records difficult, particularly when interpretations are based upon sparse observations.

The PCT will be relatively unaffected by short lived extremes in mass balance owing to the slower rate at which ice dynamics respond to climate forcing. As a result, assuming that climate is the dominant control over flow dynamics, any variation observed in PCT_a is likely to be the result of a sustained adjustment in long-term climate conditions. Consequently, extended records of PCT_a change upon glaciers are preferential over ELA records when attempting to infer long-term climate signals from glacier observations. This is particularly true when only sparse, short-term ELA data are available.

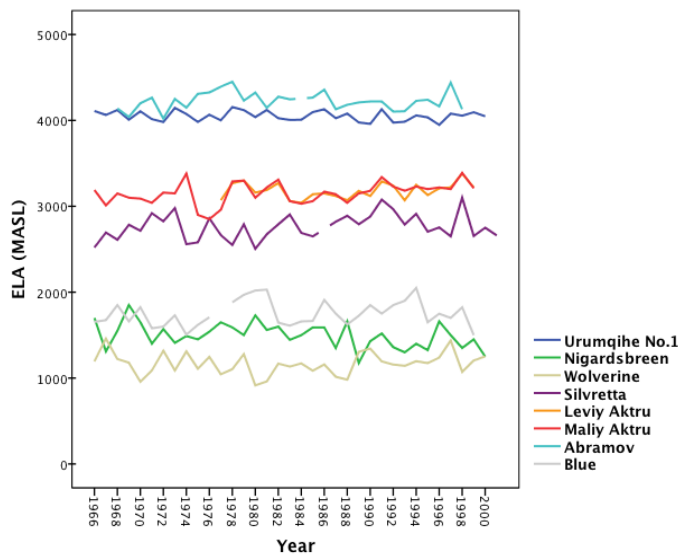


FIGURE 2.12 - ELA VARIATION
 High levels of interannual variability is visible in the ELA measurements (Data source: Fluctuations of Glacier Series (WGMS)).

However it is important to consider how the PCT may evolve through time and the difficulty that may arise when interpreting results if the only PCT_a observations are available, as is the case with ELA records when there are no accompanying mass balance records. A key problem can be identified when one considers the slow response rate of the PCT to climate forcing and the fact that the ice surface elevation itself can alter between monitoring dates. Consider the hypothetical situation in figure 2.20. At T_1 the PCT_a is recorded at elevation “Z” above sea level on the surface of the glacier. At a later date, T_2 , the PCT_a is once again recorded at the same elevation whilst having retreated “n” metres along

the X direction towards the headwall. In this scenario, ice flow dynamics have adjusted in response to a strongly negative mass balance phase whilst the ice surface has thinned to the extent that PCT_a remains unchanged between the two observation dates. Accordingly, it is recommended here that PCT movement in the X-direction (figure 2.7) should be observed and documented using the notation of PCT_x .

If one were to record PCT_a alone, it is highly likely that erroneous interpretations would be drawn from PCT data. Perhaps such erroneous interpretations have already occurred in relation to long-term ELA records due to the lack of attention paid to surface thinning and thickening. This problem could be remedied by collecting latitude and longitude coordinates at the point in which the PCT contour intersects the centre flow-line of the glacier. This would enable the PCT to be represented electronically in a GIS as a point shapefile with three-dimensional spatial coordinate attributes. As a result, changes in PCT location over time through three-dimensional space could be tracked using GIS software tools.

2.4.3 Advance and retreat scenarios

In order to fully appreciate any climate signals that may be reflected by the temporal change of PCT_x and PCT_a , it is critical that first one carefully considers the many different scenarios of glacier advance and retreat that may influence PCT behaviour over time. This understanding is of paramount importance when considering the relationship between PCT change and climate forcing.

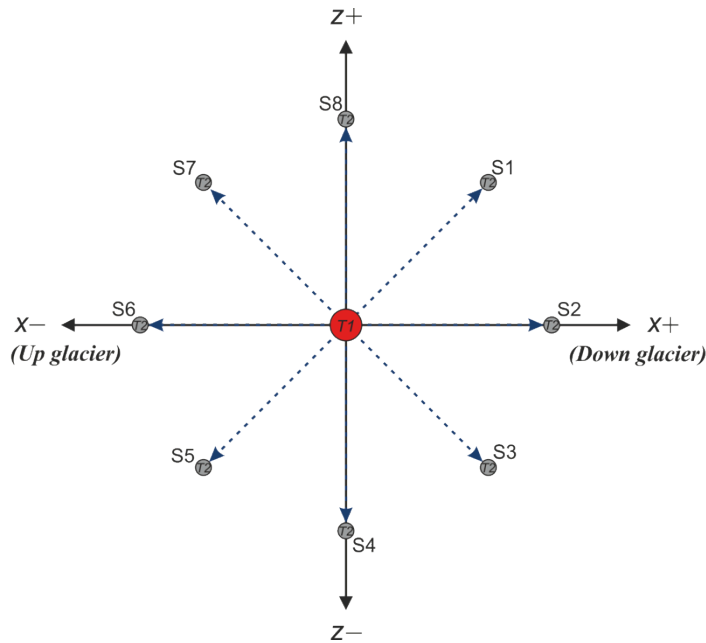


FIGURE 2.13 - PCT CHANGE SCENARIOS
Envisaged PCT “evolution scenarios” (S1-S8) that could potentially occur between initial ($T1$) and subsequent ($T2$) observations of PCT location.

Figure 2.13 highlights various possible scenarios of how PCT location changes over time. The vertical axis represents changes in PCT_a and the horizontal axis displays longitudinal changes in PCT_x upon the ice surface i.e. whether the PCT_x moves toward the snout or headwall. The intercept of the axes indicates the initial PCT location at observation time $T1$ and the surrounding points indicate the new PCT locations at $T2$ relative to the $T1$ location with n years between observations. For example in scenario 1 ($S1$), since $T1$, PCT_x has advanced towards the snout with a corresponding increase in PCT_a . In order to understand how this change in PCT location may be related to climate it is necessary to consider, in detail, the different theoretical scenarios of glacier response to climate forcing that may govern PCT evolution. It is important to note that these scenarios are speculatively based upon our current understanding of the response of glaciers to climate forcing.

2.4.3.1 Scenario 1

In this scenario the PCT_x is seen to advance towards the snout whilst PCT_a increases, relative to its initial position at the observation $T1$. However, because mountain glaciers tend to flow down relatively steep valleys, there would need to be exceptional thickening in the ablation area for the PCT to reveal an increase in elevation whilst “advancing” down glacier (figure 2.14).

To enable the PCT behaviour envisioned in scenario 1 and force such a drastic change in volume and ice surface elevation, the glacier would have required a sustained period of positive mass balance to drive this expansion. However, such drastic glacier thickening is relatively unlikely because glacier flow would adjust to balance increases in ablation area thickness, by extending glacier length in order to maintain equilibrium (Cuffey and Paterson, 2010; Hooke, 2005; Nye, 1952). As a result, strong perturbations of sustained positive mass balance are likely to result in extensive glacier terminus advance rather than substantial glacier thickening (Cuffey and Paterson, 2010). Thus, even under an extremely strong positive mass balance regime, it is unlikely that PCT_x advance could coincide with significant gains in PCT_a owing to the negative longitudinal slope. Although this may not be the case for glaciers with extremely shallow slopes, the argument stands for those glaciers located in alpine relief, which are the focus of the current study. As a result, evidence for scenario 1 is not anticipated to be observed during this study.

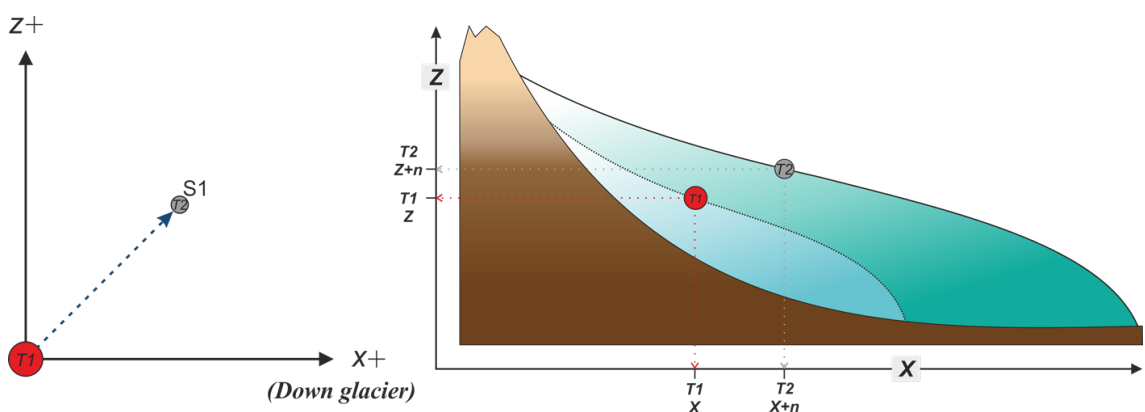


FIGURE 2.14 – SCENARIO 1

Left: The directional vector of the PCT between an initial observation at $T1$ (red circle) and subsequent observation at $T2$. Right: Idealised longitudinal glacier profile demonstrating the theoretical change in glacier volume and surface elevation required between $T1$ (dashed surface) and $T2$ (solid black line) to enable PCT increase in both X and Z .

2.4.3.2 Scenario 2

Between the observation times in this scenario, it is envisioned that the PCT_x would advance towards the glacier snout whilst experiencing minimal or no variation in PCT_a . However, owing to the negative slope towards the snout of mountain glacier ice surfaces, a degree of thickening would be required in the ablation area to maintain PCT_a between observations (figure 2.15). Any such thickening and expansion in glacier volume would require a sustained period of positive mass balance. Unlike scenario 1, this scenario is plausible in a situation where flow dynamics and thus the ice surface is shifting in response to sustained, long-term positive mass balance as demonstrated by Cuffey and Paterson (2010) through numerical modelling of the response of steady-state glaciers to sustained positive mass balance. As a result, observations of PCT behaviour that follow this schema would be indicative of glacier flow responding to positive mass balance conditions.

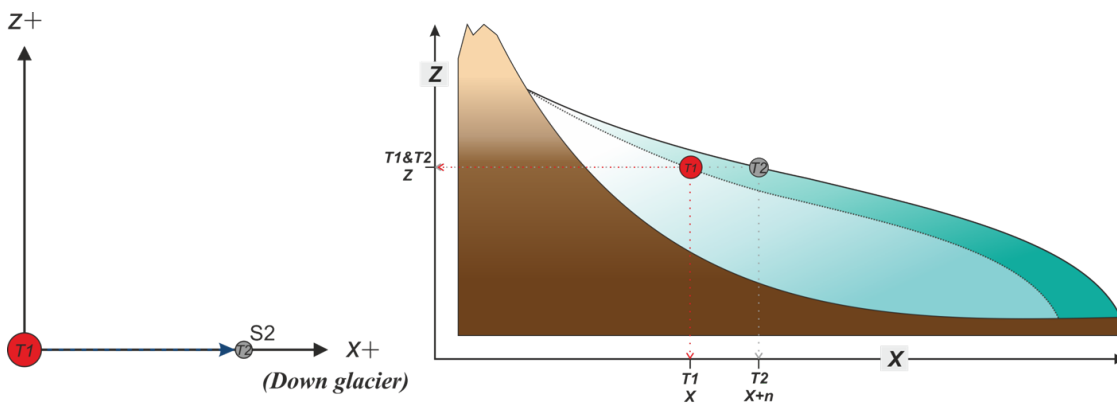


FIGURE 2.15 - SCENARIO 2
 Left: The directional vector of the PCT between an initial observation at T1 and subsequent observation at T2. Right: Idealised longitudinal glacier profile demonstrating the theoretical change in glacier volume and surface elevation required between T1 (dashed surface) and T2 (solid black line) to enable PCT increase in X with no change in Z.

It should be noted that such an interpretation may result in erroneous conclusions when assessing PCT behaviour upon glaciers that contain extremely low slope gradients within their longitudinal profile. This would be problematic where longitudinal ice surface slope values were close to 0 in the vicinity of the PCT. Here PCT_x could advance toward the snout, whilst maintaining a constant elevation, without the need for glacier thickening. This means that caution is required when interpreting PCT change on valley glaciers with low longitudinal ice surface angles.

2.4.3.3 Scenario 3

In this scenario, the PCT_x advances down glacier towards the snout whilst PCT_a decreases. The loss of elevation between observation dates is the result of PCT_x advancing along the downslope ice surface gradient towards the snout (figure 2.16).

PCT behaviour of this type would suggest that the mass balance regime upon the host glacier has been positive enough to drive PCT_x down glacier to lower elevations but not to the extent as to cause thickening in the ablation area. The glacier terminus could be expected to respond predominantly through advance under such conditions. Consequently, observations of PCT behaviour such as this could be seen as evidence of a glacier responding to a phase of positive mass balance.

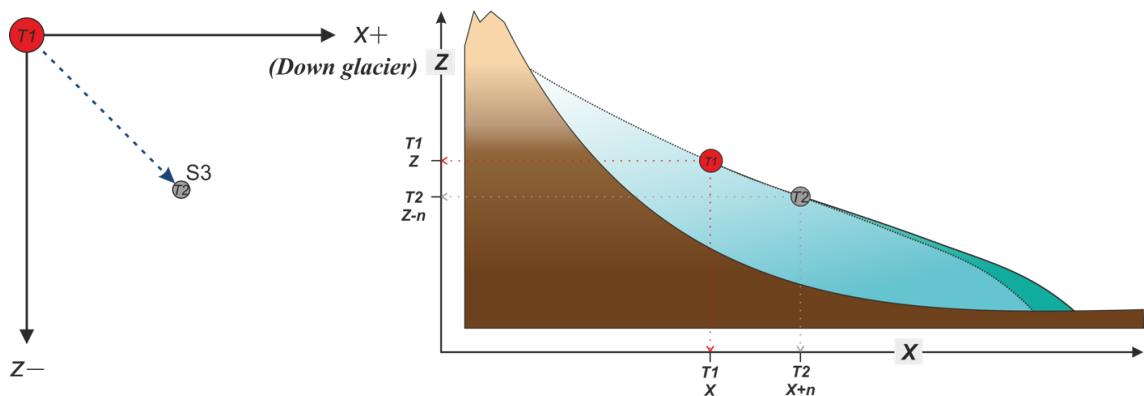


FIGURE 2.16 - SCENARIO 3
 Left: The directional vector of the PCT between an initial observation at $T1$ and subsequent observation at $T2$. Right: Idealised longitudinal glacier profile demonstrating the theoretical change in glacier volume and surface elevation required between $T1$ (dashed surface) and $T2$ (solid black line) to enable PCT increase in X with no change in Z .

Nonetheless it is important to highlight the fact that the scenarios discussed here are not distinctly separated from one another. It is probable that there is overlap through time as the different scenarios can be considered as stages through which the glacier must pass during its overall response to climate forcing. For example, under a positive mass balance regime, from $T1$ the PCT may initially display behaviour from scenario 3. Then, as positive mass balance is sustained the ablation area may thicken leading to an increase in PCT elevation, resulting in an overall PCT behaviour reminiscent of scenario 2 between $T2$ and $T3$ (Figure 2.17).

Thus it is clear that the time span between observations is an important consideration. If observations are separated by too long a time period, there is

the possibility that the initial behaviour reflected in scenario 3 would have been missed. Therefore, when recording PCT behaviour on glaciers with *positive mass balance*, one could expect to see variations in PCT location from T1 to a location reflecting aspects of both scenario 2 and 3 (see the yellow polygon in figure 2.17).

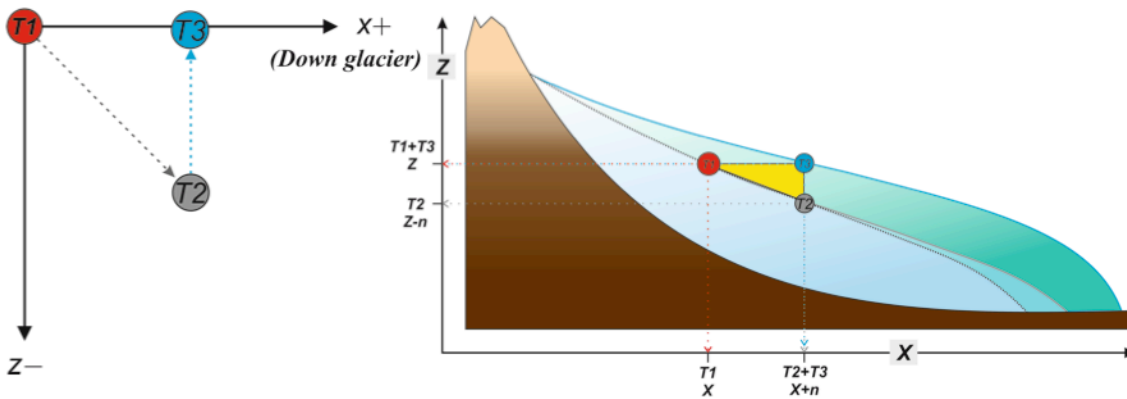


FIGURE 2.17 – SCENARIO 2/3 STAGES

Left: The directional vector of the PCT between an initial observation at T1 and subsequent observations at T2 and T3. Right: Idealised longitudinal glacier profile demonstrating the PCT behaviour through different stages between T1 and T3. Glacier surface represented at T1 (dashed surface), T2 (solid grey line) and T3 (solid blue line). The yellow triangle highlights the area of potential PCT location after T1 on glacier with sustained positive mass balance.

2.4.3.4 Scenario 4

In scenario 4 it is envisioned that whilst there is no change in PCT_x , PCT_a decreases. For this to occur, the glacier’s ice surface must lower whilst alterations to the glacier flow-field remain negligible (figure 2.18).

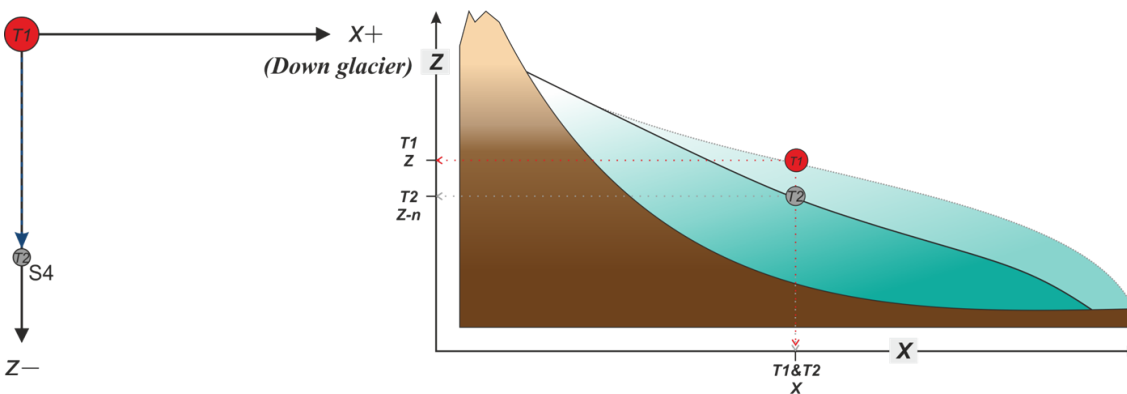


FIGURE 2.18 – SCENARIO 4

Left: The directional vector of the PCT between an initial observation at T1 and subsequent observation at T2. Right: Idealised longitudinal glacier profile demonstrating the theoretical change in glacier volume required between T1 (dashed surface) and T2 (solid black line) to enable PCT display no change in X whilst decreasing in Z.

This form of “non-dynamic” down wasting would be indicative of highly negative mass balance (Huss et al., 2010) and has been identified as being the dominant process of glacier retreat in the European Alps since 1985 (Paul et al.,

2004). Consequently, observations of PCT dynamics indicative of this scenario would represent rapid non-dynamic surface down wasting, triggered by strongly negative mass balance, at a rate greater than that of flow dynamic response.

2.4.3.5 Scenario 5

In scenario 5 the PCT_x shows evidence of retreat towards the headwall whilst PCT_a decreases. When considering the fact that glacier ice surfaces slope uphill toward the headwall, it is apparent that the glacier surface in what would have been the accumulation area at T1, must lowered between observations (Figure 2.19).

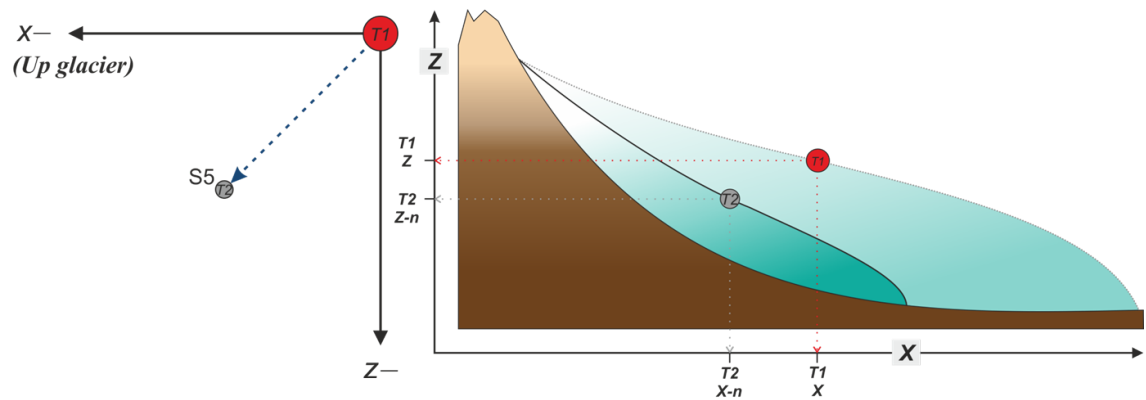


FIGURE 2.19 – SCENARIO 5
Left: The directional vector of the PCT between an initial observation at T1 and subsequent observation at T2. Right: Idealised longitudinal glacier profile demonstrating the theoretical change in glacier volume required between T1 (dashed surface) and T2 (solid black line) to enable PCT to display change in X whilst decreasing in Z

Accordingly, PCT variation of this manner would signify changes in flow dynamics and a reduction in glacier volume through surface lowering and retreat. However it is worth mentioning here that glacier margin retreat would coincide with such PCT change. This scenario is unlikely to be evidenced in the results of the current study. This is because the time span for which currently available data sources cover are not wide enough to enable observations of glacier thinning and retreat of such magnitude.

2.4.3.6 Scenario 6

In this scenario, observed PCT behaviour between T1 and T2 would display PCT_x retreat towards the glacier headwall whilst experiencing no change in PCT_a from observation T1. As with scenario 5, owing to the upwardly sloping

ice surface towards the headwall, the ice surface in what was the accumulation area at T1 must have thinned in order to maintain a constant PCT elevation between the two observation dates (figure 2.20).

Although not as extreme as the glacier volume change associated in scenario 5, PCT behaviour over time characterised in scenario 6 would signify clear evidence of a sustained negative mass balance forcing flow dynamic retreat and surface thinning.

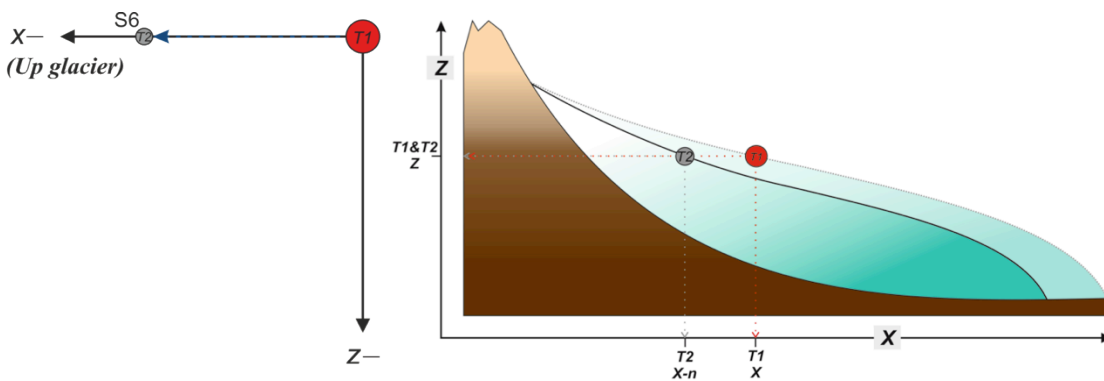


FIGURE 2.20 – SCENARIO 6
 Left: The directional vector of the PCT between an initial observation at T1 and subsequent observation at T2. Right: Idealised longitudinal glacier profile demonstrating the theoretical change in glacier volume required between T1 (dashed surface) and T2 (solid black line) to enable the PCT to display a reduction (retreat) along the X plane whilst maintaining a uniform Z value (elevation) between observations

2.4.3.7 Scenario 7

Here the PCT_x retreats towards the headwall whilst PCT_a increases. Unlike, scenarios 5 and 6, this PCT behaviour does not require surface lowering in the T1 accumulation area. The increase in PCT_a during the PCT_x retreat is likely the consequence of the upwardly sloping ice surface towards the headwall (figure 2.21).

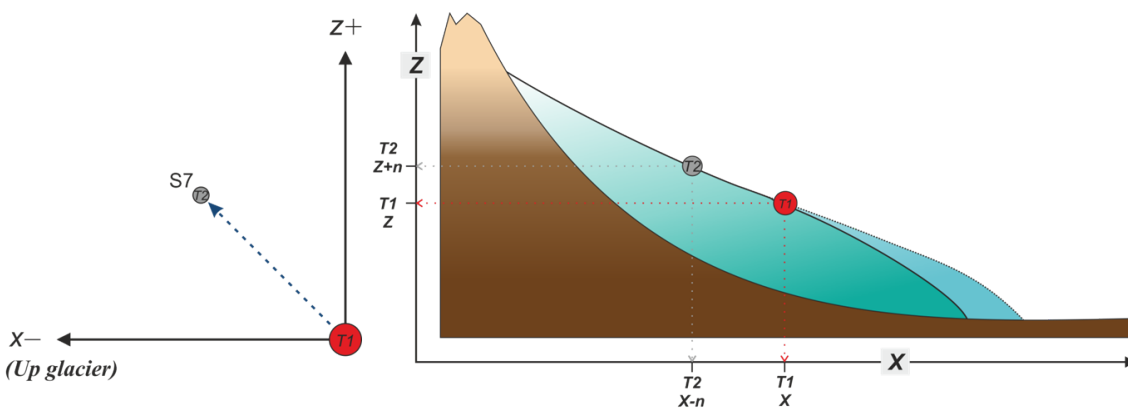


FIGURE 2.21 – SCENARIO 7
 Left: The directional vector of the PCT between an initial observation at T1 and subsequent observation at T2. Right: Idealised longitudinal glacier profile demonstrating the theoretical change in glacier volume required between T1

(dashed surface) and T2 (solid black line) to enable the PCT to display a reduction (retreat) along the X plane whilst increasing its Z value (elevation) between observations.

This display of “classic retreat” reflects a situation where the flow dynamics that control PCT_x adjust in response to a reduction in accumulation, enhanced surface ablation reaching increasing elevations or a combination of the two. This is perhaps the most recognisable glacier retreat mechanism, often associated with an increase in the ELA, where the snout retreats to higher elevations in conjunction with surface lowering in the ablation area in response to continued negative mass balance (Adhikari and Huybrechts, 2009; Huss et al., 2010). As such, surface thinning and mass loss is concentrated in the ablation area at lower elevations whilst the PCT_x retreats up-glacier in response to flow dynamic adjustments, resulting in the increase in PCT_a . As a result, the observation of PCT variation symptomatic of scenario 7 would indicate glacier retreat in response to sustained negative mass balance, but at a rate that enables variations in flow dynamic to maintain balance with glacier extent.

However, as will be discussed later in section 3.4.3.3, there is likely to be some overlap between scenarios as glaciers fully respond to climate forcing. As a result, one could expect the PCT to migrate from an initial location at T1 to any location that may reflect a permutation of scenarios 6 and 7 (see the yellow polygon in figure 2.22) under sustained negative mass balance.

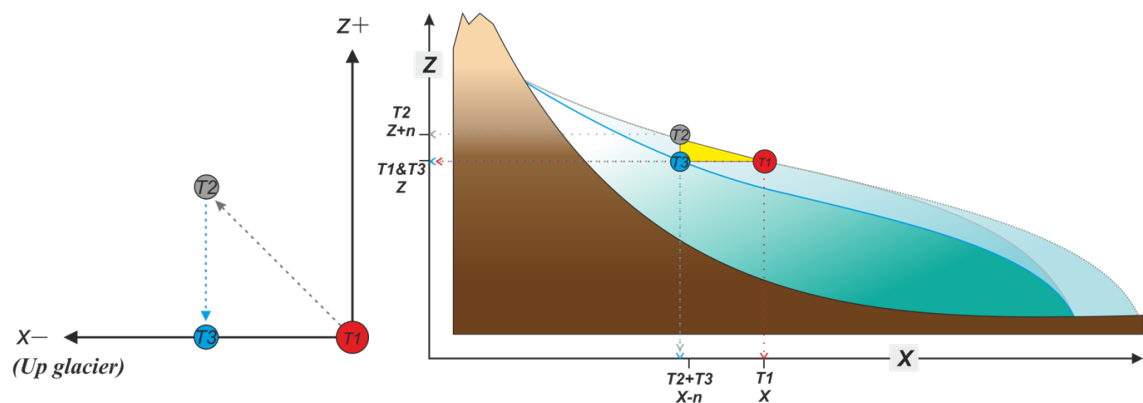


FIGURE 2.22 – SCENARIO 6/7

Left: The directional vector of the PCT between an initial observation at T1 and subsequent observations at T2 and T3. Right: Idealised longitudinal glacier profile demonstrating the PCT behaviour through different stages between T1 and T3. Glacier surface represented at T1 (dashed surface), T2 (solid grey line) and T3 (solid blue line). The yellow triangle highlights the area of potential PCT location after T1 on a glacier with sustained negative mass balance

2.4.3.8 Scenario 8

In scenario 8, the PCT_a would increase whilst PCT_x remained unchanged. In order for this to occur, the ice surface would need to rise through glacier

thickening between the two observation dates whilst flow vectors made no adjustment to the climatic forcing (figure 2.23).

However, owing to the fact that glaciers tend to accumulate in the upper regions and transport material down to lower elevations via ice flow, it is clear that overall thickening of the glacier would have to coincide with changes in flow dynamics (Cuffey and Paterson, 2010). Thus under “normal” positive mass balance conditions, where glacier mass is gained at higher elevations and distributed throughout the glacier through flow, changes in flow dynamics would be required to enable the entire glacier to thicken. As a result, PCT behaviour characteristic of scenario 8 is unlikely to be encountered during this study.

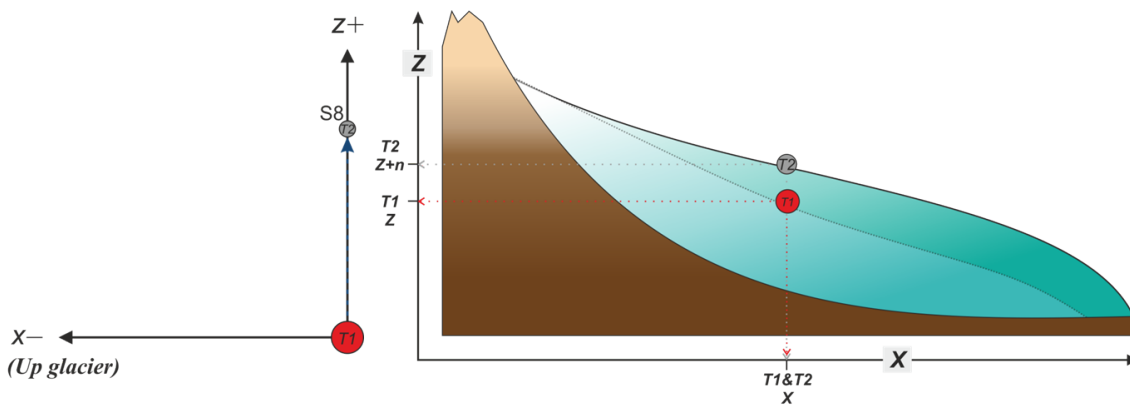


FIGURE 2.23 – SCENARIO 8
 Left: The directional vector of the PCT between an initial observation at T1 and subsequent observation at T2. Right: Idealised longitudinal glacier profile demonstrating the theoretical change in glacier volume required between T1 (dashed surface) and T2 (solid black line) to enable the PCT to display no observable movement along the X plane whilst increasing its Z value (elevation) between observations.

2.5 PCT as an indicator of glacier / climate synchronicity

2.5.1 Insights from temporal changes in PCT_p

Section 2.4 highlighted why it is imperative to record changes in PCT_x as well as changes in PCT_a . However, also important is the need to record changes in PCT_p . Assessments of the variations in time scales and characteristics of glacier extent responses to climate forcing have been well documented in the literature (Adhikari et al., 2009; Oerlemans and Fortuin, 1992; Oerlemans et al., 1998; Raper and Braithwaite, 2009; Van de Wal and Wild, 2001). However, relatively little attention has been dedicated to investigating how flow dynamics as symbolised by the PCT respond to climate changes. Accordingly, the results of a full numerical assessment concerning how PCT forming flow dynamics

should vary with modelled variations in glacier mass balance will be discussed later in this study. Furthermore, a great deal of insight could be gained empirically through observing changes in PCT_p over time.

Changes in flow dynamics and glacier inventory variables such as length, volume and area are intrinsically linked. However they do not always respond synchronously to climate forcing as changes in flow dynamics can often precede adjustments in glacier area and length (Heid and Kääb, 2012; Paul, 2004). Thus in order to assess the extent to which changes in flow dynamics and glacier extent are in unison (or asynchronous), one can interrogate the variation in PCT_p on individual glaciers between observation dates. By observing changes in PCT_p relative to glacier variables such as glacier length or altitude range, it is possible to assess the comparative scale at which both flow dynamics and inventory variables are responding to climate forcing.

With knowledge of how PCT_a and PCT_x has changed (section 2.4.3), one can then begin to interrogate changes in PCT variation in greater detail by assessing how its location has changed in terms of its proportional position upon the glacier. Figure 2.24 displays examples of changes in PCT_p upon the glacier surface over time relative to changes in PCT_a . Firstly consider the situation highlighted by the orange points. Here, between T1 and T2 PCT_a increases whilst maintaining a constant PCT_p of 0.4 between the headwall and the glacier snout. If one knows that the PCT_x has retreated towards the headwall to higher elevations the glacier snout must have retreated up valley synchronously with the retreat of the PCT_x in order to maintain a PCT_p value of 0.4. Similarly, if we know that the PCT upon the glacier represented by the green points has advanced along the X-plane whilst maintaining a constant PCT_p of 0.4, one can assume that the snout must have advanced down glacier in synchronicity with adjusting flow dynamics.

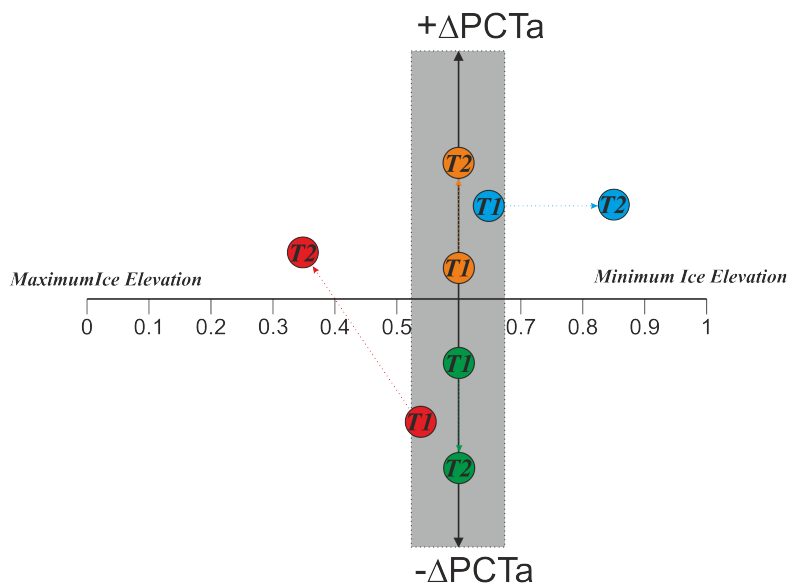


FIGURE 2.24 - POTENTIAL VARIATION IN PCT_p OVER TIME
 Theoretical changes in proportional PCT location upon the glacier surface. The horizontal axis represents the proportional elevation of the PCT between the maximum ice elevation and the minimum ice elevation. Points closer to the grey box represent glaciers displaying synchronised response to climate forcing.

Now, consider the case represented by the blue points. Here PCT_a has maintained a constant value between the two observation periods, however PCT_p has decreased from 0.35 to 0.15. Thus the PCT is in much closer proximity to the minimum ice elevation than it was at T1 despite no change in PCT_a . If prior knowledge informs us that the PCT_x retreated a small distance towards the headwall between T1 and T2, then it is clear that the snout is retreating at a far greater rate than PCT_x . This behaviour would demonstrate a situation where changes in glacier extent are unsynchronised with changes in the glacier's flow dynamics as the ice mass responds to climate forcing (see section 2.5.2).

The final example highlighted by the red points in figure 2.24 displays a scenario where the PCT_a increases whilst the PCT_p value increases. Accordingly, this suggests the PCT has moved closer to the maximum ice elevation at T2 than it was at T1 relative to the minimum ice elevation. This hypothetical PCT variation is interpreted as a situation where the glacier's flow dynamics have responded to a negative mass balance regime resulting in the PCT_x retreat up-glacier and an increase in PCT_a whilst glacier extent has responded at a slower rate or not at all. This style of behaviour could be expected on glaciers with an extensively debris covered snout. Thick debris cover on glaciers acts to insulate the ice from insolation and as a result, greatly reduces ablation rates when compared to clean ice surfaces (Anderson, 2000; Nakawo and Rana, 1999). This

protective role of the debris mantle enables the snout to remain at lower elevations where nearby “clean” snouts have been forced to retreat (Mihalcea et al., 2006; Scherler et al., 2011b). Due to the high proportion of glaciers with thick debris mantle in the Himalayas and Karakorum, a greater prevalence of glaciers with high values for PCT_p could be expected in these regions. Thus, in this scenario the PCT is evolving out of sync with glacier extent and provides another example of how one can gain greater insight into the modes by which glaciers are responding to climate forcing.

Clearly the scenarios discussed here are by no means exhaustive of all the possible modes of glacier response to climate forcing. However, they do exemplify some of the information that may be gleaned by recording and interpreting changes in PCT_p .

2.5.2 Insights from PCT_p for a single time slice

In cases where observations from numerous dates are not available, one may be required to interpret information relating to glacier health from a single time-slice. It is envisaged here that in such situations, the knowledge of PCT_p could prove to be instrumental in assessing how different glaciers are responding to climate perturbations. As glacier dynamics are driven by climate, one could expect PCT_p values to reflect this dependency upon climate control by remaining relatively constant across large glacier samples despite variations in individual glacier characteristics such as basin geometry, surface slope and aspect. Similar to studies that propose accumulation area ratios in the region of 50-60% (Dyurgerov et al., 2009; Osmaston, 2005; Rea, 2009) are required to maintain existing glacier volume and area distributions, it is suggested here that a similar benchmark value should be expected for PCT_p observations: That in order for a glacier to maintain a constant area and three-dimensional mass distribution, glacier flow dynamics must be organised in a way that enable the glacier’s area and hypsometry to remain constant. Accordingly, under steady state conditions one would expect flow vectors to be organised in such a manner that a similar PCT_p value was produced across a large sample of glaciers irrespective of case specific variations in glacier characteristics.

Let us now consider the complex relationship between flow dynamics and glacier extent and hypsometry. Although both glacier flow and hypsometry are ultimately functions of climate forcing and display substantial lags when responding to changes in mass balance, they do not necessarily display these responses or variation in unison. This is not to say that the responses of ice flow dynamics and glacier mass distribution to climate forcing are mutually exclusive but that significant variations in the rate at which each variable responds to a common forcing can occur (Pelto et al., 2008). It is suggested here that where glacier area and flow dynamics are in balance and respond in unison to climate forcing, the ice surface will tend to maintain a constant PCT_p value and are thus “*flow-balanced*”. In cases where flow dynamics and glacier extent display greatly different response rates for a single glacier to climate perturbations, the PCT_p value is expected to vary between observations. Such glaciers are to be considered as “*flow-unbalanced*”.

For illustrative purposes, let us assume that the PCT_p upon flow-balanced glaciers is approximately 0.4, where 0 is the minimum ice elevation and 1 is the maximum ice elevation. A ratio of 0.4 is suggested for the time-being for PCT_p as this figure has been used for both THAR and AAR methods when estimating ELA on both contemporary and paleo-glaciers (Benn and Lehmkuhl, 2000; Brocklehurst and Whipple, 2004; Carrivick and Brewer, 2004; Dahl et al., 2003). Thus, when analysing PCT_p values for a large sample of glaciers, we can begin to assess the extent to which glaciers are *flow-balanced* or *flow-unbalanced*. Admittedly, such information cannot provide much insight concerning glacier synchronicity with climate as a whole. However, what it may inform us of is the different modes by which, glaciers respond to climate forcing which may then provide us with hints as to their recent mass balance histories.

For example, consider figure 2.25 displaying the hypothetical distribution of PCT_p values across a large glacier sample. Glaciers with a PCT_p value close to 0.4 are considered to be flow balanced. However, it should be stressed here that such a situation would not imply that these glaciers have balanced budgets and are in equilibrium with current climate but that the response of both the flow dynamics and glacier area is synchronised. Nevertheless, it is important to consider the fact that such glaciers can still be greatly out of sync with general

climate forcing despite being “*flow-balanced*”. However, what is perhaps more interesting is the potential interpretations that can be made concerning the mode of glacier response to climate perturbations when observing the extent to which the PCT_p deviates from 0.4 and whether this variation is positive or negative.

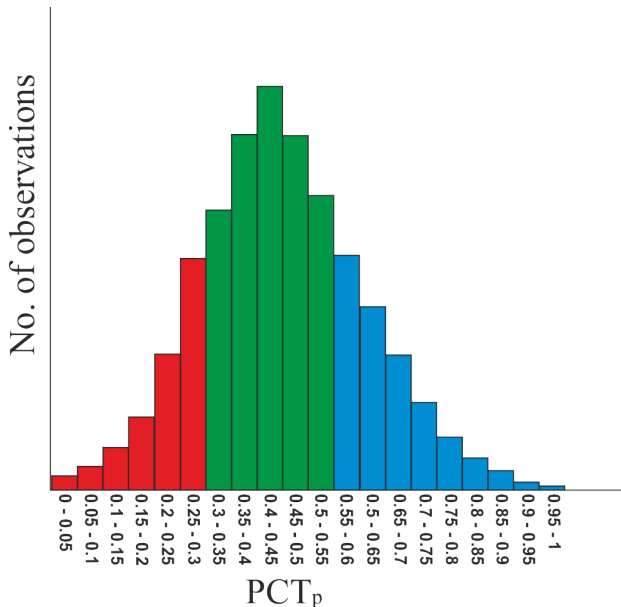


FIGURE 2.25 - HYPOTHETICAL DISTRIBUTION OF PCT_p OBSERVATIONS

In the histogram, the glaciers represented by the red columns display low PCT_p values (0 – 0.3) indicating that the PCT is located disproportionately close to the minimum ice elevation when compared to the rest of the sample. In this situation the glacier could be categorized and being “*flow-unbalanced*” as the PCT_p appears to have deviated from a balanced position. It is proposed here that in order for the glacier to display a disproportionately low PCT_p , the glacier snout and ablation area must be retreating or shrinking at a faster rate than the reorganisation of the glacier flow-field’s vectors. This observation could then tentatively be taken further when considering the climatological condition that would lead to such a rapid retreat in snout position (Ding et al. 2006; Paul et al., 2004; Paul, 2008). Of course, one can also consider the situation highlighted by the blue columns in figure 2.25 that represents glaciers where the PCT_p is disproportionately high relative to the entire sample. With the assumption that on such glaciers the PCT_p would have previously been closer to 0.4, we can then assume that changes in climate have forced the PCT to behave in one of two

ways. Firstly, PCT_x retreat has led to PCT_a increase as a result of the reorganisation of the glacier flow field. For this to occur flow dynamics would have needed to adjust prior to, or at a greater rate than, changes in glacier area in order to create *flow-unbalanced* conditions. One possible expectation is that changes in the glacier's accumulation regime could occur whilst temperatures (insolation) remain relatively constant. If such a situation occurred, it is possible to understand why the terminus would remain steady, or at least change at a slower rate, due to the maintained temperature whilst substantial changes in accumulation regime would lead to observable variations in the glaciers flow dynamics. However, unlike the situation where a brief but strong increase in warming could lead to rapid snout retreat, it should be stated that any abrupt changes in accumulation regime would need to be sustained long enough for glacier dynamics to adjust. This response mode where glacier dynamics seemingly adjust to climate forcing at a greater rate than the glaciers overall area distribution is likely to be exacerbated by the impact of supraglacial debris. As mentioned in section 2.5.1, extensive layers of thick supraglacial debris act to insulate the underlying ice from solar radiation, enabling the ice to persist at lower, relatively warm elevations. Consequently, during climatic warming or a negative change in the glacier's mass balance budget, flow dynamics will adjust accordingly, with the PCT retreating up glacier to higher elevations whilst the insulated snout remains relatively unaffected, resulting in a high PCT_p value.

The other explanation for high PCT_p values is the potential for short-term glacial advances in the form of surge events and kinematic waves to cause glacier snouts to extend down-valley without a corresponding glacier-wide adjustment in flow dynamics. During short spells of positive mass balance where rates of accumulation exceed the rate at which flow removes mass from the locality, a bulge develops in the glacier's accumulation area. The increased driving stress associated with greater ice thickness at the bulge's locality along with the sharp increase in the longitudinal slope means that it is transported down glacier at a greater velocity than the over all speed of the glacier ice as a kinematic wave. However, because the surface slope at the front (leading edge) of the bulge is steeper than that at the up-glacier end of the bulge, it travels as a greater velocity and thus localised flow acts to disperse the bulge through longitudinal extension. As a result, rather than causing extensive thickening at

the terminus, the longitudinal dispersion of the bulge results in extension of the glacier snout down valley as the increased ice mass reaches the terminus (See Cuffey and Patterson, 2010 for a more thorough description of kinematic waves). Thus in order to transport bulges resulting from increased mass gain down glacier, changes in the glacier's flow vectors tend to be surficial and concentrated around the bulge's location and thus may not have any effect upon PCT_x or glacier wide flow dynamics. Kinematic wave theory then enables one to understand how the advancing of glacier snouts in response to relatively short spells of positive mass balance would result in disproportionately high PCT_p values.

Consequently, if the hypothesis that the complex and self-regulatory relationship between flow dynamics and glacier area/volume distribution does indeed lead to a balanced flow state that tends towards a universal PCT_p value, one can then at a minimum assess the degree to which glaciers are either *flow-balanced* or *flow-unbalanced*. Furthermore, even with a lack of multi temporal data, more speculative interpretation of the PCT_p could be used to gain a great deal of information as to the mode of response to climate change by observing the different rates at which various components of the glacier system are reacting. This in turn allows one to speculate as to the type of forcing, be it increased melt or reduced accumulation, which is driving the glacier response.

Chapter 3 Planform Curvature Transition and Existing Glacier Health and Climate Measures

Chapter two highlighted the fundamental theoretical framework that shapes our understanding of why the PCT develops upon a glacier's surface and how this morphological phenomenon can be linked to climate forcing. A logical next step is to test this theory through the collection and analysis of empirical data. The following chapter examines how the PCT can be related to established glacier health measures such as ELA and mass balance. This will be achieved by comparing PCT_a data with glaciological climate variables upon glaciers with well-documented health histories. However, before focussing upon the data collected as part of this research, it is important to discuss the small number of publications that have already attempted to relate the Hess Altitude to glaciological-climatic records.

3.1 Previous Work

Since Hess's initial observations in 1904, only a handful of glaciologists have completed any work with the Hess altitude and very few papers have been published on the topic. Østrem (1966) discussed the use of the Hess Altitude as a proxy for the long-term average ELA upon a glacier when investigating the different methods used to estimate the "firn-line" or ELA. However, he failed to collect any data concerning Hess altitudes and instead focussed upon investigating the "glaciation level" in Southern British Columbia and Alberta. Similarly, Carrivick and Brewer (2004) made mention of the Hess Altitude being a recognised tool for estimating the ELA. However, like Østrem they made no attempt to further analyse the relationship between ELA and the Hess Altitude.

A paper published in 2003 by Leonard and Fountain was the first of two studies that empirically tested the relationship between climatic ELA and the Hess altitude (or the Kinematic ELA as they described it in their study). They

recorded the elevation of the straight Hess altitude contour from historic topographic maps of glacier surfaces, using only glaciers that had documented mass balance histories where the climatic ELA had been recorded each year during the glaciers' monitoring campaign. When comparing the normalised "Kinematic ELA", normalised using the same approach as outlined in section 2.4.1, with the averaged climatic ELA (normalised) for glaciers with 15 years or more of ELA data ($n = 17$), the modelled regression returned an r^2 value of 0.59 (see figure 3.1, whilst a complete list of the glaciers used in their study is displayed in table I, appendix A). Although their results provided the first clear evidence to suggest a statistically significant correlation between climatic ELA and the Hess altitude, they also identified that the Hess-derived ELA was on average 20% lower than the average climatic ELA. They attributed this 20% offset to the fact that the maps they used in the study were made before field observations were collected and that the ELA had risen in elevation since that time. They also alluded to the idea that perhaps this offset should be expected due to the organisation of glacier flow vectors (see section 2.3.1).

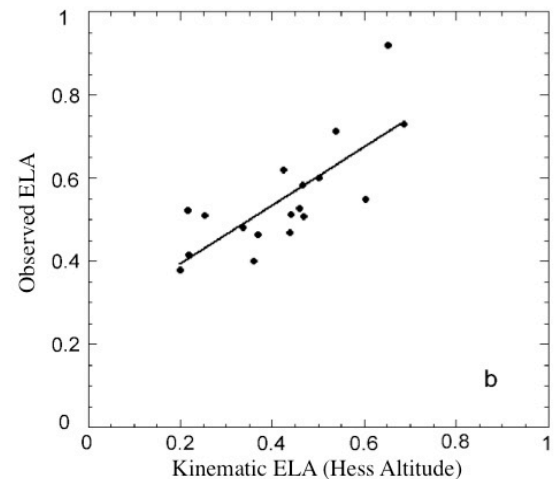


FIGURE 3.1 - KINEMATIC ELA VS CLIMATIC ELA
Relationship between normalised observed ELA and normalised Kinematic ELA (Hess altitude) taken from Leonard and Fountain (2003)

A comparable study by Cogley and McIntyre (2003) took a similar approach to assessing the relationship between climatic ELA and other "morphological estimators" such as the Hess altitude. Once again utilising topographic maps, they compared the Hess altitude with measured ELA values but for 37 glaciers. Although they did not specify which glaciers they retrieved data for, they did state that the majority were from the Western and Arctic Canada, Scandinavia and the Alps. Accordingly, it is highly likely that there is some crossover with sampled glaciers in the Leonard and Fountain (2003) study. Their results suggested that the Hess altitude provided a reliable and robust tool for estimating ELA but also commented upon its precision. However, it is worth noting that unlike Leonard and Fountain, Cogley and McIntyre did not

normalise their measurements. Thus the very high correlation between measured ELA and PCT_a (0.98) is likely to be the result of the varying elevation ranges of the sampled glaciers. Nevertheless, as with Leonard and Fountain's (2003) results, Cogley and McIntyre (2003) identified that the Hess altitude underestimated the climatic ELA on each of the 37 studied glaciers, stating that on average the Hess altitude was 130 m below the recorded ELA. However, they did not provide an explanation as to why this might be the case.

As suggested by Leonard and Fountain (2003), this systematic offset may be the result of glacier flow's lagged response to variation in ELA. However it may actually be because the Hess altitude is not a measure of climatic ELA at all, but a measure of the dynamic adjustment of flow to climate forcing that justifies being approached in a different light.

3.2 Methodology

3.2.1 Approach

This chapter takes an empirical approach to assessing the use of the PCT as a glacier health measure and extends the work of those described above. The use of freely available remotely sensed data in the form of Digital Elevation Models (DEMs) and optical satellite imagery within GIS software will provide the basis from which glacier inventory information, including PCT_a , will be extracted. PCT_a and PCT_p values will then be compared with archival records containing data pertaining to ELA and mass balance in order to gain greater understanding into how the PCT relates to other established measures of glacier health.

3.2.2 Data Sources

3.2.2.1 DEMs

Digital elevation models are one of the key data sources used in earth observation studies, with the two most utilised DEMs being that of the 90m SRTM and the 30m ASTER GDEM. These freely available topographic data sources offer almost complete global coverage and are already well established as important data sources for glacier remote sensing studies (Berthier et al., 2007; Bhambri and Bolch, 2009; Bolch et al., 2005; Huss and Farinotti, 2012;

Kääb, 2005; Le Bris and Paul, 2013; Paul, 2008). These data have been scrutinised by Frey and Paul (2011) in order to test their suitability for the specific task of glacier inventory information provision. They concluded that SRTM is slightly preferable over the ASTER GDEM owing to the fact that radar systems have advantages over optical systems for DEM acquisition due to the ability to penetrate clouds and their independence from optical contrast. The SRTM data are also preferred over the ASTER DEM due to the advantage of known acquisition dates. Accordingly, the primary source used for the collection and analysis of topographic data in the chapter was the SRTM DEM.

3.2.2.1.1 SRTM

The SRTM DEM was acquired through collaboration between the NGA (National Geospatial–Intelligence Agency) and NASA (National Aeronautics and Space Administration) during a ten-day mission in February 2000. The radar interferometry (InSAR) data was collected when a space shuttle mapped the Earth’s surface between 60°-N and 56°-S with C-band radar. The primary output from this mission was a near global DEM with 3 arc- seconds (~90m) spatial resolution. Errors and inaccuracies contained in the global DEM are well known and constrained, with Rodriquez et al. (2007) suggesting maximum elevation errors of ± 9 m and maximum planimetric errors of ± 13 m for the total dataset when comparing the DEM with ground control points (GCPs). Elevation-dependent biases have also been recorded due to penetration of the C-band radar waves into snow and ice (Rignot et al., 2001; Berthier et al., 2006). Rignot et al. (2001) identified that C-band penetration into snow and ice ranged from 1 to 10 m beneath the surface depending upon conditions (i.e. dry vs. wet) in Greenland and Alaska. However, corrections for radar penetration have rarely been attempted for the SRTM data in past studies as it is extremely difficult to correct for. This is because knowledge of the snow conditions at the time of acquisition is required but rarely available (Nuth and Kääb, 2011). Accordingly, this study does not consider errors generated by radar wave penetration. The SRTM DEM is also known to contain data voids as the result of the geometrical constraints of the acquisition method where mountainous terrain with steep slopes produce radar shadow. However, the SRTM data used in this study is a complete, void filled DEM produced by The Consultative

Group on International Agricultural Research (CGIAR) (accessed through: <http://srtm.csi.cgiar.org/>). The void-filled version (SRTM3v4) has been produced where data gaps are filled using a combination of different interpolation techniques and supplementary DEM data sources (see Reuter et al., 2007, for a full description of the methods used for the void filling).

3.2.2.1.2 ASTER GDEM

The ASTER Global Digital Elevation Model (ASTER GDEM) is a joint product developed and made available to the public by the Ministry of Economy, Trade, and Industry (METI) of Japan and the United States National Aeronautics and Space Administration (NASA). Released in 2009, the GDEM is the product of the automatic processing of stereoscopic images collected by the ASTER sensor on board the Terra spacecraft. The global DEM has a horizontal resolution of 1 arc-second (~30m) with coverage between 83°-N and 83°-S and comprises more than 1.5 million ASTER archived scenes acquired between 2000 and 2007. Vertical accuracies of the global DEM are estimated to be around ±20 m (Toutin, 2008) but this figure increases in rough mountainous terrain where RMS values of ±60 m are reported (Kääb, 2002). Furthermore, planimetric errors of ±50 m have been estimated in mountainous regions by Fujisada et al. (2005). Due to the reduced accuracy compared to the SRTM data combined with a lack of acquisition date information for specific regions, the ASTER GDEM will be applied as a secondary topographic data source for this study. Thus, it will only be utilised when SRTM data coverage is insufficient, such as for glaciers located outside of the SRTM spatial coverage or when large data voids remain in study areas. The ASTER GDEMv2 data were accessed through the USGS Earth Explorer data portal (<http://earthexplorer.usgs.gov/>).

3.2.2.2 *Optical Satellite Imagery*

3.2.2.2.1 Landsat 7 Enhanced Thematic Mapper+

Landsat 7 ETM+ tiles were selected for use during glacier delineation as recommended by Paul et al. (2009). The ETM+ images accessed through the USGS (<http://earthexplorer.usgs.gov/>) are L1T processed, meaning they come already georeferenced and orthorectified. The images consist of eight spectral bands with a spatial resolution of 30 metres for bands 1 to 7 and a resolution of 15 metres for the panchromatic band 8. Acquisition years for the selected tiles

range from 1999 to 2002 with the majority being from 2000 in order to coincide with the acquisition date of the SRTM data. Scenes with minimal cloud cover were selected from as close to the end of the summer melt season as possible where snow cover on non-glacial terrain is at a minimum to facilitate glacier boundary delineation.

3.2.2.3 *Glacier Inventory Data (ELA and Mass Balance)*

3.2.2.3.1 WGMS

Records of yearly fluctuations of mass balance and ELA have been systematically collated and published by the World Glacier Monitoring Service since 1967 as part of the Fluctuations of Glaciers series (Kasser, 1967; PSFG, 1973, 1977, 1985; WGMS, 1988, 1993, 1998, 2005, 2008, 2012). These publications have then been supplemented by less detailed biennial summaries in the Mass Balance Bulletin series (WGMS; [http:// www.geo.unizh.ch/wgms](http://www.geo.unizh.ch/wgms)). As well as yearly mass balance and ELA data, values of balanced-budget ELA (ELA_0) are calculated for a number of glaciers. This calculation, which represents the would-be ELA present on the glacier in steady-state conditions, was originally performed by Braithwaite and Müller (1980), based upon the correlation between ELA and mass balance (figure 3.2). It is calculated for a single glacier by regressing ELA data against mass balance records. The ELA_0 is extracted from the slope of the relationship where mass balance equals zero. With this in mind, the ELA_0 represents the anticipated elevation of the equilibrium line under balanced budget conditions.

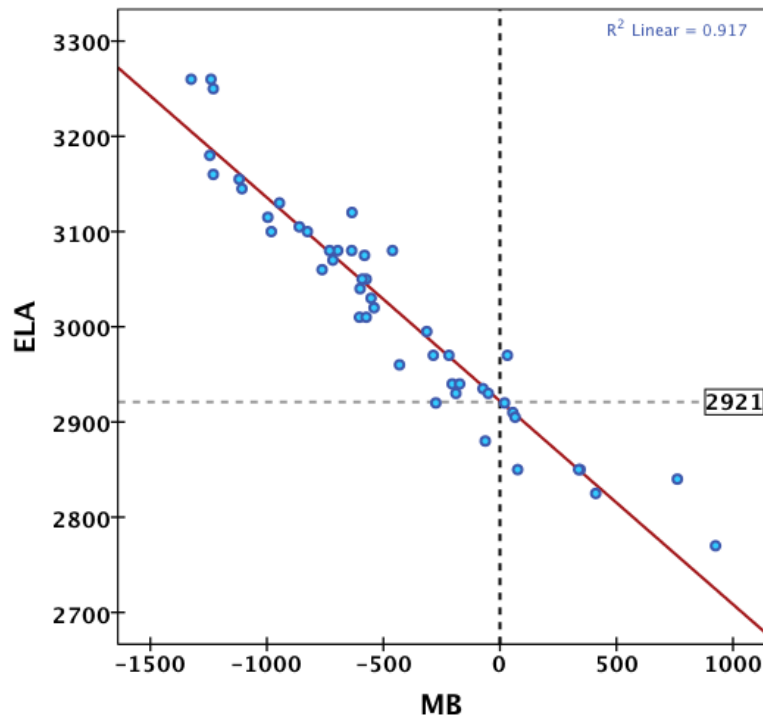


FIGURE 3.2 ELA₀ CALCULATION FOR HINEREISFERNER

The ELA₀, in this case 2921m.a.s.l., is calculated at the elevation at which the regression line intercepts MB=0 on the x-axis. The example utilises mass balance and ELA data recorded upon Hintereisferner between 1957 and 2000.

3.2.2.4 Glacier sample selection

Two different glacier sample sets were used to complete this chapter with each covered separately in the results section. The first sample of glaciers studied in the chapter were selected on account that they fulfilled the following criteria: Firstly, they are attributed with a minimum of 5 years of continuous mass balance and ELA data, and that the collection years for these data coincide with the acquisition date (± 2 years) of the DEM from which the glacier's topographic attributes are extracted. Glaciers with fewer than 5 years of continuous ELA and mass balance records are excluded as data for a single or few years could be misrepresentative. This is due to the fact that, unless proven to be representative, a single year's entry could be an extreme in annual variability, which are often observed in ELA and mass balance series (Braithwaite and Raper, 2010) (for example see figure 2.12). Secondly, the glacier's primary form must satisfy the definition of a "Valley" glacier as set out by the Global Land Ice Monitoring Service (GLIMS) (Rau et al., 2005) (Figure 3.3).

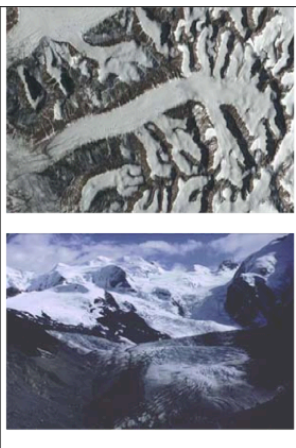
Valley glacier	<ul style="list-style-type: none"> • Accumulation area is clearly defined and limited by the topography • Ice free slopes normally overlook glacier surface • Follows a pre-existing valley 	Flows down a valley; the catchment area is well defined	<u>Excluded classification combinations:</u> <ul style="list-style-type: none"> - Cirque - Niche - Apron - Group 	
-----------------------	--	---	--	---

FIGURE 3.3 - VALLEY GLACIER CLASSIFICATION
(Extracted from the GLIMS glacier identification guidelines, Rau *et al.*, 2005)

Outlet glaciers draining ice caps, such as those on Norway’s Jostedalsbreen, are inappropriate for this study for a number of reasons. Most importantly the lack of clearly defined, topographically constrained accumulation areas means that there is not the driving force necessary for the transverse flow component to produce the concave transverse ice surface profile in the accumulation area. Similarly, the ablation area must be constrained by valley walls to enable the transverse convex surface to form. Furthermore, with no fixed upper margin there lacks a point against which glacier variables relating to elevation can be normalised (Raper and Braithwaite, 2009). Unfortunately this results in a significant number of Norwegian glaciers, with long mass balance and ELA histories, being unsuitable and thus excluded from this study.

Thirdly, only glaciers that terminate on land (Rau *et al.*, 2005) are included in this study. As a result tidewater glaciers and those that terminate and ablate via marine calving or dry terrestrial calving (cliff terminating) are excluded. This is because ice flux in such situations is greatly controlled by processes at or near the terminus and so the calving front demonstrates significant control over glacier dynamics where glacier flow regime changes and mass change can occur independently of climate perturbations, particularly in marine environments (Benn *et al.*, 2007; Howat *et al.*, 2005). Finally, only glaciers that display a clearly recognisable PCT will be included. This is due to the fact that glaciers with complex surface topography prevent the identification of a clear PCT. This is particularly pertinent when considering glaciers that contain single or multiple ice falls along their longitudinal profile (figure 3.4). Not only do icefalls

complicate the visual identification of PCTs, they may in fact maintain a degree of control over PCTs. Considering the importance of slope in PCT formation (see EQ 3), the regions of steep longitudinal slope with high longitudinal strain rates associated with icefalls may result in the formation of multiple PCT-like surfaces independent of the glacier's mass balance and climate (Nye, 1952). Table 3-1 displays a list of the 36 glaciers contained within the first sample and notes the associated Landsat tiles used to draw observations from each glacier. This dataset will be referred to as "Sample I".

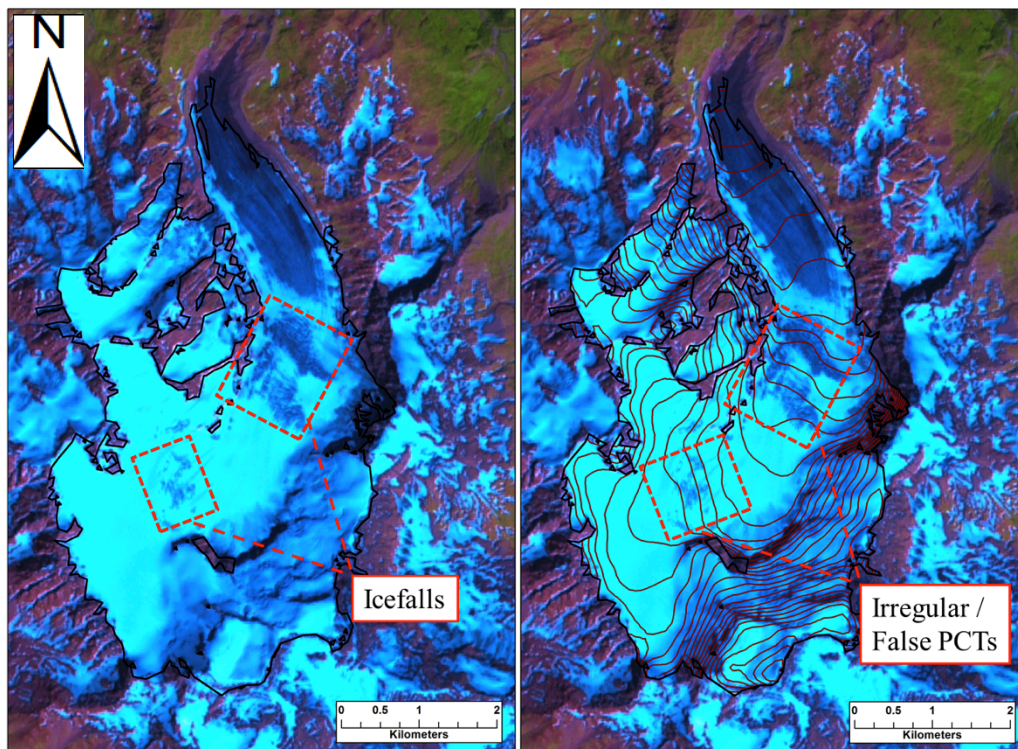


FIGURE 3.4 – SURFACE COMPLEXITY DUE TO ICEFALLS

The images highlight the impact of icefalls on identifying PCTs. Straightening of the surface contours can be observed upon Corbassière Glacier, in the Swiss Alps, where ice flows over localised steep sections in the longitudinal bed profile. (50m contours generated from SRTM DEM)

Landsat Scene Information (SPOT*)						
Name	Country	Latitude	Longitude	No. ELA record years	Path/Row	Acq. Date
Abramov	Kyrgyzstan	39°40'N	71°30'E	31	152/33	16/09/2000
Argentiere	France	45°58'N	6°56' E	5	195/28	25/07/1999
Blue	USA	47°49'N	123°41'W	40	047/27	22/09/2002
Chhota Shigri	India	32°20' N	77°50' E	5	147/38	15/10/2000
Djankuat	Russia	43°12'N	42°46'E	40	172/30	12/09/2000
Findelen	Switzerland	46°.00' N	7°.87' E	6	194/28	02/07/1999
Gebroulaz	France	45°.30' N	6°.63' E	5	195/25	30/07/2001
Golubina	Kyrgyzstan	42°27'N	74°30'E	23	151/30	06/08/1999
Gries	Switzerland	46°26'N	8°20'E	49	194/28	02/07/1999
Gulkana	USA	63°14'N	145°28'W	43	067/16	01/08/2002
Helm	Canada	49°58'N	123°00'W	32	12/305*	27/10/2008
Hinterisferner	Austria	46°48'N	10°46'E	58	192/27	28/07/2002
Jamtalferner	Austria	46°42'N	10°10'E	21	192/27	28/07/2002
Karabatkak	Kyrgyzstan	42°06'N	78°18'E	23	148/31	18/09/1999
Kesselwandferner	Austria	46°50'N	10°48'E	58	192/27	28/07/2002
Lemon Creek	USA	59°36'N	134°36'W	58	057/19	03/08/1999
Leviy Aktru	Russia	50°05'N	87°44'E	32	144/25	22/07/2000
Malavalle	Italy	46°.95' N	11°.20' E	9	119/27	26/08/2001
Marmaglacieraen	Sweden	68°05'N	18°41'E	20	197/12	31/07/2002
Midre Lovenbreen	Svalbard	78°.88' N	12°.07' E	31	220/03	26/07/2000
No. 125	Russia	50°06' N	87°42' E	30	144/25	22/07/2000
Ochsentaler	Austria	46°51'N	10°06'E	9	193/27	13/09/1999
Pasterzen	Austria	47°.10' N	12°.7' E	6	192/27	28/07/2002
Peyto	Canada	51°40'N	116°32'W	44	11/631*	29/08/2010
Rabots Glacier	Sweden	67°54'N	18°33'E	26	197/12	31/07/2002
Saint Sorlain	France	45°11'N	6°10'E	11	195/25	30/07/2001
Silvretta	Switzerland	46°51'N	10°05'E	51	194/27	02/07/1999
South Cascade	USA	48°22'N	121°03'W	45	046/26	14/08/2002
Storbreen	Svalbard	61°34'N	8°08'E	62	199/17	25/09/2000
Storglaciaren	Sweden	67°54'N	18°34'E	64	197/12	31/07/2002
Tasman	New Zealand	43°31'S	170°19'E	21	076/91	17/01/2001
TS.Tuyuksuyskiy	Kyrgyzstan	43°00'N	77°06'E	54	149/30	03/10/2002
Urumqi North	China	43°05'N	86°49'E	31	143/30	03/06/2002
Urumqi South	China	43°05'N	86°49'E	31	143/30	03/06/2002
White	Canada	79°27'N	90°40'W	47	09/004*	29/08/2008
Wolverine	USA	60°22'N	148°54'W	43	067/18	02/09/2002

TABLE 3-1 GLACIERS OBSERVED IN SAMPLE I

Because only a small number of glacier's have five years or more of associated ELA records, a second dataset ("Sample II") was used that enabled a proxy of ELA (Accumulation Area Ratio) to be compared to PCT_a. Sample II consists of 295 glaciers located in the Hindu-Kush and Karakorum mountain ranges. These regions were selected as observations of AAR values considered to be representative of long-term ELA for glaciers in the Hindu-Kush and Karakorum

have already been recorded and published (Scherler et al., 2011). Glaciers in sample II were selected upon the basis that they satisfied the same requirements as those in sample I (minus the need for five years or more of ELA records). A second sample was deemed necessary, as the 36 glaciers in sample I are predominantly simple basin glaciers and thus not representative of the wider variation in glacier characteristics that are present in the world's glacier population.

3.2.3 Digitized glacier outlines and attributes

In order to calculate glacier area in ArcDesktop, digitised glacier outlines were required. These were extracted semi-automatically using a well established threshold band ratio ($ETM+ch3/ETM+ch5$) (Paul et al., 2009; Svoboda and Paul, 2010). Areas of misclassification due to shadowing, supraglacial debris, open water and seasonal snow in the images were then manually corrected with the aid of aspect, slope and curvature layers generated from the SRTM data (Bolch and Kamp, 2006).

Information relating to glacier elevation (maximum, minimum and mid-range), surface slope and glacier length, was automatically extracted from either the SRTM or ASTER GDEM DEMs using a semi-manually digitized centreline. Following the methods recommended by Paul et al. (2009) the "maximum" glacier length was digitised. The SRTM / GDEM data were used to identify the highest point of the glacier surface, from here the flow-line was automatically digitised following the steepest downward gradient until the curvature of the glacier surface changed from concave to convex (PCT). From here the centerline was manually digitised along the central line of the trunk to the glacier terminus, ensuring that the polyline crossed perpendicular to the elevation contours (Paul et al., 2009).

3.2.4 PCT_a extraction

Elevation contours were generated at 25 metre intervals using the SRTM and ASTER GDEM data and layered upon the Landsat imagery. The PCT was visually identified as the contour that was most straight between the concave contours in the accumulation area and the convex contours in the ablation area. Identifying the PCT in this way enabled one to select the correct elevation

contour based on; the transfer of the contour lines from ice free terrain onto the ice surface, as recommended by Hess (1904), as well as take into account the overall curvature of the transverse surface profile, as recommended by Østrem (1966). To aid identification, a straight line was passed across the ice surface between the points at which the contour crossed the ice boundary in order to provide a reference against which the transverse ice surface contour was compared (figure 3.5). If multiple sequential straight contours populated the glacier surface, the contour that occurred first down glacier from the concave contours was considered to be the PCT in order to maintain a consistent approach across the glacier sample. A point was then placed upon the selected contour where it intersected the centre flow line (figure 3.5). The elevation of the point was then automatically extracted from the underlying DEM. Where the ice surface was characterised by small-scale perturbations by medial moraines, supraglacial debris or large melt water channels, identification of the broader transverse profile of the ice surface was made more difficult. To counter this problem, a 3x3 neighbourhood grid was passed over the raster in order to provide aggregated mean elevations for each grid cell and smooth the dataset to reduce the impact of smaller topographical variations. New contour lines were then generated using the smoothed DEM from which the PCT was then identified. However, it is important to note that irrespective of the PCT being identified using contours derived from smoothed DEM data, PCT_a was, in every case, extracted from the original DEM file.

It is also important to consider that PCT_a measurements will also be susceptible to errors contained within the DEM being used to identify the PCT. Accordingly, PCT_a measurements derived from SRTM data have an uncertainty of ± 9 m whilst the conservative uncertainty of ± 60 m is attributed to PCT_a measurements derived from the ASTER GDEM data.

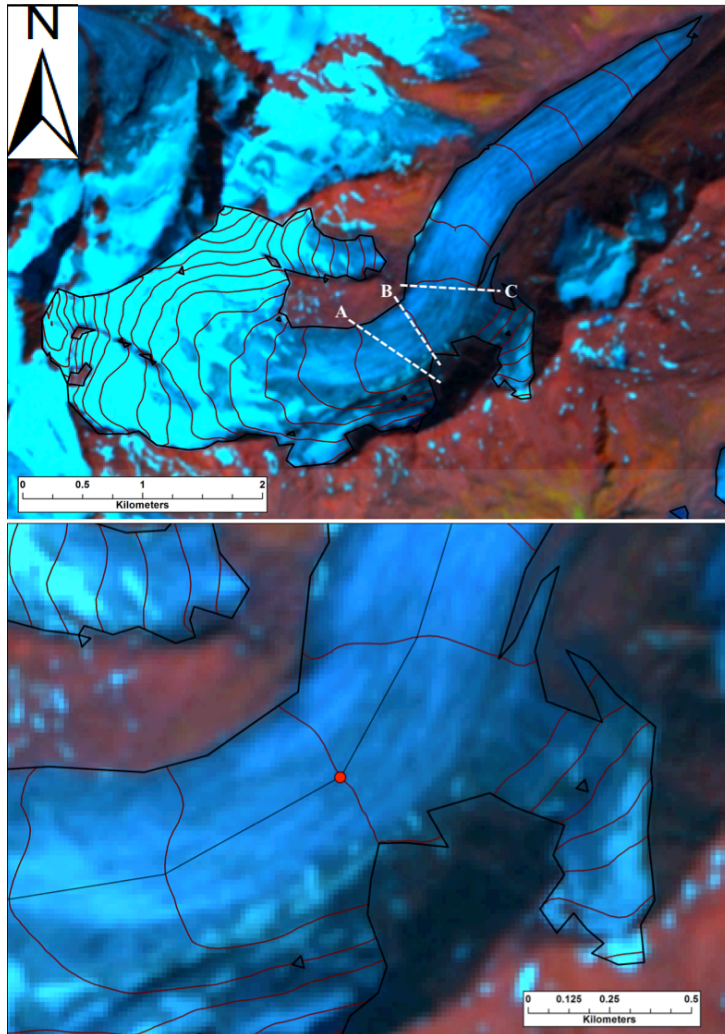


FIGURE 3.5 - PCT MAPPING AND EXTRACTION

Top: Identifying the straightest contour on Hintereisferner is assisted by passing a straight line through the points at which each contour crosses the ice margin.: A= Concave, B= Straightest, C= Convex. Bottom: Mapping of the straight contour (PCT) with a “Point” shapefile and the centreline intercept. (50m contours generated using SRTM data overlaying a FCC Landsat ETM+ image)

3.2.5 AAR and Proxy ELA calculations

Due to a lack of observational data, ELA values were calculated using Accumulation Area Ratios (AAR) for glaciers in sample II. Scherler et al. (2011) stated that AARs of 0.58 are representative for glaciers in the Hindu-Kush and Karakorum region. Similarly, Durgerov et al. (2009) recommended that an AAR of 0.58 should be applied when estimating the accumulation area for a glacier under steady state conditions. Accordingly, one can produce an estimate of a glaciers long-term ELA by calculating the minimum elevation of the accumulation area based upon a representative AAR.

In order to derive a proxy ELA using the previously published AAR value, glacier outlines were extracted using the semi-automated process presented in

section 3.2.3. The resulting glacier outlines were used as a “mask” in order to extract SRTM DEMs constrained to the coverage of each studied glacier. This was performed by clipping the DEM so that only elevation values that fell within the spatial boundary of each glacier were kept. The individual glacier DEMs were then divided into 100 elevation bands of equal area. Based upon the recommendation of Dyurgerov et al. (2009) and Scherler et al. (2011a), the elevation of the fifty-eighth sequential elevation band descending from the maximum ice elevation was recorded for each glacier producing an estimation of the minimum elevation of the accumulation area, based upon an AAR of 0.58.

3.3 Results

The following section presents observations of the relationship between PCT_a and ELA records for glaciers contained in sample I as well observations of the relationship between PCT_a and proxy ELA measurements recorded in sample II.

3.3.1 PCT_a vs ELA

NAME	PCT _a (M.A.S.L)	PCT _p	Same Yr ELA (M.A.S.L)	5Yr Mean ELA (M.A.S.L)	Full record Mean ELA (M.A.S.L)	ELA ₀ (M.A.S.L)	Area (km ²)	Length (m)	Mean Surface slope (degrees along the centre-line)	Maximum glacier elevation (m.a.s.l.)	Minimum glacier elevation (m.a.s.l.)
Abramov	3950 ±9	0.30	4130	4244	4231	4150	23.29	8458	12	4650	3650
Argentiere	2700 ±9	0.62	2698	2698	2698	-9999	13.26	9578	24	3417	1540
Blue	1537 ±9	0.21	1500	1703	1703	-9999	5.88	4168	26	2300	1331
Chhota Shigri	4725 ±9	0.37	5170	5094	5094	-9999	11.99	8563	20	5546	4245
Djankuat	3000 ±9	0.30	3400	3265	3213	3191	1.77	2623	35	3619	2734
Findelen	3025 ±9	0.49	3200	3200	3200	-9999	13.36	7365	16	3570	2493
Gebroulaz	2975 ±9	0.39	2913	3101	3101	-9999	3.24	4019	21	3452	2670
Golubina	3650 ±9	0.40	3750	3867	3874	3804	5.35	4888	19	4163	3301
Gries	2600 ±9	0.19	3037	3068	2942	2832	6.64	5253	18	3329	2425
Gulkana	1684 ±9	0.44	1704	1802	1773	1727	17.28	8277	21	2345	1161
Helm	1925 ±60	0.40	1945	2033	2086	2002	1.04	2022	16	2124	1802
Hinterisferner	2875 ±9	0.35	3050	3091	3074	2921	6.63	6809	18	3655	2460
Jamtalferner	2750 ±9	0.48	2765	2879	3004	2761	3.05	2729	26	3107	2419
Karabatkak	4075 ±9	0.49	3950	3920	3860	3860	23.35	12954	13	4651	3521
Kesselwandferner	3000 ±9	0.47	3120	3140	3134	3107	3.99	3722	16	3301	2730
Lemon Creek	1050 ±9	0.47	1050	1190	1190	1009	11.57	5958	13	1438	712
Leviy Aktru	3175 ±9	0.41	3240	3233	3184	3157	5.80	5711	27	3977	2611
Malavalle	2750 ±9	0.28	3042	3081	3081	2930	6.65	4426	18	3328	2530
Marmaglacieren	1575 ±9	0.65	1670	1619	1613	1572	3.49	3269	15	1717	1312
Midre Lovenbreen	250 ±9	0.35	425	409	399	300	5.41	4237	21	653	37
No. 125	2975 ±9	0.24	3240	3285	3222	3206	1.14	2740	34	3608	2771
Ochsentaler	2775 ±9	0.54	2850	2899	2937	2847	2.38	2301	26	3041	2465

Mountain Glacier Health Signatures Stored in Their Three-Dimensional Ice Surface Geometry
PCT and Existing Glacier Health and Climate Measures

Pasterzen	2400 ±9	0.26	2920	2920	2920	-9999	15.56	8364	15	3292	2086
Peyto	2550 ±60	0.45	2503	2709	2702	2610	12.12	4829	17	3000	2176
Rabots Glacier	1350 ±9	0.42	1411	1441	1415	1369	3.52	3891	19	1723	1077
Saint Soralain	2825 ±9	0.20	2969	2953	3026	-9999	3.02	3014	29	3417	2680
Silvretta	2625 ±9	0.28	2727	2825	2800	2766	2.99	2833	23	3076	2453
South Cascade	1925 ±9	0.49	1840	1911	1965	1892	2.02	2911	21	2223	1637
Storbreen	1525 ±9	0.21	1650	1794	1751	1724	2.77	2898	26	2002	1400
Storglaciaren	1400 ±9	0.35	1405	1465	1480	1462	3.06	3571	24	1848	1161
Tasman	1550 ±9	0.38	1748	1758	1814	1790	109.66	29125	11	2953	704
TS.Tuyuksuyskiy	3725 ±9	0.44	3780	3884	3823	3740	2.58	2859	28	4098	3429
Urumqi North	4050 ±9	0.36	4048	4041	4010	4028	0.71	1832	35	4450	3828
Urumqi South	3950 ±9	0.37	4090	4100	4088	3950	1.22	2102	25	4264	3763
White	900 ±60	0.55	1264	1099	1026	899	40.70	14675	16	1551	97
Wolverine	1012 ±9	0.49	1253	1229	1171	1152	17.07	7580	21	1633	424

TABLE 3-2 - ELA AND PCT MEASUREMENTS FROM SAMPLE 1
Data pertaining to PCT, ELA and Glacier characteristics during the year of observation (2000). Values of -9999 are indicative of data voids.

	PCT _p (M.A.S.L)	PCT _a - ELA 5 yr mean (m)	PCT _a - ELA full record mean (m)	PCT _a - ELA ₀ (m)
Mean	0.39	-164	-171	-82
Std. Error	0.01	25	19	16
Std. Deviation	0.11	152	113	87
Range	0.45	890	560	273
Max	0.65	370	39	41
Min	0.19	-520	-520	-232

TABLE 3-3 - ELA AND PCT SUMMARY

Figure 3.6 highlights the relationship between measured PCT_a and the mean ELA calculated using the full set of ELA records, PCT_a and the 5 year mean ELA and PCT_a and the balanced budget ELA_0 for 36 glaciers in plots A and B and 28 glaciers in plot C respectively. The plots were generated using the data in table 3-2.

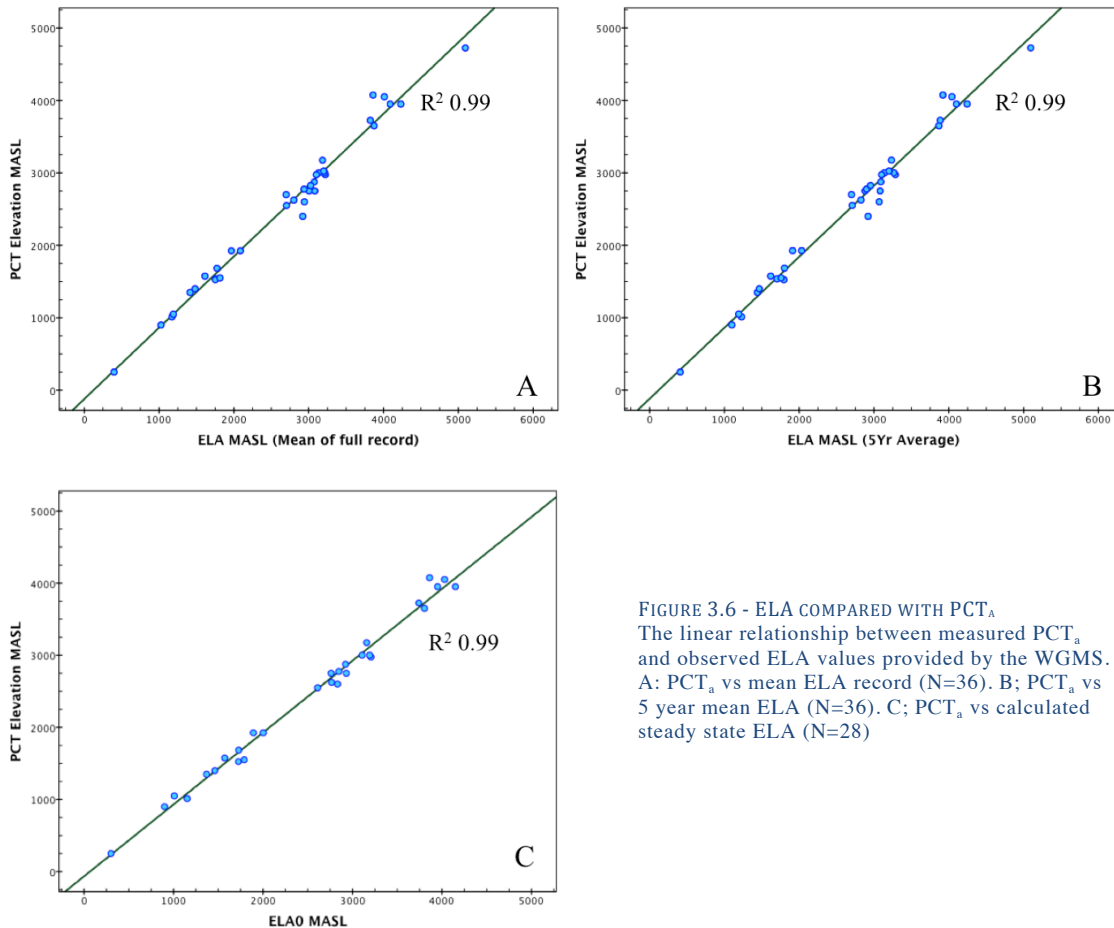


FIGURE 3.6 - ELA COMPARED WITH PCT_a
 The linear relationship between measured PCT_a and observed ELA values provided by the WGMS. A: PCT_a vs mean ELA record (N=36). B: PCT_a vs 5 year mean ELA (N=36). C: PCT_a vs calculated steady state ELA (N=28)

The plots reveal very strong, positive correlations ($r^2 = 0.99$) between PCT_a and the ELA variables, with a p-value of 0.01. This suggests that PCT_a is reliably and robustly related to the ELA. When compared with the full and 5 year mean ELA records in figure 3.6 A and B, PCT_a is recorded on average 171 and 164 metres below the ELA respectively. However, this offset is reduced considerably when comparing PCT_a with the calculated ELA for steady state conditions, ELA_0 (graph C), where the average difference between the two variables is -82 metres (Table 3-3). These offsets, which equate to ~20% of the elevation range of each glacier, between PCT_a and ELA for both the 5 year mean and total series mean ELA values correspond well with the results published by Leonard and Fountain (2003) who also identified that on each glacier, the offset between

PCT_a (Hess Altitude) and averaged ELA series records equated to 20% of the glaciers elevation range.

However, the strong relationship between the variables depicted in figure 3.6 is to be expected due to the large variation in elevation ranges observed in the sampled glaciers. This can be demonstrated by the fact that the mean elevations of the sampled glaciers range from 282 m.a.s.l. for Midre Lovénbreen in Svalbard to 4808 m.a.s.l. for Chhota Shigri in India. As a result it is highly likely arbitrarily selected altitudes on each glacier would still produce a high correlation with the ELA records. This issue has been discussed by both Leonard and Fountain (2003) and Braithwaite and Raper (2010) when attempting to estimate ELA using morphological and inventory data.

Leonard and Fountain (2003) recommend that the data be normalised using EQ 4 or a variant thereof (p. 35). The result of this normalising process is a value between 0 and 1 that represents the proportional elevation of the ELA or PCT within the individual glacier's elevation range with 0 at the snout and 1 at the maximum ice elevation.

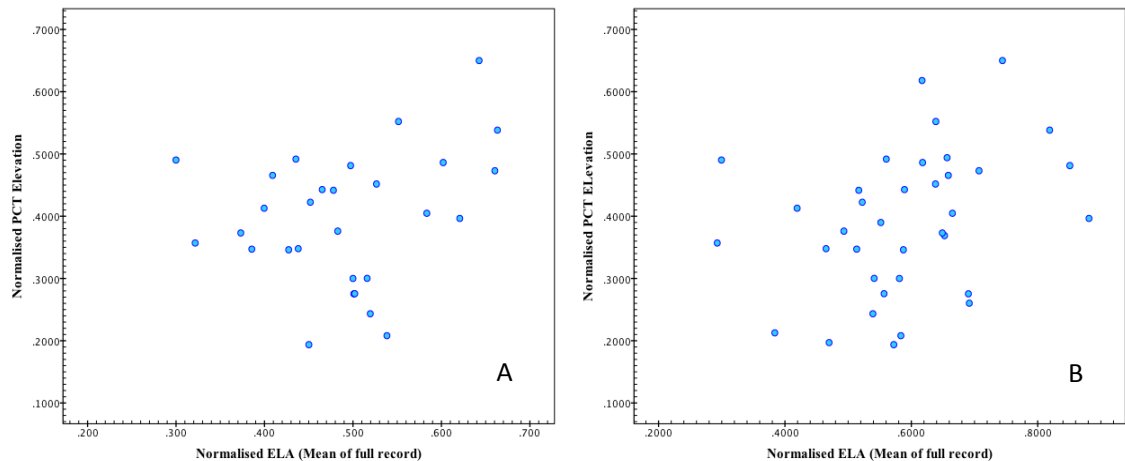


FIGURE 3.7 - NORMALISED PCT COMPARED TO NORMALISED ELA
THE RELATIONSHIP BETWEEN PCT_a AND THE MEAN OF THE FULL ELA RECORD (A) AND THE RELATIONSHIP BETWEEN PCT_a AND ELA₀ WHEN NORMALISED USING THE SAME APPROACH AS LEONARD AND FOUNTAIN (2003)

Figure 3.7 displays the relationship between PCT and ELA when the data are normalised using EQ 4. Once normalised in this manner, the strength of the relationship between the two variables is reduced to the point where no visible relationship is observed. Leonard and Fountain (2003) observed the same effect in their study when the strength of the relationship between the Hess altitude

and ELA reduced from an r^2 value of 0.99 to 0.10 after normalising their data. They attributed this extreme reduction in the strength of the relationship to bias caused by sampled glaciers with short time series of ELA data. In response they omitted glaciers with time series of ELA data of less than fifteen years. However, a closer examination of the method used to normalise their data may reveal an alternative explanation for why the relationship between their Hess Altitude measurements and ELA records was weakened.

Normalising PCT and ELA data using EQ 4 is necessary when knowledge of their proportional position on the glacier is desired. However, comparing the relationship between the resulting normalised outputs is inappropriate. By assessing the difference between two variables (PCT_a and ELA) that are normalised using elevation range, the assumption is made that the difference between the two variables is proportionate to the glacier elevation range. It is therefore assumed that the difference between PCT_a and ELA will be greater on glaciers with a larger elevation range than it will be on those with smaller elevation ranges. However, when observing the results from this study this is not necessarily the case. No statistically significant correlation could be identified between PCT_a and ELA offset and glacier elevation range. Thus by normalising the difference between PCT_a and ELA by glacier elevation range, the relatively small range of recorded offsets between PCT_a and ELA observed across the sample compared to the large variation in glacier elevation ranges could result in a relatively fixed offset between PCT_a and ELA being overlooked. For example, the data in table 3-2 display that PCT_a on Storbreen is located 226 m beneath the mean ELA, resulting in an elevation offset that is equivalent to 37% of the glaciers elevation range of 602 m. On the other hand, PCT_a on Tasman glacier is 263 m beneath the mean ELA, however when normalised by the glacier's elevation range, this accounts for an offset equivalent to only 11% of Tasman Glacier's elevation range. Hence by normalising the variance between PCT_a and ELA using glacier elevation range, the result suggests that the proportional variation between the PCT_a and ELA on Tasman glacier is smaller than the percentage offset on Storbreen when in fact actual variation is smaller on the latter.

Figure 3.8 highlights the relationship between the PCT and ELA information when normalised by maximum ice elevation only. The PCT_a , ELA and ELA_0 are normalised by subtracting each variable's observed value from the maximum ice elevation. By comparing the difference between maximum ice elevation and PCT_a with the difference between maximum ice elevation and ELA records, one is able to quantitatively assess the strength of the linear relationship between PCT_a and ELA (and ELA_0) whilst nullifying the impact of the glacier's broader elevation.

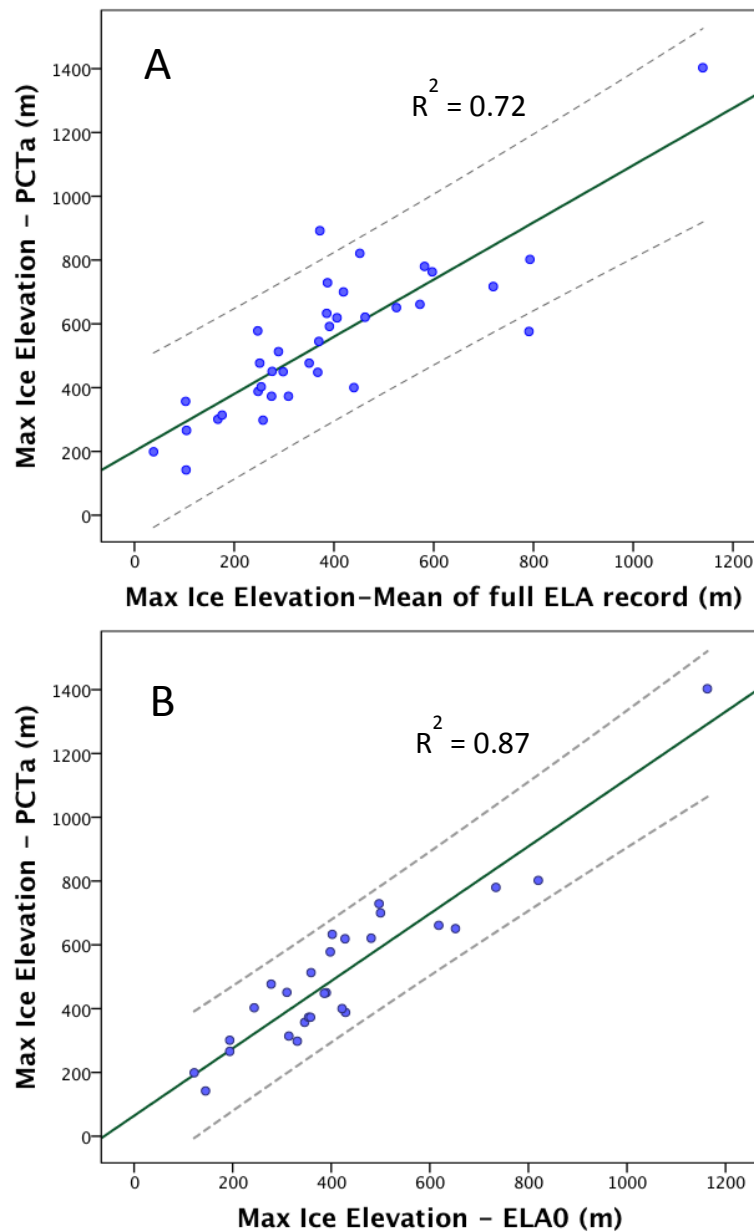


FIGURE 3.8 - NORMALISED PCT VS ELA NORMALISED USING MAX GLACIER ELEVATION

A: Normalised PCT elevation vs normalised mean of full ELA record (N=36). B: Normalised PCT elevation vs normalised ELA_0 (N=28). Normalised by dividing PCT and ELA elevation by the maximum glacier elevation. Dashed lines represent 95% confidence intervals

The results demonstrate that a strong, positive linear relationship remains between the PCT_a and ELA values after normalising for glacier elevation. The strength of the relationship is significantly greater than the r^2 0.59 that had previously been identified by Leonard and Fountain (2003) from their sample of 17 glaciers. The r^2 of 0.87 for the linear relationship between PCT_a and calculated steady state ELA is particularly high and will be discussed in detail later in the chapter.

Table 3-2 highlights an anomaly where the PCT on Karabatkak is located 155 m and 215 m above the average ELA and ELA₀ respectively. Given that the remainder of the sample display PCT_a very near to or below the observed ELA, this was initially concerning. However, a closer analysis of the health information associated with Karabatkak revealed the unusual situation where ELA and mass balance, along with AAR and mass balance, display no correlation (figure 3.9). This has also been identified by Dyurgerov et al. (2009) who attributed the lack of a relationship between mass balance and ELA/AAR to the complex basin topography where snow accumulation patterns show no clear dependencies on elevation. As a result the relationship between PCT_a and ELA may be unreliable and consequently data pertaining to Karabatkak are removed from further analysis.

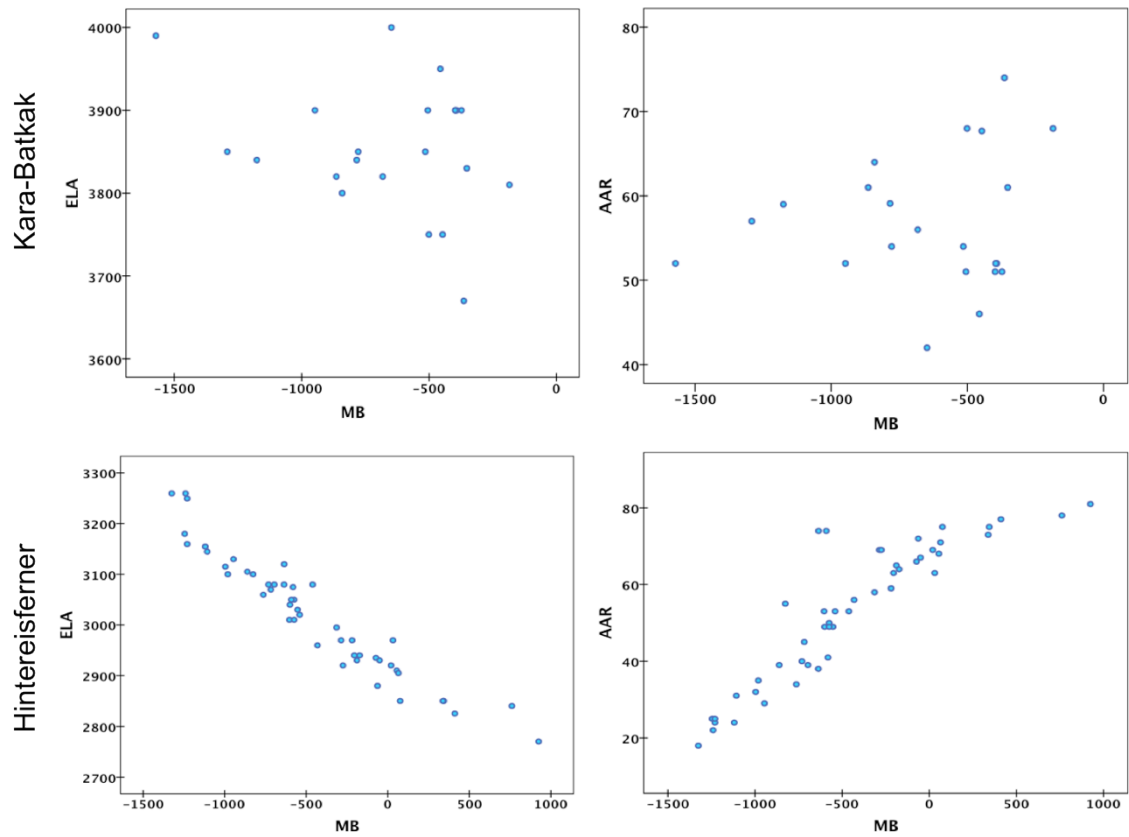


FIGURE 3.9 ELA/AAR vs MB ON KARABATKAK AND KINTEREISFERNER
The non linear or lack of relationship between ELA and mass balance (top left), and AAR and mass balance (top right) on Kara-Batkak glacier. For comparison: the strongly linear relationship between the glacier-climatic variables on Hintereisferner.

3.3.2 PCT Derived AAR vs AAR0 (WGMS)

PCT derived AAR estimates were extracted from the DEM using the outlines of the glaciers present in sample I. The derived AAR value was calculated based upon the assumption that the PCT represents the boundary between the accumulation and ablation areas. Accordingly, the glacier area above PCT_a was divided by total glacier area in order to derive the accumulation area ratio. As with the ELA₀ records the WGMS also publish calculated steady state AAR (AAR₀) estimates. The relationship between PCT derived AAR and the WGMS's AAR records can be seen in figure 3.10.

Although a linear relationship can be observed, it is significantly weaker than that observed between PCT and ELA with r^2 values of 0.18 and 0.36 for average AAR and AAR₀ respectively. This poor correlation is likely due to the impact of varying hypsometric curves throughout the glacier sample.

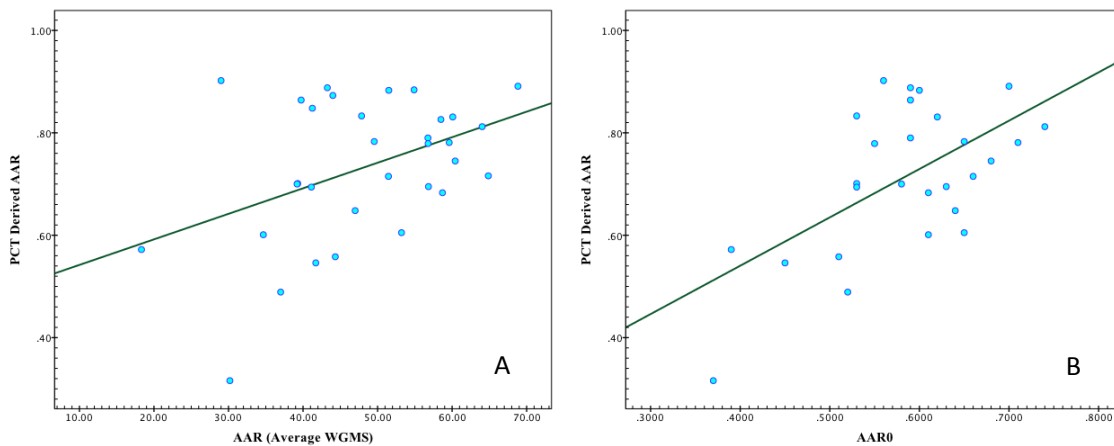


FIGURE 3.10 - PCT DERIVED AAR VS WGMS DERIVED AAR
A: PCT derived AAR vs average AAR calculated from WGMS records. B: PCT derived AAR vs steady state AAR₀ published by WGMS.

3.3.3 PCT vs proxy ELA

The following section displays the observations of the relationship between PCT_a and proxy ELA records derived from AAR values for glaciers in sample II.

Figure 3.11 displays the relationship between PCT_a and proxy ELA extracted from regional AAR values. The Proxy ELA values were extracted from SRTM data based upon a regional AAR value of 0.58 for the central Karakorum as reported by Scherler et al. (2011a) and recommended by Dyurgerov (2009). Graph A displays a strong linear relationship for the data between the two variables. The data pertaining to glaciers in sample II have been normalised using the same approach used for sample I, where the plots reveal the elevation offset between the maximum ice elevation and the recorded PCT_a and ELA elevations. Furthermore, in order to identify whether the presence of supraglacial debris has an impact on the relationship between PCT_a and AAR derived ELA, glaciers that were characterised by over 20% supraglacial debris coverage were extracted and the analysis repeated for both debris mantled and debris free glaciers in sample II (figure 3.11B and figure 3.11C). The results show that the strength of the relationship between PCT_a and AAR derived ELA is weaker upon glaciers that have more than twenty percent of their surface area covered by debris (figure 3.11B) compared to the same relationship observed upon debris-free glaciers (figure 3.11C).

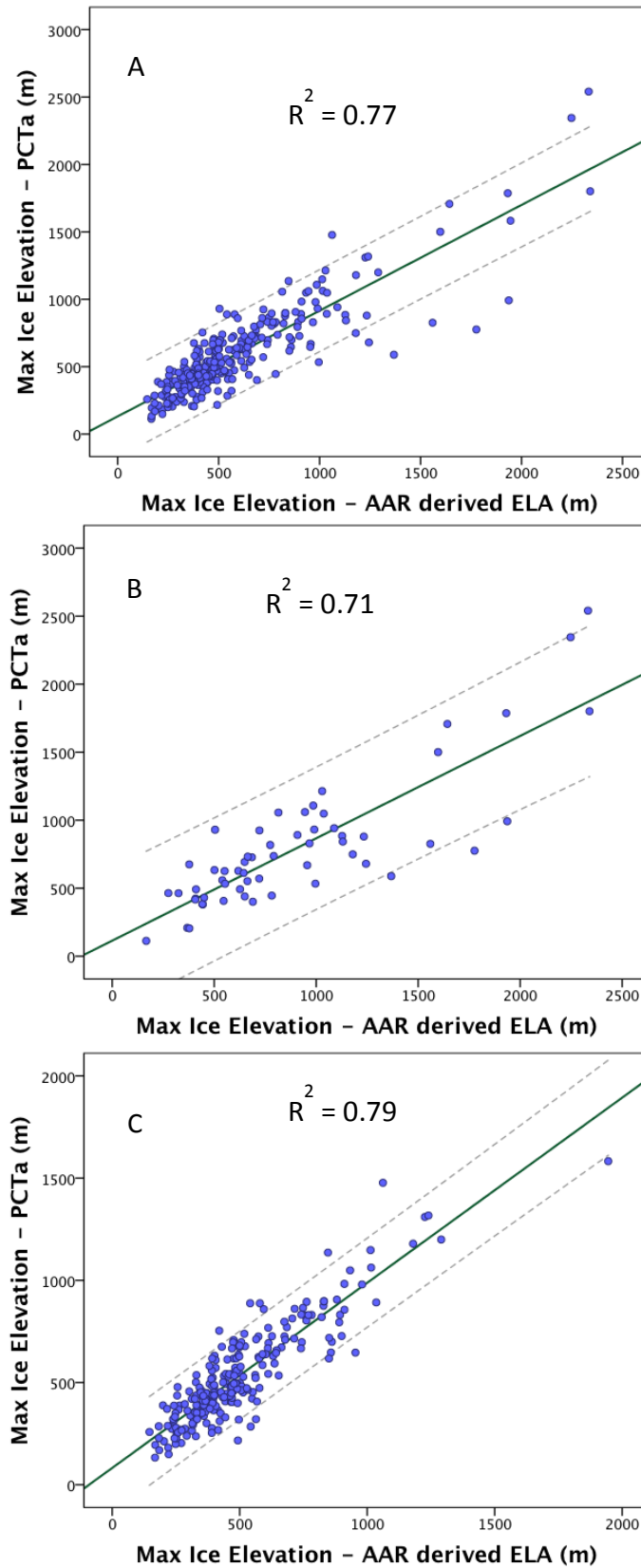


FIGURE 3.11 - PCT VS AAR DERIVED ELA IN THE HINDU KUSH – KARAKORUM
A: Normalised PCT elevation vs Normalised AAR derived ELA for entire sample (N=295). B: Normalised PCT elevation vs Normalised AAR derived ELA for glaciers with heavy debris mantles (N=58). C: Normalised PCT elevation vs Normalised AAR derived ELA for glacier with <20% surface debris mantle (N=237).

	<i>DEBRIS FREE</i>		<i>DEBRIS MANTLED</i>	
	PCT_p	PCT_a- AAR DERIVED ELA (M)	PCT_p	PCT_a- AAR DERIVED ELA (M)
MEAN	0.44	-35	0.54	110
STD. ERROR	0.01	7	0.02	38
STD. DEVIATION	0.14	111	0.14	288
RANGE	0.71	778	0.59	1426
MAX	0.85	360	0.84	1000
MIN	0.14	-415	0.25	-426

TABLE 3-4 SUMMARY STATISTICS FOR PCT AND AAR DERIVED ELA.

The table provides descriptive statistics for the PCT_p upon both debris-mantled and debris-free glaciers as well as information concerning the elevation difference between PCT_a and AAR derived ELA on the debris-free and debris-mantled glacier samples.

3.4 Discussion

The results in table 3-2 show that the average PCT_p on each glacier surface is 0.39. This observation is the first indicator that supports the theoretical assessment that the PCT is a function of mass balance (Hooke, 2005). This is because even before comparing PCT_a to observed ELA records, a mean PCT_p value of 0.39 coincides with recommended THAR (Terminus to Headwall Altitudinal Ratio) values that have been used to estimate long term ELA for contemporary and reconstructed glaciers (Benn and Lehmkuhl, 2000; Benn et al., 2005; Osmaston, 2005; Torsnes et al., 1993). Secondly, the small standard deviation in PCT_p across the dataset of 0.11 suggests that glacier specific characteristics such as longitudinal slope, hypsometry, aspect, size and basin geometry, that vary across samples, have only a minor impact upon PCT position. Thus, it is rational to assume that the PCT and its positioning are a function of a higher order control with the PCT_p being the result of the complex interaction between climate forcing (mass balance), ice flow dynamics and the topographic setting of each glacier. Hence, given that glacier length, area and slope are ultimately functions of mass balance and climate, the PCT appears to be controlled by the same driving factors, rather than being the result of individual glacier specific characteristics.

The strong relationship between PCT_a and the mean of the observed ELA data series displayed in figures 3.6 (A, B) and 3.8 (A) highlights that the PCT is closely related to the ELA in a linear fashion. Interestingly, the strength of the relationship between the variables in this study is considerably more robust,

particularly when normalised, than that observed in Leonard and Fountain's (2003) results ($r^2 = 0.59$). Initially this was thought to be due to alternative method used here to normalise the data for elevation effects. However, when comparing the RMS values for the regressed relationship between the raw values from both studies, the results showed lower RMS error here (129) compared to Leonard and Fountain's data (137). As a result, the increased robustness of the relationship here was attributed to the more rigorous approach taken in selecting appropriate glaciers for the study. Leonard and Fountain's study utilised a number of glaciers inappropriate for PCT-related studies. For example, those draining the Hofsjökull ice cap in Iceland and Jostedalbreen ice cap in southern Norway are unsuitable as they do not satisfy the conditions required for climate driven PCT generation (section 2.2.3).

However, despite the strong correlation between PCT_a and the observed ELA data, a clear offset was identified between the two variables. On average PCT_a was 171 m beneath the ELA, which equates to an offset of 20% of the glaciers' elevation range across the sample (table 3-2). This offset parallels the findings of Leonard and Fountain who also identified an offset, that equated to around 20% of each sampled glaciers' elevation range, between the Hess altitude and ELA across their sample. They proposed two possible reasons for this offset. Firstly, they identified, as was done here in section 2.3.1, that the PCT (Hess) is expected to occur down glacier of the ELA according to EQ 3 (Hooke, 2005). This is due to the fact that when $b_n = 0$, w_s must be negative and therefore ice is flowing downward into the glacier in order to balance both sides of the equation. Accordingly the physical controls that govern glacier flow, state that the mass balance derived ELA must then be located across a concave section of the glacier surface. As a result, the flat contour, where $w_s = 0$, must be located down-glacier in the upper ablation area. However, as well as the expected offset identified by Hooke (2005), another likely cause of the disparity is the slow response of the glacier flow-field in adjusting to climate perturbations compared to the rapid adjustment of the ELA in response to the same forcing (Oerlemans et al., 1998; Raper and Braithwaite, 2009; Wal and Wild, 2001).

As a result, contrary to the recommendation of Leonard and Fountain (2003), it is stated here that PCT_a should not be used to estimate contemporary ELA

values due to the likely influence of the lagged response of glacier flow to climate forcing. This then leads one to consider the usefulness of the PCT in the monitoring of glacier health. Despite the problem of lags in dynamic response preventing the use of the PCT_a as an estimator of modern-day ELA, the robust relationship between the two measures suggests that the PCT may relate to *past* steady state conditions of the glacier. This idea is given credence when observing the relationship between PCT_a and calculated values for steady state ELA (ELA₀).

Figure 3.6 (C) and 3.8 (B) display the relationship between PCT_a and calculated balanced budget ELA using the raw and normalised data respectively. The ELA₀ value was taken from WGMS publications but are essentially produced by regressing ELA data against mass balance records on individual glaciers (Braithwaite and Raper, 2010) and calculating the balanced budget ELA from the resultant regression equation between the two (figure 3.2). Thus, the ELA₀ represents the elevation on the glacier surface at which the ELA would locate in order to maintain a balanced budget for that glacier and thus maintain its current area and volume distribution. Consequently, the results displayed in figure 3.6 are interesting because they reveal that the PCT_a is more robustly related to the calculated ELA₀ on glaciers across the sample than for the mean observed ELA values. On average the PCT_a was only 82 m lower than ELA₀, which equated to an offset of only -10% of the glacier elevation range. This 82 m variance could, to some extent, be attributed to the expected offset proposed by Hooke (2005). When considering the fact that the majority of the world's monitored glaciers are experiencing continued negative mass balance (Dyurgerov et al., 2002; Dyurgerov and Meier, 2005; Meier et al., 2003; Meier et al., 2007), the close relationship between PCT_a and ELA₀ compared with the larger variation between PCT_a and observed contemporary ELA values, suggests that the PCT represents ice flow-field organisation/structure from a time when the glacier was closer to equilibrium. As a result, there is the potential to assess the degree to which measured ELA values have departed from PCT_a values in order to gauge the extent to which glacier flow dynamics are out-of-sync with current climate. This will be discussed in greater detail in the following section.

Considering the strength of the correlation between PCT_a and ELA records, the weak relationship between PCT derived AAR and the WGMS's AAR data (AAR_0 and mean observed AAR) displayed in figure 3.10 were at first surprising. However, the lack of a correlation can be explained due to the nonlinear variation of AAR with elevation change. As discussed by Dyurgerov et al. (2009) glacier areal distribution varies non-linearly with elevation and a dramatic steepening in the hypsometric curve of glacier area is observed to occur close to the long-term equilibrium line altitude (Dyurgerov et al., 2009; Pedersen and Egholm, 2013). As a result, the varying hypsometric characteristics and size of the sampled glaciers mean that large differences between PCT derived AAR and the WGMS's AAR observations are likely to occur even when the difference between PCT_a and ELA is small. Nonetheless, given the strong relationship between PCT_a and ELA_0 , one is justified in stating that the PCT can be used to calculate a dynamically-based steady state AAR. The calculation of a PCT based AAR (AAR_{pct}) would consider PCT_a to be the lower boundary of the calculated steady state accumulation area. The AAR_{pct} could then be used as a reference point with which modern day observations of AAR are compared.

The results presented in figure 3.11, which were generated using observations from sample II, reveal that PCT_a remains strongly correlated to the proxy ELA despite the much larger sample size ($n=295$) and wider variation in glacier characteristics found in this analysis compared to that of Leonard and Fountain (2003). This suggests that the relationship between PCT_a and ELA holds true for simple valley glaciers, compound basin glacier and extremely large compound basins type glaciers characterised by dendritic networks of tributary tongues. Analysis of the data revealed an average offset between PCT_a values and the proxy ELA_0 derived from calculated regional AAR values of 0.58 (Dyurgerov et al., 2009; Scherler et al., 2011a) of -6m. However, this reduced offset compared to that identified between PCT_a and observed ELA is unlikely to be due to increased robustness in the relationship. It is much more likely that ELA values are underestimated when calculated using an AAR value of 0.58. Secondly, AAR values are likely to vary greatly across the region as the sample is populated by a large number of glaciers with varying characteristics displaying heterogeneous responses to climate forcing (Fujita and Nuimura, 2011; Scherler

et al., 2011b). This is reflected by the higher standard deviation (172 m) of the observations of the elevation offsets recorded between the PCT_a and proxy ELA across sample II. Nevertheless, it is reassuring to observe that mean PCT_p values of 0.44 across the sample of debris-free glaciers are very similar to those observed in sample I and recorded in table 3-2. The small variation in PCT_p across the sample ($\sigma = 0.1$) suggests that PCT_x and PCT_a are not dependent upon glacier specific characteristics such as surface slope, glacier size, aspect and basin geometry. This supports the belief presented here that climate is the dominant control over glacier surface geometry.

Another positive outcome from the Hindu Kush – Karakorum data is the observation that debris cover appears to have only a minor impact on the location of the PCT. While the presence of debris cover may impact the relationship between PCT_a and AAR derived proxy ELA (figure 3.11 B), it can be accounted for owing to the fact that the PCT was compared to ELA values derived from a measure of glacier area distribution with elevation. Where glacier snouts are covered by a heavy debris mantle, the underlying ice is shielded from insolation (Nakawo and Rana, 1999). As a result, ablation is reduced and this can enable glacier snouts under thick debris mantles to remain at lower, warmer elevations down valley compared to debris free neighbouring glaciers (Anderson, 2000). However, observations have highlighted the fact that glacier snouts often stagnate beneath thick debris mantles and in some cases should no longer be classified as part of the active glacier system (Luckman et al. 2007; Quincey et al., 2009; Scherler et al., 2011b). Thus the consequence of debris-mantled glaciers “extending” to lower elevations is that this artificially lowers the elevation coincident with the boundary of the 0.58 AAR. This is evidenced in table 3-3 which shows that PCT_a on debris-mantled glaciers are on average 110 m higher than the AAR derived ELA, compared to PCT_a being 35 m lower than the AAR derived ELA on debris-free glaciers. Furthermore, table 3-3 exposes the small control that debris cover exerts over PCT location where PCT_p increase by only 0.1 from 0.44 on debris glaciers to 0.54 for debris-mantled glaciers. This is a welcome outcome when one considers that other glacier indices recommended for glacier health monitoring such as median, mean and mid-range elevation (Braithwaite and Raper, 2010; Kern and László, 2010; Osmaston 2005; Rea, 2009) are influenced by debris covered glaciers as

observed here. The apparent immunity of the PCT to debris effects is then even more important when taking into account that debris covered glaciers populate every mountain chain in the world (Zemp and van Woerden, 2008) and that debris covers have been observed to be increasing over time (Ageta et al., 2000; Stokes et al., 2007).

3.5 Implications for glacier/climate synchronicity assessment

Given the strong correlation between PCT_a and ELA_0 , it is fair to assert that the PCT and its location are more likely to reflect flow dynamics governed by mass balance regimes that were prevalent when the glacier was closer to being in equilibrium. Accordingly, as climate has warmed and mass balance trends have become increasingly negative, ELA values have responded faster than the glacier flow-field and resulting changes in PCT_a or PCT_x . Consequently, there is the possibility that one can assess the degree to which current glacier dynamics are out of sync with contemporary climate forcing as evidenced by ELA observations. The results in figure 3.12 reveal the difference in elevation between PCT_a and ELA_0 for each as a percentage of that glacier's elevation range. It is suggested here that knowledge of the offset between PCT_a and ELA_0 can provide information concerning the degree to which each glacier is out of sync with current climate forcing. This interpretation is based upon the assumption that under steady state conditions, PCT_a will locate close to the long-term ELA. The graph reveals that there is substantial variance in the proportional degree of the asynchronous response of glaciers to climate forcing. This supports recent observations that glaciers respond heterogeneously and non-linearly to climate forcing where response mechanisms can vary dramatically over relatively small geographic regions (Braithwaite et al., 2012). For example, the range of offset values between PCT_a and ELA_a displayed by Hinterisferner, Jamtalferner, Ochentaler and Pasterzen vary drastically despite the fact they are all located in the Austrian Alps.

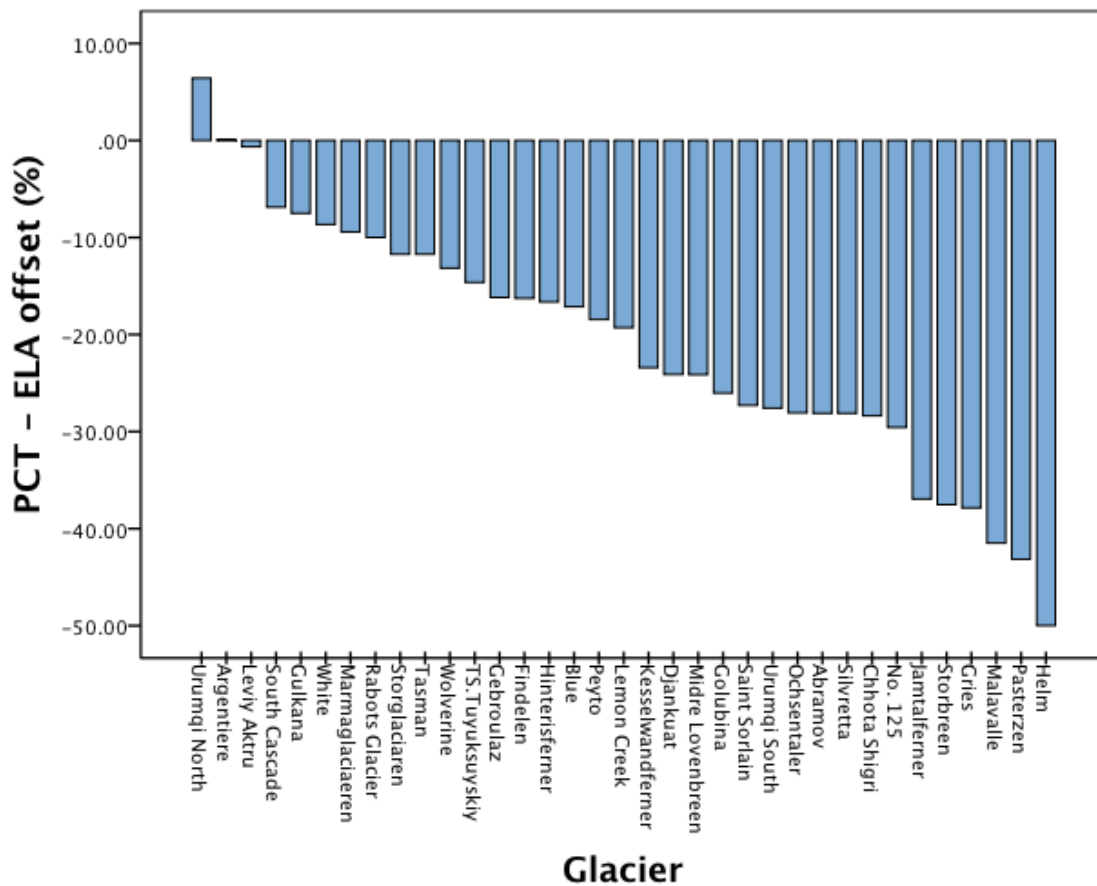


FIGURE 3.12 - PCT VS ELA OFFSET (PERCENTAGE)

In 2009 Dyurgerov et al. (2009) measured glacier displacement from equilibrium using the following simple calculation :

EQ 5

$$\alpha_d = \frac{AAR - AAR_0}{AAR_0}$$

where α_d is the percentage by which observed AAR values have deviated from that of the steady state AAR_0 . Here, negative values would indicate that the accumulation area has been shrinking and so the glacier has retreated, or will be in retreat, and positive values the opposite. Thus if PCT_a (and the systematic offset proposed by Hooke (2005) can be quantified) represents the lower boundary of the AAR_0 , it can be used not only to assess the degree to which glaciers are out of sync with current climate, but may also be utilised to provide quantitative estimates of the area the glacier must reduce by in order to reach equilibrium.

3.6 Summary of outcomes

- The small variation in PCT_p values observed across both sample I (n=36) and sample II (n=295) suggest that the PCT is the result of a complex but consistent relationship between climatological driving forces and the resulting ice flow dynamics. This interaction produces universal PCT_p values that can be observed across glacier samples irrespective of glacier size, longitudinal surface slope or basin geometry.
- The location of the PCT appears to be relatively unaffected by extensive debris mantles on glaciers in the Hindu Kush and Karakorum. Unlike current geomorphic health measures such as mean, median and mid-range glacier elevation, the PCT is appropriate for use with debris-mantled glaciers.
- The offset between the PCT_a and the observed ELA, which to some extent is to be expected even under steady state conditions (Hooke, 2005) is hypothesised to increase as glacier flow becomes increasingly out of sync with climate forcing. This is because of the lagged response ice dynamics display when adjusting to climate perturbations compared to ELA observations. As a result, the PCT_a should not be used as an estimate of modern day ELA.
- The very strong relationship between PCT_a and calculated balanced budget ELA_0 suggests that the PCT could represent the ice/flow dynamic conditions prevalent when the glacier was closer to equilibrium. Consequently, a comparison between PCT_a and contemporary ELA observations would provide insight concerning the extent with which glacier dynamics are currently out of sync with the current climate.
- A PCT derived AAR (AAR_{PCT}) can be calculated in order to assess the percentage by which modern day accumulation areas have shrunk since the glacier was closer to being in equilibrium with climate. This in turn may enable one to calculate the extent to which glacier area must reduce in order to reach equilibrium.

Chapter 4 Monitoring and Understanding PCT change over time

In chapter three, empirical observations were provided to support our theoretical understanding as to why assessing PCTs for a single time slice is important when searching for insights concerning glacier health and climate forcing. However, one of the fundamental lines of investigation required when researching climate change is the assessment of glacier variations over time. Countless studies have drawn information relating to climate forcing by observing variations in glacier snout position (Andreassen et al., 2005; Haeberli et al., 1998; Hoelzle et al., 2003; Johanneson et al., 1998; Oerlemans, 2005; Oerlemans, 2012; Vieli and Gudmundsson, 2004), changes in glacier area (Bhambri et al., 2011; Bolch, 2007; Liu et al., 2006; Narama et al., 2010; Nuth et al., 2007; Paul et al., 2004) and changes in surface elevation and velocity (Bolch et al., 2011; Bolch et al., 2008; Gardelle et al., 2012b; Käab and Vollmer, 2000; Käab et al., 2012; Surazakov and Aizen, 2006) but perhaps the most important tool for assessing climate perturbations is through the observation of mass balance trends (Benn and Lehmkuhl, 2000; Braithwaite et al., 2012; Cogley, 2009; Dyurgerov and Meier, 1997; Fischer, 2010; Hodgkins et al., 1999).

Thus in order to assess the extent to which the PCT can be used as a glacier health measure and climate signal, it is imperative that attention is paid to how this morphological phenomenon changes over time and how these changes can be related to other glaciological variables such as length and area fluctuations. Even more important is the necessity to discover the extent to which changes in PCT_x can be related to mass balance records. Accordingly the focus of this chapter will be to assess how the PCT changes over time with relevance to other variable measures.

Initially the chapter will evaluate PCT evolution and behaviour on Hintereisferner, Kesselwandferner (Ötztal Alps, Austria) and Blue Glacier (Olympic Mountains, Washington, USA), all of which have well-documented mass balance histories, in order to identify the extent to which empirical observations of PCT behaviour can be explained in terms of the glaciers' mass balance history. The work will then focus upon 47 glaciers located in the

Longyearbyen locality of Svalbard that will be assessed in order to identify how changes in PCT position over time relate to variations in glacier length. Not only will the results be used to further test the suitability of the PCT as a health measure, they will also enable us to gain significant insight into the way in which Longyearbyen glaciers have responded to climate forcing over the past five decades.

4.1 Methodology

4.1.1 Approach

Building upon the work discussed in the previous chapter, an empirical approach will continue to be the key theme when assessing the extent to which PCT changes over time can be related to other glaciological observations. Remotely sensed, GIS and inventory data continue to provide the basis for investigation. However, the data are supplemented with the use of historical and contemporary topographic maps that have been acquired and digitised for use in GIS.

4.1.2 Data Sources

4.1.2.1 DEMs

4.1.2.1.1 SRTM (2000)

Elevation contours and glacier attributes (as described in section 3.2.3) for Hinterisferner, Kessewandferner and Blue Glacier pertaining to the year 2000 were derived and extracted from SRTM DEM data. For Hinterisferner and Kesselwandferner, the SRTM tiles were converted to MGI_Austria_GK_West projection in order to enable co-registration with the LiDAR derived DEM and topographic maps. (See section 3.2.2.1.1 for details on SRTM data)

4.1.2.1.2 Tyrol LiDAR (2006)

Elevation contours and glacier attributes for Hinterisferner and Kesselwandferner from the year 2006 were derived and extracted from a 10 metre resolution DEM of the region made freely available by the Tirol Local government (accessed through: www.tirol.gv.at/applikationen/e-government/data/datenkatalog/geographie-und-planung/). The DEM was generated from aerial laser scanner (LiDAR) mass points collected in 2006 with

1 m point density and was provided readily georeferenced in MGI_Austria_GK_West projection. (figure 4.1)

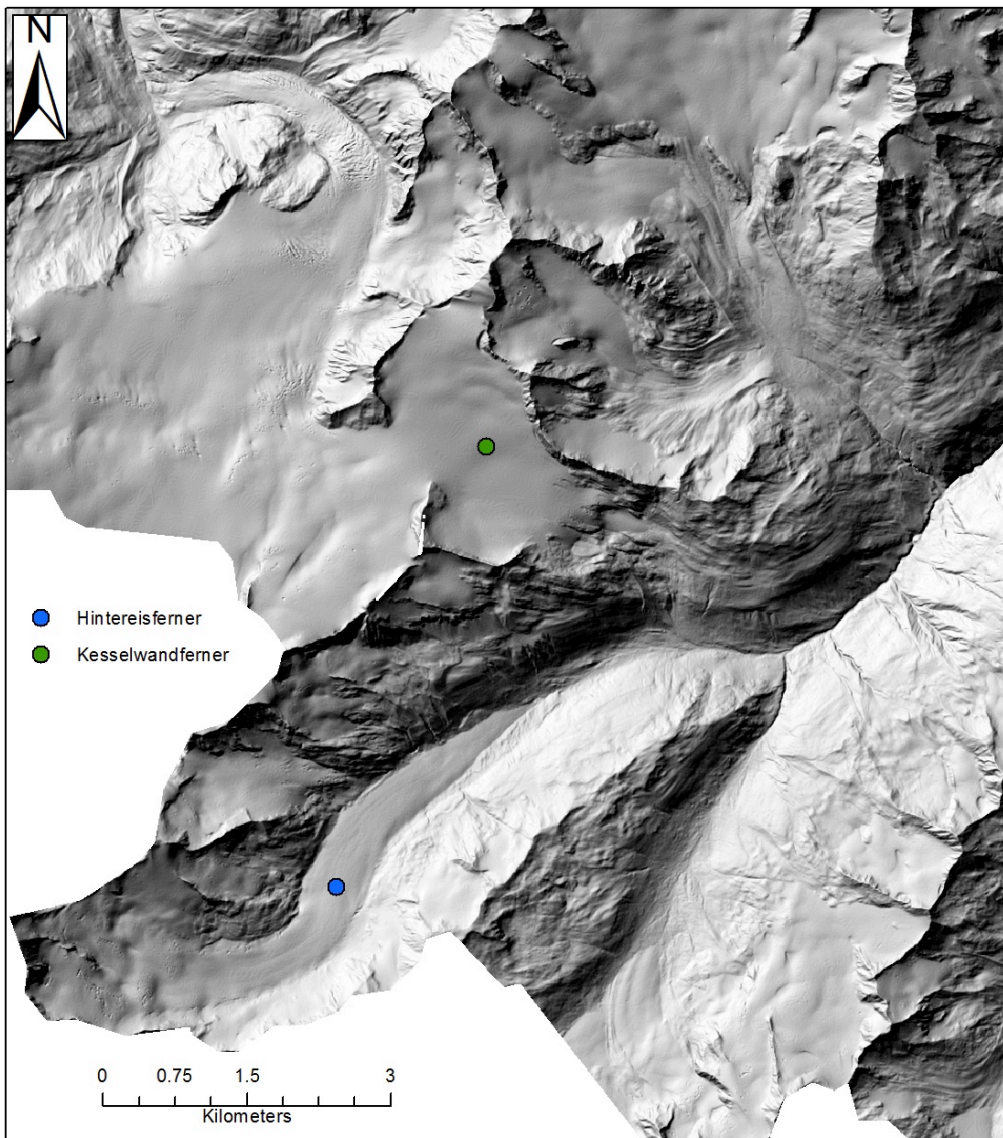


FIGURE 4.1- TIROL LiDAR
LiDAR based hillshade of Hintereisferner and Kesselwandferner in 2006.

4.1.2.1.2.1 LiDAR DEM post-processing and error assessment

The LiDAR DEM resolution was re-sampled in ArcGIS using bi-linear interpolation to the resolution of the reference SRTM DEM (90 m). The LiDAR DEM was then co-registered to the SRTM data, using a 1st-order polynomial transformation model in ErdasIMAGINE based upon 50 automatically generated tie-points on stable terrain, resulting in an average planimetric RMSE of 0.52 m. Estimations of absolute elevation errors require the use of ground control points (GCPs) from more accurate elevation datasets for the region (Nuth and Kääb, 2011). However, as no accurate GCPs or higher resolution

datasets for the area were available, the *relative* error was estimated from residuals of the difference between the 2006 LiDAR derived DEM and the SRTM DEM over ice-free terrain with slope gradients $< 20^\circ$ (Kohler et al., 2007). Measurements were taken over low slope gradients because small geolocation errors on steep slopes can lead to large elevation differences. This process produced a mean elevation offset of 0.35 m with a standard deviation of ± 11 m based upon analysis of 24,450 corresponding pixels. Given that the reported elevation errors for SRTM data are in the region of ≈ 9 m (Rodriguez et al., 2006), the small mean elevation offset of the 2006 epoch was considered negligible. The relative elevation error of the 2006 epoch DEM is considered here to reflect the standard deviation of the off-ice offsets of ± 11 m.

4.1.2.2 *Historic / Contemporary Topographic Maps*

4.1.2.2.1 Hintereisferner, Austria, 1979

PCT and glacier attribute data were generated using a 1:10,000 topographic map with 20 m interval contours of Hintereisferner accessed through the World Glacier Monitoring Service's (WGMS) data repository (Kuhn, 1981). The aerial images with which the map was photogrammetrically derived were collected on the 14th and 30th of August 1979. The paper map was drawn in MGI_Austria_GK_West projection and so was scanned into digital form, imported into ArcGIS and manually geo-referenced using the coordinate tick-marks present on the map.

4.1.2.2.1.1 1979 topographic map post-processing and error assessment

The 1979 topographic map was co-registered to the SRTM DEM in ArcGIS using manually generated tie-points located upon stable topographic features identifiable in both the 1979 topographic map and the SRTM DEM. Elevation contours at 10 m intervals were generated from the SRTM data to aid with the identification of corresponding topographic features such as mountain peaks and valley intersections. Using 32 tie-points the co-registration of the 1979 topographic map resulted in an average relative planimetric error of 13 m (RMSE). Relative elevation errors were once again estimated from the difference between the 1979 topographic map and the SRTM DEM over ice-free terrain on low gradient slopes. The off-ice locations used to assess the terrain offset were based upon 42 elevation GCPs included in the topographic map that were used

during the photogrammetry process in 1979 (Kuhn, 1981). Elevation differences at the 42 locations produced a mean offset of 5 m and a standard deviation of ± 7 m.

4.1.2.2.2 Kesselwandferner, Austria, 1971

Data for PCT and glacier attributes for Kesselwandferner were extracted from a 1:5,000 topographic map containing 5 m interval contours. Once again accessed through the WGMS data inventory with an MGI_Austria_GK_West projection, the map was generated through photogrammetry using aerial images acquired on the 18th of August 1971 (Schneider, 1976).

4.1.2.2.2.1 1971 topographic map post-processing and error assessment

The 1971 topographic map was co-registered to the SRTM DEM in ArcGIS using manually generated tie-points located upon stable topographic features identifiable in both the 1971 topographic map and the SRTM DEM. Once again, elevation contours at 10 m intervals were generated from the SRTM data to aid with the identification of corresponding topographic features such as mountain peaks and valley intersections. Using 12 tie-points the co-registration of the 1971 topographic map resulted in an average relative planimetric error of 34 m (RMSE). The higher planimetric RMSE produced here compared to that produced during the co-registration of the Hintereisferner is due to the smaller number of tie-point used. The smaller number of tie-points is the result of less topographically stable features being present on the Kesselwandferner map. Relative elevation errors were once again estimated from the difference between the 1971 topographic map and the SRTM DEM over ice-free terrain on low gradient slopes. Similar to the 1979 map, the 1971 map contained elevation GCPs that were used during the initial map production from aerial photographs. Elevation differences at the 22 locations produced a mean offset of 20 m and a standard deviation of ± 18 m. Due to the relatively large mean elevation offset between the SRTM data and the topographic map elevations, all elevation measurements taken from the 1971 map are corrected for this 20 m bias.

4.1.2.2.3 Blue Glacier, WA, USA, 1987

PCT and glacier attribute data for Blue Glacier from 1987 were extracted from a 1:24,000 scale topographic map accessed through the USGS' map archives. The

map was gridded at 1000 metre intervals in UTM 10 projection. The grid was then used to digitally geo-reference the map once it had been scanned and imported into ArcGIS. The map contains contours with 40 feet interval spacing. Accordingly, all elevation measurements taken from the map were converted into metres to ensure unit consistency.

4.1.2.2.3.1 1987 topographic map post-processing and error assessment

The topographic map of Blue Glacier was co-registered to the SRTM DEM using manually located tie-points, following the same method as described for the 1979 and 1971 topographic maps of Hintereisferner and Kesselwandferner respectively. Using 14 tie-points the co-registration of the 1971 topographic map resulted in an average relative planimetric error of 52 m (RMSE). Relative elevation errors were once again estimated from the difference between the 1987 topographic map and the SRTM DEM over ice-free terrain on low gradient slopes. As there were no GCPs available, a grid containing regular 250 m² cells was generated and layered upon the topographic map in ArcGIS to aid with the selection of sample locations. Off-ice elevation differences were recorded at locations where grid intercepts were coincident with elevation contours on the topographic map. In total, 49 locations were assessed producing a mean -3 m and a standard deviation of ± 16 m.

4.1.2.2.4 Longyearbyen, Svalbard, 1936 and 1995

Records of variation in PCT and glacier characteristics, in the Adventdalen region of Svalbard, were observed upon two 1:100,000 geomorphological maps generated by the Norsk Polarinstittutt using aerial images collected in June 1936 (C9G) and July 1995 (C9Q) (Major et al., 2000; Tolgensbakk et al., 2000). Both maps contained 50 m contour intervals and were projected in WGS_1984_UTM_Zone_33N. The paper maps were scanned into ArcGIS and digitally geo-referenced using the coordinate tick-marks present on the map.

The 1995 topographic map was co-registered to the 1936 map using 'trigonometric points' that were documented in both maps (Dallman et al., 2001; Sørbel et al., 2001). Co-registration using 38 tie-points produced an average relative planimetric error of 45 m (RMSE). Estimating the relative elevation error between two topographic maps is difficult as elevation information is only available at the location of the mapped contour lines. Using the gridded sample

approach outlined in section 4.1.2.2.3.1 but with a 2.5 km² grid size, off-ice elevation offsets were assessed at 60 locations. At each location, the elevation offset fell within one contour interval. However, as it is not possible to accurately assess elevation offsets at an inter-contour resolution on a paper map, it was decided to adopt a conservative relative elevation error of ± 50 m to reflect the contour interval spacing present on the maps.

4.1.2.3 Error Propagation

In this chapter the accuracy of the elevation data have been determined using the residual population of the difference between the reference data source (SRTM) and an alternative elevation dataset (e.g. 2006 LiDAR derived DEM) over stable terrain. These residuals represent the relative errors between elevation data sets, rather than absolute errors (Nuth and Kääb, 2011). Accordingly, when measuring changes in PCT_a between different epoch DEMs, the uncertainty in the measurement can be assessed using standard principles of error propagation (Burrough et al., 1998). For example, if the absolute error of the reference DEM, σ_1 , and the relative error of the DEM being compared, σ_2 , is known, then the resulting uncertainty in elevation differences between the two DEMs, ε_a , is defined as:

EQ 5.

$$\varepsilon_a = \sqrt{\sigma_1^2 + \sigma_2^2}$$

Furthermore, the uncertainty associated with planimetric changes between different epoch datasets can be determined. If one has knowledge of both the spatial resolution of the two datasets being compared and the relative error produced during co-registration (RMSE), the planimetric change uncertainty, ε_x , is defined as:

EQ 6.

$$\varepsilon_x = \sqrt{D_1^2 + D_2^2 + \sigma_x}$$

where D_1 is the resolution of the reference DEM, D_2 is the resolution of the second DEM and σ_x is the planimetric (relative) error produced during DEM co-registration (Hall et al., 2003; Wang et al., 2008).

4.1.2.4 Optical Satellite Imagery

4.1.2.4.1 Landsat 7 ETM+

In order to delineate the glacier boundary for Hintereisferner, Kesselwandferner and Blue Glacier for the year 2000, Landsat 7 ETM+ imagery was once again utilised. Section 3.2.2.2.1 provides details concerning the optical imagery used and a table of the Landsat data used for this chapter is available in Appendix B (Table III).

4.1.2.5 Digital Glacier Outlines, PCT Extraction and Inventory Data

When extracting glacier outlines from the Landsat imagery and other glaciological attributes from the SRTM data, the same methods as outlined in section 0 were employed. Data concerning glacier elevation and PCT location from the historic maps were manually digitised from the contours present in the digitised paper maps. The glacier outlines had already been mapped upon the paper documents and as a result, once the maps had been imported into ArcGIS, the glacier boundaries were digitised manually using the existing boundaries. As with chapter three, mass balance data were extracted from the WGMS's FOG series.

4.2 Results

4.2.1 PCT Change and Mass Balance

Changes in PCT position over time on three glaciers were observed and compared to their mass balance history in order to assess whether a clear link could be identified between the two health measures.

4.2.1.1 Hintereisferner 1979 - 2006

Year	PCT _a (m.a.s.l)	PCT _p	Glacier Length (km)	Glacier Area (km ²)	ΔPCT _a (m)	ΔPCT _p	ΔPCT _x (m)	ΔLength (km)	ΔArea (km ²)
1979	2890 ±7	0.34	7.241	9.50	N/A	N/A	N/A	N/A	N/A
2000	2890 ±9	0.33	6.835	6.52	0 ±11	-0.01	-282 ±93	-0.406	-2.98
2006	2910 ±11	0.35	6.67	6.45	20 ±14	0.02	-257 ±81	-0.165	-0.07

TABLE 4-1 SUMMARY RESULTS OF PCT CHANGE ON HINTEREISFERNER

The change in PCT_a, PCT_p, glacier length and glacier area was calculated by subtracting each observation year's value from that of the previous observation year.

Figure 4.2 displays the change in PCT_x and PCT_a between 1979 and 2006 on Hintereisferner. The satellite imagery and data in Table 4-1 clearly highlight the fact that Hintereisferner has experienced significant retreat between 1979 and 2006 where the snout has retreated by 570 m in total. However, more important is the observation that during the same period, PCT_x displayed evidence of a 539 m retreat towards the headwall. As was predicted in section 2.4, the need to record changes in PCT_x appears to be of paramount importance. This is demonstrated in figure 4.2E which highlights the fact no significant change in PCT_a was observed between 1979 and 2000 despite snout retreat. If only changes in PCT_a values were available, as is the case with ELA records, one may have been led to believe that the PCT had not adjusted between 1979 and 2000, though this is clearly not the case. Furthermore, figure 4.2E displays evidence of the expected response scenarios of the PCT discussed in section 2.4.3. Between 1979 and 2000, PCT_x retreated 282 ± 93 m whilst undergoing no change in elevation thus displaying evidence of dynamic retreat and thinning (scenario 6, section 2.4.3.6). Owing to the upward gradient of the ice surface towards the headwall, the lack of elevation change concurrent with the recorded PCT_x retreat suggests that the glacier surface must have thinned whilst ice flow dynamics were adjusting to what is expected to have been negative mass balance.

However, the change in PCT position between 2000 and 2006 reveal evidence indicative of scenario 7 where flow dynamics adjust to a negative balance regime, causing PCT_x to retreat up glacier whilst the ice surface displays little evidence of significant lowering in the vicinity of the PCT. Such changes in the response scenario between the observation dates suggests that the way in which the glacier responded to climate forcing evolved over the observation period. This idea will be covered in greater detail in the following discussion. It is also worth mentioning at this point the observation that during the entire monitoring period, the PCT_p value remained relatively constant reaching a minimum of 0.33 and a maximum value of 0.35. The significance of this will also be discussed later. The changes in PCT location were also compared to the mass balance history of Hintereisferner. Plots evidencing PCT_x retreat relative to the glacier's mass balance and ELA records are given in figure 4.3.

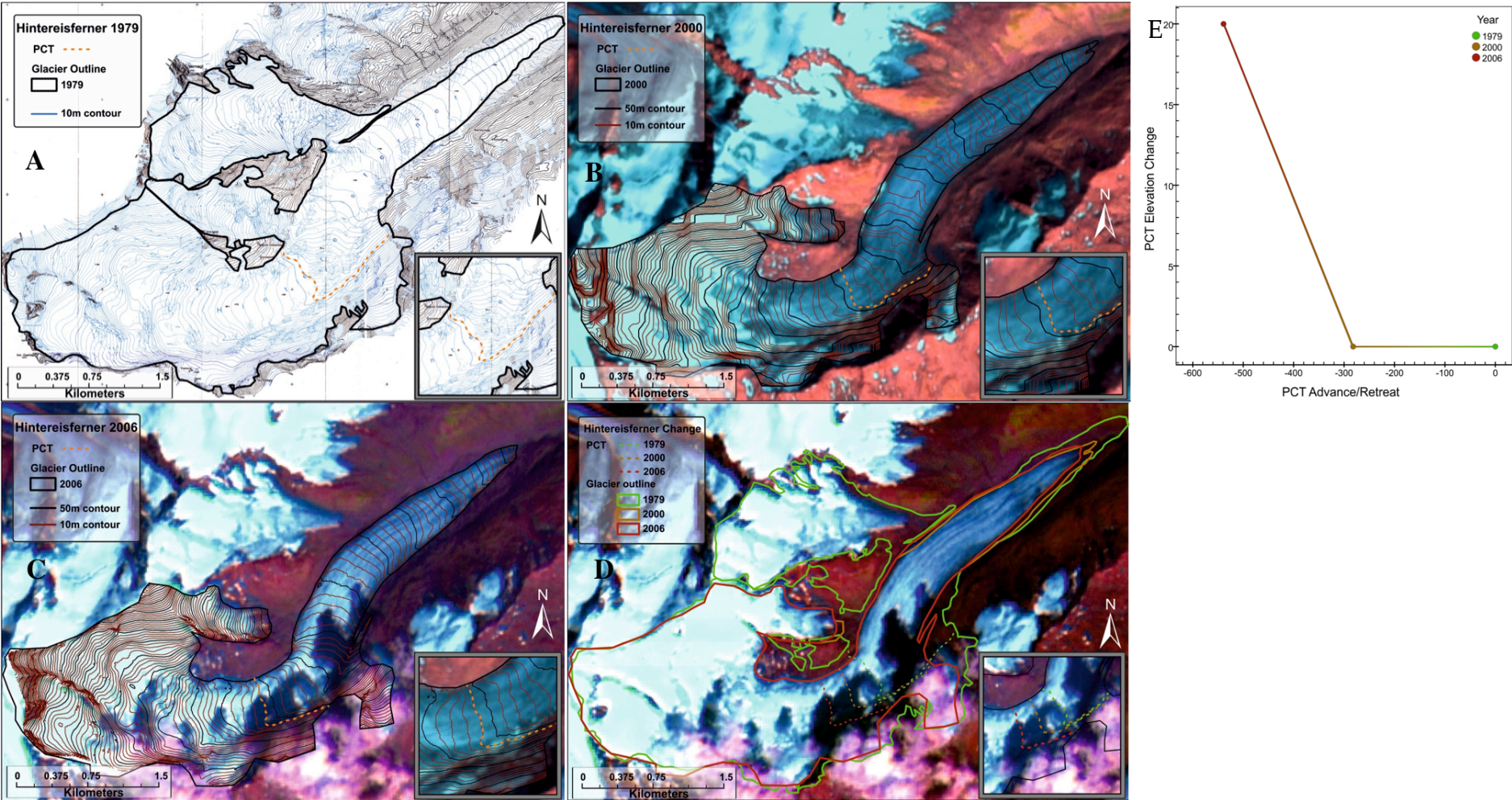


FIGURE 4.2- PCT CHANGE ON HINTEREISFERNER
 A) PCT location in 1979. B) PCT location in 2000. C) PCT location in 2006. D) Variation in PCT and terminus position between 1979 and 2006. E) Scenario plot highlighting changes in PCT location between observation date in terms of PCTa and PCTx in metres.

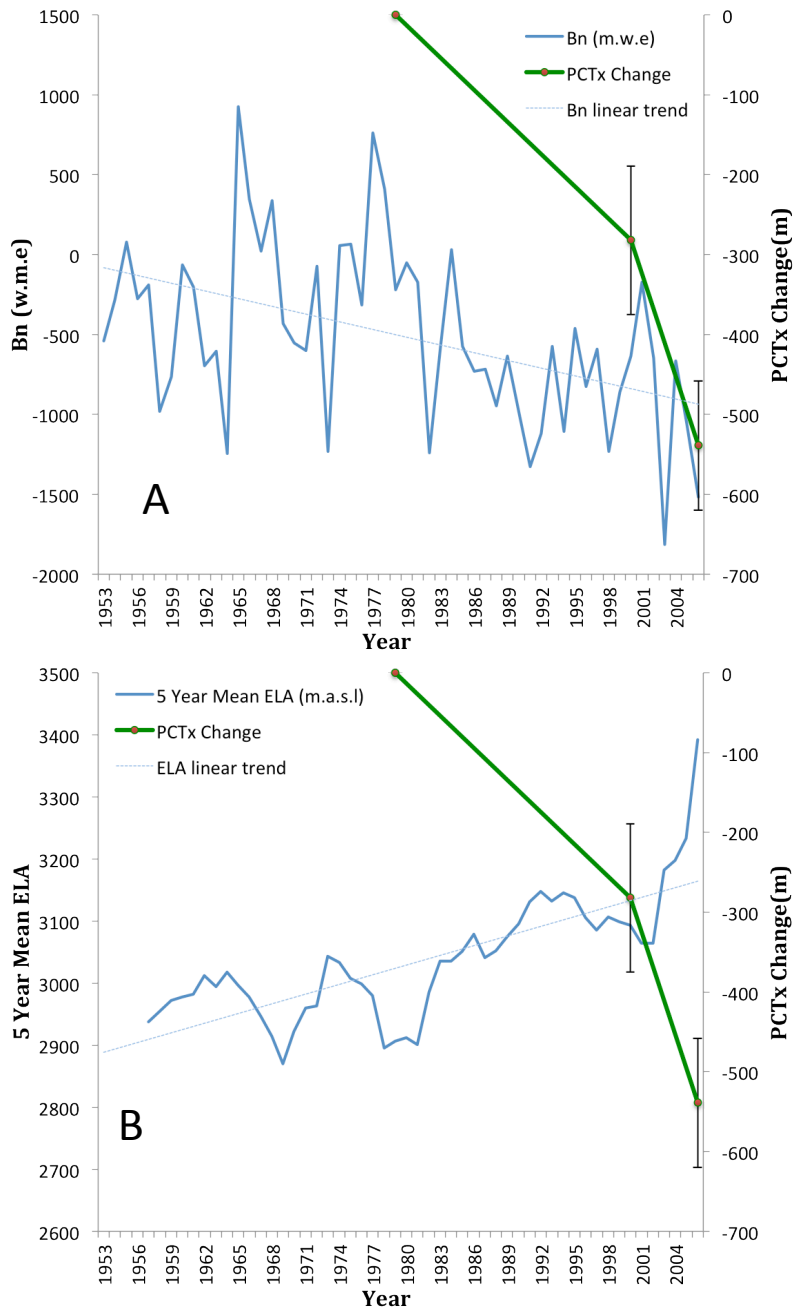


FIGURE 4.3 - PCT CHANGE COMPARED TO MASS BALANCE AND ELA ON HINTEREISFERNER
A) PCT change in the x-direction in metres vs annual mass balance m.w.e. B). PCT change in the x-direction vs 5 year running mean ELA record. Error bars reveal the measurement uncertainty in PCTx change.

Figure 4.3A shows that Hintereisferner has had an increasingly negative mass balance since records began in 1953 whilst PCT_x has been retreating since at least 1979. This negative mass balance goes some way towards explaining the observed snout retreat but also provides the first insight as to how changes in the PCT_x and PCT_a may reflect glacier health in terms of mass balance. Similarly, although not as clear as that of mass balance, the mean ELA record for the glacier suggests that there has been an overall trend of elevation

increase. These trends in mass balance and ELA and the resultant changes in PCT support the theoretical discussions held in chapter two which highlighted why one would expect the PCT_x to retreat under negative mass balance conditions.

4.2.1.2 Kesselwandferner 1971 – 2006

Year	PCT_a (m.a.s.l.)	PCT_p	Glacier Length (km)	Glacier Area (km ²)	ΔPCT_a (m)	ΔPCT_p	ΔPCT_x (m)	Δ Glacier Length (km)	Δ Glacier Area (km ²)
1971	3030 ±18	0.41	3.786	4.195	N/A	N/A	N/A	N/A	N/A
2000	3030 ±9	0.38	3.722	4.082	0 ±18	-0.03	0 ±114	-0.065	-0.113
2006	2080 ±11	0.29	3.563	4.012	-40 ±14	-0.11	82 ±81	-0.159	-0.071

TABLE 4-2 SUMMARY RESULTS OF PCT CHANGE ON KESSELWANDFERNER

The change in PCT_a , PCT_p , glacier length and glacier area was calculated by subtracting each observation year's value from that of the previous observation year.

Figure 4.4 and table 4-2 displays the variation in PCT upon Kesselwandferner between 1971 and 2006 whilst figure 4.5 displays the changes in PCT_x in relation to Kesselwandferner's mass balance and ELA history. Data from 1971 and 2000 show no significant change in PCT_a or PCT_x between the two observation dates. However, between 2000 and 2006 the PCT provided evidence for scenario 3 where changes in the glacier's flow dynamics resulted in PCT_x advance of 82 ± 81 m and a reduction in PCT_a by 40 ± 14 m whilst the snout retreated 159 m.

However, it is important to note that one can have little confidence in the observations of PCT_x behaviour upon Kesselwandferner due to the large uncertainties associated with the measured changes of PCT_a and particularly PCT_x . The high planimetric errors are the combined result of the poor availability of tie-points during co-registration and the low spatial resolution of the SRTM data. Such uncertainties indicate that small but significant variations in PCT_x and PCT_a over time may be difficult to detect when only relatively coarse resolution DEMs such as SRTM are available. This methodological constraint will be discussed in detail in section 8.5.

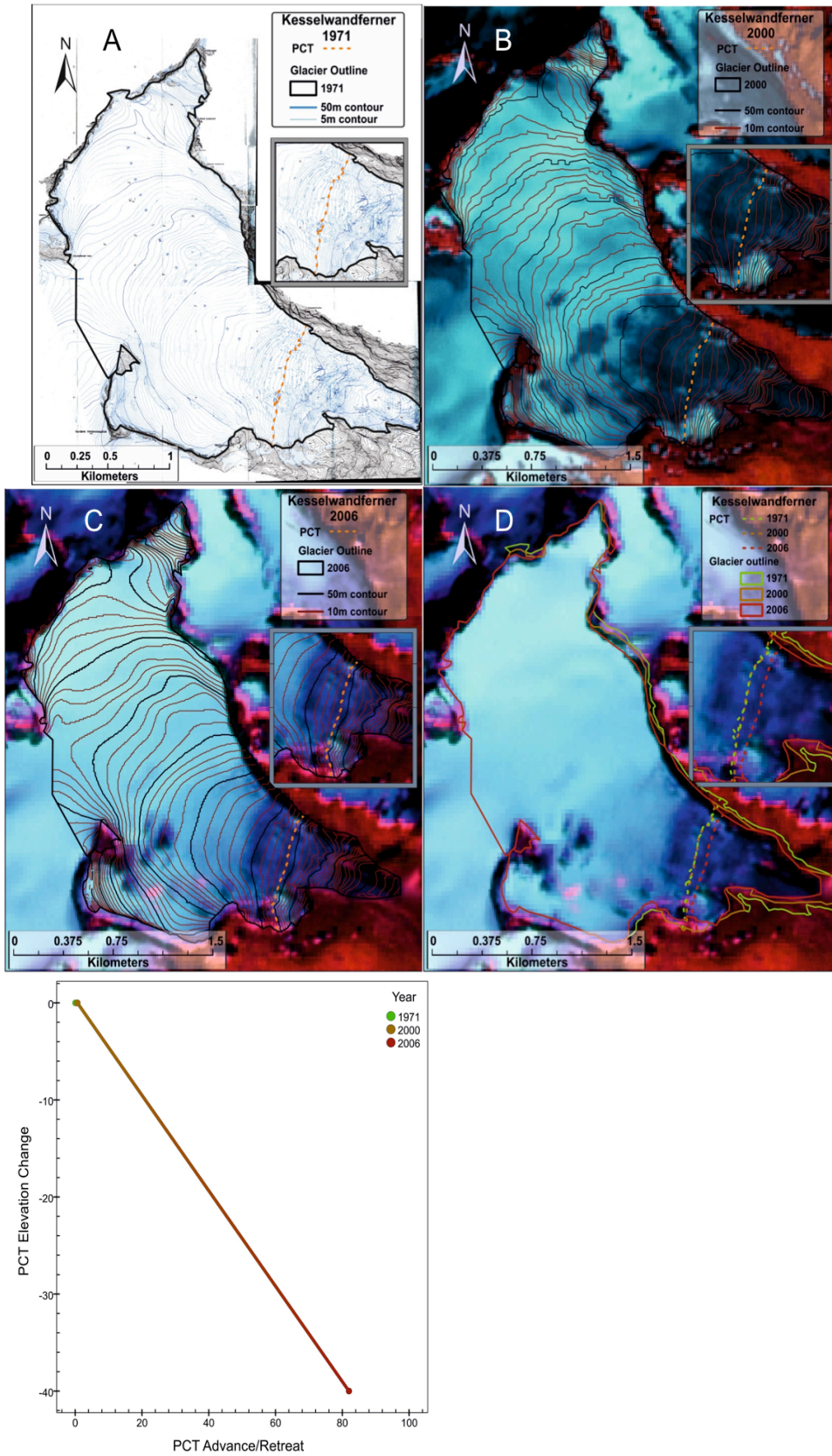


FIGURE 4.4 – PCT CHANGE ON KESSELWANDFERNER
 A) PCT location in 1971. B) PCT location in 2000. C) PCT location in 2006. D) Variation in PCT and terminus position between 1971 and 2006. E) Scenario plot highlighting changes in PCT location between observation date in terms of PCTx and PCTa in metres.

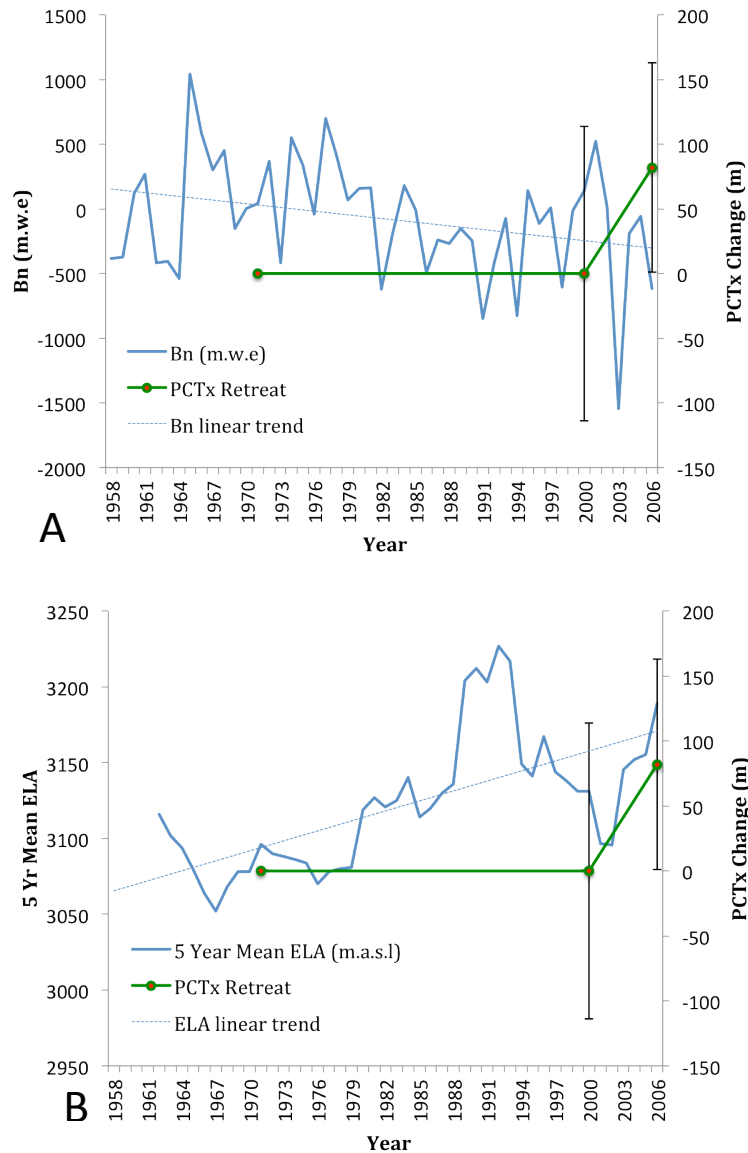


FIGURE 4.5 - PCT CHANGE VS MB AND ELA ON KESSELWANDFERNER
A) PCT change in the x-direction in metres vs annual mass balance m.w.e. B). PCT change in the x-direction vs 5 year running mean ELA record. Error bars reveal the measurement uncertainty in PCTx change.

4.2.1.3 Blue Glacier, USA, 1987-2000

Figure 4.6 displays PCT variation upon Blue Glacier between the 1987 and 2000 with the results summarised in table 4-3.

Year	PCT _a (m.a.s.l.)	PCT _p	Glacier Length (km)	Glacier Area (km ²)	ΔPCT _a (m)	ΔPCT _p	ΔPCT _x (m)	ΔGlacier Length (km)	ΔGlacier Area (km ²)
1987	1585 ±16	0.30	4.434	5.80	N/A	N/A	N/A	N/A	N/A
2000	1540 ±9	0.20	4.248	5.79	-45 ±18	-0.10	250 ±132	-0.186	-0.009

TABLE 4-3 SUMMARY RESULTS OF PCT CHANGE ON BLUE GLACIER
The change in PCT_a, PCT_p, glacier length and glacier area was calculated by subtracting each observation year's value from that of the previous observation year.

Both the maps and plot D displayed in figure 4.6 highlight the observation that between 1987 and 2000 PCT_x advanced 250 ± 132 m whilst PCT_a reduced by 45 ± 18 m. This dynamic behaviour in the PCT is indicative of scenario 3, which was proposed in section 2.4.3.3 as a potential sign of positive mass balance. As was suggested earlier, PCT behaviour of this type is believed to be the result of a period of positive mass balance where changes in the glacier's flow dynamics have caused the PCT to form down glacier at lower elevations. Thus, under such condition one would also expect the glacier terminus to advance in a phase of positive mass balance, as evidenced by PCT_x advance. However, as was the case with Kesselwandferner, the seemingly positive nature of the advancing PCT_x coincided with retreat of the snout, rather than the expected advance. Clearly there is a complexity in the response to climate that has allowed flow dynamics to advance whilst the snout has retreated. It should be mentioned here that retreat was measured and reported as the maximum observed retreat. Figure 4.6 reveals that retreat is heterogeneous across the entire snout as evidenced by the greater rate of retreat observed on the western margin of the snout between 1987 and 2000.

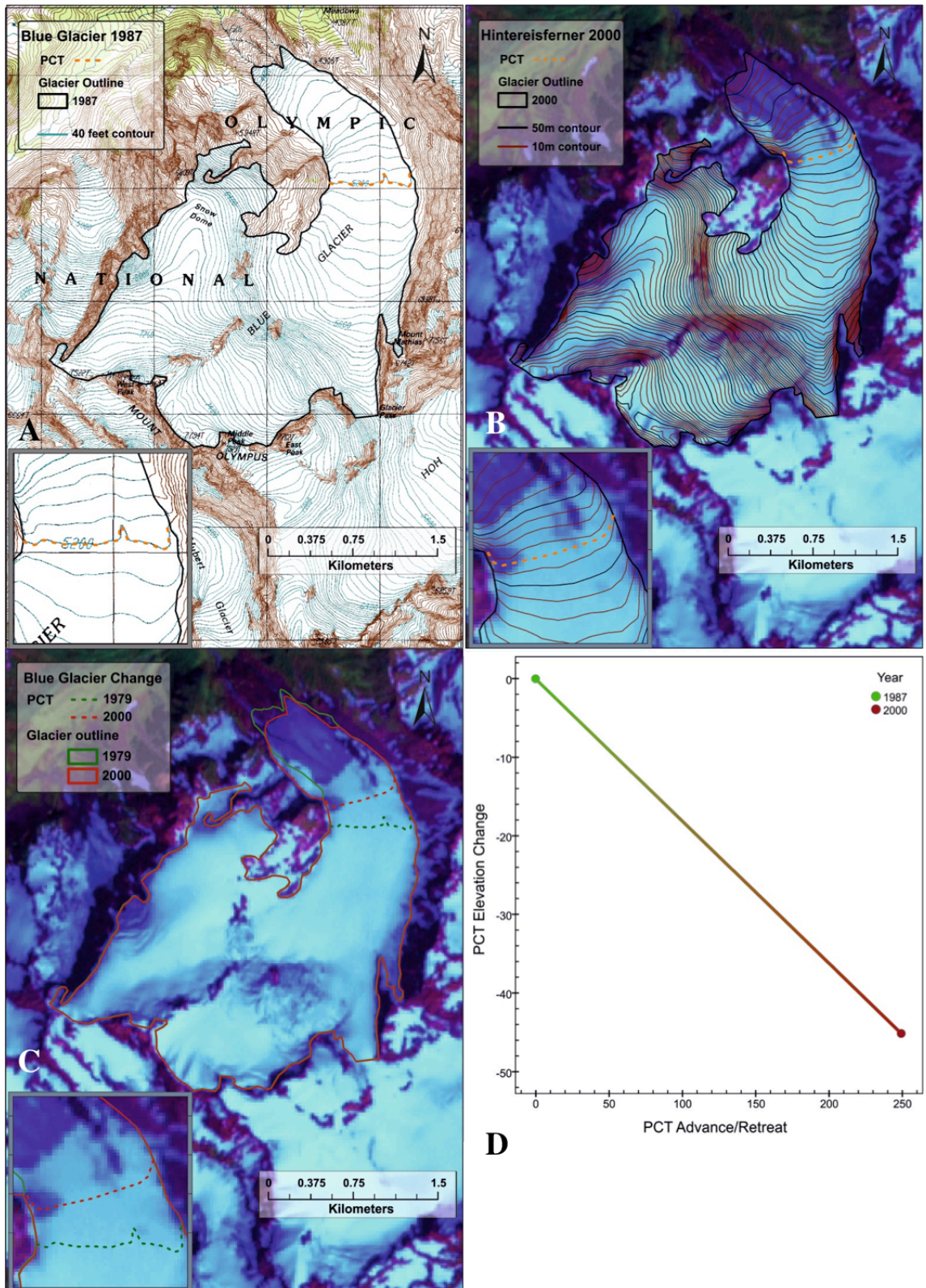


FIGURE 4.6 – PCT CHANGE ON BLUE GLACIER

A) PCT location in 1987. B) PCT location in 2000. C) Variation in PCT and terminus position between 1987 and 2000. D) Scenario plot highlighting changes in PCT location between observation date in terms of PCTx and PCTa in metres.

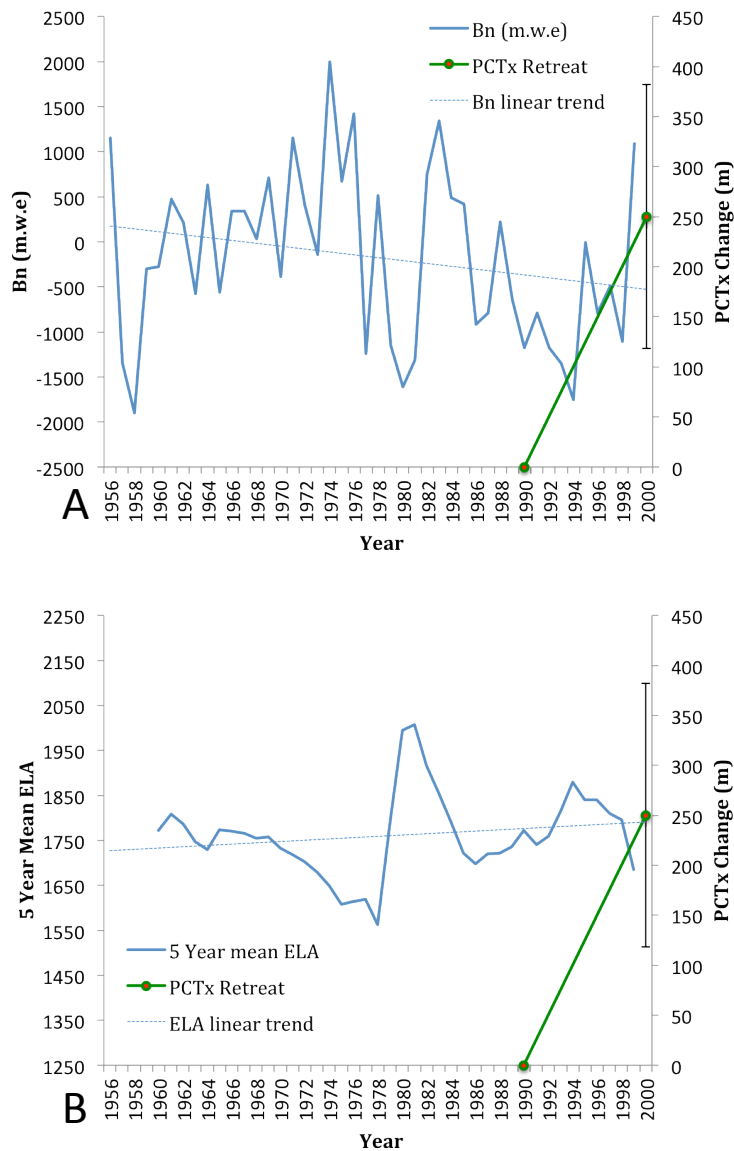


FIGURE 4.7 - PCT CHANGE VS MASS BALANCE AND ELA ON BLUE GLACIER
A) PCT change in the x-direction in metres vs cumulative annual mass balance m.w.e. B). PCT change in the x-direction vs 5 year running mean ELA record. Error bars reveal the measurement uncertainty in PCTx change.

The graphs in figure 4.7 reveal the changes in PCT_x in relation to the glacier's mass balance and ELA record. When assessing the variation in mass balance between 1955 and 2000 there is a clear trend of positive mass balance between 1960 and 1975. However, from the mid 1980's the mass balance record becomes dominated by years of negative mass balance. Similar to the mass balance record, the mean ELA signal displays great variability over the observation period. Visually, the ELA record correlates well with the mass balance record with years of high ELA correlating with years of negative mass balance and *vice versa*. Unfortunately, because only two PCT location measurements could be

taken, it is difficult to ascertain whether PCT_x advance was initiated before the 1987 observation or whether the advance commenced between 1987 and 2000. Greater knowledge of this behaviour would be useful as it would have provided information regarding the relative timings between the onset of the positive mass balance trend and the initiation of PCT_x advance, which would appear to be connected according to theory (Hooke, 2005) and the observations revealed here.

4.2.2 PCT Change in Longyearbyen

Summarised results pertaining to PCT change over time in the Adventdalen region of Svalbard are shown in table 4-4 whilst a table of the full results can be found in appendix B (Table III). A map revealing the locations of the sampled glaciers is shown in figure 4.8. Changes in PCT_a, PCT_x and PCT_p between 1936 and 1995 were recorded upon a total of 47 glaciers.

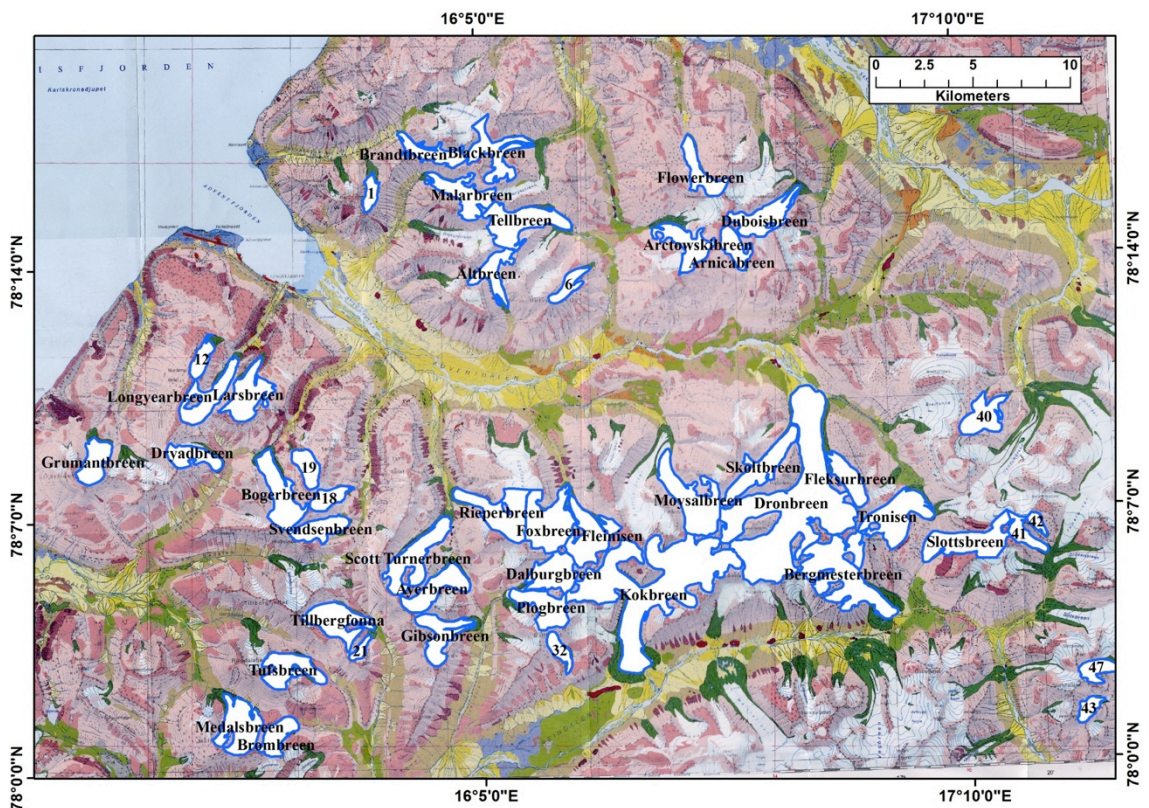


FIGURE 4.8 – MAP SHOWING THE 47 GLACIERS OBSERVED BETWEEN 1936 AND 1995 IN LONGYEARBYEN, SVALBARD.

	PCT _a (1946)	PCT _a (1995)	PCT _p (1946)	PCT _p (1995)	ΔPCT _a (m)	ΔPCT _x (m)	ΔPCT _p	Δ Glacier Length (km)	Δ Glacier Area (km ²)
Mean	530±50	520±50	0.35	0.36	-10 ±71	-154 ±52	0.005	-232	-0.79
Median	525±50	525±50	0.33	0.33	-25 ±71	-126 ±52	0.01	-209	-0.61
Std. Dev	70.64	78.76	0.09	0.13	55	457	0.1	346	0.77
Max	700±50	700±50	0.64	0.65	125 ±71	891 ±52	0.28	362	-0.04
Min	350±50	325±50	0.2	0.11	-125 ±71	-2029 ±52	-0.2	-1401	-3.62

TABLE 4-4- PCT CHANGE IN SVALBARD

Summarised information for the 47 glaciers including PCT and glacier change information between 1946 and 1995. The change in PCT_a, PCT_p, glacier length and glacier area was calculated by subtracting each observation years value from that of the previous observation year.

Table 4-4 highlights the finding that the mean PCT_p across the sampled glaciers in both 1946 (0.35) and 1995 (0.36) agree well with the mean PCT_p value of 0.39 observed and discussed in the previous chapter. When comparing the PCT_p means from the two observation dates there appears to have been little variation in PCT_p between 1946 and 1995, as indicated by the mean ΔPCT_p = 0.005. Similarly, table 4-4 suggests that between the two dates, there appears to have been only minor variation in PCT_a. This may initially lead one to believe that the PCT has remained unchanged between observations. However, this is clearly not the case as the results show that PCT_x was observed to advance 891±52 m upon on one sample whilst retreating 2029±52 on another with mean ΔPCT_x of -154 ±52 across the sample.

Due to the lack of any mass balance records in the study area, one of the few ways in which the PCT can be tested as a health measure is by comparing changes in its locality to changes in other glaciological variables such as glacier length. Accordingly the relationship between ΔPCT_x and changes in glacier length is shown in figure 4.9.

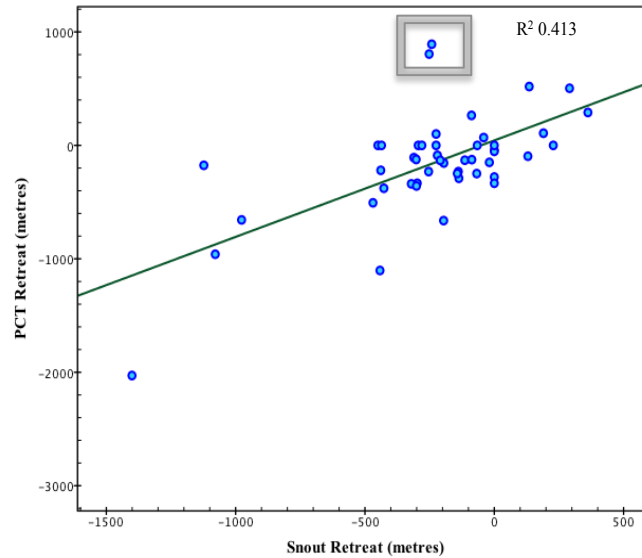


FIGURE 4.9 – ΔPCT_x COMPARED WITH $\Delta GLACIER$ LENGTH

The relationship between changes in PCT_x and changes in terminus position (advance / retreat) between 1936 and 1995. Grey box indicates glacier where PCT_x has advanced whilst the glacier snout has undergone retreat

Although the strength of the relationship is not extremely strong, there is a clear indication that PCT_x retreat occurs with snout retreat and vice versa. Furthermore the glacier upon which PCT_x displayed the largest retreat also experienced the highest degree of recorded snout retreat. However, this relationship could not be stated for the glacier upon which PCT_x experienced the greatest advance. This is owing to the two outliers, Scott Turnerbreen and Ayerbreen, highlighted by the grey box (included in the r^2). These glaciers represent the unusual occurrence where PCT_x has advanced whilst the glacier snout has undergone retreat. This observed behaviour is in keeping with that of Kesselwandferner and Blue Glacier and is interpreted to be due to the influence that variations in accumulation regimes have upon the observed glaciers, a point that will be developed in the following section.

As well as comparing ΔPCT_x with changes in glacier length, changes in PCT_a were compared to ΔPCT_x and PCT_p .

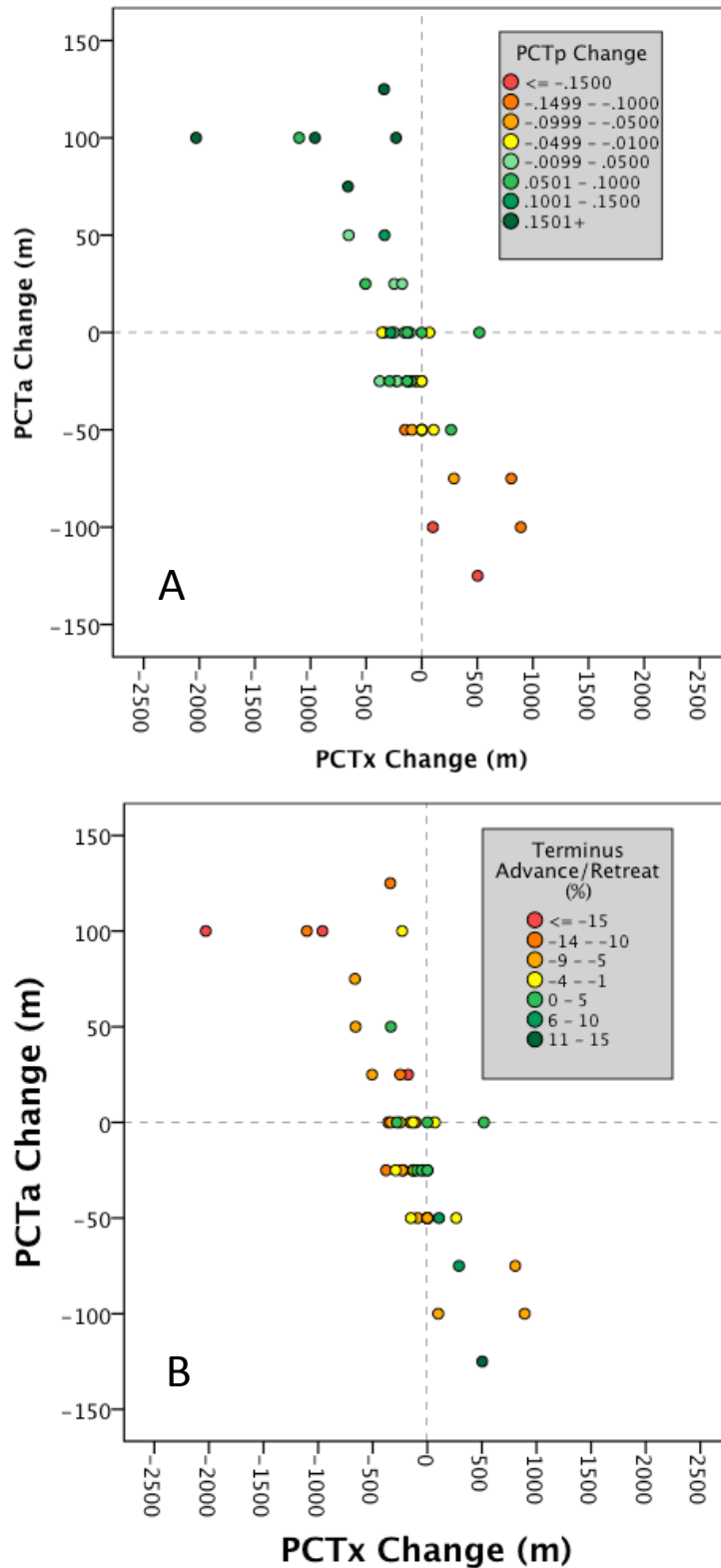


FIGURE 4.10 - PCT LOCATION CHANGE IN LONGYEARBYEN, 1936 – 1995
A) Plot highlighting planar (X) and elevation (Z) changes in PCT position with the points coloured according to changes in PCT_p between observation dates. B) Plot highlighting planar (X) and elevation (Z) changes in PCT position with the points coloured according to the percentage of snout advance / retreat (% of the total length of the observed glacier).

Figure 4.10 highlights the variation in PCT change during the observation period. The plots highlight that most of the glaciers demonstrated PCT_x retreat, with the highest levels of PCT_x retreat also resulting in the greatest increases in PCT_a (as was predicted in section 2.4 due to the upwardly sloping ice surface towards the headwall). Plot A also shows that the highest levels of PCT_x retreat and PCT_a increase occurred in tandem with increases in PCT_p as indicated by the clustering of green points in the upper left-hand side. Moreover, plot B highlights the observation that glaciers demonstrating high levels of PCT_x retreat experienced the greatest proportional reductions in length by snout retreat. The PCT on Dalburgbreen showed no variation in elevation or movement in the x-direction yet its PCT_p increased from 0.33 to a relatively high 0.53. Owing to the lack of horizontal or vertical motion observed in the PCT, this change in PCT_p is attributed to the lowering of the minimum glacier elevation through the observed advancing of the snout by 228 metres. This glacier snout advance despite apparent PCT inactivity cannot be explained in terms of glacier advance under positive mass balance as this would require the PCT to advance down glacier in tandem. Thus this anomalous observation could be attributed to glacier surging resulting in glacier advance nonsynchronous with climate forcing (see section 2.5.2).

However, the most basic information that can be extracted from the plots in figure 4.10 is that of the PCT response scenarios, first introduced in section 2.4.3 and figure 2.13, observed across the sampled glaciers. As one would expect, there was no evidence of scenario 1 or 8 throughout the sample however the results do highlight the variability in glacier response scenario to climate forcing displayed across the region. The frequencies of the response scenarios are provided table 4-5.

It is important to highlight the alarming observation that for a quarter (12 cases) of the sample, the PCT exhibited behaviour characteristic of scenario 5, where the PCT has retreated *and* reduced in elevation. As discussed in 2.4.3.5, the situation where the PCT reduces in elevation whilst retreating is

Scenario	Frequency	Percentage
2	2	4.3
3	7	14.9
4	9	19.1
5	12	25.5
6	7	14.9
7	10	21.3
Total	47	100.0

TABLE 4-5 SCENARIO FREQUENCIES.

indicative of rapid glacier wastage and surface thinning. Furthermore, the second most frequently observed response (10) is that of scenario 7 where the PCT retreats up-glacier to higher elevations, a behaviour that is interpreted to be indicative of a negative mass balance regime. The majority of the remaining glaciers (9) displayed PCT movement symptomatic of scenario 4, which is suggested here to be an indication of down wasting due to increased atmospheric temperatures and enhanced melt rates in the ablation area. Of the glaciers that displayed evidence of scenarios 2 and 3 (9), there was evidence of both snout advance and retreat. Assuming that PCT_x advance is evidence of flow dynamics adjusting to positive mass balance, the concurrent snout retreat with PCT_x advance observed here further highlights the complexity that lag times present when assessing glacier response to climate forcing. Based upon observations from Kesselwandferner and Blue Glacier, the PCT_x advance concurrent with glacier terminus retreat is likely to be the result of a prior period of positive mass balance.

Nevertheless, as discussed previously, in order to identify how different components of the glacier system, in this case flow dynamics and areal/length extent, respond to climate forcing, it is important to assess how their PCT_p value varies over time. Figure 4.10A reveals how PCT_p values varied between 1946 and 1995 in relation to changes in PCT elevation and planar position. It should first be observed that, although there was clear variation in PCT response, overall changes in PCT_p values were relatively small across the sample as evidenced by the fact that only 7 glaciers displayed PCT_p change $\geq \pm 1.5$. This perhaps suggests that flow dynamics and glacier extent are generally responding to climate forcing at a similar rate and that the glaciers are demonstrating some form of dynamic balance between glacier flow, glacier extent and three-dimensional surface shape. However, as highlighted in figure 4.10 there is clear evidence that responses still do vary across the sample and that there are certainly cases where glacier retreat and thinning is occurring at rate far greater than the response of flow dynamics and vice versa.

One benefit of using GIS in this research is that it enables one to assess whether there is a spatial pattern that may explain the variation in glacier and PCT response to climate forcing that has been observed. Figure 4.11 displays the

spatial distribution of PCT response scenarios across the study region. The glacier outline are colour according to the response scenario whilst the solid points represent change and PCT_p and hollow points indicate changes in terminus position as a percentage of the glaciers length. The figure shows that the fastest glacier retreat and shrinkage appears to have occurred in the southwest of the region where the majority of the glaciers can be categorised under scenarios 4, 5 and 6 according to the associated PCT behaviour. Furthermore, this region appears to be dominated by the situation where PCT_p values have lowered despite providing evidence of PCT inactivity or PCT_x retreat. Furthermore, an alarming observation is the prevalence of glaciers displaying evidence of scenario 5, which in section 2.4.3.5 was predicted to indicate glacier thinning, coupled with the lowering of the PCT_p value perhaps evidences concerning levels of glacier retreat.

Towards the more central region there appears to be a higher proportion of glaciers characterised by scenario 7 where PCT_x has retreated up glacier at a greater rate than glacier thinning. Interestingly, these glaciers have also experienced the highest rates of snout retreat yet their PCT_p values have either remained relatively constant during the retreat or have in fact increased by moving disproportionately closer to the maximum ice elevation (headwall). Despite the very high snout retreat rates observed on these glaciers, it appears that PCT_x retreat rate has exceeded the snout retreat rate resulting in the increases seen in PCT_p value. Such observed behaviour may provide some insight into how high PCT_x retreat rates lead to increased snout retreat. This will be developed in the discussion section.

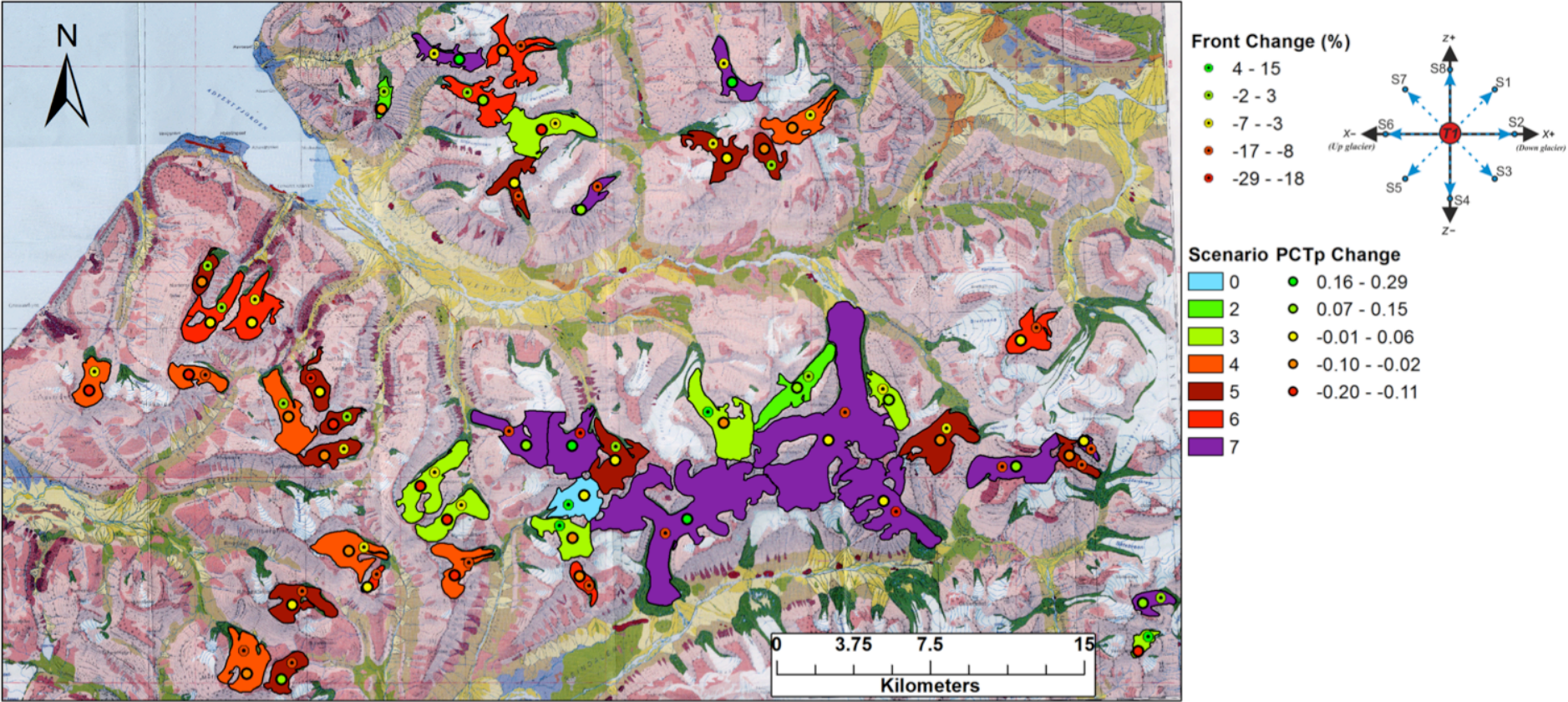


FIGURE 4.11 – PCT CHANGE ACROSS THE STUDY REGION
 The polygons represent glacier extents coloured according to the PCT change scenario between 1936 and 1995. The hollow points represent the percentage of snout retreat and advance whilst the solid points account for the change in PCTp between observation dates. Points and polygons overlay the 1995 OS map of the Longearbyen region.

4.3 Discussion

The following discussion takes place in two parts with different foci. The initial discussion will consider whether the results provide evidence that support the idea that the PCT can be used for monitoring glacier health over time and therefore be used as a climate signal. The second part of the discussion will then switch the approach by assessing the observed changes in PCT over time with the view of gaining insights into how the studied glaciers are responding to climate forcing and whether these responses are spatially consistent.

4.3.1 Supporting evidence for the PCT as a glacier health measure

The first observation of note from the sample of Svalbard glaciers and the three case-study glaciers is the validation of the prediction made in section 2.4 that proposed the need to record planar variation in PCT evolution (PCT_x), something that is not done with current ELA monitoring campaigns. Consequently, by recording PCT_x changes as well as changes in PCT_a , PCT records enable one to identify whether glacier thinning or thickening is occurring in tandem with dynamical changes to the glacier's flow. This is an insight that ELA records alone are unable to provide.

Another fundamental observation that supports the assertion that the PCT is a function of climate controlled flow dynamics is provided by the PCT_p observations. The mean PCT_p value for all glaciers discussed in this chapter for all recorded dates is 0.36. This value falls well within 95% confidence interval (0.34 – 0.42) for the sampled glaciers discussed in section 3.4 and further supports the belief that the PCT is produced by the complex relationship between climate, mass balance and glacier flow as glaciers tend towards dynamic balance. Furthermore, the standard deviation in PCT_p across the dataset (0.11), once again suggests that glacier-specific characteristics such as longitudinal slope, hypsometry, aspect, size and basin geometry, that vary across different samples within the dataset, have only a minor impact upon PCT position.

The relatively small changes in PCT_p values observed for the majority of glaciers in Svalbard suggests that glaciers in the region are tending towards equilibrium flow (Pelto et al., 2008) in response to changes in mass balance and

climate forcing. Furthermore as suggested in section 2.5.1 and figure 2.24, by focussing attention upon those glaciers that have experienced large variations in PCT_p one can assess the degree to which glaciers are *flow-unbalanced* and identify which aspects of the glaciers' system are responding to climate forcing fastest. For example, the observation that PCT_x and PCT_a upon Hintereisferner adjust to the negative mass balance regime at the same rate as the glacier's terminus suggests that the glacier is *flow-balanced* where changes in the flow dynamics are synchronised with variations in glacier extent. Alternatively, Kesselwandferner is dynamically imbalanced where flow is accounting for a previous spell of positive mass balance despite snout retreat under current negative mass balance forcing. Accordingly, situations where glacier dynamics are out of synchronicity with current glacier mass balance regimes, as is the case with Kesselwandferner and Blue Glacier, can be identified through time variable observations of PCT_p .

Another observation suggesting that the PCT is suitable for use as an indicator of glacier health and climate forcing is that PCT evolution displays statistically significant correlation with glacier snout retreat. Observations of glacier snout fluctuation have long been established as one of the fundamental indicators of climate change (Dyurgerov et al., 2002; Hoelzle et al., 2003; Oerlemans, 2005; Oerlemans, 2012). Figure 4.8 reveals the linear relationship observed between variations in terminus position and variation in PCT_x position. PCT_x is observed to retreat upon glaciers that display snout retreat while glaciers experiencing snout advances also tend to display PCT_x advance as well. This observation further supports that the PCT is driven by, and therefore is indicative of, climate as PCT evolution appears to be driven by the same mechanisms that drives glacier advance and retreat. However, it is important to consider the observations of discordant behaviour between PCT_x and the glacier terminus observed upon Kesselwandferner and Blue Glacier. This highlights the interpretational complexity that results from the lagged response of glacier flow-field changes to climate perturbations.

The hypothesis that the PCT is a function of climate and thus glacier health is then given even greater credence when one compares PCT evolution with the recorded glacier mass balance histories in section 4.2.1. Theory suggests that if

climate in a region were to remain constant for a long time (decades – centuries), the geometry of non-surging glaciers in that locality would adjust so that the local submergence and emergence velocities were equal everywhere to specific net balance (Hooke, 2005). Net mass balance over the entire glacier, B_n , would equal zero resulting in a steady-state glacier and an unchanging three-dimensional surface. Thus as climate forcing and mass balance varies, so too must the glacier's flow dynamics in order to achieve a new geometric distribution that can remain in balance with mass balance and climate (Hooke, 2005). This can be observed upon Hintereisferner where PCT_x has visibly retreated as flow dynamics have been responding to an extended period of negative mass balance. As mass balance becomes increasingly negative and glacier retreat hastens across the European Alps due to rising temperatures (Braithwaite et al. 2012; Paul 2004; Oerlemans 2005), the flow dynamics of Hintereisferner begin to adjust so that emergent velocities can balance the loss of mass at the surface through increased melt. Therefore it is proposed here that as increased temperatures have caused surface melting to occur at higher elevations, flow dynamics have responded by driving emergent ice flow to the surface at higher elevations, forcing the planform curvature transition up-glacier, resulting in PCT_x retreat and increased PCT_a .

However, perhaps the more interesting observation is that PCT_x upon Kesselwandferner and Blue Glacier advanced during the observation period (figures 4.4 and 4.6). This is surprising given the evidence of glacier retreat over the observation period due to negative mass balance recorded at both localities. However, the picture becomes somewhat clearer when the PCT change is compared to the glaciers' mass balance history. Unlike Hintereisferner where data from field monitoring campaigns reveal long term, sustained negative mass balance, the plots in figure 4.5 and figure 4.7 reveal that both Kesselwandferner and Blue Glacier underwent prolonged periods of positive mass balance between 1964 -1981 and 1960 – 1976 respectively. It is proposed here that the longitudinal advance and reduction in elevation of the PCT_a observed on both glaciers is the result of the reorganisation of the flow-field driven by these extended periods of positive mass balance. As B_n becomes positive, thickening occurs over time in the accumulation area which increases the driving stresses (Hooke, 2005: section 2) resulting in faster flow and

longitudinal extension (section 2.2.2). Over time, these flow perturbations together with pre-existing velocity patterns non-uniformly redistribute the added mass as they move down glacier. Thus the redistribution of increased mass, through the reorganisation of glacier flow, resulted in the observed PCT_x advance.

These observations, although supportive, once again highlight the complexity that lag times present when assessing how glaciers are responding to climate forcing. Response times are to a large extent dependent upon longitudinal bed slope, mass balance gradient and the glacier's area-altitude distribution (Oerlemans, 2005). Accordingly, it has been proposed that response times for temperate alpine glaciers generally lie in the region of between 15 and 60 years (Cuffey and Paterson, 2010). This belief is supported by the observation of PCT_x advance between 1990 and 2000 on Blue Glacier and between 2000 and 2006 on Kesselwandferner, 14 and 19 years after the termination of each glacier's recorded period of positive mass balance. Despite this interpretational complexity these observations provide empirical evidence that the PCT is driven by climate albeit it on a delayed scale. However, great caution is required when making such claims due to the small and therefore non-representative nature of the sample. Unfortunately there is a dearth of data that enable comparisons between mass balance records and changes in the three-dimensional shape of valley glaciers, which means that studies such as this will be limited to working with small samples.

One final point worth consideration is the observation that overall PCT_x retreat on Hintereisferner was greater between the shorter time period between 2000 and 2006 (-282 m) than was recorded between 1971 and 2000 (-257 m). Even with potential lag times taken into account, the increase in PCT_x retreat may reflect observations that mean glacier area loss per decade in the Alps from 1985 to 1999 had accelerated by a factor of seven compared to the period 1850–1973 according to Paul et al. (2007). Thus the *increasing* rate with which PCT_x on Hintereisferner appears to be adjusting to climate forcing reflects similar observations of increasing rates of glacier wastage in the area (Haeberli et al., 2007; Hoelzle et al., 2003; Paul et al., 2004; Zemp et al., 2006).

By observing how the PCT changes in relation to changes in glacier extent and mass balance, we are able to improve our understanding of how and why the PCT relates to glacier health and climate forcing. Additionally, based on the results discussed thus far and those in chapter three, there is increasing evidence that enables one to accept the hypothesis that the PCT is indeed a function of glacier health and climate forcing. With this in mind, one can investigate what the PCT can tell us about how these sampled glaciers are responding to climate forcing.

4.3.2 Insights Provided by the PCT

4.3.2.1 *Hintereisferner, Kesselwandferner and Blue Glacier*

With our understanding of why PCT_x should advance or retreat under different regimes of mass balance and climate forcing, one can now begin to assess whether the glaciers are dynamically balanced or whether flow dynamics are out of synchronicity with each glacier's contemporary mass balance, which if so could lead to further changes in glacier extent.

As was suggested in section 2.5, studying PCT_p changes over time also enables one to identify whether different aspects of the glacier system are responding heterogeneously to climate forcing. On Hintereisferner, the PCT_p value remained relatively constant at a value between 0.33 and 0.35 between 1979 and 2006. However, PCT_p varied from 0.41 in 1971 to 0.29 in 2006 on Kesselwandferner and 0.34 in 1990 to 0.25 in 2000 on Blue Glacier. The relative constancy displayed by the PCT_p on Hintereisferner suggests that dynamic changes in the glacier's flow field are adjusting to climate perturbations at a similar rate to which the glaciers area/extent is. Thus one would consider this glacier to be flow or dynamically balanced where the glacier's flow-field vectors are adjusting to the increasingly negative mass balance (figure 4.3A) regime at a similar rate to which the glaciers areal extent is (Hagen et al., 2005).

This, however, cannot be said for Kesselwandferner and Blue Glacier as PCT_x on both glaciers displayed observable advances down glacier despite significant snout retreat on both. This resulted in lowering of the PCT_p values for the glaciers and thus indicates that both are dynamically out of balance and thus considered to be *flow-unbalanced*. As was stated earlier, PCT_x advance is

considered here to be a lagged response in flow dynamics to the extended periods of positive mass balance previously experienced by both glaciers. However, the slow response of glacier dynamics to climate perturbations resulted in PCT_x advance occurring during a time of negative mass balance as evidenced by the observed snout retreat. Thus it is clear that both Blue Glacier and Kesselwandferner are dynamically imbalanced. These findings are supported by the observations of Pelto et al. (2008) on Taku Glacier where the snout continued to advance and the glacier's flow continued to display evidence of being driven by a positive mass balance regime despite the glacier experiencing a negative mass balance at the time of observation in 2006. Pelto et al. (2008) attributed this behaviour to an extended spell of positive mass balance between 1946 and 1987. Similarly, they also identified snout thinning due to the prevailing negative mass balance regime towards the end of the monitoring period.

With this observation in mind, one could be left to wonder: what will happen to Kesselwandferner and Blue Glacier, and all other glaciers that display such behaviour for that matter, if negative mass balance trends are sustained and PCTs begin to migrate back up glacier as flow dynamics catch up with climate forcing? The PCT_x advance observed on both glaciers suggests that, at that time, the glacier flow dynamics were adjusting in an attempt to balance the effects of a positive mass imbalance. It would be fair to presume then that during PCT_x advance, the volume of ice transported down glacier from the accumulation area also increased, particularly if the previous spell of positive mass balance was due to increased accumulation. Nevertheless, the glacier termini continued to retreat despite the fact that flow dynamics were likely transporting disproportionately high levels of mass under positive flow balance conditions. This suggests that melt rates at the snout were high enough to negate the increase in mass being transported down glacier. The concern for the glaciers' sustainability then increases when one considers the fact that the flow dynamics will eventually have to "catch-up" with climate forcing. If the current negative mass balance trends on these glaciers are in part the result of reduced accumulation and should persist, PCT_x retreat will occur, resulting in a reduction in the volume of ice being transported to lower altitudes. Considering that these glaciers continued to retreat during PCT_x advance, it is likely that

these glaciers will retreat at an even greater rate as flow dynamics adjust towards equilibrium with current mass balance and climate forcing.

Nevertheless, not only does the PCT enable one to assess the degree to which glaciers are dynamically balanced, it also enables greater insight as to the mode in which glaciers are responding to climate perturbations. As shown in figure 4.2E between 1979 and 2000, the PCT on Hintereisferner displayed evidence of scenario 6 undergoing planar retreat whilst maintaining a constant elevation (or producing elevation variance too small to be detected with the available data). As was discussed in section 2.4.3.6 this suggests that surface down-wasting has occurred and that changes in glacier surface elevation are due to high melt rates rather than changes in the flow dynamics. Consequently, this observation suggests that although flow dynamics are changing in response to negative mass balance on Hintereisferner, the rapid glacier retreat is likely to be due to very high melt rates rather than changes in accumulation. These high melt rates are likely the result of increased temperatures, resulting in surface down-wasting. This idea is supported by figure 4.12 that displays winter and summer mass balance relative to annual mass balance. The plot shows that despite a positive trend in winter balance (accumulation), the summer trend appear to become increasingly negative due to increased temperatures leading to greater melt rates, driving the overall negative annual mass balances.

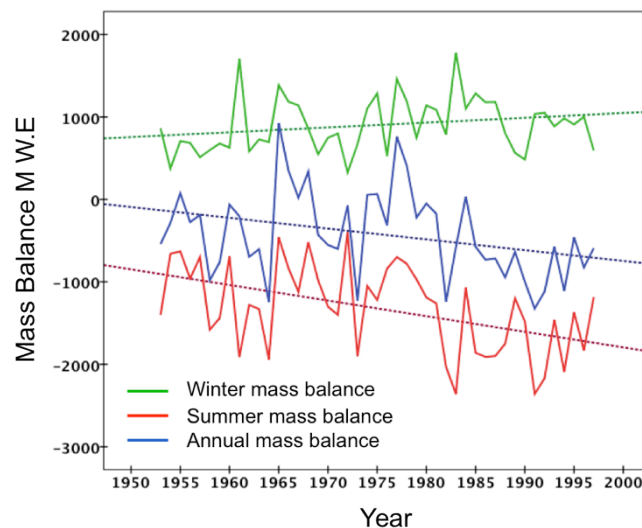


FIGURE 4.12 – HINTEREISFERNER MASS BALANCE
Comparison of summer and winter mass balances and their influence over the annual mass balance of Hintereisferner

The observation that the PCT suggests down-wasting is occurring on Hintereisferner is supported by observations from numerous studies (e.g: Haerberli et al., 2007; Hoelzle et al., 2003; Paul et al., 2004; Paul and Haerberli, 2008; Paul et al., 2007). Most suggest that increases in temperature are the main cause for the glacier retreat and down wasting recorded in the European Alps. Paul et al. (2007) added that their observations of increasing rates of glacier down-wasting in the European Alps indicated that the glaciers were not able to primarily adjust to the current climatic conditions by a dynamic retreat towards higher elevations. Instead enhanced melting resulted in surface elevation reduction through down-wasting, an occurrence that has clearly been observed on Hintereisferner. However, the accelerated PCT_x retreat observed on Hintereisferner between 2000 and 2006 suggests that the glacier's flow dynamics may be closer to dynamic equilibrium with the glacier's mass balance than they were between 1979 and 2000. This once again highlights the need to take time lags into account when assessing glacier response to climate forcing.

In a similar vein, work published by Oerlemans (2005) and Braithwaite and Zhang (2000) supports the opinion that glacier fluctuations over decades to centuries are primarily driven by temperature changes and that a 25% increase in annual precipitation is typically needed to compensate for the mass loss due to a uniform 1 K warming. These observations may go some way in explaining why PCT_x advance on Blue Glacier and Kesselwandferner, possibly due to increases in accumulation, did not result in glacier advance. Unfortunately, precipitation and melt data do not exist for these glaciers. Accordingly, it is not possible to verify whether PCT_x advance did not result in glacier terminus advance due to increases in temperature and melt at the snout.

Finally one of the drivers behind this research was the question of the representativeness of benchmark glaciers when extrapolating their mass balance records across the entire glacier populous (Braithwaite, 2009; Fischer, 2010; Hoelzle et al., 2003). This is because glaciers close to one another have been observed to display different responses when adjusting to relatively uniform climate forcing over a regional scale (Braithwaite et al., 2012; Paul et al., 2004). This is reflected in the results where the PCT on Hintereisferner and Kesselwandferner display dramatically different behaviour over the same

monitoring period, despite both glaciers being located in the same valley system with termini only 2 km from one another and being subjected to similar climates. These variations in glacier response can, to an extent, be accounted for by each glacier's different area-altitude mass distribution (Raper and Braithwaite, 2009). Nevertheless, the observations suggest that monitoring the PCT is extremely useful as it enables one to identify heterogeneous glacier responses to climate forcing on a regional scale. Furthermore, the high variability in PCT change observed between Hintereisferner and Kesselwandferner may also be due to varying accumulation histories on each glacier. As highlighted by Oerlemans (2005), precipitation anomalies normally have smaller spatial and temporal scales than those of temperature anomalies, therefore changes in temperature, in this case warming, tend to be spatially homogenous on a regional scale whilst spanning larger timescales. As a result, it is suggested here that the period of positive mass balance that provided the driving force for PCT_x advance observed Kesselwandferner was the result of *increased accumulation*. However, PCT_x advance occurred whilst temperatures continued to rise, which explains why the snout continued to retreat despite the advancing PCT_x driven by increases in accumulation. Increases in glacier accumulation during atmospheric warming can be explained by the fact that a uniform 2K rise in atmospheric temperature could potentially increase the atmosphere's moisture carrying capacity by 15% and lead to an increased frequency of heavy precipitation events (>30 mm/day) by more than 20% (Frei et al., 1998). Over high elevation topography, such as the Alps, these heavy precipitation events would fall as snow.

4.3.2.2 Svalbard

The minimal change in average PCT_p across the region between the two observation dates suggests that overall, glacier flow and glacier extent responses to climate forcing are generally occurring at similar temporal scales. Vastly different response rates of flow dynamics compared to variations in glacier extent would have been evidenced by a large deviation from the 0.35 average PCT_p recorded in 1936. Nonetheless despite the low variation in mean PCT_p between the two dates, the results suggest that there is a great deal of spatial variation in how glaciers in the region are responding to climate forcing.

As had been identified elsewhere (Paul and Haeberli, 2008; Paul et al., 2007; Scherler et al., 2011b), considerable variation in the response to climate forcing over a relatively small geographical region was observed in the Adventalen glaciers. The variety of glacier responses and thus scenarios of PCT change observed in the sample may to a degree be influenced by non-climatic variables such as glacier aspect, glacier hypsometry and thermal regime. However, it is suggested here that a further driver for the variability observed in PCT evolution in the Advantalen region is heterogeneous accumulation rates across the sample. As was discussed in the previous section, relative to changes in temperature, changes in precipitation and thus accumulation tend to be more variable, both spatially and temporally and are thus likely to provide the driving force behind variable PCT response. It is important to point out here that longitudinal bed slope plays an extremely important role in PCT evolution due to the close relationship between bed slope and glacier ice flow velocity (Oerlemans, 2012). However the importance is more relevant when assessing the lag times that occur between climate forcing and PCT response. It is fair to assert that assessments of bed gradients would not explain why some PCTs advanced in the region whilst others retreated. Such variable behaviour is thus believed to be an indicator of spatially variable climate controls, namely variations in accumulation rates. As was the case with Kesselwandferner and Blue glacier, this observation, along with the fact that the PCT requires longer to respond to climate forcing than variations in terminus position go some way in explaining why a number of the glaciers in the sample continued to retreat despite concurrent PCT_x advance (see figure 4.8).

In figure 4.11 the variable responses of PCT across the sample reveals regional patterns of PCT and glacier variation. For example, the high proportion of glaciers displaying scenarios 4 and 5 in the southwest of the study area suggests that rapid melt and down-wasting is occurring in this locality at a rate faster than which flow dynamics can respond. Alternatively, the high proportion of scenario 6 glaciers located more centrally suggests that in this locality, flow dynamics are responding to changes in glacier mass balance at a faster rate. However, it is important to consider the possibility that partial glacier surges may be misinterpreted as rapid response to climate change, due to the thinning in the upper regions of a glacier as a consequence of mass displacement. This is

plausible considering results from Sund et al. (2009) suggest that a majority of current Svalbard glaciers are surge type, as already proposed by Liestøl (1969). As a result the thinning in the accumulation of the southwest glaciers could be considered to be the result of partial glacier surges. However, the vertical resolution of the utilised maps is too poor to clarify the situation because even if thickening had occurred in the ablation area in response to a surge event, the resulting snout thickening would not have been visible in the maps to verify this proposition.

Nonetheless this observation highlights the importance of understanding how glacier dynamics are behaving as attributing observations of glacier thinning and thickening directly to climate forcing can lead to misinterpretation (Hagen et al., 2005). Hagen et al. demonstrated that glaciers in Svalbard can still thin or thicken even if mass balance is zero. This is due to short-term variations in flow that are unrelated to climate forcing. They stated that the longitudinal surface profile on a surge-type glacier would gradually change during a long quiescent phase, with increasing altitude in upper parts and decreasing altitude in lower parts even if the net surface mass balance is zero and in balance with the current climate. As a result, longitudinal centreline geometry changes alone cannot be used to assess the surface mass balance without knowledge of the dynamics. This is where observing PCT evolution comes to the fore. By observing long-term PCT evolution in tandem with geodetic mass balance observations, one can be confident that any significant glacier thinning observed alongside PCT retreat is likely to be the result of variations in mass balance and climate rather than surge events.

As previously mentioned, observations of changing PCT_p values can be used to identify the degree to which glaciers are *flow balanced*. The results displayed in figure 4.11 highlight that there is much greater variation in PCT_p between the two dates in the southwest coastal glaciers, which can be explained by the high rates of snout retreat and thinning, relative to the slower retreat of PCT_x . This suggests that glacier flow dynamics are adjusting at a slower rate to climate forcing and negative mass balances than that of the glacier's area and length. As was mentioned earlier, this may also be evidence that the current observed glacier retreat is driven predominantly by an increase in temperature rather

than a reduction in accumulation. This idea is supported by meteorological records from Longyearbyen which show that summer temperatures have been rising since the 1960s (Førland et al., 2003) with a warming trend $0.04^{\circ}\text{C yr}^{-1}$ in the summer months (JJA) for the 30-year period between 1967 and 2006. This indicates that the driver for Svalbard glacier changes is warmer summer temperatures causing additional melt (Kohler et al., 2007).

However in the central region of the study area, PCT_x retreat is much higher and appears to have exceeded snout retreat. This rapid change in PCT position could potentially be driven by a continued reduction in accumulation as Hagen et al. (2003) identified a decreasing trend in winter accumulation since 1990. Similarly, James et al. (2012) observed enhanced thinning in the accumulation areas of glaciers located in Western Svalbard. They suggested that the observed thinning may have been due to an imbalance between mass input and submergence velocities in the accumulation area. Thus one could then suggest that as the reduction in accumulation has driven PCT_x retreat and PCT_a increase, the reorganisation of the glacier flow-field coupled with the identified regional warming may have had a hand in the extremely high rates of snout retreat observed in the central region of the study area. The fact that these glaciers' snouts have retreated over 5 times the average distance of that observed across the entire sample suggests that the observed PCT_x retreat and the associated reduction of mass being transported down glacier has led to the extremely high snout retreat rates. This observation justifies the concern that Blue Glacier and Kesselwandferner will retreat at a faster rate when their PCTs retreat up-glacier in response to current negative mass balance.

4.4 Summary of outcomes

- As anticipated, the results highlight that recording planar changes in the position of the PCT (PCT_x) is imperative to ensure that observations of PCT_a constancy are not misinterpreted as evidence of the PCT or glacier being in an equilibrium state.
- The mean PCT_p of 0.36 generated from all glaciers across the observation sample compares well to the mean PCT_p (0.39 ± 0.11) observed in chapter three. This consistency lends support to the assertion that the PCT is a dynamic characteristic of glacier flow that reflects the glacier's self-organising nature and attempts to remain in balance with climate forcing.
- PCT_x retreat was observed as flow dynamics adjusted in response to sustained negative mass balance trends. Conversely, PCT_x advance was observed in response to an extended period of positive mass balance. However a lag in PCT response to climate forcing (mass balance records) was identified. This needs to be carefully considered when using observations of PCT change to gain insight into how glaciers are faring in today's climate. Nevertheless, this observation provides strong evidence to support the belief that the PCT is a climatically driven glacier health signal.
- Observations of PCT_p variation across all glaciers in this chapter demonstrate how the PCT can be used to assess the degree to which flow dynamics and glacier extent (length / 2D-geometry) are responding to climate forcing (a)synchronously.
- Hintereisferner displayed evidence of being flow balanced where changes in flow dynamics (PCT) occurred at a similar rate to glacier retreat that resulted in negligible variation in PCT_p values between observations. However, observations of significant changes in PCT_p were identified on Kesselwandferner, Blue glacier and a number of glaciers in the Svalbard sample. Accordingly, flow dynamics present in these glaciers are responding at a different rate to climate forcing than other glacier variables such as length. This suggests that these glaciers are flow unbalanced and thus further dynamically imbalanced with climate forcing than those that display minimal variation in PCT_p between observations.
- PCT observations in Svalbard reveal that the majority of glaciers displayed evidence of scenarios 4, 5 and 6 suggesting that the glaciers in the region have experienced high rates of thinning and retreat since 1946. Particularly concerning is the high frequency of scenario 4 and 5 glaciers identified in the southwest of the region. Here PCT observations

highlight the situation where surface thinning and mass ablation is occurring in response to climate forcing at a far greater rate than that of the flow dynamics.

- The highest levels of snout retreat in Svalbard occurred on those glaciers that experienced the greatest levels of PCT_x retreat. This suggests that a change in glacier flow that causes the PCT to retreat up-glacier is likely to result in greater rates of snout retreat than would have occurred with similar warming but no variation in flow dynamics and PCT_x position.

Chapter 5 Guidelines for PCT Assessments

Chapter two developed the theoretical understanding as to why PCTs form upon glacier surfaces and how this formation process is strongly controlled by the influence of climate. The chapter then went on to discuss the ways in which PCTs are expected to behave under differing forms of glacier response to climate forcing. These theorised assertions were then supported and enhanced in chapters three and four through empirical testing by recording and comparing PCT position and evolution with other glacier-climate measures such as mass balance, ELA, AAR and length changes. The results so far appear to confirm our theoretical understanding that the PCT is, to a large degree, a function of climate forcing and that there is potential to use the PCT to inform us of glacier-climate interactions in regions where few data exist. Accordingly the ultimate goal is to use observations of the PCT from a large sample of glaciers, about which relatively little is known, in order to identify their health state and gain insight into how climate in the study area may have been changing.

However before this takes place it is necessary to highlight how the theoretical understanding of the PCT developed in chapter two combined with the observations from chapters three and four can be translated in a way that enables PCT observations to be applied to the task of assessing glacier health and climate forcing. Accordingly, the following section will take stock of our newly developed understanding of the PCT and will detail how PCT observations may provide information concerning health and climate information for glaciers about which very little is known, based on the existing understanding and observations developed in earlier chapters.

The final step in strengthening our understanding of PCT – climate interactions is to test the guidelines and hypotheses developed in this chapter through a number of glacier forcing experiments using the iSOSIA glacier flow model developed by David Egholm (Egholm et al., 2011) (chapter six).

5.1.1 Observations of PCT_a

As discussed in chapter two, PCT formation results from differential ice flow regimes present in the accumulation and ablation area. As a result, the PCT represents the boundary between the submergence flow driven, concave transverse ice surface in the accumulation area and the emergence flow driven, convex transverse ice surface observed in the ablation area. Under long-term steady state conditions, this boundary is hypothesised to be located close to the glacier's ELA. This is supported by the findings of section 3.3.2 where the PCT_a was observed to correlate well with ELA₀, which represents the calculated position for the ELA under steady state conditions (figure 3.6 and 3.8). However, as was identified in section 3.4, the majority of glaciers observed are not in steady state as evidenced by the negative mass balances observed as well as the large elevation offsets observed between the ELA and ELA₀. Accordingly, unless the glacier is known to be in steady state, the PCT_a is not an appropriate measure for estimating climatic ELA (Cogley and McIntyre, 2003).

Nevertheless, PCT_a observations still provide an extremely useful measure as they provide insight into the dynamic response of glaciers to climate forcing. Observations of the differing rates of response to climate forcing displayed by the climatic ELA and PCT lead to the finding that the flow driven PCT is believed to lag considerably behind the ELA. As a result, by comparing contemporary ELA (or proxies such as the end of summer snowline) to the PCT_a, it enables one assess the extent to which glacier flow is out of synchronicity with the current climate. Furthermore, differences in PCT_a across a region will reflect the spatial variations in temperature and precipitation that occur across a study area.

Chapters two and four also demonstrated a further utility of the PCT by discussing and highlighting its effectiveness in recording changes in glacier state over time. Observations of changes in PCT position over time confirmed the assertion that it is necessary to record changes in planar position (PCT_x) as well as elevation in order to prevent misinterpretation of PCT variation. Furthermore, observations from chapter four supported the idea proposed in the previous chapters that PCT is a function of climate that can be recorded in a similar manner to that of the ELA. This is due to the observation that down-

glacier advances of PCT_x to lower elevations could be explained by evidence of positive mass balance or glacier advance. Similarly, strongly negative mass balance and glacier retreat most commonly occurred with increases in PCT_a and PCT_x retreat. Therefore it is hypothesised here that, as has been done with ELA records, long-term monitoring of PCT_x and PCT_a changes through time can be used as evidence of changes in glacier mass balance and thus climate. Specifically, observations of PCT_x retreat and increases in PCT_a are indicative of negative glacier mass balance due to reduced accumulation and/or increased melt and that PCT_x advance, concurrent with PCT_a lowering, provides evidence of positive mass balance changes due to increased accumulation and/or reduced melt. However, it is key to reiterate the need to consider the lag times involved between climate forcing and dynamic glacier response when drawing climate and glacier health signals from PCT observations.

5.1.2 Proportional PCT elevation (PCT_p)

Observations from chapters three and four provided intriguing insights concerning how PCT_p could be utilised to inform us of the way in which glaciers are responding, and perhaps will respond, to current climate forcing. The limited spread of PCT_p values, recorded across a wide and diverse sample of glaciers, evidences the complex and self-regulatory adjustment mechanisms that glaciers undergo in order to be balanced with the forcing climate. It is hypothesised here that the common PCT_p values observed indicate that glacier flow-fields adjust and respond to climate forcing in such a way that glacier three-dimensional ice surface geometry remains homogenous, irrespective of variations in constraining basin geometry, glacier size, thermal

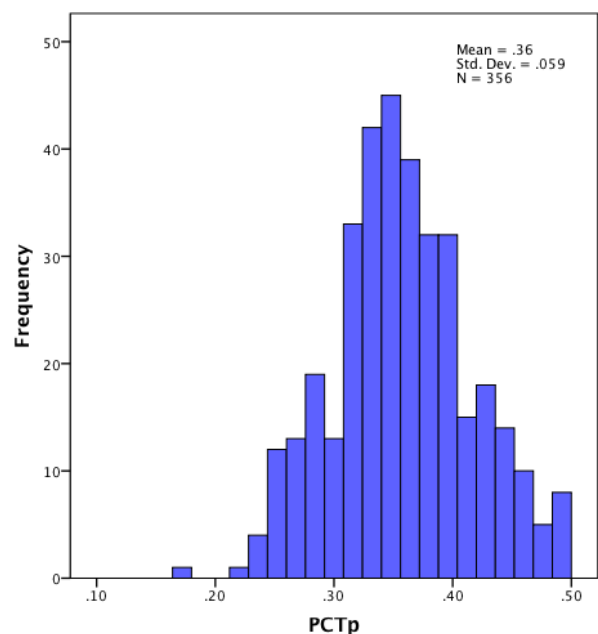


FIGURE 5.1 - PCT_p VALUES
 PCT_p values for all outputs from each glacier in chapter three and four

regime, aspect or longitudinal slope profile across samples.

Furthermore, the observations in the previous two chapters and the histogram displayed in figure 5.1 highlights the situation where the PCT_p tends towards a mean value of 0.36, where the PCT is located 36% of the total ice elevation range above the minimum ice elevation. Due to this apparent tendency for glaciers to adjust their surface so that the PCT is located 36% up-glacier in elevation from the minimum ice elevation, it is speculated here that glaciers will display a PCT_p around 0.36 when flow balanced. With this in mind one can then begin to infer information concerning how glaciers are responding to climate forcing by observing whether their PCT_p values deviate significantly from a range of ~0.3 to 0.5 and how these values change over time. It is important to note here that the 0.3 – 0.5 range is an initial estimate based roughly upon the variance within the observed PCT_p values recorded thus far. However, deciding upon suitable, informative PCT_p ranges is a complex task and one that requires greater attention and consideration. Accordingly, this issue will be discussed at length in section 8.4.

In chapter four a number of cases were identified where PCT_p values remained relatively uniform for individual glaciers despite clear evidence of PCT_x advance and retreat between different observation dates. This further supports the assertion that glaciers adjust the structure of their flow-field, and maintain a uniform PCT_p , in order to preserve “*flow-balance*” with their three-dimensional mass distribution and extent. However, PCT_p values were also observed to deviate significantly from the 0.3 - 0.5 range, both spatially and temporally. These observations provide us with the opportunity to use empirical evidence in order to formulate hypotheses as to the driving mechanisms that would produce such deviating PCT_p values.

Based upon the observations from chapter four, it could be identified that the lowest PCT_p values occurred when PCT_x remained stationary or advanced during glacier terminus retreat, or when glacier retreat rates exceeded that of the PCT_x . Such observations are evidence of glaciers being “*flow-unbalanced*” where changes in the organisation of the glacier flow-field are out of sync with variations of glacier area and length. This can be attributed to the lag times associated with climate forcing and the resulting dynamic response of the

glacier (Oerlemans and Fortuin, 1992; Oerlemans et al., 1998; Raper and Braithwaite, 2009). Accordingly chapter four also revealed the situation where PCT_p values were disproportionately high (close to the maximum ice elevation). This often occurred in situations when the PCT was observed to retreat to higher elevations at a rate greater than that of the glacier snout. This could also be identified in the Karakorum glaciers discussed in section 3.3.3 where heavy debris mantles influenced the lowest elevations at which the snout could remain. Not only do such observations enable us to assess the degree to which flow dynamics and glacier extent are responding to climate forcing at different rates for “*flow-unbalanced*” glaciers, it also enables one to formulate theories as to the forcing mechanisms that would drive these discrepancies in glacier response to climate perturbations evidenced by varying PCT_p .

It is hypothesised here that disproportionately high PCT_p values are likely to be the result of variations in mass accumulation. This is because a prolonged reduction in accumulation is envisioned to lead to PCT_x retreat to higher elevations, while little to no change in ablation at the snout results, in the short term, in relative snout constancy. As a result, until the impact of the reduced accumulation propagates down-glacier to the ablation area, PCT_x will retreat at a rate greater than the terminus. Furthermore, it could be suggested that a high PCT_p value acts as a precursor to high snout retreat rates. The reduction in accumulation, evidenced by the PCT retreat, is expected to propagate down glacier with time, starving the snout of mass replenishment leaving ablation unabated resulting in ice wastage and retreat. This is evidenced to a degree by the observations from the central study area of Svalbard in chapter four whereby the highest rates of snout retreat were recorded upon glaciers that displayed the highest levels of PCT_x retreat. Thus, if high PCT_p values do indeed reflect changes in flow dynamics due to reduced accumulation, such observations can be used to identify glaciers that may be, or soon to be, undergoing accelerated rates of snout retreat.

Comparably, it is then suggested here that disproportionately low PCT_p values are the result of increased snout retreat caused by temperature and thus melt increases. The occurrence where glacier snout retreat occurs despite no or little change in PCT_x is believed to be evidence of “passive retreat”. The description

of passive is suggested because in such situations, the glaciers reveal little evidence of a dynamic response in ice flow. Such occurrences are suggested here to be due to the faster speed with which glacier snouts retreat under increased melting when compared to that of flow dynamic adjustments. This is not to say that the glacier will not eventually demonstrate a dynamic adjustment, or that no changes in accumulation rates have occurred, more that climate forcing has altered abruptly whereby the only observable response is by mass wastage at lower elevations during a short time frame. Accordingly it is hypothesised here that low PCT_p values are evidence of passive glacier retreat whereby changes in ice mass area are driven predominantly by increased temperatures and thus greater melt at the snout.

Although it has been stated that glaciers that are flow balanced will display a PCT_p between 0.3 and 0.5, this is not to say that all glaciers with flow dynamics adjusted to display a PCT_p of ~ 0.36 are in steady state. This is because PCT_p values in this numerical region may be indicative of a *flow-balanced* glacier but the glacier's state may still be out of balance with climate in a more general sense. This situation is evidenced by Hintereisferner, chapter four, where PCT_p values remained relatively uniform through time, despite the glacier being out of synchronicity with climate as evidenced by its negative mass balance record. Such a situation could also be verified by comparing PCT_a with the modern day ELA (or proxy of), where the glacier can be considered to be nearer equilibrium, the closer PCT_a locates to the ELA.

The empirical observations from the previous two chapters, combined with the developed understanding of the importance of three-dimensional ice surface geometry in chapter two, have been utilised to develop the hypotheses and propositions put forward in this chapter. The next step is to now test these hypotheses and validate the empirical observations made thus far through computational ice flow simulations.

Chapter 6 Computational Ice Flow Simulations

In order to test the hypotheses and propositions put forward in chapter five, PCT evolution and characteristics will be observed during numerous glacier flow simulation experiments. This chapter uses the iSOSIA glacier flow model developed by David Egholm (Egholm et al., 2011) to focus upon how the PCT changes upon glaciers with differing characteristics under various forcing mechanisms. These simulations will also shed some light on the extent that the PCT is controlled by non-climatic, confounding factors.

6.1 Methodology

6.1.1 iSOSIA

Previous models used to simulate the flow of alpine glaciers in steep rugged terrain have often built upon the shallow ice approximation (SIA)(Hutter, 1983) where ice is driven by local gradients in ice surface elevation and ice thickness. However, the SIA was developed to approximate flow in larger interior portions of ice sheets and thus neglects the longitudinal and transverse stress gradients that characterise the complexity of mountain glacier flow. The iSOSIA model overcomes these drawbacks through the depth integration of these “higher order” stresses by including extra terms from the full second-order shallow ice approximation (SOSIA) (Baral et al., 2001). This is of great significance given the importance of longitudinal and transverse stress gradients in PCT formation (section 2.2.2). The model’s ability to reproduce processes and glacier characteristics that are observed empirically has been scrutinised and reported upon positively (Egholm et al., 2011; Pedersen and Egholm, 2013). For a thorough description of the model frame work and example testing, the reader is directed to Egholm et al. (2011). The model runs were conducted using a grid resolution of 100 m and a variable time step that depended upon ice flux. The time step varied from 14 days for the highest ice flux to 36 days during the lowest ice flux.

The modelling was conducted by D. Egholm and the design of the experiments and the analysis of the results were conducted by R. Hayes.

6.1.2 Study area

The study area used for the model simulations is displayed in figure 6.1. It consists of an ice free, previously glaciated topography covering an area of around 240 km² in the southern Chilean Andes roughly 400 km south of Santiago (Lat-36.894° Long-71.147°). The four main trunk valleys (numbered in the figure) oriented northeast into the large valley to the centre-right of the image in figure 6.1 are the focus of the glacier simulations. This area was chosen due to the varying geometric characteristics of the valleys contained within. Valleys 1 – 4 range from small, steep sided, cascading, single basins (1) to larger, even, compound basin type valleys (2). They also display varying degrees of “V” to “U”- shape valley cross-profiles. These variations in valley type will provide insight as to the degree in which the geometry of the constraining topography controls the locations and characteristics of the PCT.

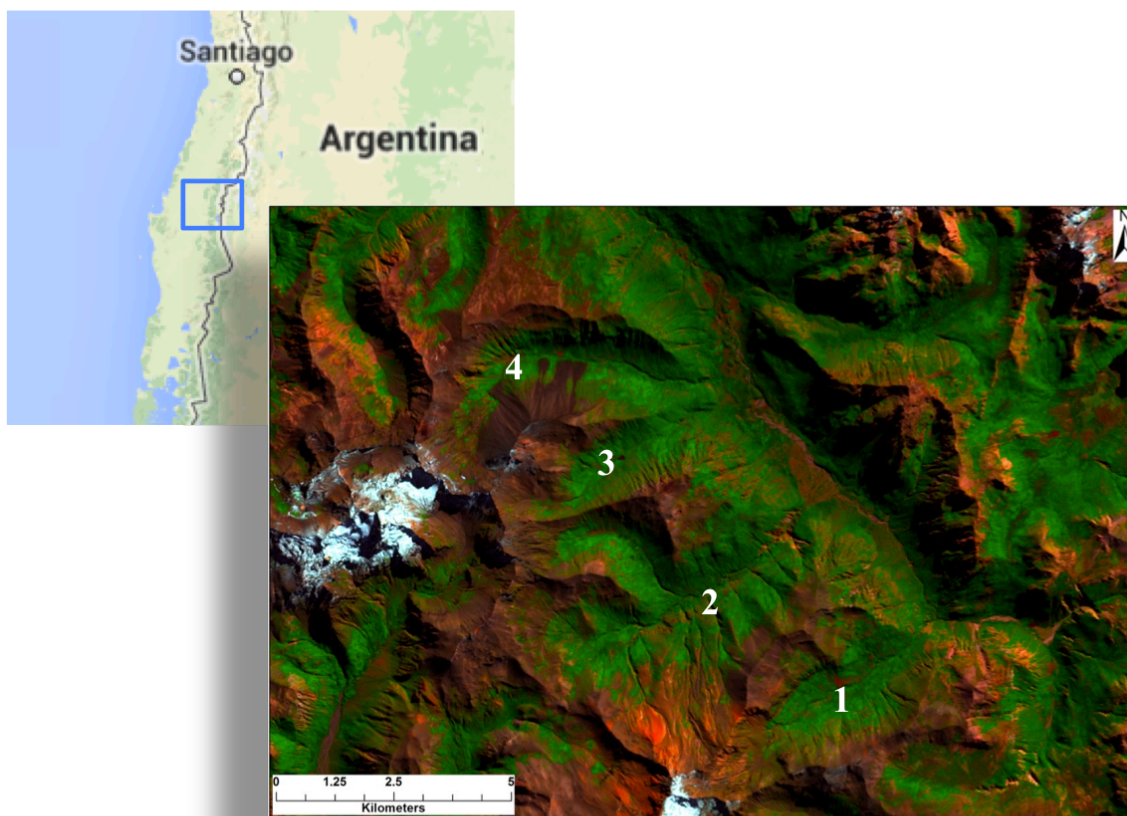


FIGURE 6.1 – MODELLING STUDY AREA.
Landsat image of the study area in the Chilean Andes (Lat-36.894° Long-71.147°)

6.1.3 Model runs

To test how PCT behaviour varies under differing topographic and climatic conditions, glacier fluctuations were forced through numerous simulations with different climate drivers. These included forcing glacier fluctuations through changes to accumulation rates, changes to ablation rates and adjustments of the ELA. Given the importance of plastic deformation in the formation of the PCT, model runs were also conducted with and without basal sliding enabled in order to test whether sliding has an observable effect on PCT behaviour. Furthermore, the variable valley geometries in the study area will provide useful insight into the extent to which valley shape influences PCT behaviour.

6.1.3.1 ELA variation

To test the impact of changes in ELA upon the location of the PCT, three experiments were conducted. The first was designed to identify how the PCT responds to a gradual change in ELA, slow enough so that the glaciers remained in steady state. The second and third were designed to test how the PCT responds to abrupt but sustained glacier advance and retreat caused by a lowering and raising of the ELA respectively, thus allowing the glaciers to depart from steady-state conditions.

6.1.3.1.1 Steady state advance

In this experiment, the glaciers were forced to advance / retreat using the fixed mass balance curve displayed in figure 6.2 and gradually reducing the ELA from 1950 masl to 1750 masl over a 10,000 yr simulation in order to enable the glaciers to remain in steady state. This experiment not only enables one to test the relationship between the PCT and ELA on glaciers in steady state, it allows one to assess the degree to which gross valley geometry affects PCT position. Confounding factors that are known to influence glacier flow velocities such as changes in valley width, ice falls, valley confluences and variable longitudinal bed slope (Nye, 1952) can be observed to see whether they exert an measurable influence over the PCT.

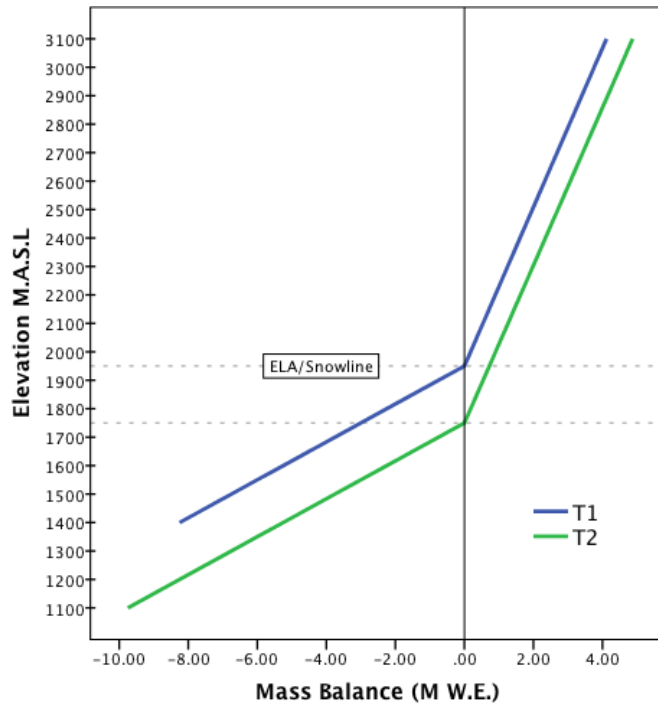


FIGURE 6.2 – STEADY STATE MASS BALANCE FORCING
Mass balance curves used to force gradual glacier advance by lowering the ELA 200 metres

6.1.3.1.2 Abrupt ELA decrease and glacier advance

In order to gain greater insight into the lag times associated with changes in ELA and the response of the PCT (an interpretational limitation highlighted in section 3.4) it was necessary to perturb the ELA abruptly and observe the response of the PCT. In this and the following experiments, the model parameters allow the glaciers to depart from equilibrium and re-adjust until an equilibrium state is reached. For this model run, the same mass balance curve was used again (figure 6.2). However in this case, after allowing the glaciers one hundred years to equilibrate with an ELA at 1950 masl, the ELA was abruptly lowered to 1750 masl. The PCT_p was also monitored throughout this experiment in order to assess whether changes in PCT_a and PCT_x preceded or lagged behind changes in the glaciers terminus position.

6.1.3.1.3 Abrupt ELA increase and glacier retreat

The setup for this experiment follows that of 6.1.3.1.2 however with the alteration that the ELA increases in elevation abruptly from 1750 to 1950 masl.

6.1.3.2 Variable retreat forcing mechanisms

As glacier extent and mass balance are determined by rates of both accumulation and ablation, a change in either of these forcing mechanisms is

likely to have an observable affect on glacier size, dynamics and ultimately health. Consequently, forcing glacier retreat through a reduction in accumulation whilst leaving the ablation curve unperturbed may produce distinctly different PCT behaviour than where glacier retreat is forced by increased ablation alone. Accordingly, separate glacier retreat simulations were run using these different forcing regimes. These simulations are outlined below.

6.1.3.2.1 Accumulation-forced retreat

As with the *Ablation forced retreat* simulation, the glaciers were perturbed in the 101st year. However, in this case the gradient of the mass balance curve above the ELA reduced from 3/2 to 1/2 metres of melting ice per year per degree (temperature lapse rate: 0.6K per 100 m in elevation) resulting in a reduction in accumulation by a factor of three whilst maintaining the original ELA and ablation conditions figure 6.4.

6.1.3.2.2 Ablation-forced retreat

The glaciers remained in steady state for the initial one hundred year cycle with the ELA constant at 1950 m.a.s.l with the mass balance curve displayed in figure 6.3. On the 101st year, the gradient of the mass balance curve in the ablation area increased from 20/9 to 60/9 metres of melting ice per year per degree (temperature lapse rate: 0.6K per 100 m in elevation) in the ablation area, effectively tripling the ablation rate, whilst leaving the ELA and accumulation gradient unperturbed. The change in the mass balance forcing was sustained and the model run continued until the glaciers achieved a new equilibrium state.

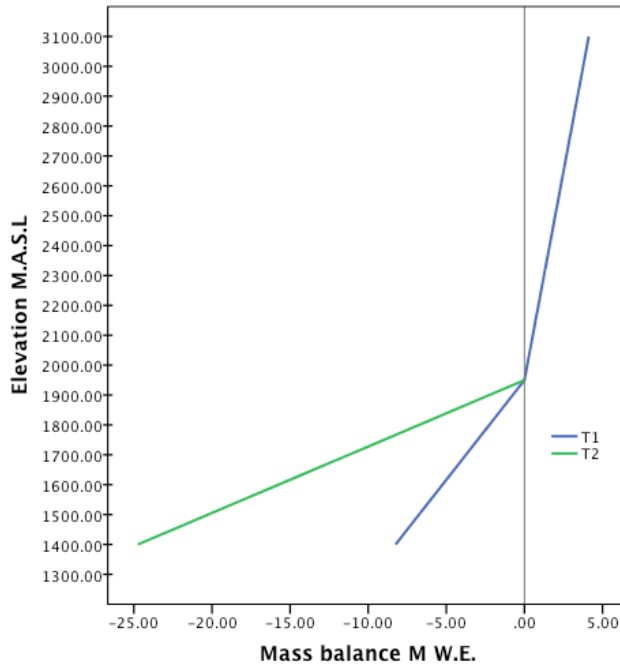


FIGURE 6.3 – ABLATION FORCED CHANGE
 Glacier retreat forced from initial conditions (T1) by increasing ablation rates whilst holding accumulation and ELA constant (T2).

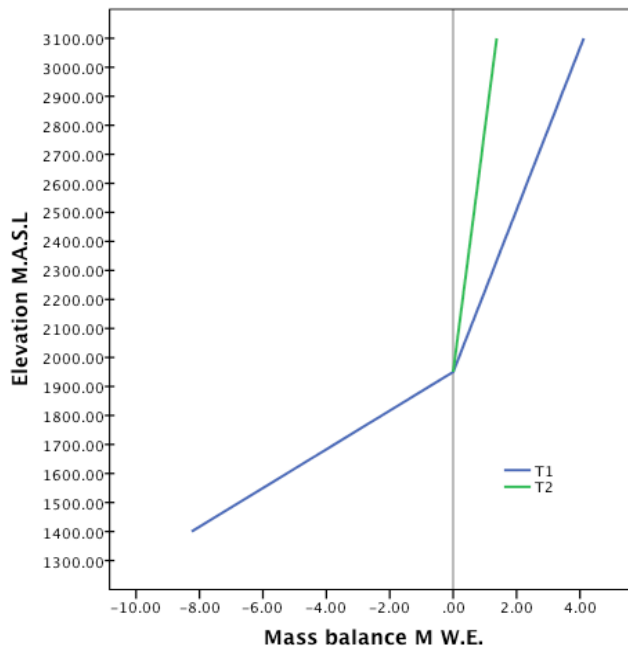


FIGURE 6.4 – ACCUMULATION FORCED CHANGE
 Glacier retreat forced from initial conditions (T1) by decreasing accumulation rates whilst holding ablation rates and the ELA position constant (T2).

6.1.3.3 Basal sliding vs no basal sliding

Given the importance of internal deformation in the creation of the PCT (chapter 2), an experiment was conducted to identify whether glaciers experiencing basal sliding produced PCTs in a manner not compatible with our

interpretations thus far. Using the mass balance curve displayed by the blue line in figure 6.2 the glaciers were forced to equilibrium with an ELA at 1950 masl during two simulations. In the first simulation, glaciers were restricted to mass transport through internal deformation only. In the second simulation, the iSOSIA model enabled basal sliding to be controlled according to the bed roughness parameter derived from Schoof's (2005) formulation. For the sliding experiment, the C (roughness) parameter of 0.42 was chosen.

It should be noted that sliding was enabled for all of the other experiments outlined in section 6.1.3.

6.1.3.4 Assessing confounding factors

As identified by Nye (1952), topographic characteristics can have a significant impact on longitudinal strain rates and given the importance of longitudinal strain rates in forming the PCT, the model runs in this chapter provide a good opportunity to identify how PCTs evolve in various topographic settings. The key topographic features expected to cause variation in longitudinal strain and thus effect PCT location, include areas of valley narrowing, ice confluences and ice falls (localised increases in longitudinal bed slope) (figure 6.5). The experiments also offer the opportunity to assess how variable glacier hypsometry affects PCT location, for example the potential accumulation basin in valley 2 is substantially larger than that of valley 3.

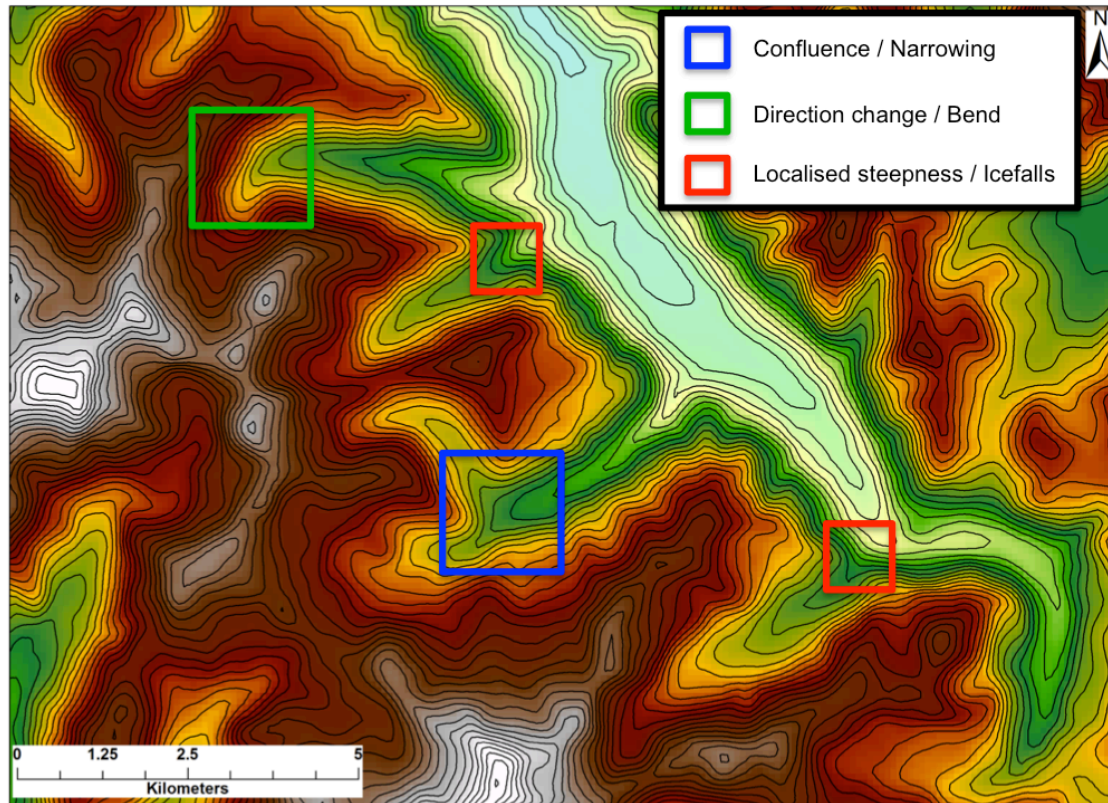


FIGURE 6.5 – POTENTIAL TOPOGRAPHIC CONTRLS ON PCT FORMATION
STRM DEM of the study area with potential confounding factors highlighted

6.1.4 PCT and glacier attribute extraction

The topography upon which the glacial simulations were forced was generated from a clipped SRTM tile in UTM projection (see section 3.2.2.1.1 for technical details for SRTM data). The model simulations generated two key outputs, a DEM file of the ice surface and an ice mask file for each time-slice, both at 100 m resolution. Elevation contours with 25m interval spacing were then generated using the output ice surface DEMs.

PCTs were visually identified and mapped using the guidelines described in section 3.2.4. The ice mask outputs were converted to polygon shapefiles in order to provide the glacier outlines. The maximum and minimum values of the ice surface DEMs for each time-slice were recorded as the maximum and minimum ice elevations for each of the modelled glaciers.

6.2 Results

6.2.1 ELA variation

6.2.1.1 Steady state advance / retreat

During the model run, a single output was produced for the initial conditions and then for every 1,000th year resulting in PCT data collected from each glacier for 11 time slices. Owing to the fact that the forcing in ELA change was so gradual that it enabled all of the generated glaciers to remain in steady state, the results can be considered evidence of glacier advance or retreat. For clarity, the results discussed for this particular experiment will be analysed and presented in terms of long-term glacier advance, although the same results would be true for a retreat scenario. The results are displayed in table 6-1 and displayed in figures 6.6 to 6.10.

Glacier	Mean PCT Elevation (m.a.s.l)	Mean PCT _p	Total PCT _x advance (m)	Total PCT _a change (m)	Snout advance (m)	Mean ELA - PCT _a (m)
1	1703	0.33	2025	-181	3560	-146
2	1647	0.36	3827	-334	4115	-203
3	1684	0.35	1622	-266	2523	-166
4	1712	0.31	3005	-292	2938	-138

TABLE 6-1 - STEADY STATE ADVANCE SUMMARY RESULTS
 The table shows changes in PCT and Snout position for the full 10,000 yr simulation.

Figure 6.6 displays outputs from three time slices during the model run as well as the evolution of the glaciers and related PCTs over the entirety of the simulation. The outputs provide a clear indication that the PCT is dynamic feature where its position adjusts in response to forcing variations. In this case, PCT_x can clearly be seen advancing down glacier with each time-slice as the ELA gradually reduces in elevation from 1950masl (6.6 B) to 1750 (6.6 D). Another observation worthy of note concerns the clustering of PCT location on glaciers 1 and 3 during the later stages of the model run. As was highlighted in section 6.1.3.4, the valleys in which these glaciers are constrained displayed sections of steep-topography that were considered likely to produce icefalls. The clustering of PCTs in these identified regions, along with the tightening of contours as seen in figure 6.6A and B, suggest that perhaps the subglacial

topography played a role in PCT location once the snout had advanced over these areas of localised steep topography. This will be discussed in greater detail when assessing the confounding factors in PCT formation and location.

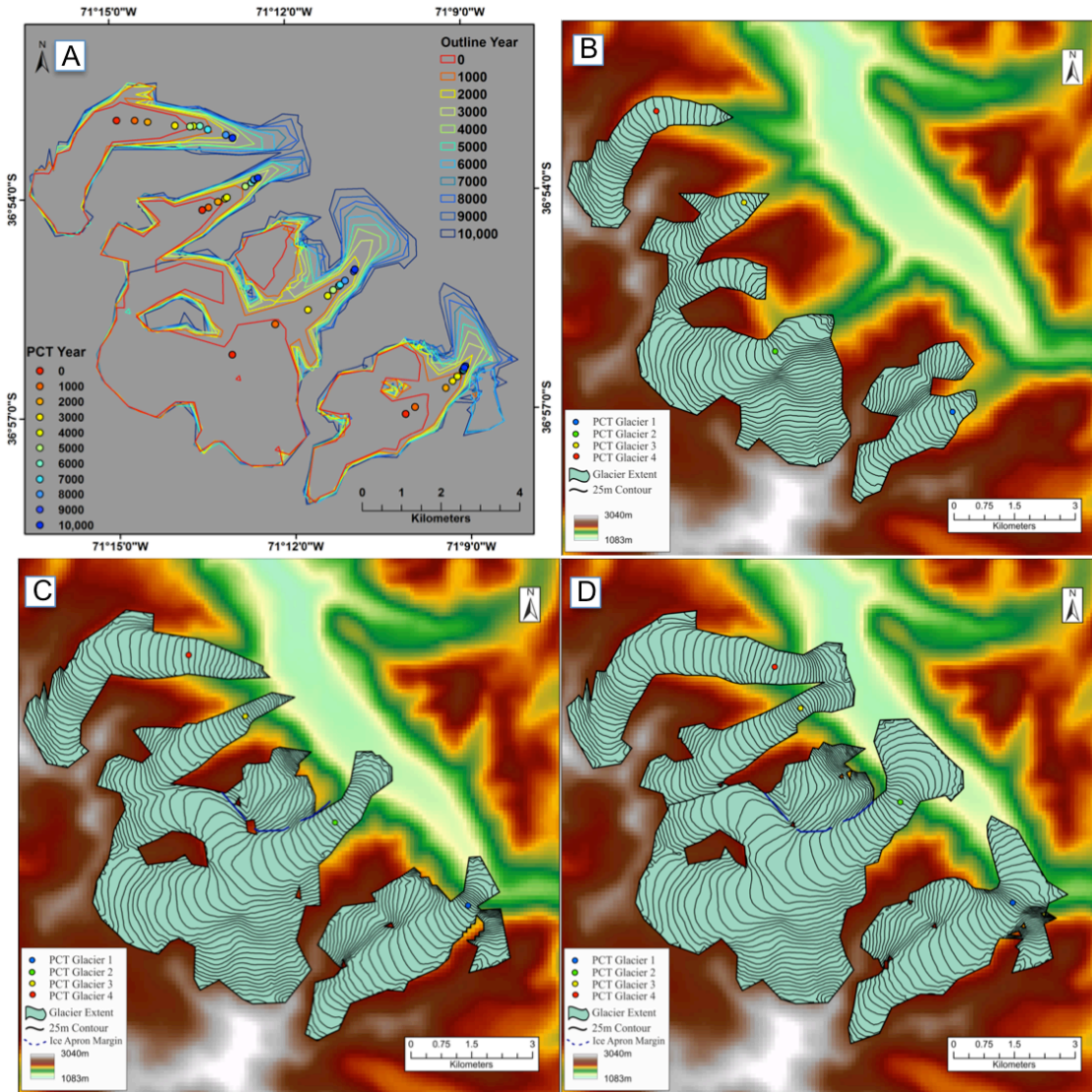


FIGURE 6.6 PCT MIGRATION UNDER LONG-TERM STEADY STATE ADVANCE
 A: PCT migration and changes in glacier extent over the 10,000 year forcing during ELA decrease from 1950 to 1750 masl. Each point and line represents the location of the PCT and glacier boundary for each time-slice respectively. B: PCT location at the beginning of the forcing (ELA = 1950). C: PCT location at 5000 years (ELA = 1850). D: PCT location at 10,000 years (ELA = 1750).

As displayed in table 6-1 PCT_x on the four glaciers not only advanced but PCT_a also reduced between the initial conditions and the final output after the 10,000 year simulation.

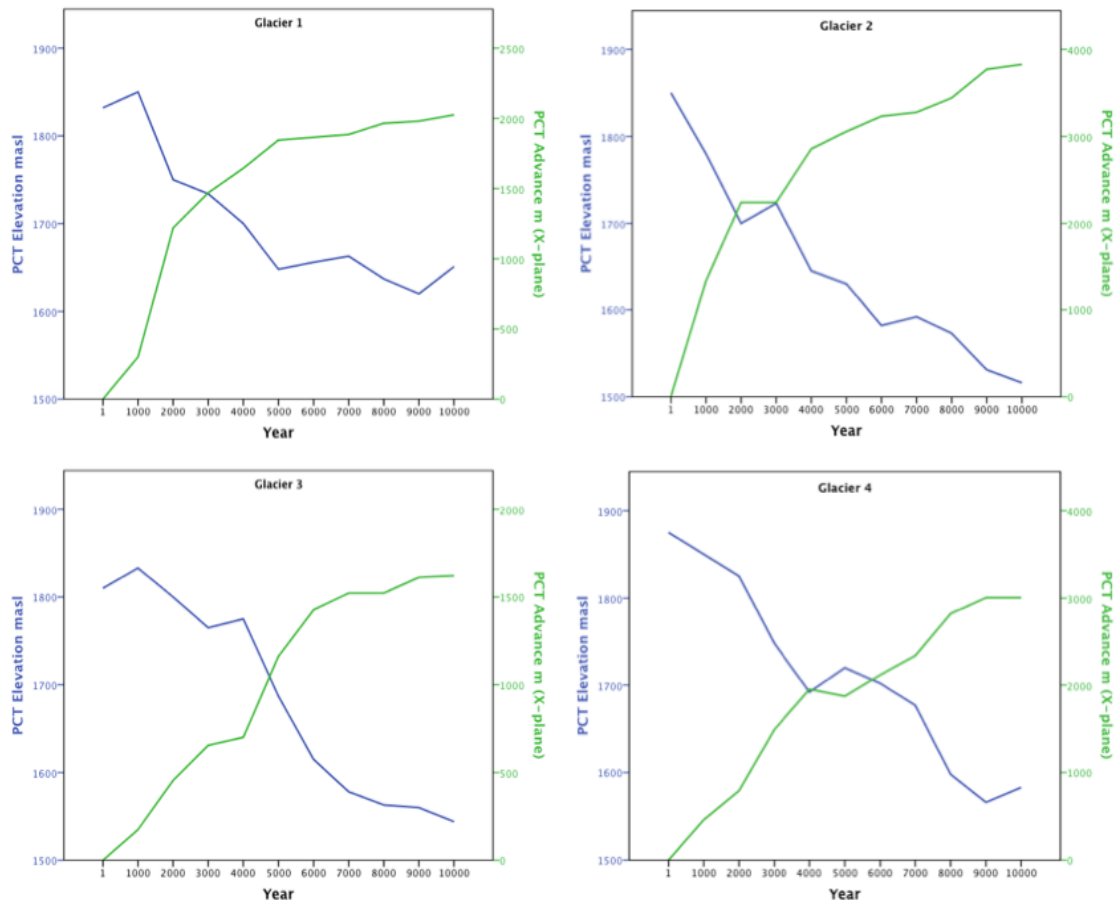


FIGURE 6.7 - PCT CHANGE OVER TIME.
 Cumulative change in PCT_a over the 10,000 year simulation compared with PCT_x advance.

The changes in PCT_a for every 1000th year in figure 6.7 display a clear trend in PCT_a reduction over time. This reduction in PCT_a can be readily explained by PCT_x advance down the longitudinal ice surface slope. Interestingly, but perhaps unsurprisingly, the PCTs tracked on the smaller glaciers (1 and 3) exhibit a slightly smaller range in elevation reduction, compared to the larger glaciers 2 and 4, despite experiencing the same change in forcing. PCT_a change appears relatively linear with time upon glaciers 2 and 4. However, there appears to be evidence of greater irregularity present in the elevation change displayed by glaciers 1 and 3. As glacier 1 and 3 are smaller, and thus likely to be shallower, than glacier 2 and 4, they are more susceptible to control of localised topography over flow dynamics. Particularly for glacier 3 in figure 6.7 where PCT_a experiences a sharp decline after the 4000 year time-slice. When comparing this sudden dip in PCT_a to the position of the PCT markers displayed in figure 6.6A, one could suggest that the steep reduction in elevation

coincides with the point at which the PCT is located at the predicted icefall zone (figure 6.5).

The trends in PCT_a also reveal periods of elevation increase during the overall decreasing trend. These occur when the rate at which the PCT_x advance reduces whilst glacier thickening continues (figure 6.7). This can also be seen in figure 6.8 displaying the “advance scenario” of the PCT between each time slice and over the entire simulation (refer to section 2.4.3 for the introduction of this concept).

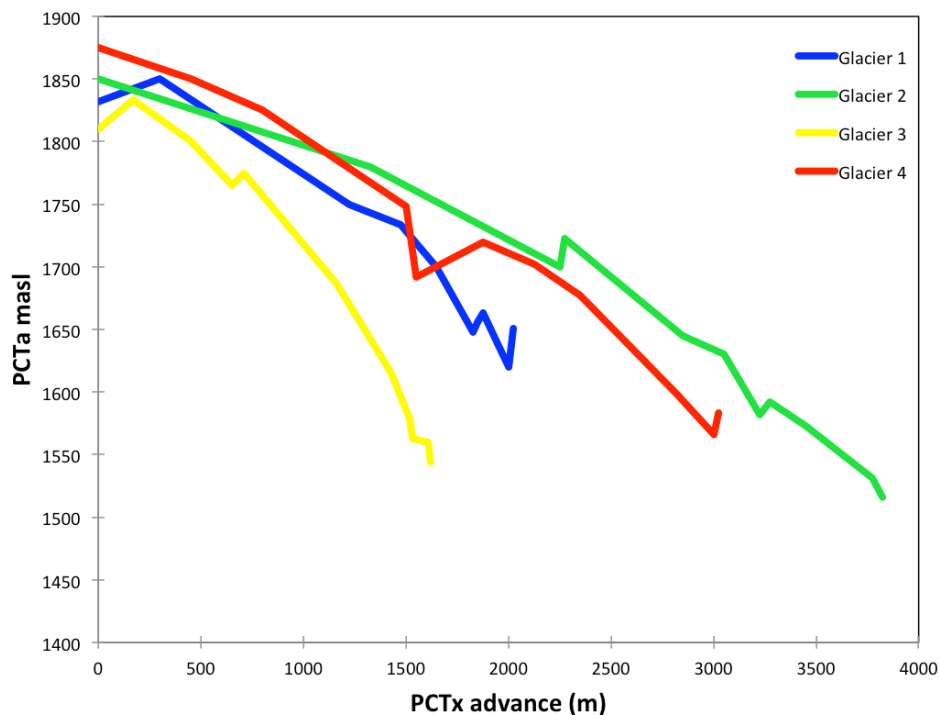


FIGURE 6.8 - ADVANCE SCENARIOS
PCT advance scenarios observed upon the 4 glaciers generated in the study region.

It is clear that the PCT displays a similar trajectory of migration on each of the glaciers as it advances down glacier to lower elevations. However, the PCT trajectory upon glacier 4 appears to reveal an anomalous result where the PCT_a suffers a pronounced dip in elevation, at around $X = 1600$ m, compared to the general trend of the line. A thorough investigation of the DEM at this point revealed no local topographic feature that could cause the ice surface to dip so substantially during steady state advance. The anomalous data point is considered to be the consequence of an irregular cell value in the output DEM. Nevertheless, the distance that PCT_x was observed to advance highlights the importance of the assertion made in section 2.4.2 that stated the necessity of

monitoring changes in PCT_x as well as PCT_a . Figures 6.6 to 6.8 highlight the dynamic nature of the PCT and the clear relationship between climate forcing driven by ELA lowering and the responding evolution of the PCT.

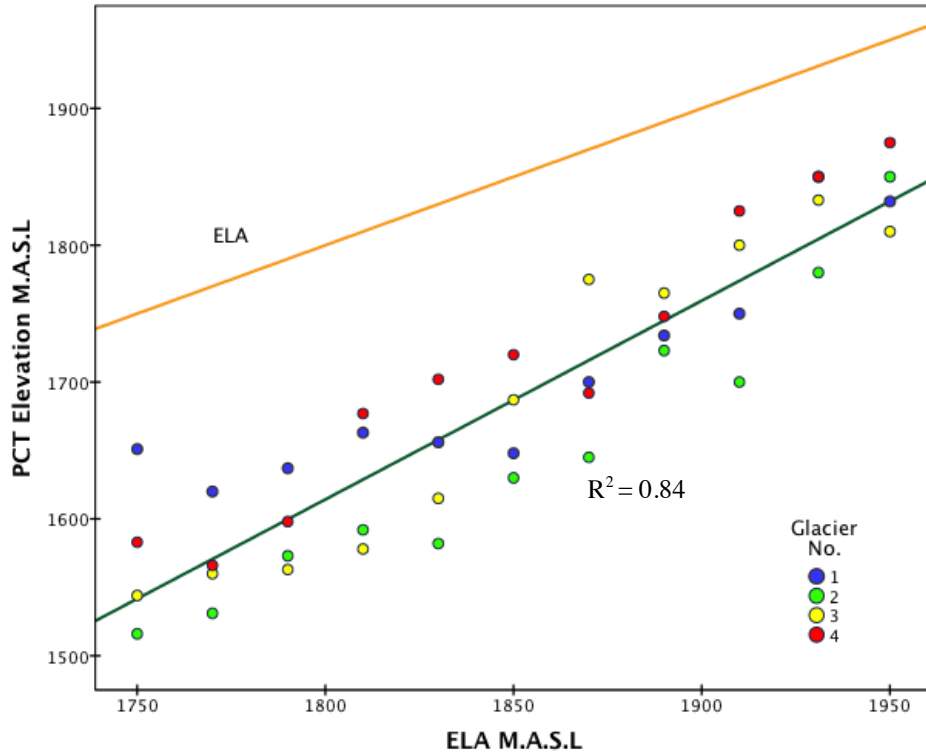


FIGURE 6.9 - PCT VS ELA

The relationship between PCT elevation and ELA for each glacier at all time-slice outputs. The yellow line represents the 1:1 trajectory of the ELA to aid comparison

Figure 6.9 highlights the relationship between the ELA value at each time-slice and the corresponding PCT_a located on the four studied glaciers. The plot reveals a robust linear relationship between PCT_a and ELA ($r^2 = 0.84$) however, an offset is present where PCT_a is, on average, 163 m in elevation beneath the ELA across all glaciers (Table 6-1). This observation is rather striking when one considers that the results from the empirical observations discussed in chapter three also identified a mean elevation offset of 163 m between PCT_a and ELA. Not only does this provide support for the model's ability to replicate empirically observed glacier dynamics, it also reinforces the interpretation that the PCT is intrinsically linked with mass balance.

During the model run, the PCT_p was also recorded alongside changes in PCT_a . Changes in PCT_p over time are displayed in figure 6.10.

The plot highlights that despite the significant changes in PCT_a and PCT_x as well as glacier advance and areal expansion, as evidenced in figures 6.6 – 6.8, PCT_p variance was minimal during the simulation. Across all 4 glaciers, the mean PCT_p value was 0.34 ($\sigma = 0.04$). Interestingly, the plot reveals that during the initial time-slice, the PCT_p value appeared disproportionately low on glaciers 1 and 3 (figure 6.6B). These two glaciers represent the smaller, in length and area, of the sample and as a result the unusually low PCT_p values may suggest that a minimum glacier size is a pre-requisite and thus a confounding factor in PCT positioning. This will be covered in greater detail in the following discussion.

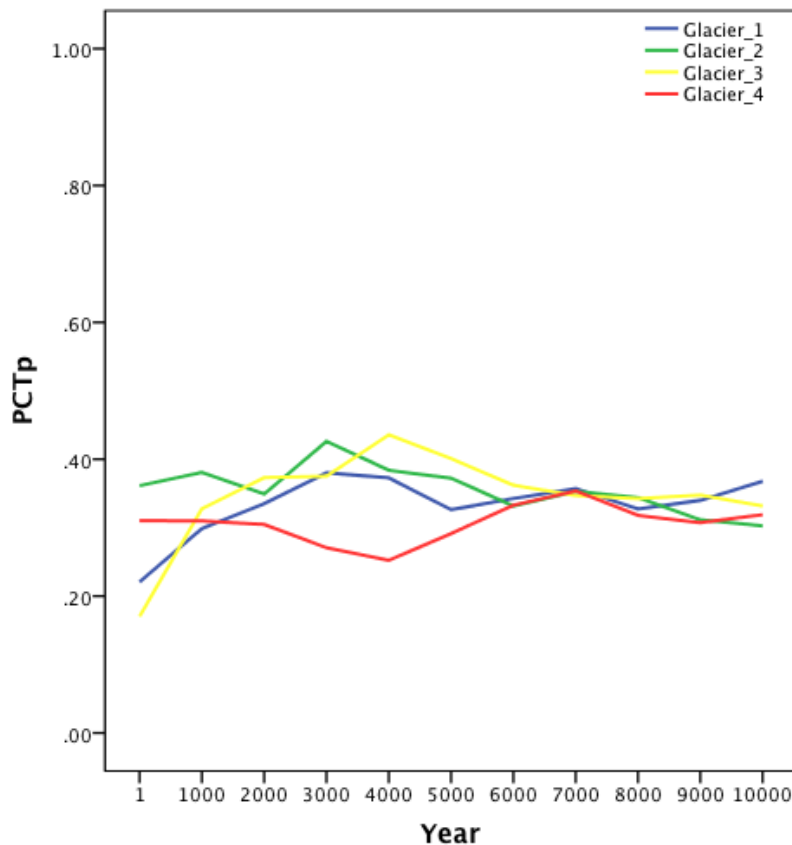


FIGURE 6.10 - PCTP VARIATION
Variation in proportional PCT position upon each glacier over the entire simulation.

6.2.1.2 Abrupt ELA decrease and glacier advance

Owing to the potential for localised increases in bed steepness to produce icefalls and influence PCT location, glaciers 2 and 4 are focused upon for the remaining experiments.

Although the simulation required a 300 year period to allow the glaciers in the experiment to regain equilibrium, as expected (Hooke, 2005; Oerlemans et al., 1998; Raper and Braithwaite, 2009), the majority of the dynamic response in glacier and PCT to the sudden drop in ELA occurred during the 100 year period immediately after the perturbation, with little observable change occurring during the last 200 years. Accordingly, to gain a high-resolution picture of how the PCT responds to a sudden change in climate forcing, PCT and glacier snout positions were recorded for every two-year time-slice for the first 100 years after the ELA perturbation. To gain a complete picture, PCT and glacier information was then recorded for the 200th and 300th years after the ELA drop.

Glacier	Mean PCT _a (m.a.s.l.)	Mean PCT _p	Total PCT _x change (m)	Total PCT _a change (m)	Mean ELA- PCT _a (m)
2	1644	0.38	3558	-185	-110
4	1655	0.32	3136	-252	-98

TABLE 6-2 SUMMARY RESULTS FOR ABRUPT ADVANCE EXPERIMENT

The changes in PCT_a and PCT_p values upon glaciers 2 and 4 immediately following the 200m reduction in ELA are displayed in figure 6.11 and figure 6.12.

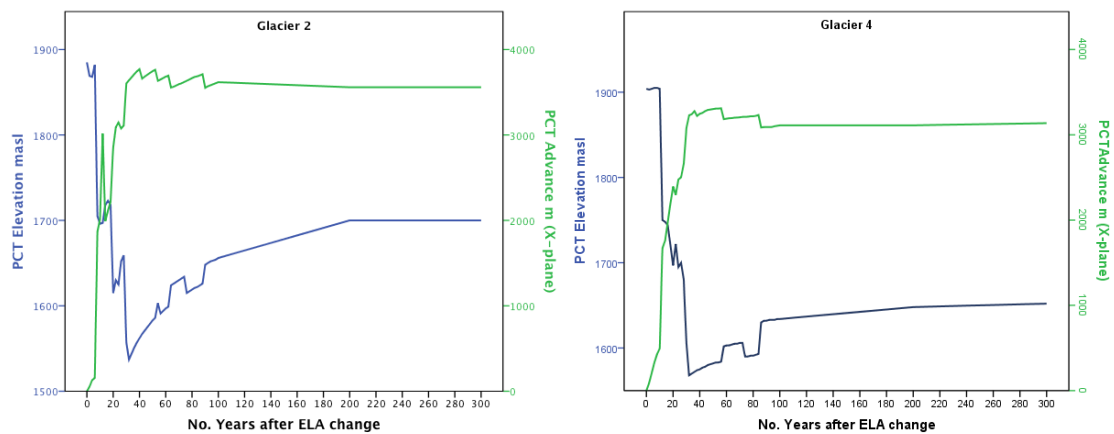


FIGURE 6.11 – PCT_a AND PCT_x PLANAR CHANGES
Plots display the variation in PCT_x and PCT_a (masl) immediately after the ELA decreased from 1950 to 1750 masl.

The plots display that shortly after the decrease in ELA, PCT_a decreased rapidly upon both glaciers. The rapid decrease in PCT_a was sustained until the minimum PCT_a of 1537 and 1568 masl was attained on glaciers 2 and 4 respectively. Interestingly, the minimum elevation was reached 32 years after

the ELA perturbation on both glaciers. This rapid fall in PCT_a coincided with the highest rates of PCT_x advance. PCT_a can then be seen to increase at a reducing rate until a constant elevation was sustained. When comparing the trend in PCT_a with changes in PCT_x , particularly with glacier 2, it is clear that PCT_a increases despite little variation in PCT_x between 100 and 200 years after the ELA perturbation. This suggests that the planar adjustment of the PCT_x reached an equilibrium state before the glacier itself had reached its equilibrium state. This is evidenced by the fact that ice thickening appeared to continue for almost two hundred years after PCT_x reached an equilibrium state.

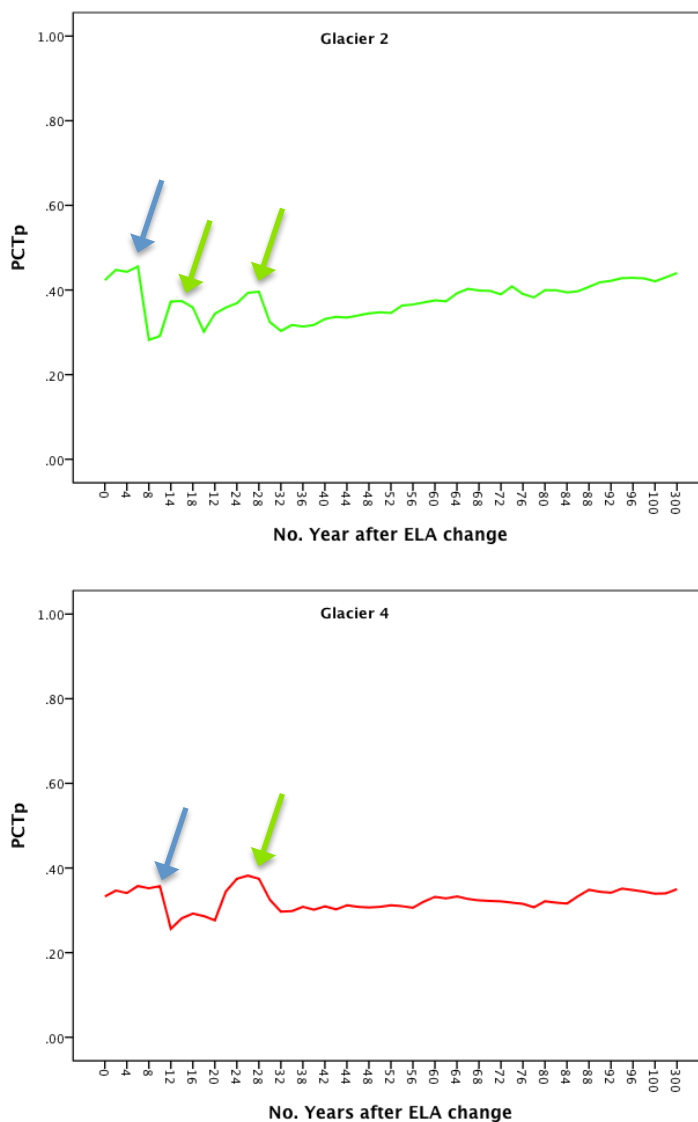


FIGURE 6.12 - - PCT_p VARIATION DURING ABRUPT GLACIER ADVANCE
 Variation in the proportional elevation position of the PCT on both glaciers during abrupt, ELA driven advance. Note that the X-Axis is truncated between 100 and 300 years after the climate perturbation due to the minimal variation observed in PCT_p during this period

Fluctuations in the proportional PCT position upon glaciers 2 and 4 throughout the experiment are displayed in figure 6.12. As was identified with the results from the gradual, steady state advance experiment (figure 6.10), there is very little difference in the PCT_p value when comparing the PCT position during maximum and minimum ice extent at year 300 and 0 respectively. For the entire run, mean PCT_p was 0.37 ($\sigma=0.04$) and 0.32 ($\sigma=0.02$) for glacier 2 and 4, respectively. During the simulation an initial drop in PCT_p (blue arrows) occurred upon both glaciers. This suggests that the PCTs advanced down-glacier to lower elevations at a rate greater than the response of the glacier snout. This is an indication that flow dynamics and the resulting PCT may have adjusted faster to climate forcing than changes in glacier extent. The PCT_p values then continued to display moderate fluctuations whilst PCT_a and PCT_x experienced significant changes (figure 6.11). The “bumps”, annotated by the green arrows, are interpreted to be the result of short periods where the rate of snout advance exceeded the rates of PCT_x and PCT_a change. This is likely the result of the termini advancing down the slightly steeper longitudinal slope into the large trunk valley to the northeast of the study area. After 32 years, PCT_p values upon both glaciers then demonstrated very gradual increases as the PCT_a slowly rose relative to the minimum ice elevation.

6.2.1.3 Abrupt ELA increase and glacier retreat

Glacier	Mean PCT_a (m.a.s.l)	Mean PCT_p	Total PCT_x change (m)	Total PCT_a change (m)	Mean ELA- PCT_a (m)
2	1757	0.45	-3806	166	-188
4	1813	0.39	-3023	255	-131

TABLE 6-3 SUMMARY RESULTS FROM ABRUPT RETREAT EXPERIMENT

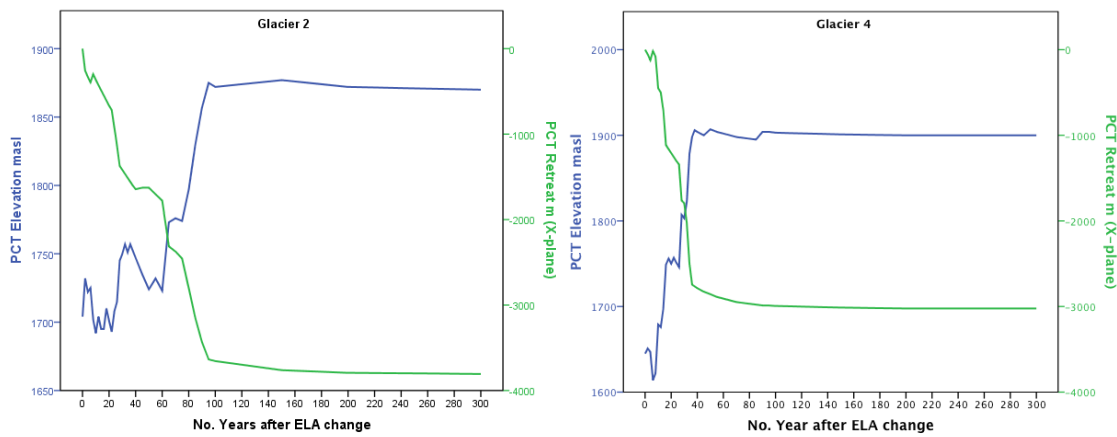


FIGURE 6.13 - PCT ELEVATION AND PLANAR CHANGE RETREAT
 Plots display the variation in PCT planar position and PCT elevation (masl) immediately after the ELA increased from 1750 to 1950 masl.

As with the previous section, most of the glaciers' response to the ELA increase occurred shortly after the initial climate perturbation. Accordingly, this period remains the focus for the following analysis.

Changes in PCT elevation and planar position on glacier 2 and 4 following the abrupt increase in ELA from 1750 masl to 1950 masl are displayed in figure 6.13. PCT_a upon both glaciers initially displayed a rapid increase in elevation corresponding to the high rate of PCT_x retreat that occurred almost immediately after the ELA perturbation. After forty and one hundred years for glaciers 4 and 2 respectively, PCT positioning appeared to equilibrate where changes in elevation and planar position became virtually negligible. This observation is unusual given that there was a clear "overshoot" in PCT_a when ice flow was responding to an abrupt drop in ELA. The lack of a PCT_a "overshoot" in response to an abrupt increase in ELA suggests that flow dynamics that control PCT position undergo variable responses to climate perturbations that dependant on the nature of the forcing (i.e. through an abrupt increase in B_n and vice versa). The physical reason for this difference in the response of PCT_a to the two modes of forcing observed here will be explored in section 6.3.

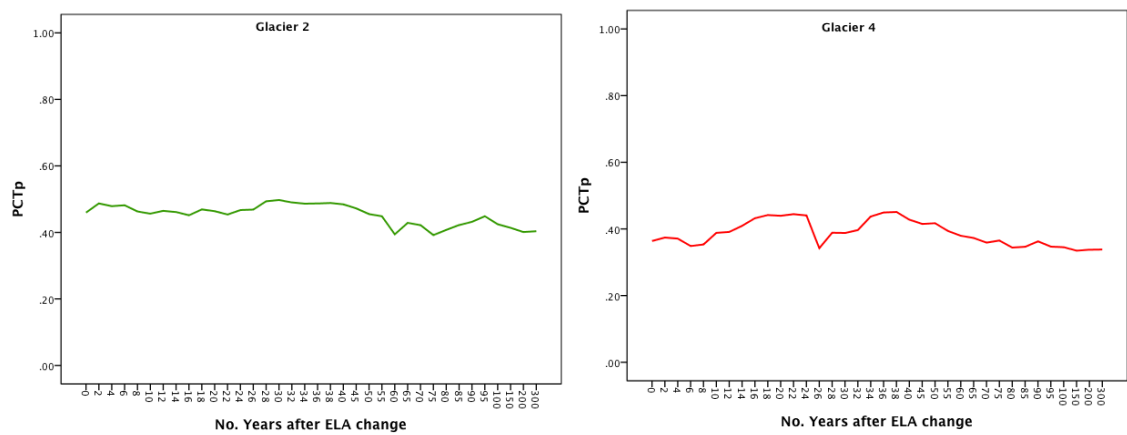


FIGURE 6.14 - PCT_p VARIATION DURING ABRUPT GLACIER RETREAT
 Variation in the proportional elevation position of the PCT on both glaciers during abrupt, ELA driven retreat. Note that the X-Axis is truncated between 100 and 300 years after the climate perturbation due to the minimal variation observed in PCT_p during this period

Figure 6.14 reveals the variation in PCT_p during glacier retreat forced by the abrupt change in ELA. Once again, the plots reveal that there is relatively little change in the PCT_p upon the glacier surface despite clear changes in its elevation and planar location. Mean PCT_p for glaciers 2 and 4 for the duration of the simulation were 0.45 ($\sigma = 0.03$) and 0.38 ($\sigma = 0.04$). However, it is interesting to note that PCT_p values on the two studied glaciers are higher during the abrupt retreat than they were during the advance scenario. Another indication that the PCT responds to climate forcing faster than glacier extent is evidenced by the observations that PCT retreated up glacier, under negative mass balance forcing, faster than the retreat of the minimum ice elevation leading to higher PCT_p values.

6.2.2 Variable retreat forcing mechanisms

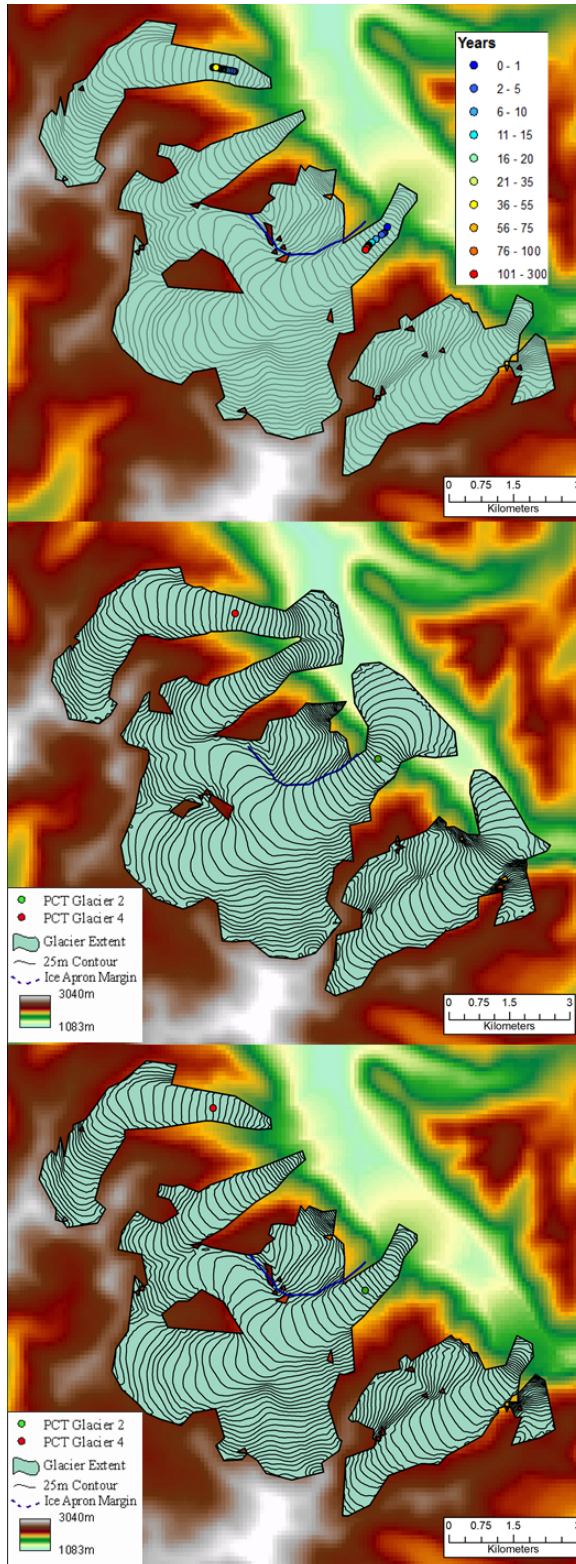


FIGURE 6.15 - ACCUMULATION DRIVEN PCT EVOLUTION
Changes in glacier extent and PCT position (Top) throughout simulation, (Middle) Pre accumulation change, (Bottom) Glacier extent once an equilibrium state was reached.

6.2.2.1 Accumulation-forced retreat

As with the rapid ELA perturbation experiments, the majority of the glacier and PCT response occurred during the decades immediately following the mass balance perturbation. Accordingly, the following results highlight changes in PCT location on a yearly basis for the first 2 decades of response. After 20 years, the PCT was recorded every 5 years until 100 years after the onset of accumulation reduction. The final two observations display the position 200 and 300 years after the initial perturbation. By the 300th time-slice, the glaciers had regained equilibrium.

Changes in glacier extent and PCT location are displayed in figure 6.15 with a summary of the results tabulated in table 6-4. It is clear from the Arc outputs and results table that the PCT displayed a dynamic response to a change in accumulation levels. However, when compared to the extent of PCT retreat observed due to changes in ELA, the PCT variation forced by changes in accumulation appear to be somewhat smaller.

Glacier	Mean PCT _a (m.a.s.l)	Mean PCT _p	Total PCT _x change (m)	Total PCT _a change (m)	Mean ELA- PCT _a (m)
2	1627	0.37	-752	58	-223
4	1698	0.32	-521	-2	-152

TABLE 6-4 SUMMARY RESULTS FROM ACCUMULATION DRIVEN RETREAT EXPERIMENT

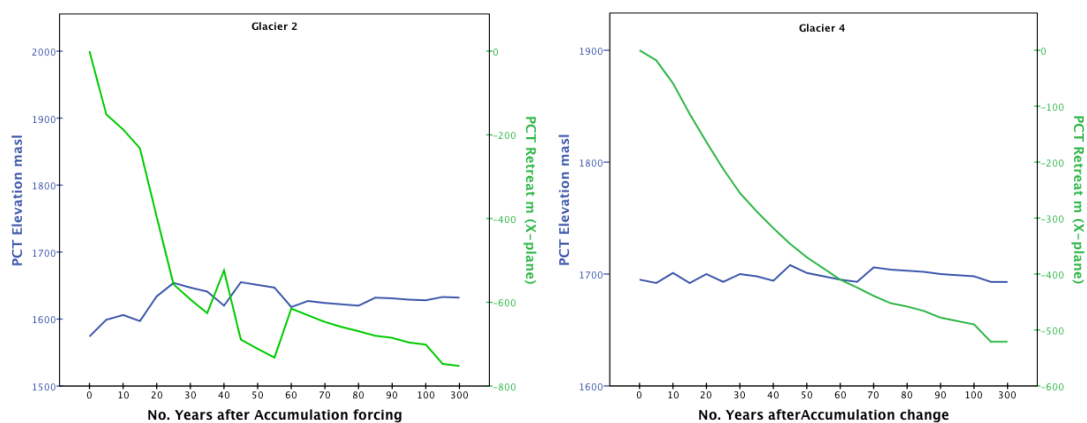


FIGURE 6.16 - ACCUMULATION-DRIVEN PCT CHANGE

Changes in PCT_a and PCT_x on glaciers 2 and 4 forced by a reduction in accumulation. Note that the X-Axis is truncated between 100 and 300 years after the climate perturbation due to the minimal variation observed in PCT_a and PCT_x during this period.

The plots in figure 6.16 reveal evidence of PCT_x retreat on both glaciers as a result of the reduction in accumulation. This PCT retreat occurred relatively

rapidly upon glacier two following the mass balance perturbation. However the high rate of retreat is not sustained beyond year 30, as the rate of PCT_x begins to decrease. On the other hand, PCT_x retreat rate on glacier 4 reduced gradually during the entire 300 year period after the change in accumulation.

Perhaps the most interesting observation to be drawn from the results displayed in the plots and in the images in figure 6.15 is the fact that despite evidence of PCT_x retreat, PCT_a shows minimal change. Furthermore, compared to PCT change forced by ELA variation, PCT_x retreat and change in PCT_a are substantially smaller when forced by a significant change in the accumulation. This is demonstrated by PCT_x retreat of around 4 km and 3 km on glacier 2 and 4 respectively after an abrupt increase in ELA compared to PCT_x retreat of 752 m and 521 m when forced by accumulation reduction. The same observation can be made concerning changes in PCT_a . The physical explanation for this disparity in PCT responses to different climate forcing modes will be discussed in section 6.3.

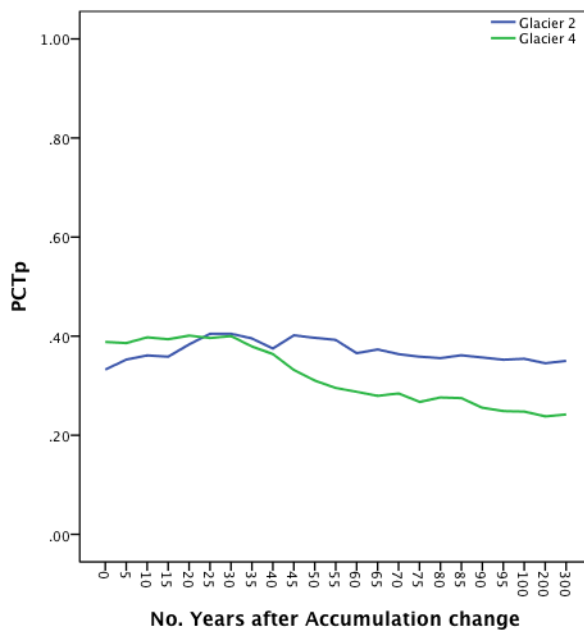


FIGURE 6.17 - PCT_p VARIATION DRIVEN BY ACCUMULATION CHANGE
 Changes in the proportional position of the PCT on glaciers 2 and 4 after a sustained decrease in accumulation.

Changes in PCT_p during the accumulation reduction model run are shown in figure 6.17. The PCT_p upon glacier 2 displays very little variation with an average value of 0.37 ($\sigma = 0.02$). This lack of variation reflects the fact that the small increase in PCT_a was accompanied by a similar increase in minimum

glacier elevation during the model run. On the other hand, PCT_p upon glacier 4 displayed a reduction from 0.4 to 0.24 during the model run. This reduction in PCT_p has occurred because the PCT_a did not change whilst the glacier's minimum ice elevation increased.

6.2.2.2 Ablation forced retreat.

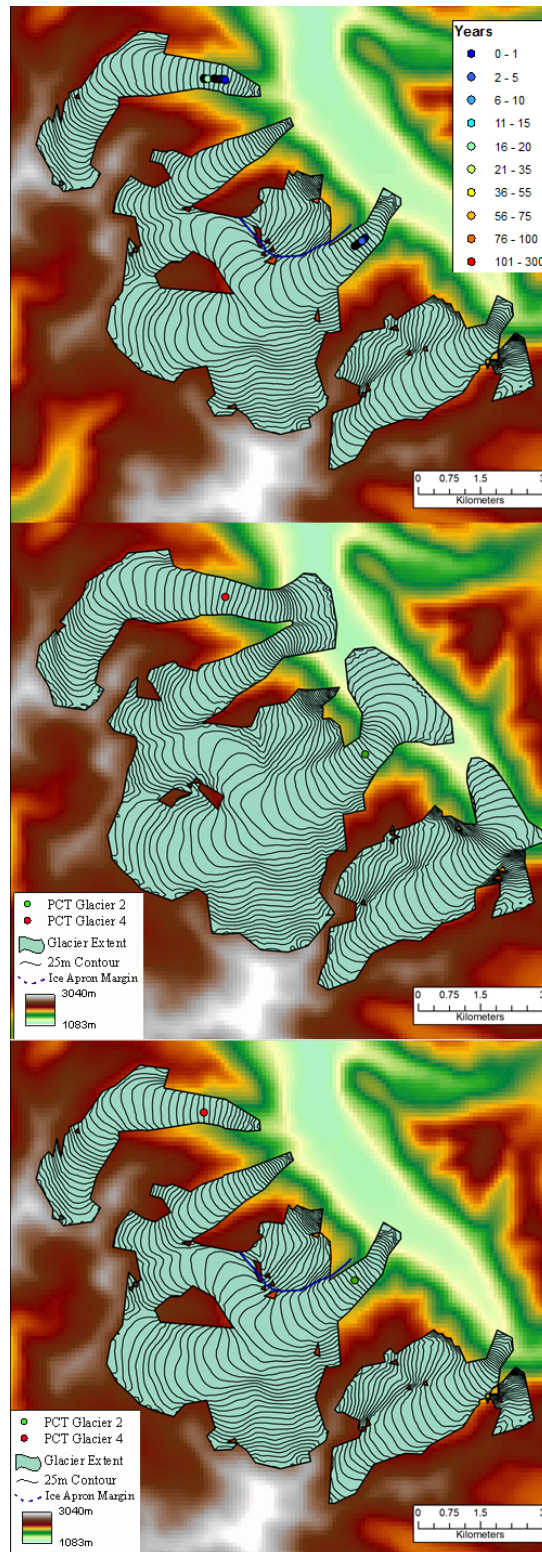


FIGURE 6.18 – ABLATION-DRIVEN PCT EVOLUTION

Changes in glacier extent and PCT position (Top) throughout simulation, (Middle) Pre accumulation change, (Bottom) Glacier extent once an equilibrium state was reached.

Figure 6.18 displays the evolution of glacier extent and PCT location in response to a significant increase in ablation. The plots in figure 6.19 reveal changes in PCT elevation and planar position throughout the simulation.

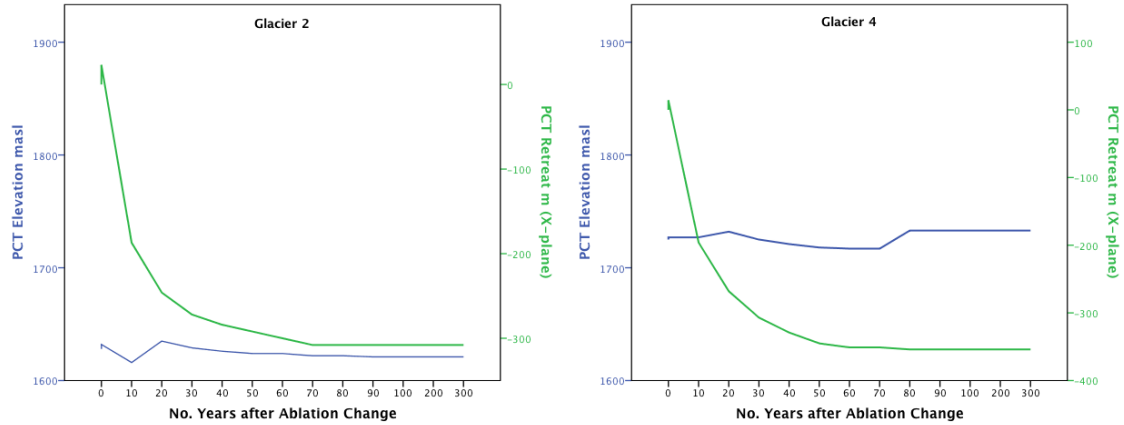


FIGURE 6.19 - ABLATION DRIVEN PCT CHANGE
Changes in PCT elevation and planar position on glaciers 2 and 4 forced by a reduction in accumulation.

The plots reveal that during glacier retreat forced by increased ablation, the PCT displays behaviour similar to that evidenced during accumulation driven retreat. PCT_x on both glaciers experience fairly rapid retreat, albeit it over short distances, for the first 50 years or so after the ablation increase. Once again, the PCT_a demonstrated very little variation during the entire simulation. This is particularly interesting given the clear evidence of PCT_x retreat displayed by both glaciers. The minimal PCT_a change despite evidence of PCT_x retreat is the result of ice thinning occurring synchronously with PCT_x retreat. The mechanism by which ice thinning maintains PCT_a during PCT_x retreat will be considered in more detail in section 6.3

Glacier	Mean PCT _a (m.a.s.l)	Mean PCT _p	Total PCT _x change (m)	Total PCT _a change (m)	Mean ELA-change PCT _a (m)
2	1625	0.35	-308	-8	225
4	1725	0.30	-354	8	125

TABLE 6-5 – SUMMARY RESULTS FROM ABLATION DRIVEN RETREAT EXPERIMENT

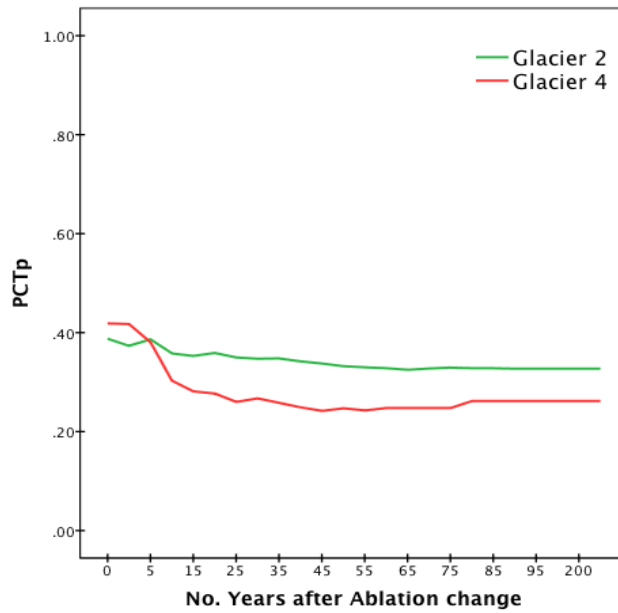


FIGURE 6.20 - PCT_p VARIATION DRIVEN BY ABLATION CHANGE
Changes in the proportional position of the PCT on glaciers 2 and 4 after a sustained increase in ablation.

Changes in PCT_p during ablation driven glacier retreat are displayed in figure 6.20. Despite relatively low levels of PCT retreat and elevation variation relative to the retreat rate of the glacier snout (see table of results and images in figure 6.13) the PCT_p remained relatively unchanged on glacier 2. PCT_p values may have maintained a relatively uniform value on glacier 2, despite high rates of snout retreat relative to PCT_x retreat due to the shallow longitudinal profile of the lower valley in which the lobed terminus was located. The shallow gradient of the lower valley means that despite significant snout retreat under increased ablation, the minimum glacier altitude increased by only 109 m. As a result, despite very little change in PCT_x and PCT_a, the PCT_p decreased only slightly from 0.39 to 0.32. On the other hand, glacier 4 displays an apparent PCT_p reduction from 0.39 to 0.24. Unlike glacier 2, the terminus of glacier 4 began to leave the lower valley and migrate up the bed slope of the glacier's parent valley. As a result, the glacier's minimum elevation increased by 328 m. Given the minimal variation in PCT position, the terminus encroaches upon the PCT resulting in a lowering of the PCT_p value.

6.2.2.3 Basal Sliding vs Plastic Deformation

Figure 6.21 suggests that the glacier flow mechanism, whether through plastic deformation only or a combination of deformation and basal sliding, has a minor impact upon PCT_x location. Between the two model runs, there was no

observable change in PCT_x position under sliding and non-sliding flow settings. However, PCT_a were recorded to be 20 m lower on average for the sliding enabled experiment. This observation suggests that one must be mindful of the role of basal sliding when quantifying the offset between PCT_a and ELA. However, the results from this experiment confirm that the presence or absence of basal sliding in glacier flow exerts no influence over a glacier's ability to generate a PCT.

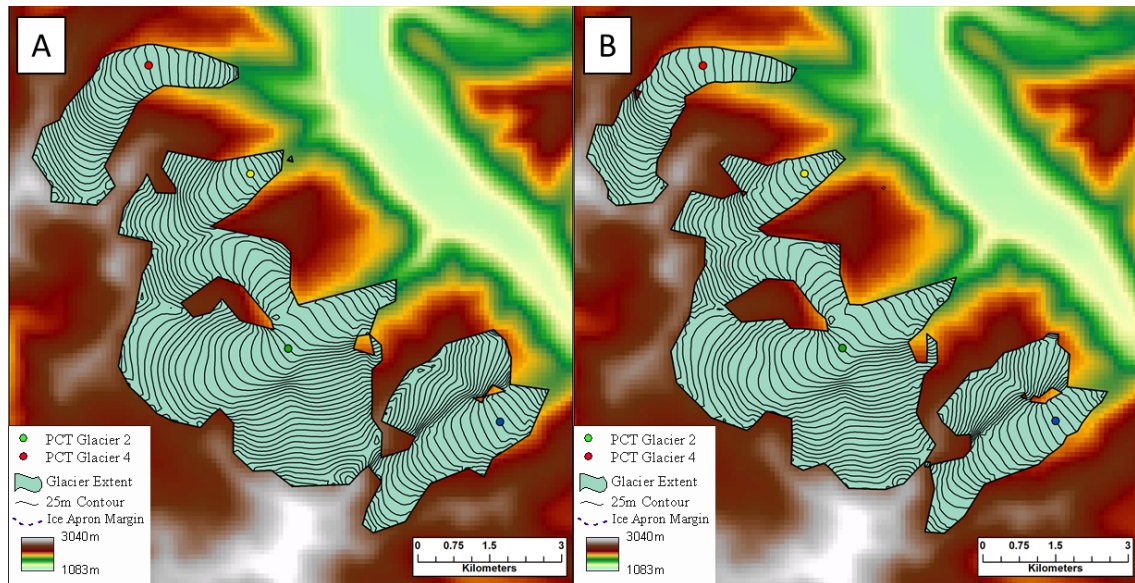


FIGURE 6.21 - PCT LOCATION UNDER DIFFERENT SLIDING REGIMES
 A: PCT location for plastic deformation only. B: PCT location when sliding enabled.

6.2.3 Assessing confounding factors

As displayed in figure 6.6A, sharp increases in longitudinal bed slope result in longitudinal extension as ice accelerates down the slope and longitudinal compression as the ice then decelerates when it reaches a shallower profile. Just as the (mass) balance gradient-controlled longitudinal stress gradient (see section 2.2.2) forms climatically-derived PCTs, this localised variation in longitudinal stress creates non-climatic or “false” PCTs. This is clearly the case on glaciers 1 and 3 where PCT_x remained at the location where ice overrides the short but steep descent into the lower, shallow valley. Accordingly this observation confirms the prediction expressed in section 3.2.2.4 that icefalls have a strong influence over the transverse ice surface profile and accordingly, when the influence of icefalls prevent the climatically-derived PCT from being identified, glaciers containing icefalls should be excluded from PCT analysis.

The study area was purposefully selected as it displayed varying valley geometries from small, single basined valleys to large compound basins with tributary valleys. This enabled one to assess the degree to which PCT location was a function of valley size and geometry. The results from the discussed experiments reveal that the wider topography of the region has relatively little impact on PCT position. This is highlighted by the fact that PCT_p values and the correlation between PCT_a and ELA displayed in figures 6.9 and 6.10 were very similar across all glacier, despite their having different extents and geometries.

In a final experiment, the ice extent was forced to fill the large lower valley in order to identify whether ice confluences resulted in false PCTs similar to those resulting from icefalls. With the ELA fixed at 1750 m.a.s.l, the accumulation gradient used to force ice flow in the steady state advance experiment was increased by a factor of 2 to increase glacier extent. The resulting glacier extent and PCT location is displayed in figure 6.22.

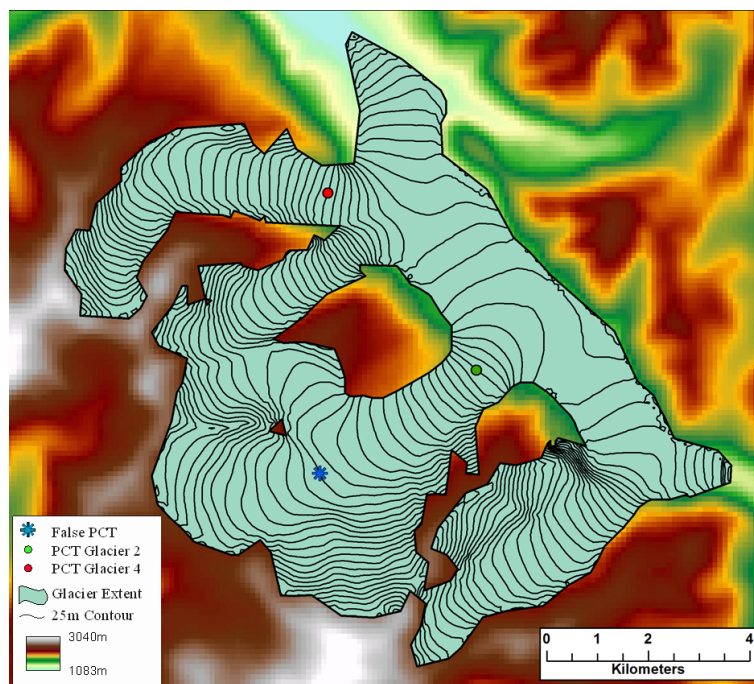


FIGURE 6.22 - ICE CONFLUENCES AND PCT LOCATION
PCT location for glaciers 2 and 4 during maximum ice extent under steady state conditions. ELA at 1750masl.

When observing the two PCTs in figure 6.22, although they have formed in relatively close proximity to the junction of multiple ice flows, the results suggest that this is perhaps coincidental. The PCT_a was located at 1700 m.a.s.l on glacier 2 and 1650 m.a.s.l on 4. Furthermore they displayed PCT_p values of 0.41 and 0.36, which are within the range of PCT_p values displayed during

steady state advance (in which the glaciers did not merge in the lower valley). This suggests that the PCTs are climatically controlled rather than a function of topography. However, also highlighted by the blue star is the occurrence of what is termed here as a “false PCT”. Glacier two highlights a situation whereby a straight contour can be identified on the northern tributary valley feeding the main trunk immediately. It is suggested here that the localised increase in ice-flux required to conserve mass would result in acceleration and longitudinal stretching (Hooke, 2005; Cuffey and Paterson, 2010). As a result, this localised variation in ice flow dynamics has produced a false PCT, however this is clearly a brief perturbation to the overall ice surface geometry as the surface and corresponding contours soon become concave down glacier after the confluence until the climatic PCT is reached. In situations where the ice surface quickly returns to a concave transverse profile downstream of the confluence, non-climatic or “false” PCTs can be easily interpreted and accounted for. However, in cases where the transverse ice surface profile becomes convex after the ice confluence, interpreting the PCT to be either climatic or topographic in nature can become difficult. In such situations, great care should be taken when deciding whether to include such a result in the final analysis.

6.2.4 Synthesis of Results

Figure 6.23 reveals the relationship between ELA and PCT_a for all glaciers during each of the experiments. The plot reveals that during steady state glacier adjustment and ablation and accumulation driven glacier change, the PCT_a displays a linear relationship with ELA where PCT_a is on average 171 m beneath the ELA. Alternatively, during the abrupt changes in ELA experiments (green and orange circles) it is clear that the PCT_a can be located above the ELA during glacier advance as well as much lower beneath the ELA during glacier during abrupt ELA driven retreat. This result is interesting as it suggests that perturbing glacier extent by altering accumulation and ablation amounts has relatively little effect on the offset between the ELA and PCT. Alternatively, forcing glacier extent with an abrupt change to the ELA leads to dramatic variation in the offset between ELA and the PCT_a whilst glacier are in a transitional phase. Furthermore, as was also highlighted in figure 6.11 and

figure 6.13, the PCTs in the abrupt ELA change experiments (green and orange circles), display rapid adjustments in elevation until the offset between ELA and PCT_a approaches a new equilibrium as the rate of change in PCT_a decreases.

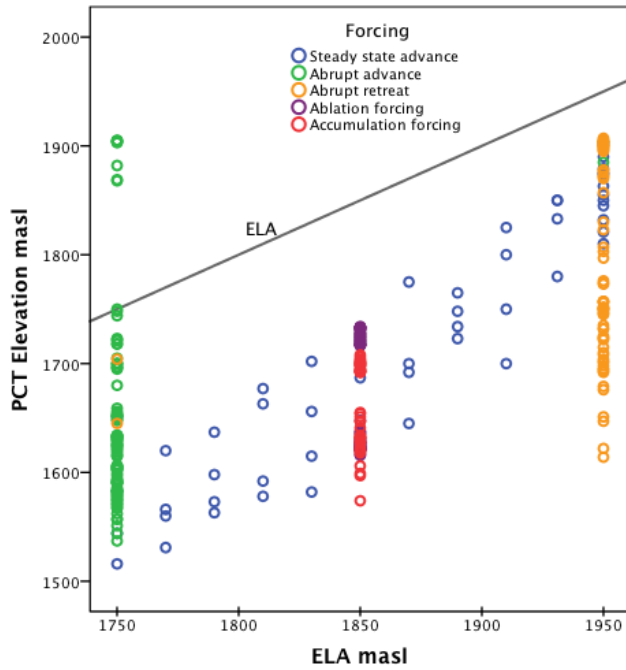


FIGURE 6.23 - PCT vs ELA ON ALL GLACIERS
 The relationship between PCT and ELA for all glaciers under the 5 forcing regimes.

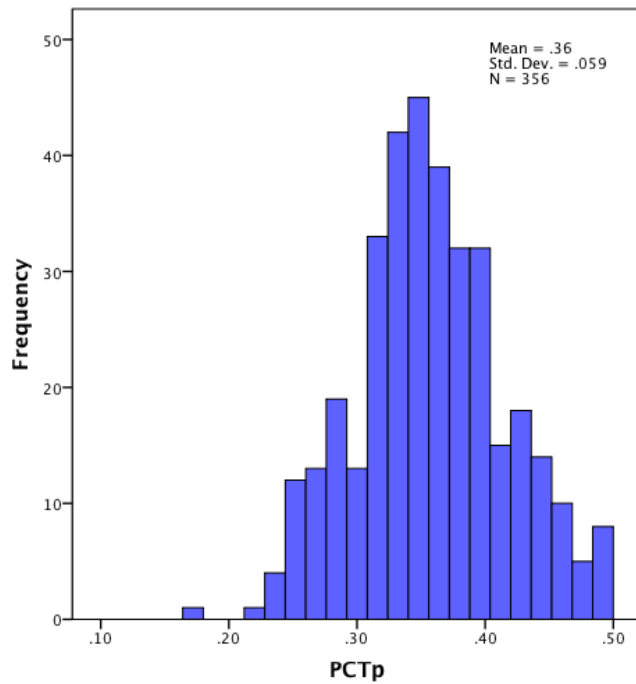


FIGURE 6.24 - MODELLED PCT_p VALUES
 PCT_p values for all outputs from each glacier

Figure 6.24 reveals the histogram for PCT_p values recorded upon each glacier for each output time-slice for all experiments. The plot reveals a relatively normal distribution of PCT_p values with a mean of 0.36 ($\sigma = 0.06$). The small spread in observed PCT_p values highlights the tendency of the glaciers' three-dimensional surface geometry to adjust towards equilibrium states in response to heterogeneous forcing mechanisms.

6.3 Discussion

Before discussing how different climate forcing regimes appear to control PCT behaviour or suggest how these observations can be used to assess glacier health, it is imperative that one is fully confident that the model accurately replicates PCT forming flow dynamics.

The results of this investigation generate a great deal of confidence that the model does indeed accurately reflect realistic dynamics that generate the idealised glacier surface geometries observed by Raymond (1969), discussed in chapters three and four and covered by the theoretical literature (Cuffey and Paterson, 2010; Hooke, 2005; Nye, 1952). Not only did the model outputs produce clearly identifiable PCTs (Figure 6.6, 6.15, 6.21 and 6.22), the modelled glaciers and the resulting PCT characteristics and behaviour over time appear to be indistinguishable from that of the real glacier observations in chapters three and four.

Figure 6.25 displays the PCT_p values calculated for all "real" glaciers that were monitored in chapters three and four. When comparing the spread of PCT_p values produced by the model simulations (figure 6.24) with those from the empirical observations, it is clear that the model runs produced PCT_p values that reflect real world observations. Furthermore, as well as displaying a very similar distribution of PCT_p values, they both display a mean PCT_p value of 0.36. However, it is worth noting the range of PCT_p values recorded from the empirical observations was greater than the range of PCT_p values produced during the model runs. The smaller range of PCT_p values produced by the model runs, compared to the range of PCT_p values observed empirically, may reflect the fact that empirical observations were limited to a small number of glaciers. However, it is also possible that the climatic variations used to drive

the glacier simulations were not strong enough to elicit a glacier response that would produce extreme PCT_p values.

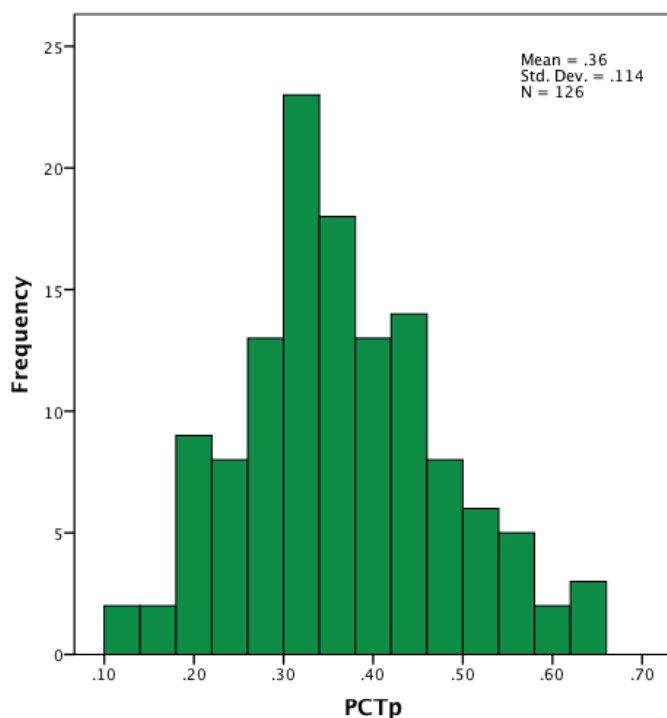


FIGURE 6.25 - PCT_p VALUES FROM "REAL WORLD GLACIER" OBSERVATIONS
 PCT_p VALUES CALCULATED FOR ALL GLACIERS OBSERVED IN CHAPTERS 3 AND 4.

Nevertheless, the model does accurately replicate the flow dynamics that generate the PCT in real world glaciers. Therefore the next step is to further test our understanding and hypotheses by analysing the climate forcing experiments in order to understand the effect that different climate forcing mechanisms exert over PCT behaviour.

One of the most unsurprising, yet promising observations from the modelling experiments is the evidence for the PCT being a dynamic feature. As had been identified in chapter four when observing changes in PCT_x upon well-documented glaciers over time, the PCTs produced during the experiments showed significant positional variation with climate forcing. Furthermore, as was predicted in chapter five, PCTs displayed a common response across all glaciers where they advanced down glacier under sustained positive mass balance and glacier growth and retreated up glacier during sustained negative mass balance and glacier shrinkage. However, when recording changes in PCT_x , the results of this study highlight the importance of taking certain topographic

aspects into account. As expected, abrupt, localised changes in the longitudinal bed slope profile can significantly influence the flow characteristics that determine the location of the PCT. This resulted in occasions where, upon glaciers 1 and 3, the PCT underwent reduced variation in response to glacier advance / retreat when the ice was overriding the steep bed slope. Regions of ice mass convergence also exerted a similar influence over PCT location whereby the acceleration of ice flow required to increase discharge and conserve mass results in a PCT formative process. As discussed in section 6.2.3, this can lead to erroneous interpretation of the ice surface geometry. As a result in such situations, great care is needed to ensure that the PCT being assessed is the result of climatically driven ice dynamics rather than a consequence of localised topography. A similar concern was the effect that different flow regimes would have on PCT formation and location. However, the results displayed in figure 6.21 allayed any such fears as they imply that PCT_x is not dependent upon whether flow is by plastic deformation or basal sliding. Personal communication with David Egholm revealed that this was to be expected. This is owing to the fact that when basal sliding occurs, the overall discharge does not increase but that sliding takes away from the mass transport that would have been internally deformed. However, PCT_a observed during the sliding enabled experiment was around 20 m lower than the PCT_a recorded during the sliding-disabled experiment. This variation in ice surface elevation was not restricted to the location of the PCT but was observed across the total glacier area. Accordingly, the small offset in ice elevation, and the resulting PCT_a , between the sliding and non-sliding model outputs is suggested here to be the result of the model's limitations. Despite the possible pitfalls of topographic influences when interpreting ice surface geometry, the results are encouraging given the clear link between PCT evolution and glacier fluctuations (figure 6.6).

Tracking changes in PCT location during the simulated advance and retreat enabled one to assess how the relationship between PCT, mass balance and ELA manifest under different climate forcing mechanisms and rates of change. The results reveal that as expected, PCT_x retreated towards the headwall under an increase in negative mass balance forcing and glacier retreat whereas during glacier advance under positive mass balance conditions, PCT_x advanced down-glacier towards the minimum ice elevation. Furthermore, the model results

shown in figure 6.9 support the findings of chapter three where there was a strong correlation between PCT_a and ELA. As with the empirical observations, when the ELA was maintained at a constant elevation the model reproduced an offset of -171 m between PCT_a and ELA ($\sigma = 51$ m) and an offset of -150 m ($\sigma = 51$ m) when the entire glacier mass was in equilibrium. These offsets are comparable to those observed in chapter three. Not only does this finding further verify the accuracy of the iSOSIA model in replicating the complex relationship between climate forcing, flow dynamics and three-dimensional ice surface geometry, it further strengthens the finding that the PCT is a climatically based measure of glacier health comparable to the ELA. Interestingly the small standard deviation contained within the results suggest that the offset appears to remain relatively constant irrespective of glacier size or areal distribution, particularly when the glaciers remain in steady state.

However, one of the key purposes of conducting the modelling work was to assess how the PCT behaves when glaciers are no longer in synchronicity with climate forcing. Specifically, how does the offset between ELA and PCT_a alter with varying degrees of glacier-climate synchronicity? The results displayed in sections 6.2.1.2 and 6.2.1.3 reveal once again that as ELA rises (falls) the PCT is observed to retreat up-glacier to a higher elevation (advance down glacier to lower elevations). Furthermore, during the initial and final steady state glacier conditions, the offset between ELA and PCT_a were inline with the steady-state model results, empirical observations and results from previously published studies (Cogley and McIntyre, 2003; Leonard and Fountain, 2003). However as figure 6.23 reveals, the offset varies greatly as the dynamic response of the glaciers lagged behind the change in ELA during both advance and retreat.

During glacier advance driven by a 200 m drop in ELA from 1950 to 1750, figure 6.11 reveals that the PCTs on both glaciers rapidly advanced down-glacier to lower elevations in response. Additionally, the plots in figure 6.11 suggest that PCT_x shows a faster dynamic response to climate forcing than that of the glacier overall. This is evidenced by glaciers 2 and 4, where PCT_x appears to reach an equilibrium position between 30 and 40 years after the ELA perturbation. However, PCT_a continues to increase in elevation upon both glaciers despite minimal PCT_x change. This gradual increase in PCT_a is the

result of continued ice thickening at the location of the PCT (and across the entirety of the glacier) until around 300 years after the change in ELA position when the glacier reaches equilibrium. One mechanism that could explain the PCT_a “overshoot” relates to the rapid response time of w_s compared to the rate at which u_s is able to transport mass gained, through the lowering of the ELA, down glacier. The observation suggests that w_s in the locality of the ‘new’ ELA is able to respond quickly to the climate perturbation in order to adjust the surface geometry and generate the PCT close to the new ELA. This adjustment in surface geometry is by the time increased u_s , and thus increased ice flux, is able to transport mass added to the ice surface during the 200 m ELA decrease. As a result, the ice surface at the PCT begins to rise as the glacier thickens whilst the increased mass in the, now larger, accumulation area is transported down glacier.

This experiment provides useful insight concerning the lag times between climate perturbations and PCT variation where changes in PCT_x, and thus organisation of the glacier flow-field, demonstrate response times on the order of decades, whereas changes in glacier extent and hypsometry need timescales on the order of centuries to reach new equilibrium states. This observation suggests that recording changes in PCT may provide evidence of early glacier response to climate change that would take longer to identify through terminus change observations (Andreassen et al. 2005; Hoelzle et al., 2003; Oerlemans 2005; Oerlemans, 2012;) or through geodetic surveys (Cogley 2009; Fischer, 2011; Joerg and Zemp, 2014; Wang et al., 2014). PCT adjustments in response to an abrupt increase in ELA on the other hand appear to experience a slightly slower response (figure 6.13). Here, PCT_x appeared to reach planimetric equilibrium between 30 and 90 years following the ELA increase. However, unlike the PCT during the abrupt advance experiment, the PCT during the abrupt retreat experiment displayed no PCT_a “overshoot”. Instead, PCT_a and PCT_x appeared to reach an equilibrium state synchronously. This lack of PCT_a “overshoot” during the 200 m ELA increase suggests that the ice surface in the accumulation area had lowered to an equilibrium elevation prior to, or in tandem with, PCT_x retreat.

Perhaps unsurprisingly, the PCT on glacier 2 took almost double the time of that upon glacier 4 to reach an equilibrium position after the forcing perturbation. As glacier 2 is much larger than glacier 4, this difference in PCT response can be explained by the observation that response times scale with glacier size (Oerlemans, 2012; Oerlemans et al., 1998; Raper & Braithwaite, 2009; Wal and Wild, 2001).

The rapid changes in PCT position in response to abrupt changes to the ELA further support the belief that the two variables are linked through the shared driving force of glacier mass balance. However, the clear lags that have been observed between climate forcing and glacier dynamics, or more importantly between changes in climatic ELA and the responding PCT_a , confirm the finding PCT_a should not be used as a tool for estimating present day ELA.

Although the variability in glacier-climate synchronicity prevents the use of the PCT_a as a proxy for the modern day ELA, as was identified in section 3.5, the results suggest knowledge of the offset between the PCT_a and the modern day ELA may be of great use. Considering that the offset between PCT_a and ELA during the steady state experiments showed minimal variation (150m, $\sigma = 55m$) and that during rapid changes in climate forcing the PCT adjusted rapidly to maintain the steady-state offset when the glaciers regained equilibrium suggests that the PCT_a -ELA offset may indeed be used to assess the degree to which glacier dynamics are out of sync with climate. Although assessment of the offset could not realistically produce accurate quantitative projections for future glacier retreat, the information could be used to generate ballpark estimates of glacier retreat as well as identify which glaciers are most likely to be *more* synchronised with contemporary climate forcing. This style of analysis would follow on from the legacy of Mark Dyurgerov where he compared balanced budget AAR value to modern day AAR values to gain similar insight (Dyurgerov et al., 2009). Such knowledge would be particularly useful when deciding upon which glaciers are most representative of the current climate during for future mass balance field-data campaigns.

The apparent link between the PCT and ELA is then further illustrated when observing how variations in PCT_x and PCT_a remained relatively muted when the ELA was held constant and glacier changes were forced by perturbing

accumulation or ablation rates only. Figures 6.15, 6.16, 6.18 and figure 6.19 reveal that although PCT_x retreat occurred in response to negative mass balance forcing, the rate and extent of retreat was on much smaller scale than was observed during the ELA forcing experiments. Accordingly, this lack of planar variation may provide more information concerning the relationship between PCT behaviour and glacier mass balance.

When developing our understanding of why the PCT forms, it was clear that the literature and resulting theory focused heavily upon the controls of surface mass balance over flow dynamics (Cuffey and Paterson, 2010; Hooke, 2005; (Raymond, 1969). Furthermore, the results from the abrupt advance and retreat experiments driven by ELA change revealed how the redistribution of the surface mass balance in a spatial sense, had a significant effect on PCT position. Accordingly, PCT monitoring may provide direct evidence of surface mass balance change when driven by ELA variation. However this also suggests that the PCT may be unresponsive to non-surficial changes to glacier mass balance caused by basal and internal accumulation through refreezing and thus limited in providing evidence of wider glacier volume changes. Nevertheless, the results from the accumulation and ablation forcing experiments verify one of the central beliefs of this work that was proposed in section 2.4, which identified the imperativeness of recording changes in PCT_x as well as PCT_a .

The primary purpose of the accumulation-driven retreat experiment was to test the hypothesis that significant reduction in accumulation rates would drive PCT_x retreat, increase PCT_a and ultimately result in high PCT_p values. However, the results in table 6-4 suggest that this might not be the case. This is because despite clear evidence of PCT_x retreat under accumulation forcing, elevation changes remained muted. This lack of an observed increase in PCT_a can be explained by the fact that the reduction in accumulation resulted in surface thinning in the upper region of the glacier above the initial PCT location (figure 6.26).

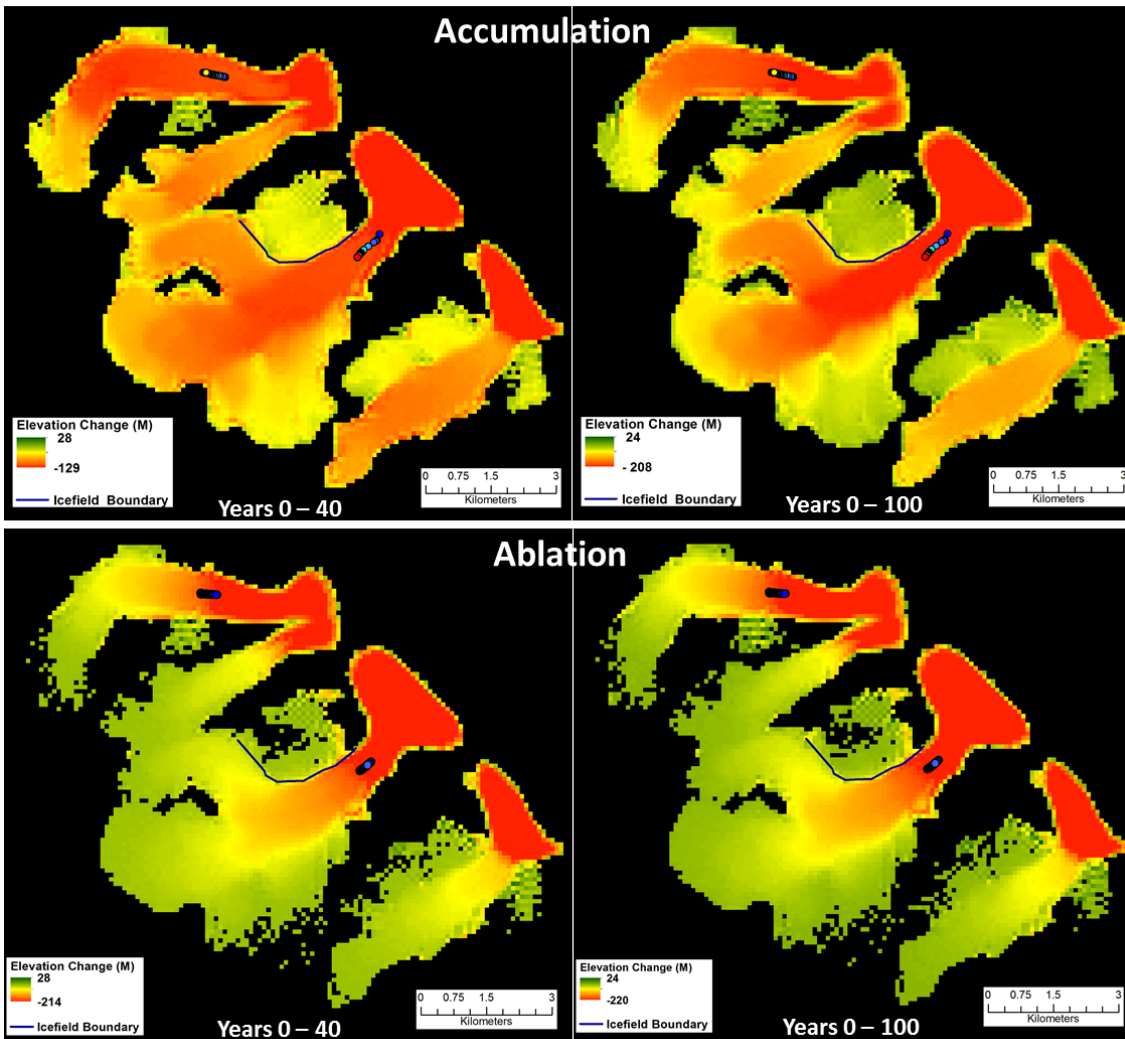


FIGURE 6.26 - ICE SURFACE THINNING

Ice surface thinning 40 years and 100 years after abrupt reduction in accumulation / increase in ablation. Note the larger degree of thinning in the accumulation area during the accumulation driven experiment.

As a result, despite PCT_x retreat, surface thinning in the accumulation area meant that instead of retreating up the longitudinal ice surface slope to higher elevations, PCT_a remained relatively fixed as PCT_x retreat and ice surface thinning occurred synchronously (figure 6.27).

This observation highlights the importance of monitoring changes in PCT_x position as well as PCT_a changes and supports the simple but important concept of change scenarios introduced in section 2.4.3. Without knowledge of PCT_x , analysis of the PCT_a data alone in this instance could have been interpreted as evidence of equilibrium conditions.

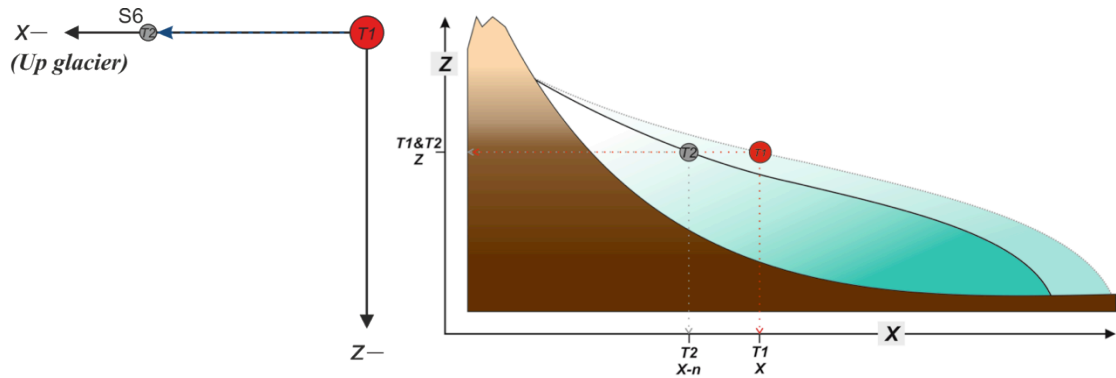


FIGURE 6.27 – SYNCHRONISED RETREAT AND THINNING

Left: The directional vector of the PCT between an initial observation at T1 and subsequent observation at T2. Right: Idealised longitudinal glacier profile demonstrating the theoretical change in glacier volume required between T1 (dashed surface) and T2 (solid black line) to enable the PCT to display a reduction (retreat) along the X plane whilst maintaining a uniform Z value (elevation) between observations.

This idea forces one to re-evaluate the way in which the ELA, a staple tool in assessing glacier-climate interactions (Braithwaite and Raper, 2007; Braithwaite and Raper, 2010; Chinn et al., 2005; Dyurgerov et al., 2009; Zemp et al., 2007), has been recorded and utilised for subsequent climate analysis for the past 6 decades (Braithwaite, 2002; Braithwaite 2009; Fischer 2010). In currently available datasets, the ELA has either been visually identified through field measurements or more often than not has generally been determined, in the context of mass-balance measurements, by fitting a curve to data representing surface mass balance as a function of altitude (such as in figure 6.2). However, information concerning the planar position of the ELA, i.e. the geographic coordinates at the point where the ELA intersects the centre flow line, has been neglected. Accordingly there is the potential that periods of limited change observed in long-term ELA records, without the context of mass balance information, could have been misinterpreted as evidence of a steady climate. This is because ELA records may neglect to take into account the possibility that the ice surface has thinned over the monitoring period to the extent that the migration of the ELA closer to the headwall has occurred without the corresponding elevation increase. Considering the occurrence of a globally negative mean mass balance (Braithwaite et al., 2012; Dyurgerov and Meier, 2005; Zemp and van Woerden, 2008) and the more recent observations of glacier wastage (Farinotti et al., 2009; Fujita and Nuimura, 2011; Kohler et al., 2007; Paul 2008) there is the potential that ELA records alone do not represent the true extent of the climate perturbations that have driven this globally negative trend.

Another fundamental aspect of PCT monitoring is the calculation of the proportional PCT position or PCT_p . Earlier empirical observations suggested that glaciers tend towards a three-dimensional surface geometry where the transition from the concave transverse surface profile to the convex transverse surface profile occurred at very similar proportional positions across glaciers of different size, hypsometry, thermal regime and so on. The observations presented here have led to the belief that knowledge of the PCT_p could provide insight concerning the degree to which flow dynamics and glacier extent have responded, and are responding, to climate forcing at different rates. The empirical observations indicate that glaciers tend to produce a PCT_p of around 0.4 when flow dynamics and glacier extent are balanced or varying in unison.

The results from the steady state advance experiment (figure 6.10) show that PCT_p values vary little across the sample despite significant differences in glacier area, length and hypsometry and valley geometry. This observation supports the proposition that PCT_p evidences the glaciers' ability to adjust glacier flow dynamics in response to climate forcing and tend towards a common geometric surface required to maintain a steady glacier hypsometry and three-dimensional shape. Furthermore, the mean PCT_p value observed during the steady state experiments (0.34) compares well to the prediction made in chapter five. In view of these results one could understandably be tempted to state that glaciers demonstrating PCT_p values close to the observed mean are near to being in steady state. However, when comparing the mean PCT_p values from the steady state simulations (0.34) to the empirical observations made in chapters three (0.39) and four (0.36), it is clear that there is very little difference between the observations. We know that the glaciers observed in chapters three and four were not in steady state through knowledge of their mass balance and terminus fluctuation records, yet they share comparable PCT_p values. Further still, the results from the abrupt advance and retreat experiments (figure 6.12 and 6.14) display that PCT_p values for all observed glaciers largely remained within the 0.3 to 0.4 range despite the glaciers departing from equilibrium states. As a result it can be concluded here that specific PCT_p values, irrespective of the chosen values, cannot be considered representative of a glacier being in steady state. Nevertheless, the results support the interpretation that glaciers tend towards dynamic balance

when the organisation of the flow field is in a state capable of maintaining the glaciers extent and hypsometry *at the time of observation*. This means that glacier extent must adjust if there is a change in the glacier flow-field's structure, evidenced by a change in PCT position, and *vice versa*. Accordingly, it is possible to understand how a glacier can then be dynamically balanced, or *flow-balanced*, but remain out of synchronicity with climate.

With this in mind, observations of unusually high and low PCT_p values in chapters three and four led to the suggestion that such "extreme" values were indicative of glaciers where flow dynamics and glacier extent / three-dimensional mass distribution were responding to climate forcing independently at differing rates termed as being "flow-unbalanced". It was hypothesised that high PCT_p values were indicative of changes in flow dynamics driven by a reduction in accumulation where the PCT would retreat up-glacier, due to a reorganising of the glacier flow-field, at a rate faster than that of terminus retreat. However the results of the modelling experiments did not support this interpretation. As figure 2.26 suggests, surface thinning above the PCT driven by the reduction in accumulation resulted in limited elevation variation despite observable PCT_x retreat. As a result the PCT is unlikely to reach disproportionately high elevations through the proposed mechanism, and so if one was to base conclusions upon these modelling experiments alone, the hypothesis linking high PCT_p to changes in accumulation rates would have to be rejected.

However, when comparing PCT_x retreat recorded during the accumulation and ablation driven experiments, it is clear that PCT_x retreat was much greater during accumulation-driven retreat. This suggests that changes in accumulation are more likely to lead to an adjustment in the organisation of the glacier flow field, and thus changes in PCT position, than that which would occur during glacier retreat driven by enhanced ablation alone. As a result, one could justifiably expect a significant reduction in accumulation to lead to high PCT_p values. However, the model experiments were unable to replicate or recreate the extremely high PCT_p values that were recorded during the empirical observations. This forces one to question whether the climate perturbations imposed during the accumulation driven retreat experiment were strong

enough. Given that the PCT showed a significant response to accumulation forcing, perhaps a more severe reduction in accumulation rates would have lead to the formation of much higher PCT_p . This is an experiment that will contribute to the future work of this thesis.

The second hypothesis proposed in chapter five concerning how PCT_p values may be used to infer specific climatic forcing was concerned with PCTs observed at disproportionately low elevations upon glacier surfaces. Specifically that low PCT_p was indicative of an abrupt increase in ablation at lower elevations due to temperature increases resulting in snout thinning and retreat faster than PCT forming flow dynamics could respond. When observing the results in figure 6.19 and figure 6.20, the data displays evidence of the PCT_p lowering where the snout retreats to higher elevation whilst the PCT remains relatively stationary, presumably due to a lack of adjustment in glacier flow-field. This variation in retreat rates of the two glacier components is further evidenced by the fact that on glaciers 2 and 4, PCT_x was observed to retreat 328 m and 370 m compared to snout retreat of 1906 m and 1778 m respectively. However, the PCT_p values in the simulated results do not reach the same low values (0.10) that have been identified through empirical observations in chapters 2 and 4. This is attributed to the shallow gradient upon which the glaciers' initial retreat was located. Accordingly, it is suggested here that the lowering of the PCT_p would have been amplified had the glaciers snouts retreat up the steeper longitudinal valley of the main ice mass. Yet, it is also worth mentioning once again that perhaps the model results did not produce the same low PCT_p values observed in chapters three and four due to the fact that the simulated climate forcing was not as extreme as has been experienced by real world glaciers. As a result, the model simulations may have underestimated the extent of the climate forcing that is currently driving the previously observed glacier responses. It is also important to consider the results of the abrupt advance experiment displayed in figure 6.12. The blue arrows indicate that PCT_p values dropped rapidly shortly after the ELA perturbation. This drop in PCT_p was the result of rapid PCT_x advance and PCT_a decrease whilst no change in minimum ice elevation occurred. This is evidence of the glacier being in a transitional phase where flow dynamics are changing but the glacier's mass has not yet been fully redistributed in order to achieve equilibrium. This

observation complicates interpretations of low PCT_p values as it means that low PCT_p values are not always be evidence passive glacier retreat. However, one can be confident that glaciers displaying low PCT_p values are not *flow-balanced* but are in fact in transitional phase where ice flow and glacier extent is adjusting to a significant climate perturbation.

The modelling experiments have been extremely useful in verifying the interpretation that the PCT is closely related to glacier mass balance and how PCT_p observations can be used to infer information concerning how glaciers are adjusting to climate forcing. The experiments have also been particularly useful in developing our understanding concerning how glaciers tend towards dynamic equilibrium and how the degree of glacier *flow-balance / unbalance* can be assessed using PCT_p records. However, the modelling results were unable to fully elucidate why very high PCT_p values were observed upon the glaciers discussed in chapters three and four. The modelled results produced a maximum PCT_p value of 0.5 compared to 0.66 calculated from the empirical observations. However, one potentially useful insight provided by the modelled results is that of the total 356 PCT_p measurements, 77 cases showed PCT_p values >0.40 . Of these 77 cases, the majority (60%) were recorded during the abrupt glacier retreat experiments where PCT and glacier changes were driven by a sharp 200 m increase in the ELA. This result suggests that, as with the abrupt advance results, the PCT retreated at a rate greater than the glacier snout, resulting in a slightly higher PCT_p value.

6.4 Summary of outcomes

- The model simulations successfully produced observable PCTs and three-dimensional ice surface geometries resembling those recorded in real glaciers. Furthermore, the locational characteristics of the modelled PCTs agree well with the observations made in chapters three and four.
- The dynamic nature of the PCT where its elevation and planar location varied in response to adjustments to the ELA highlights the close relationship between the two variables. The results suggested that changes in PCT position are driven changes in the spatial distribution of mass balance. This is further supported by the observation that the PCT displayed minimal variation when the equilibrium line was held

constant and changes to glacier mass balance were forced through increased melt/decreased accumulation.

- However, the variance in the PCT_a - ELA offset during periods where the glaciers were forced out of sync with climate, and were thus in a transitional phase, support the interpretation that PCT_a cannot be used as a proxy for modern day ELAs.
- The results suggest that the PCT_x responds fairly rapidly to changes in ELA by retreating / advancing in order to reduce the offset between the two variables. The simulations computed here suggest that the PCT reaches a new equilibrium location on the order of decades after the initial climate perturbation.
- It is suggested that during ELA driven glacier advance, the PCT reaches a new equilibrium position before total glacier extent and hypsometry reaches equilibrium. This is evidenced by the fact that ice surfaces continued to thicken in response to positive mass balance for a number of decades after PCT_x had reached equilibrium.
- PCT_p values cannot be used to identify whether glaciers are in steady state with climate forcing. This is due to the observation that PCT_p values upon glaciers generated during the ELA forcing experiments remained relatively constant irrespective of being in equilibrium or not.
- However, the small variation in PCT_p values produced during the ELA variation experiments reveal that glaciers tend towards a state whereby the PCT locates 30 – 50% up-glacier from the terminus elevation. Initially observed upon real world glaciers, the results from the model runs support the idea that glaciers can be “flow-balanced” when flow vectors, indicated by the PCT, are in a state of organisation capable of maintaining the glacier’s areal extent and hypsometry at *that moment in time*. The stipulation of a specific timeframe is important to consider as the flow dynamics will need to adjust as glacier extent varies in response to the climate forcing and vice versa. Accordingly, glaciers can be *flow-balanced* but still out of sync with climate.
- The observation of steady PCT_a despite evidence of planar retreat highlights the need to record changes in PCT_x when assessing glacier changes based upon PCT observations.
- The results from the ablation forced simulations and the abrupt glacier advance experiment highlight the potential to use low PCT_p as evidence of glaciers being in a transitional phase where glacier flow and glacier extent are adjusting at different rates to climate forcing.

- The modelling simulations did not reproduce the extremely high proportional PCT positions recorded from real world empirical observations. This suggests that the model forcing was not severe enough to replicate the forcing currently being experienced by real glaciers in many regions of the world. However, the modelling does hint towards the idea that high PCT_p values may be the result of rapid changes in flow dynamics, in response to a rise in the ELA and changes in accumulation, at a rate greater than that of the response of glacier extent.

Chapter 7 PCT Observations in the Hindu Kush-Karakoram-Himalayas

The work completed thus far has been to gain insights into how the PCT relates to climate and glacier dynamics. This has been achieved initially in chapter two by discussing the physical processes that form the idealised three dimensional ice surface geometry as a result of the complex relationship between climate forcing and ice-flow dynamics. With the fundamental theoretical understanding of why PCT formation is related to climate, chapter three and four then assessed whether the relationship between PCTs, climate and glacier health could be empirically observed. The hypotheses, developed based upon the observations and theoretical knowledge of the PCT, concerning the ways in which PCT observations may provide insight into how glaciers are responding to climate forcing, were then tested through computer simulations.

One is now in a position to switch the approach of this investigation. Instead of assessing PCT behaviour upon known glaciers in order to better understand the physical controls over PCT behaviour, PCT observations will be used to gain insight into how unknown glaciers are responding to climate. The focus however will not be upon assessing how individual glaciers are responding to climate forcing but how the PCT can be used to assess glacier-borne climate signals on a large scale. Consequently, this chapter aims to record the PCT on a large sample of glaciers in the Hindu-Kush, Karakorum and Himalaya region (HKKH) in the hope of developing a better understanding as to how the general glacier populous of the region is faring in today's climate.

7.1 The Current State of HKKH Glaciation

Recent estimates of glacier coverage in the high mountainous regions of Asia range from 118,629 km² (Radić and Hock, 2010) to 128,444 km² (Hirabayashi et al., 2010) with 60,000 km² of this contained in the HKKH region alone (Kääb et al., 2012). Consequently, the region represents the third highest concentration of perennial ice outside of the polar regions (Rasmussen, 2013). Glaciers in the HKKH are a vital resource to the region's large population as they store water in years of high snowfall and release it in years of low precipitation.

Additionally Barnett et al. (2005) suggested that glacier melt-water in High Mountain Asia accounts for more than half of all stream flow in the region's main rivers. Furthermore, calculations of global glacier volume and ice thickness distributions suggest that glaciers in High Mountain Asia have the potential to raise global sea levels by 24 mm (Huss and Farinotti, 2012). However, despite the clear significance of this region, a dearth of direct glaciological data is hindering our understanding of how glaciers in the HKKH are faring in today's climate. Of the >21,000 glaciers that populate the Greater Himalayan region (Cogley, 2011) only 12 have ever been the subject of direct mass balance measurements and of these, only the minority provide a continuous record of more than 5 years. Furthermore, all but one of these monitoring programs have been terminated, with only Chotta Shigri glacier in the Indian Himalayas continuing to be directly monitored (WGMS, 2012). As a result, annual amounts of ice and snow melt, along with seasonal and spatial variability, are all uncertain (Bolch et al., 2012). This lack of *in situ* measurements can be attributed to the remote and dangerously rugged terrain, coupled with the complex geopolitical relations that characterise the region, which make physical access difficult.

The lack of understanding, and the recent controversies concerning future projections of Himalayan glaciation (Cogley et al., 2010), has fuelled the urgency amongst glaciologists to gain greater insight into the state of glaciers in the region. Accordingly, this situation has provided an opportunity for remote sensing studies to act as a substitute for *in situ* measurements and enhance our knowledge of how glacier characteristics and thus climate is changing in the HKKH.

A mass budget of $-5 \pm 6 \text{ Gt yr}^{-1}$ was calculated for glaciers in the HKKH ($-4 \pm 20 \text{ Gt yr}^{-1}$ for the entire High Mountain Asia) between 2003 and 2010 based upon satellite gravimetry (GRACE) (Jacob et al., 2012). However, their results contained high errors and also identified high inter-annual variability in the region's gravitational signal, which can be problematic when determining mass loss rates over short periods (Jacob et al., 2012). Nevertheless, the observations suggested that although the region was losing ice mass, the losses were low relative to the volume of ice in the HKKH compared to other regions around to

globe. Kääb et al. (2012) postulated a similar observation when producing geodetic mass balance estimates for the HKKH. By comparing glacier surface elevations between 2000 (SRTM) and 2008 (ICESat laser altimetry) they estimated mass balance of the HKKH to be $-0.21 \pm 0.05 \text{ m yr}^{-1}$, significantly less negative than other estimates of the global average for glaciers outside of Greenland and Antarctica based upon *in situ* measurements of around -0.75 m yr^{-1} (Braithwaite, 2009; Cogley, 2009; Dyurgerov and Meier, 2005; WGMS, 2012). Perhaps more important though was the spatial heterogeneity in glacier mass change that they observed across the study area. Their results highlighted widespread glacier wastage in the eastern, central and south-western regions of the HKKH with maximum thinning rates of $-0.66 \pm 0.09 \text{ m yr}^{-1}$ whilst glaciers in the Karakorum thinned by only a few centimetres each year. This spatial variability in glacier response to climate change in the HKKH has also been identified through glacier terminus and flow velocity observations by Scherler et al. (2011b). Their results were similar to those of Kääb et al. in that the glaciers in the east, south and central Himalayas displayed the highest frequencies of retreat whilst the majority of glaciers in the Karakorum region either remained unchanged or even advanced. However, unlike Kääb et al. who stated that debris cover had little impact on glacier wastage, Scherler et al. attributed much of the observed heterogeneity in glacier response to the varying degrees of debris cover identified upon the glaciers across the sample.

Regional scale studies of glacier mass balance based upon a small number of *in situ* measurements (Fujita and Nuimura, 2011; Wagnon et al., 2007; WGMS, 2012), estimations of glacier volume change (Berthier et al., 2007; Bolch et al., 2008; Bolch et al., 2011) and changes in glacier aerial extent (Bhambri et al., 2011; Ren et al., 2006; Scherler et al., 2011b) have identified that glaciers in the east, south and central Himalayas are retreating and are doing so at increasing rates. However this cannot be said for the north-western regions of the HKKH where glacier expansion has been observed in the Karakorum. Such observations are particularly interesting due to their anomalous nature when taking into account the global trend of glacier recession (Dyurgerov and Meier, 2005).

Hewitt (2005) was among the first to suggest that the Karakorum was showing signs of anomalous glacier advance. The proposition was based upon field

observations of both rapid and gradual snout advances, coupled with evidence of increased winter precipitation, declining summer temperatures and reduced summer discharge recorded at stations downstream. These indirect measurements indicative of positive glacier mass balance were then confirmed by Gardelle et al. (2012b) who measured the geodetic mass balance for a large region of the Western Karakorum. Comparisons of ice surface elevation from two co-registered DEMs (SRTM and a photogrammetrically derived DEM from 2008 SPOT imagery) revealed glacier thickening between 1999 and 2008 demonstrative of an annual mass balance for the 5,615 km² study area of $+11 \pm 22$ m yr⁻¹ w.e. A more recent study by Gardelle et al. (2013) reports a regional mass balance estimate for the Eastern Karakoram of $+0.11 \pm 0.14$ m yr⁻¹ w.e. between 1999 and 2010.

Considering the observed regional variation in glacier behaviour across the HKKH, one could also expect to see regional differences in glacier flow dynamics. As a result, the observations discussed above provide an excellent opportunity to see whether regional differences in PCT_a and PCT_p location reflect the geographical variation in glacier behaviour identified by previous studies throughout the HKKH. Furthermore, drawing upon the insights gained from the previous chapters, PCT observations may go some way in accounting for the spatial heterogeneity observed in glacier behaviour and shed some much needed light on the response of the region's glaciers to climate perturbations.

7.2 Methodology

7.2.1 Study Area

7.2.1.1 Geographical extent

The study area spans over two thousand kilometres, from Tajikistan in the northwest to Bhutan in the southeast, passing through Afghanistan, Pakistan, India, China and Nepal (figure 7.1). The studied region consists of the Hindu Kush, Karakorum, Greater Himalayas and the Kunlun Shan mountain ranges with a total glaciated area exceeding 60,000 km² (Kääb et al., 2012).

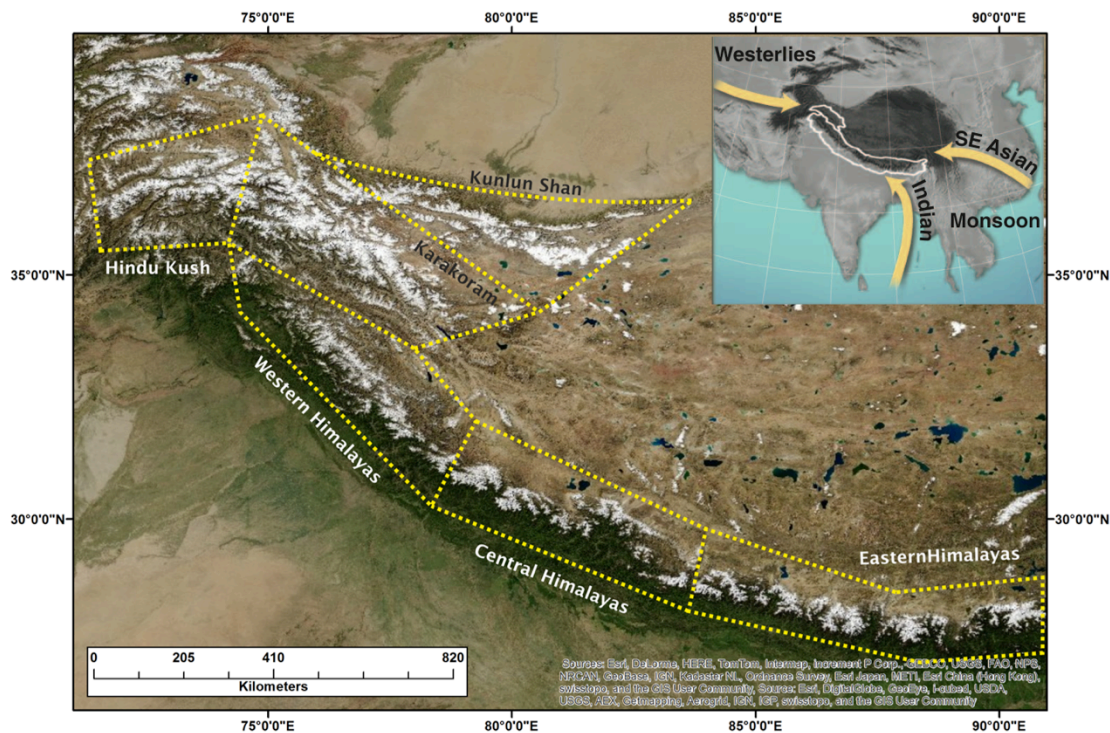


FIGURE 7.1 – HKKH STUDY AREA

The dashed lines represent the boundaries of the studied mountain ranges. Range delineations are estimated, based upon those defined by Kääh *et al.* (2012) and Gardener *et al.* (2013). The inset highlights the key weather systems that influence the study area.

7.2.1.2 Climate of the HKKH

The study area also provides a unique opportunity to identify how PCT characteristics differ on glaciers under differing climate regimes. This is because glaciers in the central and eastern Himalayas experience a different climate to those 2000 km west in the Karakorum-Hindu Kush ranges. Glaciers in these two areas experience markedly different climate, especially in terms of the source and type of precipitation, and reveal great variation in their behaviour and dynamics (Armstrong, 2010). However, there is no abrupt division between these two climatic systems; rather, conditions change gradually across the HKKH region.

The varying dominance of the Asian monsoon and Westerlies across the HKKH results in the distinct climate gradient observed across the region (Bolch *et al.*, 2012). In the north western region of the HKKH, glaciers in the Karakorum and Western Himalayas rely upon moisture brought in by westerly cyclones. Here, over two thirds of the annual high-altitude snowfall that accumulates in the winter months is due to westerly circulations (Bookhagen and Burbank 2010).

However towards the east into the central and eastern Himalayas, over 80% of snow precipitation is provided by the summer monsoon (Bookhagen and Burbank, 2010). The very high elevation of the HKKH mountains also block the transfer of moisture to the Tibetan Plateau. This results in a sharp precipitation gradient that decreases north/north-eastward present in both the monsoon and westerly dominated region respectively (see figure 7.1 insert).

Trends in air temperature have also varied largely over the HKKH in recent decades. Shrestha et al. (1999) reported increasing temperature trends of up to 0.12°C per year in most regions of the central and eastern Himalayas in recent decades. Similarly Shekhar et al. (2010) identified an increase in maximum and minimum temperatures of 1.0 and 3.4°C across the Himalayan region between 1988 and 2008. Furthermore, these temperature increases have been accompanied by decreasing trends in precipitation (Shekhar et al., 2010). In contrast, decreasing temperature trends have been observed in the Karakorum (Armstrong, 2010). Along with increasing trends in precipitation (Fowler and Archer, 2006), the Karakorum range has experienced a decrease in maximum and minimum temperatures of 1.6 and 3.0°C, respectively between 1988 and 2008 (Shekhar et al., 2010).

Owing to the climate gradient across the HKKH, glacier accumulation and ablation patterns also differ distinctly across the region. In the east, central and parts of the western Himalayas, both maximum accumulation and ablation typically occur during the summer monsoon season. Here accumulation occurs at the highest elevations whilst concurrent melt occurs below. However, in the west (Karakorum), maximum accumulation rates generally occur during the winter while melt reaches a maximum in the summer, similar to North America and Europe. According to Armstrong (2010), in the west glacier termini tend to extend to lower elevations (approximately 2500 masl) compared to those in the east (~4000 masl). This is primarily due to the lower temperatures at higher latitudes of the more western mountain ranges (Armstrong, 2010).

7.2.2 Sample Glacier Characteristics

PCT data have been extracted from 2409 individual glaciers across the HKKH with a further 309 PCTs measured upon tributary ice masses that form part of

the “compound basins” (Rau et al., 2005) that account for ~7% of the sample. “Compound basins” are glacier systems where two or more individual valley glaciers issuing from tributary valleys coalesce to form a single glacier system (figure 7.2 C). “Compound basin” type glaciers, where multiple accumulation basins feed a single glacier trunk (figure 7.2 B), constitute ~18% of the sampled glaciers while the remaining ~ 75% of the sample is composed of simple basin formed glaciers (figure 7.2 A). However, despite “compound basin” and “compound basins” type glaciers accounting for only a quarter of the total population, the areal coverage of these large, complex glaciers systems accounts for 70% of the total ~27,300 km² area of the sample (based upon Randolph Glacier Index outlines). Such observations highlight the need for glacier monitoring networks to pay attention to how these large glacier systems are responding to climate perturbations. Currently, available *in situ* mass balance measurements, from which global estimates are extrapolated, are limited to small, simple basin mountain glaciers (Braithwaite, 2002). Accordingly, due to the relative ease with which PCT data can be collected, this study has the potential to assess the health state for a much more representative sample of glaciers than *in situ* mass balance measurements alone could. Glaciers with extensive debris mantles on the surface of the ablation area are also underrepresented in glacier mass balance databases. In this sample, 120 or 5% of glaciers have an extensive debris mantle, as defined by Rau et al. (2005). Although this may seem small, the debris mantles are commonly observed on the larger compound basin/basins type glaciers and as a result account for >4500 km² of the HKKH’s glaciated area.

As with chapter three, only glaciers that demonstrate “normal” terrestrial termination (Rau et al., 2005) are included in this study due to the control over glacier dynamics exerted by processes at fronts that calve into ice dammed lakes. In such cases, flow regime and mass changes can occur independently of climate perturbations, particularly in lacustrine environments (Benn et al., 2007; Howat et al., 2005). As a result, glaciers terminating in proglacial lakes have been discounted from the sample. Also, only glaciers that display a clearly recognisable PCT were included due to difficulty arising when extremely complex surface topographies prevent the identification of a clear PCT. As a result, glaciers with single or multiple icefalls present in the area where one

would expect to locate the PCT, have been excluded from the final analysis (figure 7.3). (See section 3.2.2.4 for a more detailed reasoning concerning the exclusion of glaciers with icefalls.)

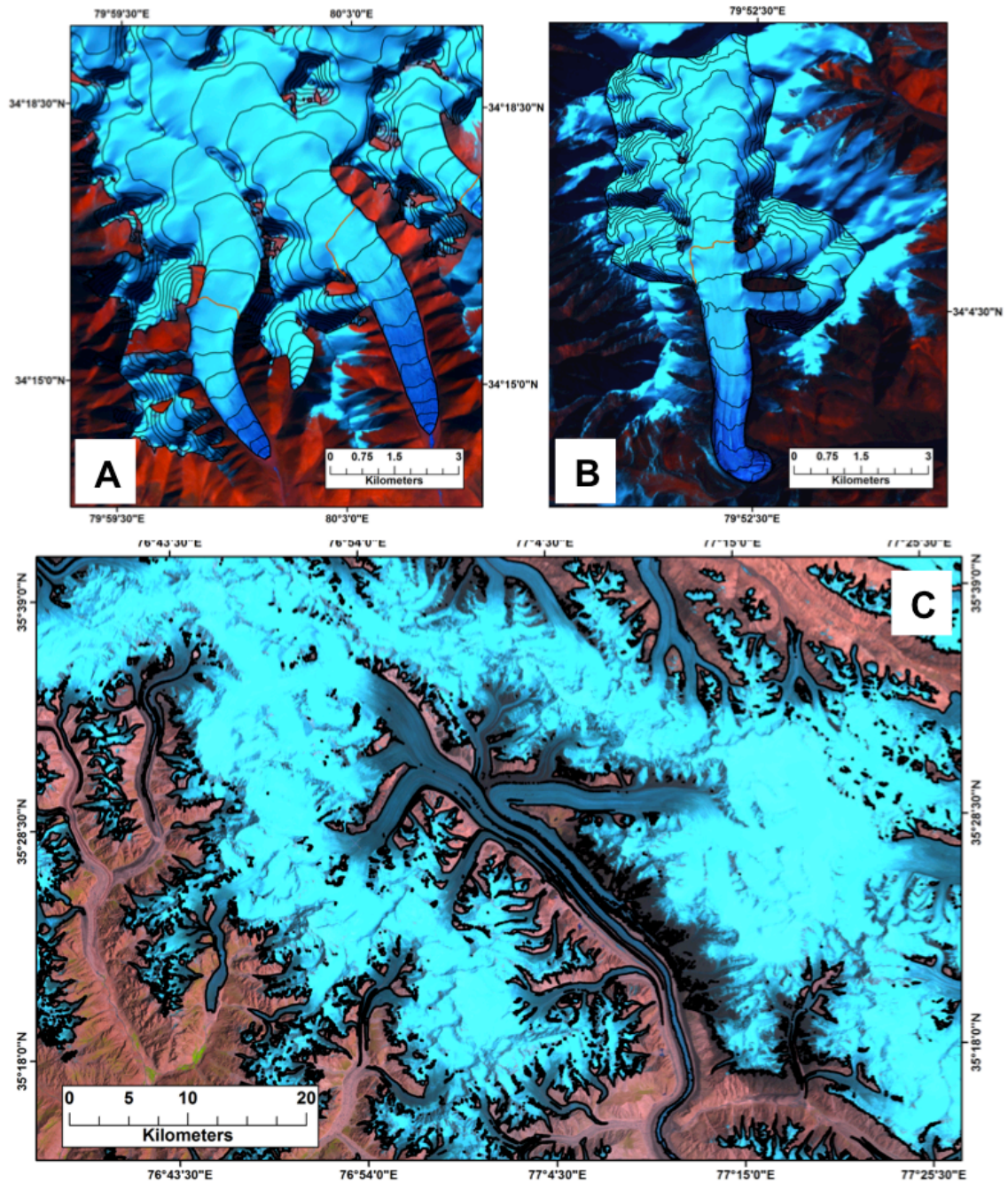


FIGURE 7.2 – GLACIER TYPES ACROSS THE HKKH

A: Simple basin – develops a glacier tongue from a single/two basins. B: Compound basin – Multiple accumulation basins feeding a single glacier system. C: Compound basins - Two or more individual valley glaciers issuing from tributary valleys and coalescing.

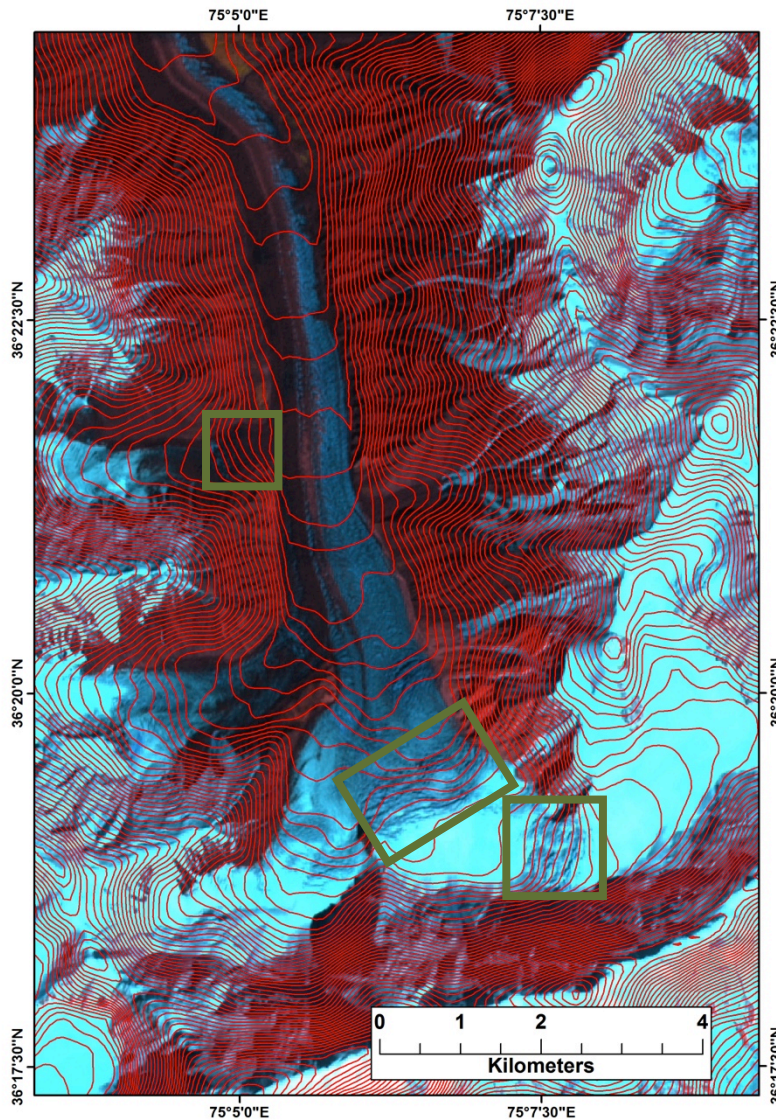


FIGURE 7.3 – COMPLEX GLACIER SURFACE
Zones of localised steepness in the longitudinal slope gradient combined with tributary confluencing (indicated by the green boxes) create complex ice surface geometries that make accurate PCT delineation difficult.

7.2.3 Data Sources

7.2.3.1 Landsat 7 ETM+

Table IV, appendix C, lists the Landsat tiles used in this chapter for the purpose of identifying glacier locations and boundaries for the collection of the inventory data.

See section 3.2.2.2.1 for technical details of the optical imagery used.

7.2.3.2 SRTM

The SRTM DEM with ~90 m resolution generated from interferometry (InSAR) data from February 2000 was used to derive elevation measurements for glacier

and PCT attributes. Maximum elevation errors of ± 9 m and maximum planimetric errors of ± 13 m for the total dataset have been reported by Rodriquez et al. (2007) when comparing the DEM with ground control points (GCPs).

7.2.4 Extraction of PCT and Inventory Data

The PCT was visually identified and PCT_a recorded using the same approach as outlined in section 3.2.4. Due to the large-scale nature of the mapping effort and the high frequency of debris-covered glaciers populating the HKKH, glacier outlines were not digitised due to time constraints. However, maximum, minimum and mid range elevation, glacier length and information pertaining to longitudinal slope profile were extracted from the semi-manually generated centre-line. Refer back to section 3.2.3 for a reminder of the collection method.

7.3 Results

7.3.1 PCT elevation

Summary results pertaining to PCT characteristics across the entire study area are displayed in table 7-1 whilst the distribution of PCT observations and their elevation is displayed in figure 7.4.

Region	Mean PCT _a (MASL)	Mean PCT _p	Mean mid-range Ice elevation
Hindu Kush	4294	0.4	4951
Karakoram	5418	0.38	5510
Kunlun Shan	5745	0.4	5803
W. Himalaya	5217	0.43	5239
C. Himalaya	5582	0.44	5639
E. Himalaya	5647	0.3	5787
HKKH	5317	0.39	5488

TABLE 7-1 - SUMMARY RESULTS OF PCT CHARACTERISTICS ACROSS HKKH AND SUB REGIONS

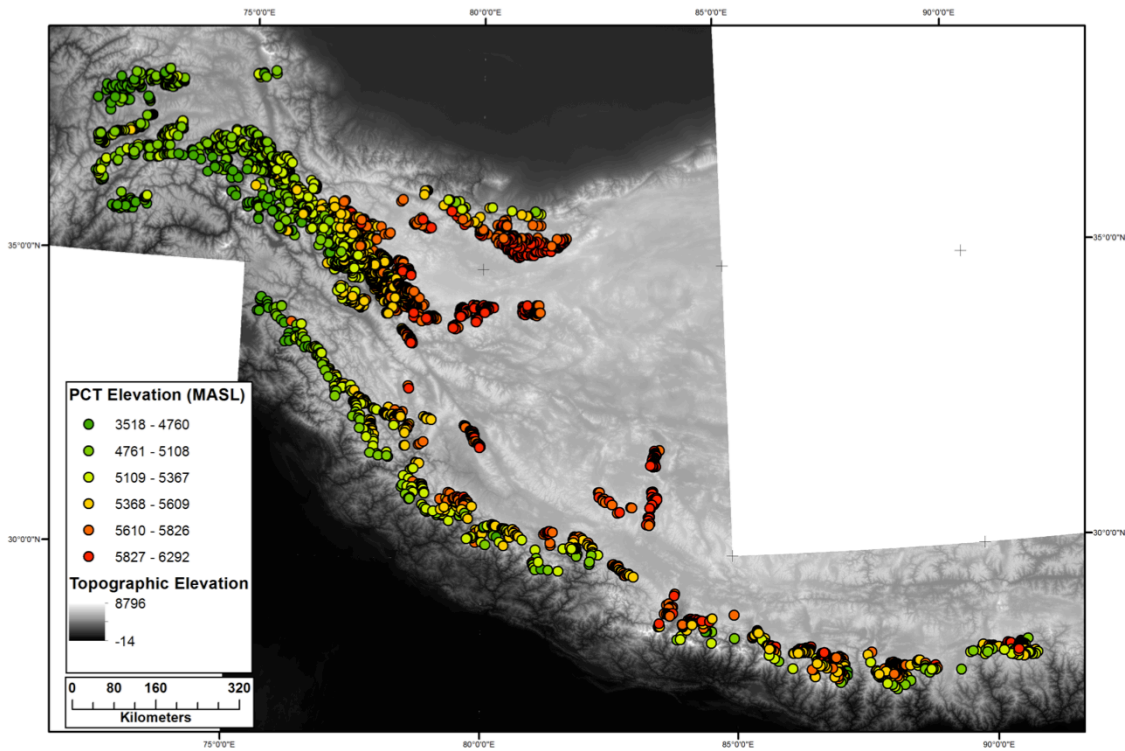


FIGURE 7.4 - PCT ELEVATION
Raw PCT elevation in metres above sea level spanning the Hindu Kush – Karakorum – Himalaya mountain ranges.
n=2718

The above figure reveals that PCT_a measurements display clear regional patterns across the HKKH. PCTs display a trend of increasing elevation travelling from the southern/western slopes of the ranges to the more continental Tibetan plateau. This trend appears more uniform in the westerlies dominated Hindu-Kush – Karakorum regions compared to the more uneven variations in PCT_a observed in the Indian summer monsoon dominated eastern and central Himalayas.

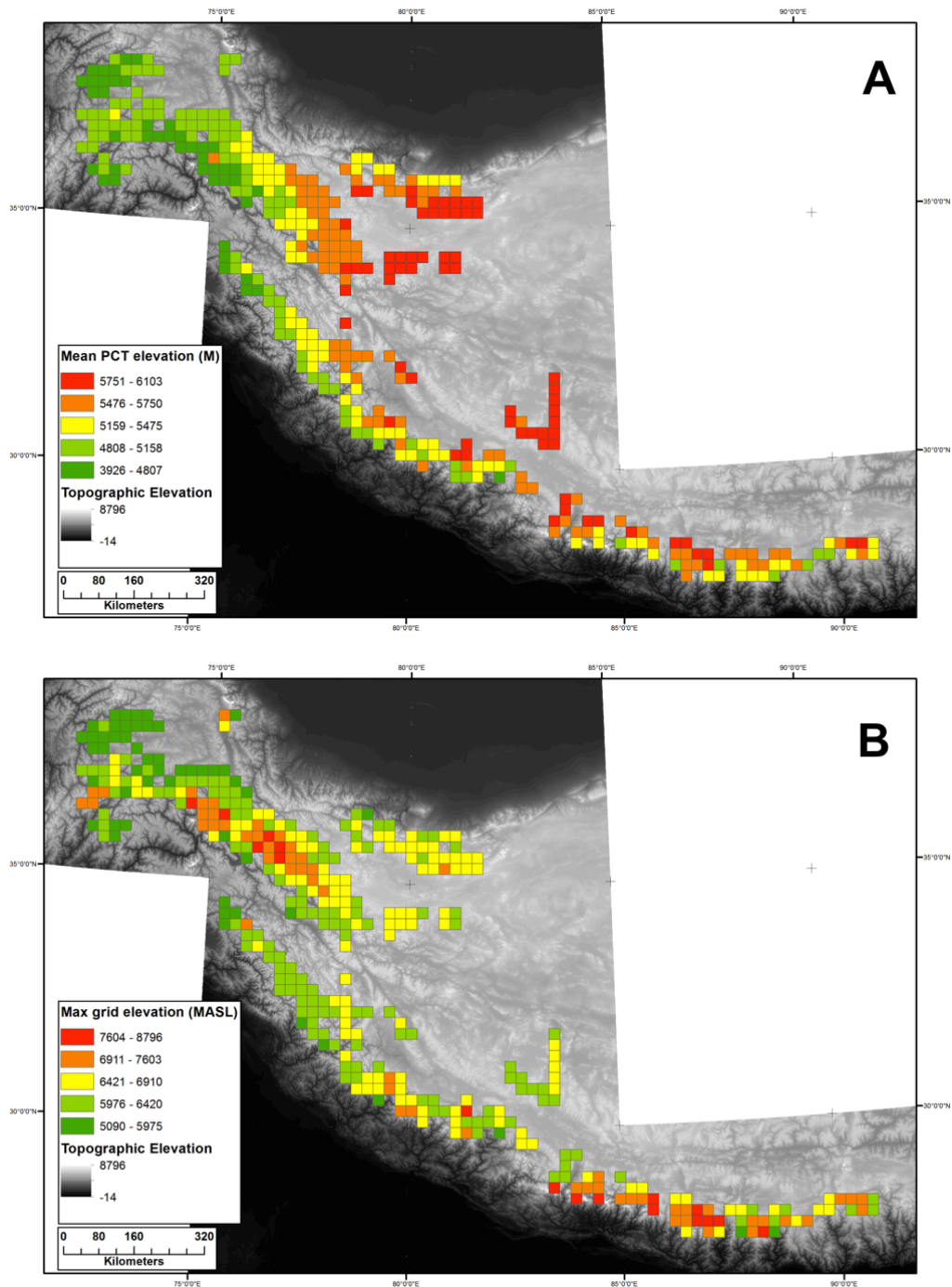


FIGURE 7.5 - PCT VS TOPOGRAPHY MAP

A) The mean elevation of all the PCTs located within the cell boundary. B) The maximum elevation of the topography within the grid cell.

Before taking the analysis of these results further, it is important to rule out the possibility that this striking pattern is not simply a reflection of the elevation of the underlying topography. In order to test this, PCT_a observations were aggregated using a 25 km cell grid in ArcGIS. This process produced a gridded

dataset with each grid value representing the mean of the PCT_a values recorded in that 25 km² area and enabled the mean PCT_a and maximum topographic elevation for each cell to be compared to one another. Figure 7.5A and B reveal the mean gridded PCT_a and maximum gridded topographic elevations recorded across the HKKH. Visually, the PCT_a trend appears to be independent of the general topographic elevation. The two variables were also tested for a statistically significant correlation. However, as with the visual assessment, no statistical correlation was identified (correlation coefficient: 0.24) between PCT_a and topographic elevation (see figure 7.6).

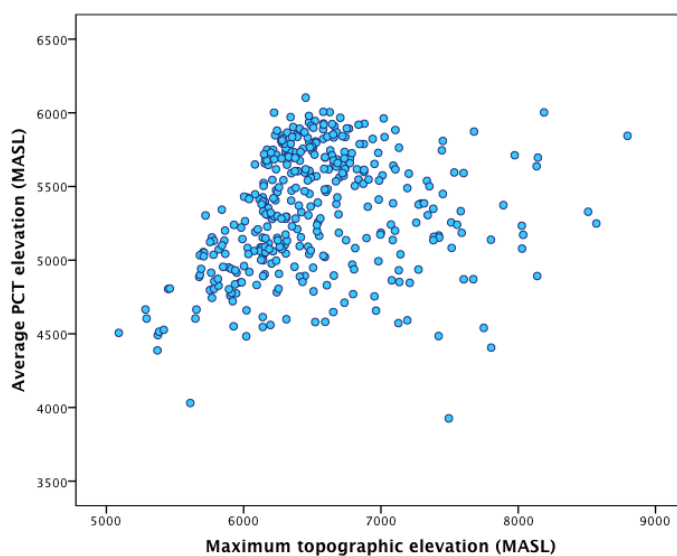


FIGURE 7.6 – PCT_a COMPARED TO THE MAXIMUM TOPOGRAPHIC ELEVATION RECORDED IN EACH 25 KM² CELL

7.3.2 PCT_p

Figure 7.7 reveals a histogram of the PCT_p values measured across the HKKH. Due to the need for minimum snout elevation for the calculation of the PCT_p , only glaciers with land terminating snouts were included. This means that tributary ice masses were excluded from the PCT_p analysis due to the impossible task of assessing the point at which they terminate and the flow dynamics of the recipient snout take over control of the adjoining ice mass. Furthermore, owing to the role that heavy debris mantles play in insulating unusually low terminus elevation from climatic forcing (section 3.3.3), glaciers with over 20% (estimated) of their snout covered by supraglacial debris were also excluded.

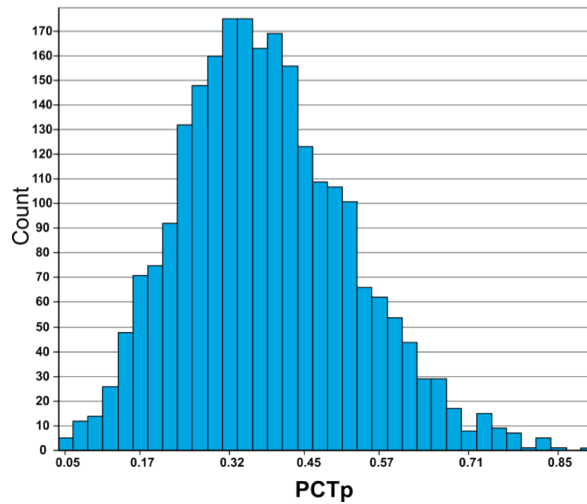


FIGURE 7.7 - PCT_p VALUES ACROSS HKKH
N=2289

The histogram reveals that PCT_p values across the HKKH display a normal distribution around a mean value of 0.39 (σ 0.13). However, it is important to note that the spread of values (0.05 to 0.86) is far greater than has been recorded hitherto during empirical observations and model runs.

The distribution of PCT_p values across the HKKH region is displayed in figure 7.8. Due to the clustered nature of glacier distributions across the HKKH, the results were aggregated using the same 25 km cell grid used in figure 7.5 in order to facilitate the identification of possible regional trends in PCT_p. The results of the aggregated PCT_p values are displayed in figure 7.9.

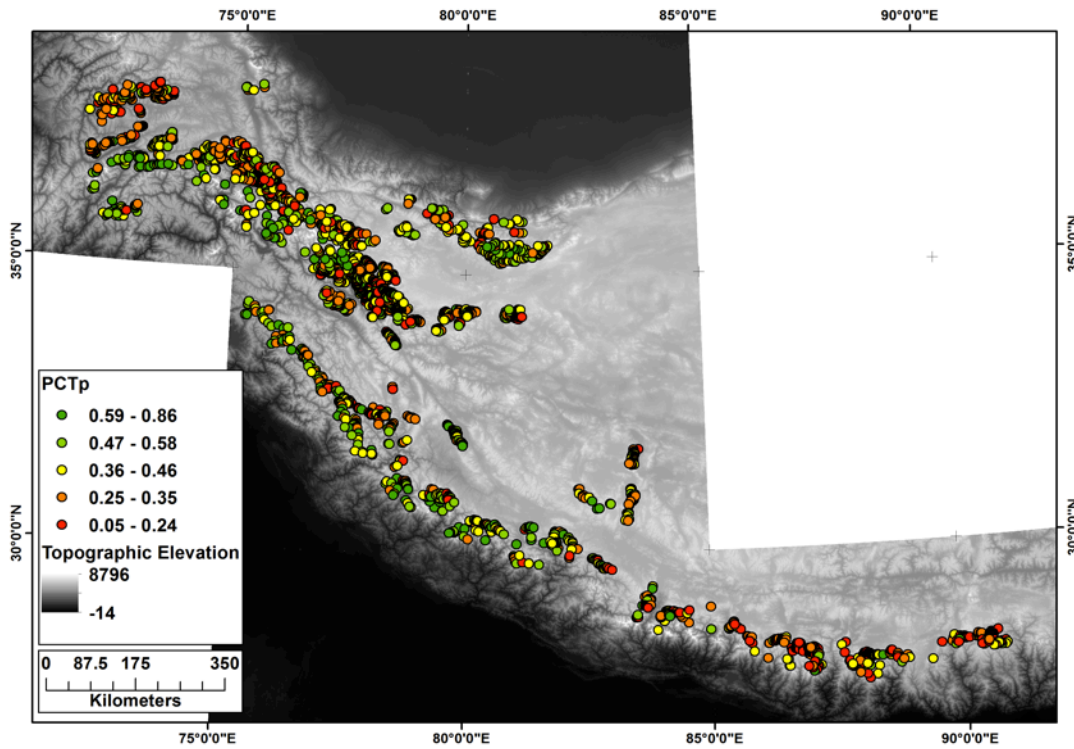


FIGURE 7.8 - PCT_p ACROSS THE HKKH

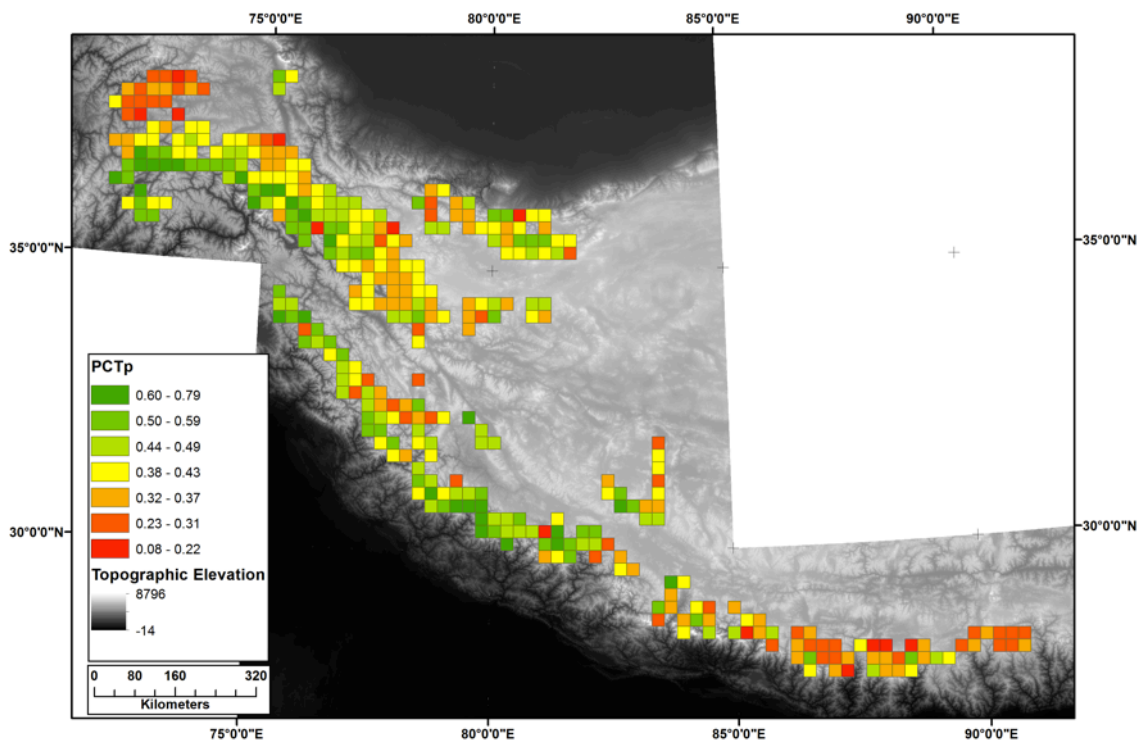


FIGURE 7.9 - AGGREGATED PCT_p VALUES ACROSS HKKH
 Each cell value indicates the mean PCT_p for that 25 km² area.

Although not as apparent as the PCT_a results, the distribution of PCT_p values in the gridded output (figure 7.9), which shows mean PCT_p values recorded over

gridded 25 km² areas, reveals evidence of spatial clustering. Although the majority of PCT_p values recorded were close to the mean value of 0.39 (0.47 for glaciers with more than 20% of their surface mantled by debris), the results also highlight the fact that very high and very low PCT_p values were not uncommon.

Figure 7.9 demonstrates that regions of very low PCT_p, indicated by the darker orange / red cells were most frequently observed in the northern Hindu Kush and much of the Eastern Himalayas. The central Karakorum region is characterised by PCT_p values ranging between 0.32 and 0.49. Particularly interesting though is the observation that the strongest patterns of regional PCT_p values are amongst glaciers displaying disproportionately high PCT elevations (darker green). Regions dominated by high PCT_p values appear to be located on the southern / western margins of the Hindu Kush and Karakorum ranges. This pattern of high PCT_p values continues into the western and central Himalayas until the PCT_p values drop when entering the ISM (Indian summer monsoon) dominated eastern Himalaya. However, despite the general patterns in PCT_p value observed across the HKKH, it is possible to identify significant variations over relatively small areas.

7.4 Discussion

The PCT_a observations displayed in figure 7.4 and 7.5A exhibit a clear spatial trend in PCT_a irrespective of the local topographic elevation. This is important to consider because if topography is not the determining factor for PCT_a, the observed spatial trend must be the result of the spatially variable climatic conditions experienced across the HKKH (Armstrong, 2010). As it has already been identified that PCT_a is closely related to the balanced budget ELA, these PCT observations can be used to infer climatic variations across the region that would account for the striking pattern.

It is interpreted here that regions characterised by lower PCT_a experience cooler or greater accumulation, or a combination of both than those characterised by high PCT elevations, which experience warmer and/or more arid conditions. Accordingly the results suggest that the Hindu-Kush, western

Karakorum and regions of the western Himalaya experience cooler temperatures and/or greater solid precipitation (snow) than areas of low PCT_a in the Eastern and Central Himalaya, Eastern Karakorum and continental ranges of the Tibetan plateau such as the Kunlun-Shan. The observed pattern of PCT_a also illustrates the sharp precipitation gradient caused by the blocking nature of the main HKKH chain where the more continental glaciers exhibit higher PCT_a than the sample mean (5408 m.a.s.l) (Armstrong, 2010; Bolch et al., 2012; Rasmussen 2013). Accordingly, the PCT_a measurements observed here represent the spatially variable climate that characterises the study region.

It is worth mentioning here that the same result could have been achieved using records of median or mid-range glacier elevation as recommended by Brathwaite and Raper (2010). However, it is proposed here that the PCT remains the preferred measure due to the reduced acquisition time required during data collection. Furthermore, although the distribution of PCT_a across the HKKH reflect the variable climate forcing displayed across the region, the real intrigue in the results concerns the extent to which PCT_p observations can inform us of the way which glaciers are responding to climate forcing across the study area.

The histogram displaying PCT_p frequencies recorded upon glaciers in the HKKH compares favourably with the results from chapter three, four and six. Once again, the mean PCT_p value across the study area of 0.39 is strikingly similar to that observed in the previous chapters (0.39 from empirical observations and 0.36 for the modelling experiments). This adds additional weight to the proposition that glacier flow dynamics tend towards an equilibrium state that produce steady surface geometries that result in homogenous PCT_p values despite differences in glacier specific variables such as accumulation area, hypsometry and valley geometry. However, the greater extremes in PCT_p values present in the HKKH compared to previous empirical observations from chapters three and four, or those produced during the model experiments in chapter six, suggest that a small proportion of the glaciers in the study area are undergoing significant variation which is producing a wider range of PCT_p values across the study region than has been seen previously in

this study. This observation then takes on greater meaning when observing the spread of PCT_p values across the HKKH region.

Although not as strong as the trend in PCT_a across the study area, figure 7.9 shows an observable pattern in PCT_p distributions. The results display that glaciers in the Eastern Himalayas and a region in the northern Hindu Kush demonstrate low PCT_p values. The results from the abrupt advance experiments, discussed in chapter six, suggest that these low PCT_p values maybe indicative of the glaciers being in a transient phase following an abrupt spell of positive mass balance (figures 6.11 and 6.12). However, without knowledge of how PCT_a has changed on these glaciers over time, such an interpretation can only remain speculative. The more likely explanation is that the low PCT_p values observed here are evidence of negative mass balance where melt and snout retreat is driven by increasing temperatures in these regions. As a result, these glaciers are considered to be in a transient phase, *flow-unbalanced* and thus likely to experience further retreat with alongside adjustments in the glaciers' flow-field to the climate perturbation. This interpretation is in agreement with the limited number of observations and estimates of glacier mass balance in the Eastern Himalayas and Northern Hindu Kush / southern margin of the Pamir range published in a small collection of studies. Gardner et al. (2013) through geodetic methods estimated regional glacier thinning of -0.89 ± 0.18 m yr⁻¹ and -0.44 ± 0.20 m yr⁻¹ between 2003 and 2009 for glaciers in the east and central Himalayas respectively. Others have used geodetically acquired surface thinning measurements in order to calculate mass balance estimates in water equivalent terms. For example, mass balance in the Everest region between 1970 and 2007 has been estimated at -0.32 ± 0.08 m w.e. a⁻¹ decreasing to -0.79 ± 0.52 m w.e. a⁻¹ between 2002 and 2007 (Bolch et al., 2011). For the same area, Nuimura et al. (2012) estimated a regional mass balance of -0.40 ± 0.25 m w.e. a⁻¹, which agrees well with geodetic work by Gardelle et al. (2013) and Kääb et al. (2012) who produced estimates of -0.26 ± 0.13 m w.e. a⁻¹ and -0.39 ± 0.11 m w.e. a⁻¹ between 1999 and 2010 and 2003 and 2008 respectively. Furthermore, Gardelle et al. (2013) and Kääb (2012) also produced mass balance estimates for Bhutan for the same time periods of -0.22 ± 0.12 m w.e. a⁻¹ and -0.52 ± 0.16 m w.e. a⁻¹. Negative mass balances in the east and central Himalayas have also been proposed based upon observations of

increased glacier shrinkage and retreat (Bhambri et al., 2011; Ren et al., 2006; Scherler et al., 2011b). Furthermore, evidence of glacier stagnation in the central and eastern Himalayas (Quincey et al., 2009; Luckman et al., 2007; Scherler et al., 2011b) coupled with the observed retreat supports the hypothesis that low PCT_p value can be indicative of passive retreat. Passive retreat occurs when PCT forming flow dynamics do not adjust in response to climate perturbations whilst the snout undergoes significant retreat, or “melt-back” (see figure 7.10).

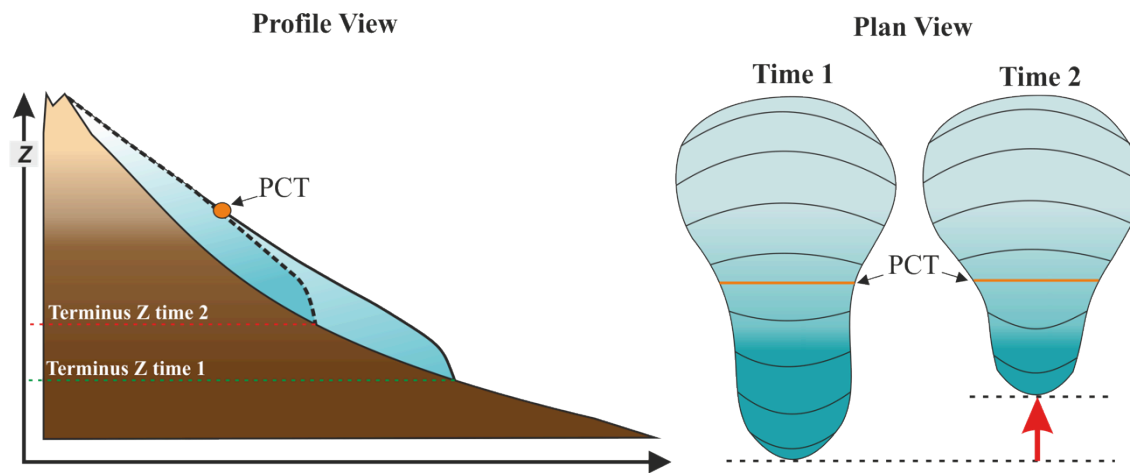


FIGURE 7.10 – SCHEMATIC OF PASSIVE REATREAT

The low PCT_p values that characterise the central and eastern Himalayas are likely to be explained by the fact that the Indian summer monsoon has been weakening for the past 60 years (Bollasina et al., 2011) which could have contributed to a reduction in accumulation in the region. However, perhaps more important is the reporting of increasing maximum temperatures in the central in eastern Himalayas for the past 40 years (Shrestha et al., 1999). Furthermore, summer accumulating, Indian summer monsoon (ISM) affected glaciers are more sensitive to temperature increase than glaciers that accumulate mass during the winter months. This is due to the fact that temperature increases not only increase surface melt but also directly reduce the availability of solid precipitation. The reduction in snow accumulation then exacerbates melt rates by reducing the albedo of the glacier’s surface (Fujita, 2008). This greater sensitivity of central Himalayan glaciers to temperature changes is manifest in the PCT_p results in the region.

The other region dominated by low PCT_p values displayed in figure 7.9 is located at the far north-western margin of the study area in the northern Hindu-Kush / southern Pamir mountains. Although less attention has been

paid to this region in the literature, reports suggest that glaciers in the region have been retreating for the past four decades (Haritashya et al., 2009). Haritashya et al. (2009) also identified that during the observed retreat, there was very little evidence of snowline variation between 1979 and 2003. This observation is particularly pertinent given that low PCT_p were generated during the modelling experiments in chapter six when glacier retreat was forced through increased temperatures at lower elevations whilst maintaining a constant ELA.

In the central and southern Karakoram, figure 7.9 reveals that the region is characterised by glaciers displaying PCT_p values in the “normal range” (0.36 – 0.49 according to Jenks natural breaks classification). Based upon knowledge generated in this work concerning PCT dynamics, this observation suggests that the glaciers in this region are *flow-balanced*. This is not to be confused with being in steady state where glacier extent and flow dynamics are in sync with climate forcing, but that the organisation of the glaciers’ flow-fields are suitable for maintaining the glaciers’ current extent and three-dimensional shape. This is not to say, however, that the glaciers will not advance or retreat as flow dynamics adjust in response to climate perturbations that may be occurring in the in region. However, it should be said that a *flow-balanced* glacier can be in steady state with climate whereas a *flow-unbalanced* glacier is likely to be in a transient phase following a shift in climatic conditions.

The Karakorum mountain range has become a region of particular interest in recent years due to the small number of observations that suggest the region’s glaciers are either stable or in fact showing evidence of slight mass gains and advance. Gardelle et al. (2013) produced geodetic mass balance estimates of $+0.11 \pm 0.14$ m w.e. yr^{-1} and $+0.09 \pm 0.18$ m w.e. yr^{-1} for the east and western Karakorum during the first decade of the 21st century based upon a glaciated area covered by a pair of overlapping SPOT tiles. Similarly, Kääb et al. (2012) estimated the regional mass balance of the Karakorum to be only very slightly negative (-0.04 ± 0.04 m w.e. a^{-1}) based upon relatively sparse laser altimetry points. Additionally, unlike the observations of glacier stagnation in the central and eastern Himalayas (Luckman et al., 2007; Quincey et al., 2009; Scherler, et al., 2011b), Copland et al. (2009) used feature tracking upon glaciers in the

vicinity of and including Baltoro glacier. The results highlighted that all of the glaciers in the region were active and displayed no evidence of stagnation. The stability and advance of Karakoram glaciers has been attributed to increasing precipitation trends observed in the upper Indus basin since 1961 (Archer and Fowler, 2004) and over the Pamir and Karakorum (Yao et al., 2012). Furthermore, mean summer temperatures in the Upper Indus Basin have been decreasing for the past four decades (Fowler and Archer, 2006), whilst the Karakorum range has experienced a decrease in maximum and minimum temperatures of 1.6 and 3.0°C, respectively since 1988 (Shekhar et al., 2010). Accordingly the high frequency of *flow-balanced* indicative PCT_p values across the Karakoram reflects the previous observation that the glaciers in the region have remained stable over the past decade (Gardelle et al., 2012).

Thus far the regional-scale PCT_p values recorded across the HKKH and the interpretations based upon them are in agreement with observations made in other studies concerning how glaciers in this vast region are faring in the current climate. However, a surprising result can be seen when observing the frequency and distribution of high PCT_p values.

Figure 7.9 reveals that one of the strongest spatial trends observed in the results concerns regions characterised by high PCT_p values. Much of the southern Hindu Kush and northwest Karakoram and the majority of the Western Himalaya display higher PCT_p values than have been observed elsewhere in the HKKH or even from previous chapters. However, the interpretation of this observation is proving to be much more challenging. This is in part due to the fact that such high PCT_p values did not emerge during the modelling experiments despite forcing glacier fluctuation through a number of climatic driving mechanisms. Although, as was discussed in chapter six, this may have been due to insufficient forcing magnitudes during the model runs. Nevertheless, one plausible mechanism that could account for high PCT_p values is glacier surging. Monitoring PCT positions during or immediately after an active phase of glacier surging could explain why the snout would extend to disproportionately low elevations compared to PCT_a. However, although surging glaciers have been observed in the Karakoram with increasing frequency (Copland et al., 2009; Gardelle et al., 2012b; Hewitt, 2007; Quincey et

al., 2011; Quincey and Luckman, 2013), this does not explain why the western Himalayas appear to be characterised by glaciers with high PCT_p .

The western Himalayas are home to the most complex climate across the HKKH owing to the transition from ISM to mid latitude westerlies that occurs in the region. Furthermore, Gardelle et al. (2013) identified that between 1999 and 2011 the Western Himalayas displayed the highest rates of mass loss in the HKKH with geodetic mass balances of -0.32 ± 0.13 m w.e. a^{-1} and -0.45 ± 0.13 m w.e. a^{-1} in western Nepal and the Spiti Lahaul region respectively. The findings by Gardelle et al. (2013) support the suggestion from chapter six that high PCT_p values may be the result of a sharp, sustained increase in ELA where PCT forming dynamics adjust faster than the glacier snout. Accordingly, despite the weak signal provided by the modelling runs, it is speculated here that high PCT_p values are the result of the glacier being in a transitional phase where the flow-field is adjusting to a sustained reduction in accumulation, driven by an increase in ELA. This forcing would lead to high PCT_p as the glacier's flow-field and the resulting PCT adjusted to the reduction in accumulation prior to an observable response by the glacier snout. The snout would display a delayed response to such forcing because mass changes in the upper reaches of a glacier have to be propagated down-glacier through longitudinal flow before the effects of the perturbation are felt in the ablation area. Nevertheless, as well as the measured glacier mass loss in the Western Himalaya, increases in maximum and minimum temperature of 1.0°C and 3.4°C have been identified in the region (Shekhar et al., 2010). Accordingly, one can be relatively confident that high PCT_p values can be related to negative mass balance, warming and glacier retreat. However, the precise mechanism as to how increasing temperatures in the Western Himalaya have led to high PCT_p values in the region cannot be ascertained here without greater knowledge of how the organisation of the glacier flow-fields and corresponding PCTs have evolved over time.

The results discussed here suggest that the PCT can be used to assess the broader variation in climate experienced across large regions and also that knowledge of regional variations in PCT_p can be used to draw insight into how climate may have been changing regionally. The PCT observations and the associated interpretations of their meaning also reflect the broad findings of the

limited amount of previous work conducted in the HKKH. However, it should be stated here that the interpretations are made with a degree of caution as they are limited by the fact that only a single snapshot in time has been observed. It is advised that the interpretations made here would have been made with a greater degree of confidence had data pertaining to changes PCT_x and PCT_a over time been available. This is because being able to track changes in PCT_x and PCT_a over time enables one to generate a much clearer understanding of how glacier dynamics and general glacier state are changing under climate forcing.

Nevertheless, the results here demonstrate one of the fundamental advantages of using the PCT: The extremely large geographical extent for which it can be employed to assess the dynamic balance and equilibrium state of mountain glaciers. This is particularly important given that, despite the advances in the quality and quantity of geodetic mass balance studies attempting to assess glacier health and climate across the HKKH, the area still remains somewhat of an enigma due to the limited spatial and temporal extent of previously published work (Miller et al., 2013).

7.5 PCT derived insights for the HKKH

The discussion so far has revolved around identifying how interpretations of climate forcing and glacier state, based upon PCT observations, compare with findings from the few studies that have produced glacier mass balance/mass loss estimates for the region. Attention will now focus upon what interpretations of the PCT record can tell us about the state of glaciers and the style of their response to climate forcing across the HKKH at the time of observation.

The spatially variable values of PCT_p recorded across the HKKH suggest that the region's glaciers are not controlled by a uniform climate forcing. This comes as no surprise given our knowledge of the complex weather systems that influence the HKKH. However, what is interesting is that the PCT_p observations suggest that the style of glacier response to climate forcing varies across the HKKH in a spatially heterogeneous manner. The results from this chapter suggest that in 2000 (SRTM acquisition year), glaciers in the Northern Hindu-

Kush and the Khumbu and Bhutan regions of the Eastern Himalayas in particular, had been, or were undergoing extensive retreat. This is based on the interpretation that low PCT_p values are the consequence of rapid snout retreat, or “passive retreat”. This style of glacier retreat is hypothesised to be the result of increased temperature at the lower reaches of the glacier. Furthermore, the tendency of the glaciers in these regions to display “extreme” PCT_p values indicated that they are displaying a non-equilibrium response to climate forcing and are *flow-unbalanced*. This is where the glacier’s extent has reduced at a rate greater than the response of the glacier’s flow. As a result, the glacier’s flow field structure is unsuitable for the glaciers’ extent and must adjust in order to restore a dynamically balanced state. This reorganisation of the flow-field could then potentially result in further glacier retreat.

High mean PCT_p values recorded in the Central and Western Himalayas as well as the southern Hindu-Kush, suggest that the glaciers found in these regions were also *flow-unbalanced* and thus displaying non-equilibrium responses to climate forcing. However, the tendency of these glaciers to display high PCT_p values perhaps suggests that they were demonstrating a different style of response to climate forcing than those with low PCT_p values. Although the modelling results in chapter six could not provide conclusive evidence, the interpretation remains that high PCT_p values in these regions are the result of glacier flow adjusting to climate forcing prior to a change in glacier extent. This is interpreted as being the result of a significant reduction in accumulation. Under these circumstances, the glaciers are deemed to be *flow-unbalanced* and thus in a transitional phase as the organisation of their flow-field is incapable of maintaining the glacier’s extent and hypsometry at the time of observation. As a result, glacier extent would need to reduce in order to regain equilibrium with glacier flow and so these glaciers could be expected to undergo high rates of retreat in the future. It is then interesting to note that glaciers in the western Himalayas, which were characterised by high PCT_p values in 2000, have displayed the highest rates of mass loss in HKKH throughout the following decade (Gardelle et al., 2013). This leaves us with an intriguing question: Can high PCT_p values be considered a precursor of glacier retreat?

The glaciers in regions displaying PCT_p values closer to 0.39 mean are interpreted to have been dynamically balanced, whereby the organisation of the flow-field is appropriate for maintaining the glaciers' hypsometry and three-dimensional shape at the time of observation. This does not necessarily mean that these glaciers were in steady state. Without knowledge of PCT variation over time, it is difficult to ascertain whether these glaciers were advancing, retreating or maintaining a constant extent. However, their dynamically balanced nature, as suggested by the PCT_p , indicates that they were displaying an equilibrium response to climate forcing.

7.6 Summary of outcomes

- Here, for the first time, data pertaining to glacier “health” and dynamic state has been recorded at high spatial resolution and analysed for the entire HKKH region.
- The geographical variation of PCT_a displayed a strong trend where PCT_a increased with increasing continentality, reflecting the blocking nature of the HKKH mountain chain in preventing moisture penetration into the Tibetan Plateau.
- The distribution of PCT_p value agrees well with those from chapters 3 and 4 as well as the model outputs. Considering the large sample size and the very wide range of glacier characteristics present in the HKKH, the relatively small spread of PCT_p values around the mean provides further observational evidence that glaciers tend towards a steady surface geometry where the PCT forms around 40% up-glacier from the minimum ice elevation.
- PCT_p values display regional clustering where the Eastern and Central Himalayas and Northern Hindu Kush are characterised by low PCT_p values interpreted to be indicative of *flow-unbalanced* glaciers and retreat. Alternatively, the central Karakorum is characterised by high frequencies of normal PCT_p values (0.36 – 0.49) considered to be evidence of *flow-balanced* glaciers where their flow dynamics are capable of maintaining the glaciers' current extent and hypsometry.

- The interpretations drawn from PCT_p values agree well with observations of glacier shrinkage and negative mass balances in the Central/East Himalayas and glacier constancy and advance in the Karakorum based upon sparse and sporadic geodetic mass balance studies.
- Clear trends in high PCT_p values that characterised the western Himalayas and southern Hindu-Kush agree well with observations of rapid glacier retreat in the same regions (Gardelle et al., 2013), suggesting that high PCT_p values are indicative of glacier's being in a transitional state with near-future snout retreat being likely.
- Low PCT_p values suggest that glaciers in the northern Hindu-Kush and the Eastern Himalayas were displaying non-equilibrium responses to climate forcing interpreted to be driven by increased temperatures and melt at lower altitudes. Furthermore, glacier in the Central and Western Himalayas were displaying evidence of an imbalance between glacier flow and glacier extent, interpreted as the result of a reduction in accumulation. Additionally, the high PCT_p values observed in the western Himalayas were suggested to be a precursor for high rates of glacier retreat. This interpretation is supported by observations of high mass loss rates in this region a decade later by Gardelle et al. (2013).

Chapter 8 The PCT: What have we learned?

The format of the thesis is such that the majority of the discussion has taken place within each of the respective chapters. Nevertheless, the following section will act as a “discussion of discussions” and aims to assimilate the observations made and knowledge gained thus far in order to ascertain whether the PCT is a suitable tool for monitoring glacier health and climate signals. This will be achieved by explicitly linking the observed PCT phenomenon with mass balance and climate forcing mechanisms. The chapter will then focus upon specifically assessing what the PCT can tell us about glacier health and how it can be utilised in future work to gain greater insight into the state of the world’s glaciers. Furthermore, the practicalities involved in, and recommendations for, PCT monitoring will be discussed along with the limitations that are inherent with such a method of glacier-climate monitoring.

8.1 The PCT, a function of climate?

Before the PCT can be used as a signal of glacier health or climate variation one must be confident that the PCT is indeed a function of these rather than the result of individual glacier characteristics such as hypsometry, aspect or valley geometry and so on. The theory discussed in chapter two highlights the formative role that mass balance plays in determining PCT_a and PCT_x by controlling the distribution of emergence and submergence velocities at the ice surface. Furthermore, the empirical observations of PCT characteristics upon glaciers with long established monitoring records go some way in supporting this theory. The observations highlight how PCT characteristics correlate strongly with well-established glacier-climate measures, particularly when comparing PCT_a with ELA_0 . Furthermore, observations of PCT changes over time display how PCT_x varies in response to climate-driven, mass balance fluctuations.

The modelling work assessed how PCT behaviour varied under different climate forcing mechanisms in greater detail. The results generated in the experiments, where glacier fluctuations are forced by changes in the ELA, displayed that the strong relationship between PCT_a and ELA corresponds with

the empirical observations from chapters three and four. Furthermore the modelling results suggest that PCT_x is a function of the surficial distribution of mass balance rather than the overall volume of mass change. This was demonstrated by the minimal change in PCT_x observed during glacier retreat where the glacier's mass balance was changed without altering the ELA. However, when glacier fluctuations were driven by changes in ELA, substantial adjustments in PCT_x were observed in response to the forcing. Accordingly this observation highlights an interesting finding, with respect to the linkage between mass balance and glacier flow. It suggests that changes in glacier flow are not simply the result of changes in glacier-wide volume but that it is, more importantly, the changes to the spatial distribution of surface accumulation and ablation that leads to significant adjustments in the flow-field of the glacier. This observation supports the assertion that the PCT reflects the relationship between long-term surface mass balance conditions and the resulting glacier flow structure.

However, perhaps the key observations that convinces one that the PCT is a function of climate are those concerning the proportional position of the PCT (PCT_p).

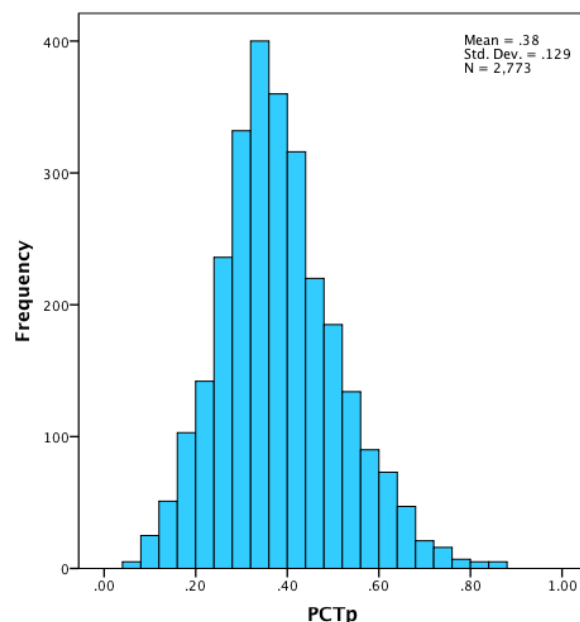


FIGURE 8.1 - PCT_p FOR ALL GLACIERS IN THE STUDY
The spread of PCT_p values, both observed and generated through modelling, for each glacier included in this study.

Figure 8.1 displays the histogram of all PCT_p values recorded upon each glacier observed in this study (tributary ice masses excluded). Given the wide range of

glacier types included in this study with varying thermal regimes, elevation distributions, sizes, longitudinal slope gradients, valley geometries, climate forcing, flow mechanisms, velocities and so on, the relatively small deviation of values around the mean is indicative of a higher order, shared forcing. As was stated in section 3.4, it is rational to assume then that the PCT and its positioning is a function of a climatic control that overrides glacier specific variations such as those listed above. Accordingly, the PCT_p is indicative of the complex interaction between climate forcing (mass balance), ice flow dynamics and the topographic setting of each glacier whereby flow dynamics strive towards an equilibrium state where flow vectors are organised in a manner that enables the glacier to maintain a steady three-dimensional shape and flow structure whilst accounting for the local topography. Consequently the PCT is the manifestation of this complex glacial balancing process.

8.2 So what is the PCT?

The Planform Curvature Transition is the location upon a glacier's surface where there is an observable change in the transverse ice surface profile. This transition is identified by the first consistently straight elevation contour that indicates the departure from the concave transverse ice surface profile in the accumulation area. However, more fundamentally, it is the manifestation of the complex interactions that ensue between climate forcing, glacier flow, and underlying topography as glaciers strive to achieve equilibrium with their physical and climatic surroundings. As a result, by observing and recording PCT information and changes thereof, we gain significant insight into how this complex relationship forms and evolves.

Until now, the PCT, or Hess altitude/Kinematic ELA (Cogley and McIntyre, 2003; Leonard and Fountain, 2003) as it has been labelled previously, has only been discussed in terms of its use as a tool for estimating ELA. However, the substantial lag times that can occur between climate perturbations and the responding changes in the glacier flow-field (Oerlemans et al., 1998; Oerlemans, 2012; Raper and Braithwaite, 2009), as demonstrated by the modelling results, in addition to the expected offset between the ELA and PCT_a upon steady-state glaciers (Hooke, 2005), highlights the inappropriateness of the PCT_a as an ELA proxy. Accordingly, the PCT should be considered as a glacial measure in its

own right rather than an estimator for other more established measures and so should be routinely recorded upon glaciers as is currently done with ELA. However, rather than being an indicator of annual weather variations controlled by short term changes in surface gains and losses like the ELA, the PCT is the result of a more fundamental relationship between glacier flow and mass balance and climate forcing. Thus it is suggested here that the PCT goes beyond simply identifying short term variations in surficial mass gains and losses, it acts as an indicator of the state of a glacier's inherent flow structure, particularly when observed over time. With this in mind, one can state that whilst the term "planform curvature transition" or PCT is a suitable description of the observable ice surface characteristic, it does not fully capture the fundamental nature or significance of the phenomenon at hand. Leonard and Fountain (2003) appeared to be thinking along similar lines when they labelled the Hess altitude: the kinematic ELA. However, in an attempt to distance the phenomenon further from comparisons with ELA it is given a new term. Accordingly, the PCT can be considered an expression of *Kinematic Partitioning*. The phenomenon is deemed as such owing to the insistence that the distinctly different internal flow structures that define the upper and lower parts of the glacier, and thus form the opposing transverse profiles in the respective regions, is worthy of study in its own right irrespective of the formative role of mass balance. Accordingly, the *kinematic partition* represents the boundary between these two dynamically distinct glacier regions. The choice of the term "Kinematic" is due to the definition of kinematics: A branch of classical mechanics concerned with the motion of bodies without consideration of the causes of motion (Taylor, 2005). Accordingly, this term enables us to conceptualise the dynamic state of glaciers separately from the context of climate forcing.

Given that the formative processes that account for *kinematic partitioning*, and the resulting PCT, are well understood in terms of continuum mechanics, it is surprising that relatively little attention has been (or still is) paid to the three dimensional shape of mountain glaciers. In universities and schools across the world, one of the first aspects of glaciology taught is the concept of mass balance and the ELA. Perhaps due to the way in which we prefer to break complex systems into smaller, easily defined sections, in order to aid our

understanding, we are taught that mountain glaciers can be divided into two distinct zones; the accumulation area and the ablation area, and that these two regions are separated by the ELA. However, it could be suggested that the ELA actually tells us relatively little about glacier state or dynamics unless the ice-mass is in steady state. Unfortunately, the majority of the world's glaciers are far from experiencing a balanced budget (Dyurgerov, 2005). As a result the ELA, and mass balance data, is extremely useful for informing us of surface mass gains and losses, and the year on year variation in the amount and spatial distribution of these exchanges. However, ELA and mass balance records cannot inform us of a glacier's flow state, or whether a glacier's flow regime is capable of maintaining or achieving an equilibrium state under current climate forcing. Of course a strong, sustained trend in ELA change is likely to have a significant impact on glacier stasis, however as mentioned previously, large but short-lived extremes in inter annual ELA variation, although interesting from a weather point of view, tell us little about the state of the glacier. In fact, such short-lived extremes are likely to have little impact upon glaciers in the long-term. Accordingly, it would be fair to consider ELA and glacier mass balance records to be more akin to climatological tools rather than glaciological ones. This is not to say that we should ignore the concepts of mass balance and ELA when understanding glaciers however, as these concepts are still pivotal in our understanding of cryosphere - climate interactions. Long-term mass balance records also play a crucial role in providing evidence of climate change. Rather, it seems clear that the intense focus upon the mass balance paradigm has masked the importance of observing and understanding the fundamental characteristics that define mountain glaciers. This then forces one to reassess the reasons behind the glaciological communities apparent ignorance of the general three-dimensional shape of glaciers and the resulting *kinematic partitioning* phenomenon.

This highlights an important philosophical observation concerning how the essence of what characterises a glacier may have been somewhat lost amongst the glaciology community where mass balance has become the overarching paradigm used to inform us of what is "important" about glaciers. With the increasingly apparent threat of climate change (Vaughan et al., 2013), mountain glaciers have become the "poster child" of the climate debate. This is illustrated

by the use of Folgefonna glacier as the front cover of the IPCCs fifth assessment (Vaughan et al., 2013). Although this is fully justified, as glacier fluctuations provide unequivocal evidence of climate change (Oerlemans, 2005), the continued focus upon mountain glaciers based solely upon their use as indicators of climate change means the fundamental characteristics that define glaciers as intriguing phenomena in their own right have been somewhat overshadowed.

It is suggested here that the *kinematic partition* represents a more fundamental part of a glacier system that can provide information concerning a glacier's state that cannot be gleaned through observations of ELA and mass balance alone. If we take an abstract approach to our understanding concerning what characterises a glacier for a moment, it is possible to consider the hypothetical situation where a modern day glacier is temporarily removed from all climatic influence. Under such circumstances, there would be no such concept of mass balance or the ELA as accumulation or ablation would not exist. However the glacier could still be divided into two distinct zones in the upper and lower regions of the ice mass, based upon the characteristics of the internal flow structures separated by the *kinematic partition*, by observing the location of the PCT and the resulting three-dimensional shape of the ice.

This hypothetical observation highlights that, although we have the ability to identify fundamental characteristics and processes occurring within the glacier system (PCT / dynamics partition), where the upper and lower region of glaciers display a distinct morphology, flow structure and behaviour from one another, we continue to define these two distinct glacier zones in terms of climatic processes that occur on their surface whilst the fundamental flow structure of the glacier is overlooked. Accordingly, although long-term records of ELA and mass balance are useful in identifying significant trends in climate change, the glaciological community should not become overly reliant upon partitioning distinct processes occurring within the glacier and assessing its state based upon the location of the ELA alone. This thought is particularly important when considering the large inter-annual variability observed in the ELA records. Thus, given the interpretation that the *kinematic partition* is a function of the relationship between *long-term* glacier mass balance, the

constraining topography and the resulting organisation of the ice-flow-field, it is suggested here that this thesis has produced, for the first time, evidence of a *single* observable index that can inform us of the complex relationship between climate forcing and glacier state. Accordingly observations of this phenomenon, through the mapping of the PCT, may be used to provide insights concerning the flow state, dynamic balance and even the long-term future of mountain glaciers.

8.3 What does the PCT tell us?

The discussion above highlights that knowledge of *kinematic partitioning* and the resulting PCT provides insight into the self-regulatory nature of mountain glacier systems. However, the true value of these observations may lay in the information that can be drawn concerning the relationship between climate forcing and glacier response.

Given the finding that PCT location is largely controlled by surface mass balance and thus climate, PCT observations from a single snapshot in time can inform us of regional variations in climatically-driven flow dynamics and thus *long-term* climatic conditions, similar to the way in which the ELA has been used to compare short-term climatic variations amongst different glaciated regions (Benn and Lehmkuhl, 2000; Dyurgerov, 2005; Dyurgerov et al., 2002; Meier et al., 2003). This assertion is based upon the strong relationship observed between ELA_0 and PCT_a . However, contrary to the recommendation of Leonard and Fountain (2003), PCT_a is not an appropriate tool for estimating modern day ELA upon glaciers that are not in steady state due to the lag times associated with the response of glacier flow to climate perturbations.

However, it is perceivable that PCT_a can be compared to modern day ELA records (or proxies of) in order to identify the degree to which glacier flow dynamics and current climate forcing are discordant. Owing to the argument that under steady state conditions the PCT_a shares a similar elevation with the long term ELA (Hooke, 2005), one can use the observed offsets between modern day ELA and PCT_a to estimate the extent that glaciers will retreat if current climate forcing is sustained at its current level. Accordingly, comparing ELA measurements with PCT in this manner may provide clues towards the future

response of glaciers. It is also interesting to note that the presence of extensive debris mantles appeared to have little if any impact on the recorded PCT_a when compared again PCT_a on debris free glaciers in close proximity. This presents an advantage of using the PCT over other glacier state indices such as area and length fluctuation measurements that are significantly influenced by the presence of substantial debris mantles.

The PCT also provides the potential to gain new insights into how glaciers are responding to climate perturbations by observing changes in PCT characteristics over time. One of the key findings of this work has been in identifying the necessity to record changes in PCT_x as well as changes in PCT_a over time. Records of PCT_a change through time alone are insufficient for understanding how glacier dynamics are adjusting to climate forcing because changes in ice surface elevation have been shown to occur synchronously with flow dynamic adjustments (figure 6.26) and PCT_x retreat.

This observation provides the opportunity for one to reflect upon whether the impact of ice surface lowering has been taken into account when inferring climate signals from ELA records. Given that the ELA is generally determined by fitting a curve to data representing surface mass balance measurements as a function of altitude (Cogley et al., 2011), ice surface lowering during long observation periods could result in ELA records underestimating the true extent of glacier change. As a result, it is possible that climate inferences based upon ELA records alone may underestimate the true magnitude of the climatic signal.

Nevertheless, observations from chapter four and the modelling experiments detailed in chapter six provide evidence of how PCT changes over time can be used as evidence of mass balance forcing. The results from these chapters showed that observations of PCT_x advance down glacier can be used as evidence of positive glacier mass balance and conversely, observations of PCT_x retreat can be considered evidence of long-term negative mass balance. These results highlight the potential to use PCT observations as indicators of the broader long-term mass balance *regime* (i.e. positive or negative, not m.w.e. estimates) that are present upon glaciers with no direct measurement records. However, when inferring mass balance regime from such observations, it is

important to consider the lag times associated with the dynamic response of glaciers to climate forcing. This was demonstrated in chapter four when PCTs on both Kesselwandferner and Blue Glacier were observed to advance in response to previous spells of positive mass balance despite the contemporary negative mass balance exhibited by the glacier. Lag times have been suggested to occur on the scale of decades to a century for mountain glaciers (Raper and Braithwaite, 2009); this suggestion is confirmed by the modelling results in chapter six.

Perhaps the most important information that can be drawn from observing the three-dimensional surface geometry of mountain glaciers relates to the proportional position of the PCT upon the ice surface (PCT_p). It was initially considered whether PCT_p observations could be used to identify steady state glaciers where the organisation of glacier flow, or “glacier dynamics” (Hagen et al., 2005), were in steady state with climate. For example, that glaciers displaying a PCT_p value between 0.3 to 0.5 were in steady state with climate. The modelling results went some way in supporting this claim by revealing that steady state glaciers do indeed display a PCT_p value between 0.3 and 0.5. However, the experiments also highlighted that similar PCT_p values can occur when glaciers are in a transitional phase (figure 6.12). This observation could be attributed to the possibility that the abrupt changes in glacier mass balance during the modelling experiments were not strong enough to elicit the kind of glacier response that produces the extreme values of PCT_p recorded during empirical observations. However, the observation that PCT_p values remained relatively unchanged on Hintereisferner between 1979 and 2006, despite evidence of glacier retreat, thinning and a negative mass balance record (section 4.2.1.1), confirms that PCT_p observations cannot be used to identify glaciers that are in steady state.

However, given that the results of this study highlight how glaciers tend towards a surface geometry that produces a common PCT_p value irrespective of individual glacier characteristics (figure 8.1), it is suggested here that the PCT_p measure can still be used to glean information concerning glacier state. This is because if the PCT is indeed the manifestation of the balancing effort between climate forcing, glacier flow and the containing topography, extremes in PCT_p

that deviate substantially from the norm may be indicative of imbalances within this dynamic process. Accordingly, similar to work conducted by Harrison et al. (2009) who assessed “dynamic glacier health” by comparing measured mass balance to reference surface mass balance, it is believed here that the PCT_p can be used to assess whether glacier flow is in a state appropriate for maintaining the glacier’s volumetric and aerial extent at the time of observation with respect to the prevailing climate forcing. Furthermore, observing changes in PCT_p over time or observations of a departure from the “normal” PCT_p range can be used as an indication of non equilibrium glacier response to climate (Harrison et al., 2009).

Accordingly, it is suggested here that observations of PCT_p , and changes thereof, can inform us of the dynamic state of glaciers and thus relates to the interpretation, developed throughout this thesis, that glaciers can be *flow-balanced* or *flow-unbalanced*. Specifically, flow balanced glaciers displaying a *normal* PCT_p exhibit a state of flow capable of maintaining the glacier’s current extent and are thus displaying a gradual, equilibrium response to current climate condition. On the other hand, glaciers with extreme PCT_p values, or those that display large variations in PCT_p over time, are flow unbalanced with a flow field structure incapable of maintaining the glacier’s current area-volume extent. Such glaciers are considered to be in a transitional phase where the glacier is currently displaying a non-equilibrium response to a sustained perturbation in climate forcing. Accordingly, these findings suggest that PCT observations may assist in identifying high-risk glaciers in today’s climate and inform *speculative* assessments as to how they may behave in the near future. For example, consider a situation where a glacier displays a low PCT_p value of say 0.09. If the glacier is to maintain a steady three-dimensional surface profile and extent, and a PCT_p value in the region of 0.38 is indicative of an ice flow structure capable of doing so, one can assume that either the flow structure or the extent of glacier must adjust until the PCT_p reaches a equilibrium value close to 0.38. Given that the low PCT_p is likely the result of a reduction in glacier extent at rate faster than the response of glacier flow, as was identified in chapter four upon Blue Glacier and Kesselwandferner, one can assume then that the flow structure of the glacier must adjust to the climate forcing that is causing the reduction in glacier extent. Conversely, consider the situation

where a glacier possesses an extremely high PCT_p value of 0.9. Here the structure of the flow field is incapable of maintaining the glacier's current extent and so, in order to achieve flow-balance and equilibrium, glacier extent must reduce until the PCT_p lies within the "normal" range. Although these assertions are, to a degree, speculative in nature, the results discussed in chapter seven are supportive of these claims. This is due to the fact that the regions of the HKKH that are characterised by glaciers with very high or very low PCT_p values also display the highest rates of glacier wastage and disequilibrium (Gardelle et al., 2013; Gardner et al., 2013; Jacob et al., 2012; Kääb et al. 2012).

Furthermore, empirical observations from chapter four and the results from the modelling experiments in chapter six suggest that observations of PCT_p may provide information concerning the source of potential glacier disequilibrium. For example, very low PCT_p values are believed to be indicative of flow unbalanced glaciers where snout retreat is occurring at greater rate than the response of the glacier's flow-field. This is because the structure of the glacier's flow-field is likely to be a remnant from a time when the glacier had a greater extent. This disparity between glacier extent and glacier flow is hypothesised to be due to increased temperatures driving higher melt rates at lower elevations resulting in glacier thinning, volume reduction and a new glacier extent to which the three-dimensional glacier flow-field must adjust.

When considering the driving mechanisms that would lead to very high proportional PCT values, it was hypothesised that a significant reduction in accumulation would lead to the reorganisation of the glacier flow-field and potentially generate the high PCT_p values that were observed in chapter three, four and seven. Unfortunately, the modelling experiments in chapter six failed to provide conclusive evidence to link high PCT_p values with reduced accumulation rates. This may be due to the fact that the forcing in the accumulation specific experiment was not strong enough to realistically replicate real world forcing that results in high PCT_p values. Nevertheless, the PCT showed much stronger response to accumulation driven glacier change than it did to ablation driven glacier retreat. Accordingly, even though the results of the modelling experiments proved to be less conclusive than one had

hoped, there is still the possibility that high PCT_p values can be attributed to substantial changes in accumulation rates.

Nevertheless, despite the uncertainty concerning the driving mechanisms that lead to extremes in PCT_p , focus should remain on the results generated by this thesis that provide convincing evidence that PCT_p observations can provide important information concerning the dynamic balance and flow state of mountain glaciers.

8.4 Proposed applications for the PCT?

Given the evidence to suggest that changes in PCT_a and PCT_x are driven by, and so, indicative of long-term variations in surface mass balance, it is recommended here that future glacier monitoring campaigns include information pertaining to the position and elevation of the PCT. Not only would this provide a long-term climate signal that can be recorded on an extremely large geographical scale through remote sensing, PCT observations through time could be compared to climate simulations in order for us to better understand the rate at which glacier flow is adjusting to climate forcing. Consequently, these data should be routinely compared to ELA records in order to assess whether today's climate continues to depart further from harmony with the flow states of contemporary glaciers. Furthermore, with knowledge of the discrepancies between contemporary ELA and PCT_a , we can then infer ballpark estimates of future glacier retreat even if climate were to stabilise at its current state.

In a situation where PCT_a is substantially lower than the ELA in elevation, and if current ELA records represent long-term trends and not just short-term extremes, based upon the assumption that PCT_a must locate close to the ELA in order for the glacier to achieve equilibrium, flow dynamics will need to adjust to the prevailing surface mass balance distribution resulting in PCT_x retreat and a rise in PCT_a . This would lead to a reduction in mass being transported down glacier and increased snout retreat. Accordingly, because the PCT_a can be recorded on a very large sample of glaciers, global scale mapping could reveal regions characterised by larger PCT_a – ELA offsets and thus indicate regions where the largest rates of glacier retreat is to be expected. However, for this

approach to be developed, a greater level of knowledge is required concerning the expected offset between ELA and PCT_a on steady state glaciers. The modelling results suggest that this offset is in the region of -163 m. However the moderate variation in volume, length, area and so on between the glaciers generated during the model runs, relative to the variability observed in nature, suggests the -163 m offset may not be fully representative. Furthermore, it is unlikely that ELA – PCT offsets upon balanced glaciers can be characterised by a globally uniform value. It is more likely that this offset should, to some degree, scale with glacier size. This scaling was not observed in the results in chapter three. This is likely due to the relatively limited range of glacier sizes present the sample for which ELA records were available.

When ELA records are not available for comparison against PCT_a records, the results from this study suggest that knowledge of the PCT_p can be utilised in order to formulate predictions as to which glaciers are dynamically or *flow-unbalanced* and displaying non-equilibrium responses to climate forcing. The information that can be gained from observing PCT_p has been discussed in detail in the previous section and chapters, however some uncertainty remains as to how this approach to assessing glacier state can be practically implemented.

The uncertainty relates to the methodological requirement to define which PCT_p values represent *flow-balanced* glaciers compared to those that are indicative of *flow-unbalanced* glaciers. Owing to the histograms presented in figure 7.9, figure 8.1 and the results of the modelling experiments discussed in section 6.2.1.1, glaciers that display a *kinematic partition* producing PCT_p values close to 0.38 are considered to be *flow-balanced* and thus undergoing an equilibrium response to climate forcing. Similarly, one can be confident that glaciers displaying extreme PCT_p values, such as 0.9 or 0.05, possess a flow-field structure that is incapable of maintaining the glacier's extent under current climate forcing and can be considered to be *flow-unbalanced*. However, complexity is envisioned to arise when trying to infer glacier state from PCT_p values in-between the end member values. This forces one to question how glacier PCT_p should be categorised. Should we enforce fixed boundaries to PCT_p values where glaciers are categorised as balanced or unbalanced according to which side of the boundary

they sit? Or should variations in glacier flow-state be assessed in terms of a gradual change where, for example, glaciers with a PCT_p of 0.7 are considered to be less “healthy” than those with a PCT_p of 0.4 but “healthier” than a glacier with a PCT_p of 0.9 (figure 8.2)?

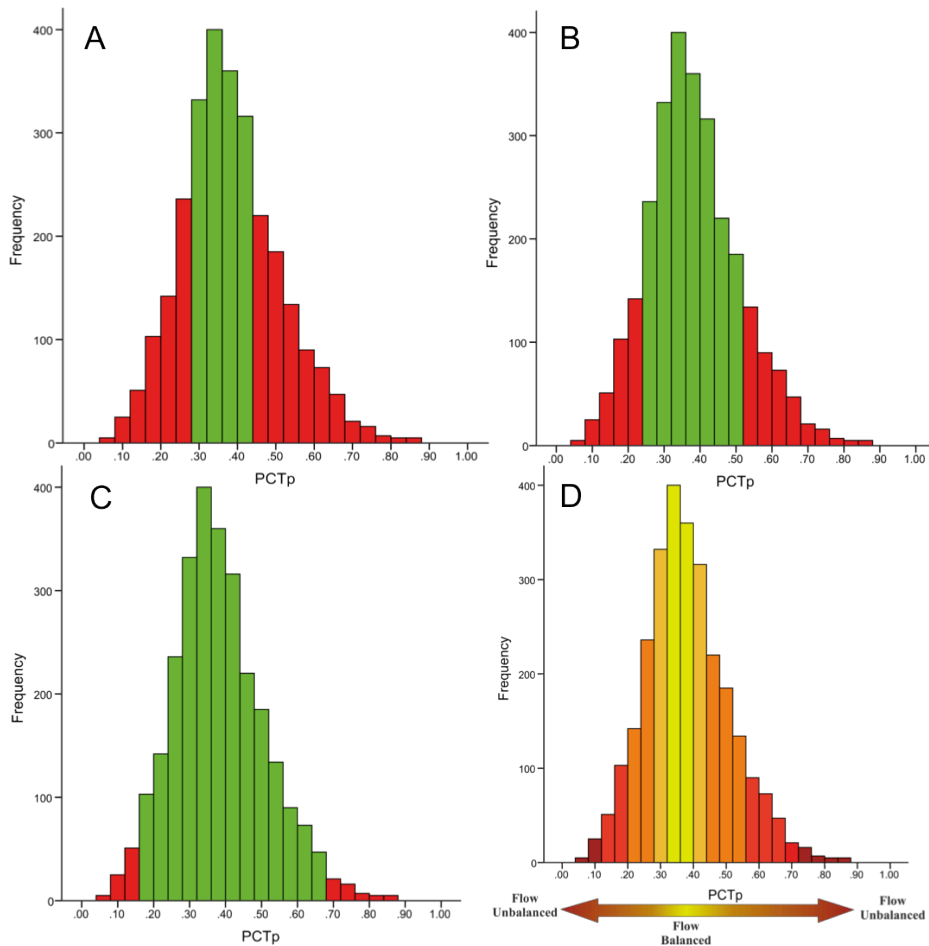


FIGURE 8.2 - PCT_p BOUNDARY ISSUES

A: Abrupt boundaries based upon σ where green glaciers are flow-balanced and red are flow-unbalanced. B: Abrupt boundaries based upon natural breaks (jenks). C: Abrupt boundaries at extreme values. D: Gradual/Blurred boundaries change from flow-balanced (equilibrium response) to flow-unbalanced (non-equilibrium response) glaciers.

This issue clearly requires greater consideration and although a solution to this quandary is beyond the capability of this thesis. It is likely that modelling flow structure evolution and thus PCT_p variation for a broader sample of glacier characteristics would elucidate some answers concerning this issue. Accordingly, this highlights a potential area for future investigation.

Irrespective of these methodological considerations, the fact remains that PCT_p observations may be used to identify whether glaciers are dynamically balanced and thus provide clues concerning their future behaviour. The

importance of this discovery cannot be overstated given the extremely large scale upon which the PCT can be recorded on individual glaciers. It means that the PCT can be employed to enable very large-scale reconnaissance studies into glacier state and thus glacier health. Such studies would enable glaciologists to identify regions characterised by dynamically unbalanced glaciers and thus direct our attention to those areas that are likely to display the greatest rates of glacier retreat. Furthermore, from a climatic point of view, large-scale reconnaissance studies may also aid in identifying regions where climate has undergone the most significant change in recent years. Take figure 8.3 for example. Even without prior knowledge of the region's climatic or glacial history, the extreme values of PCT_p that characterise the Western and Eastern Himalayas and northern Hindu-Kush would highlight these sub-regions as areas of glacier displaying non-equilibrium flow regimes. Accordingly, closer investigation using more time consuming and expensive methods would reveal that these areas are indeed experiencing the highest rates of glacier thinning and retreat across the entire HKKH (Gardelle et al., 2013; Gardner et al., 2013). It is suggested here that the use of the PCT then has the potential to provide such insights for the entirety of the world's glacier population.

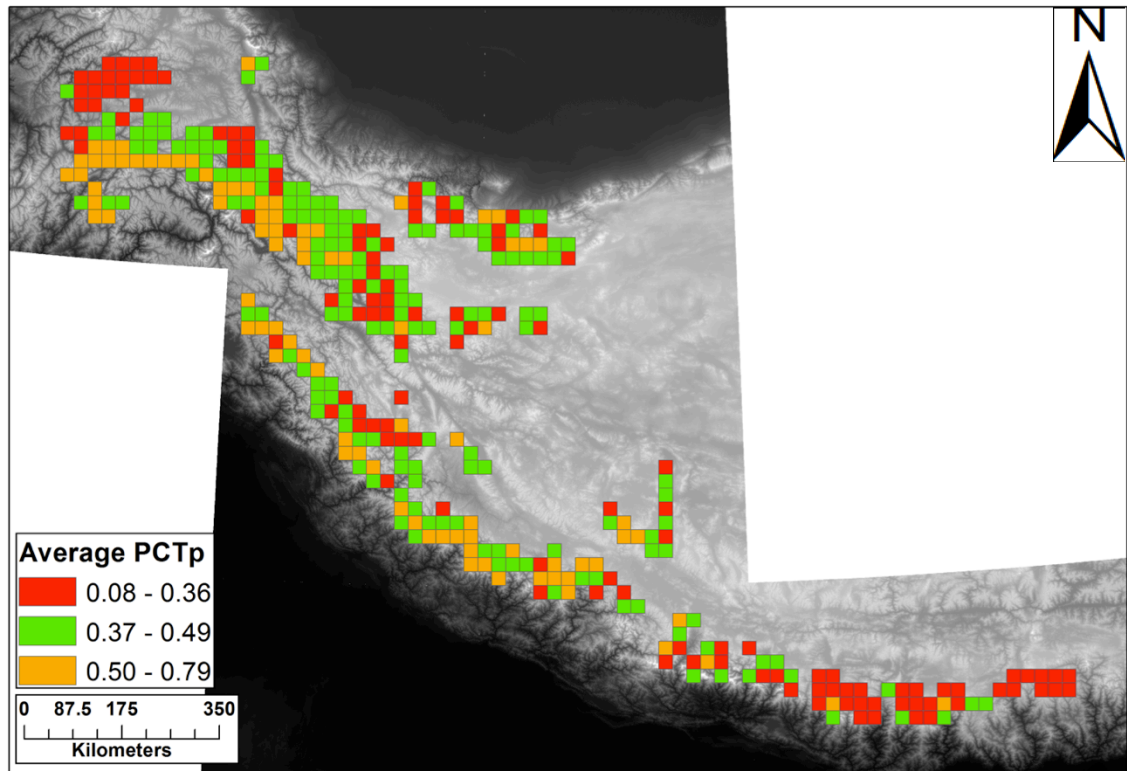


FIGURE 8.3 – GLACIER FLOW-STATE IDENTIFICATION
PCT_p across the HKKH reveal clusters of unbalanced glaciers in the Eastern Himalayas and North Hindu Kush (red = low PCT_p) as well as in the Western Himalayas and Southern Hindu Kush/West Karakoram (orange = high PCT_p). PCT_p binning based upon natural breaks (Jenks) in the sample.

8.5 Limitations and practicality considerations.

PCT data pertaining to only a single snapshot in time can be difficult to interpret as was discussed when interpreting the HKKH PCT record. This is in part due to the problem of equifinality. For example, without knowledge of how PCT_a and PCT_x have been varied over time, PCT_p records alone cannot inform us whether a glacier is in steady-state with climate or not. This is due to the modelling results that demonstrated how PCT_p values remained relatively constant upon glaciers when they were both in and out of balance with climate. As a result, observations of regionally homogenous PCT_p values in the Karakoram were interpreted as evidence of the glaciers in the region being *flow-balanced* rather than in steady state. Unfortunately, without knowledge of variations in PCT_a or PCT_x over time it is difficult to identify whether these glaciers are unchanging, retreating or advancing. The principle of equifinality also makes it difficult to interpret the meaning of low PCT_p values when data are available for only a snapshot in time. The abrupt advance modelling experiment revealed that glaciers can produce low PCT_p values during the

transitional phase as PCT_x advances and PCT_a decreases after a drop in ELA. However, the results discussed in chapter 4 revealed that low PCT_p values can also occur when the snout retreats at a greater rate than PCT_x retreat and the corresponding PCT_a increase. Accordingly, this suggests that knowledge of PCT_a and PCT_x changes over time are required if one is to have greater confidence in the interpretations drawn from PCT_p records. Nevertheless, one can be confident that when PCT_p values deviate largely from the norm, the exhibiting glacier can be considered *flow-unbalanced* and thus out of synchronicity with climate.

Another limitation worth consideration is associated with the observations and theory that suggest ice surface geometry to be ultimately a function of surface mass balance. Although this finding contributes substantially to our understanding of the relationship between mass balance forcing and glacier flow, it does mean however, that changes in ice volume due to non-surface exchanges, such as internal accumulation, refreezing and terrestrial calving will not be reflected in PCT records.

The PCT is easily identifiable upon simple, single basin valley glaciers (figure 8.4) and during personal communication with Graham Cogley (December, 2013), it was agreed that, as a rule of thumb, PCTs can be clearly and easily identified upon 75% of glaciers. However the author is aware that for more complex glacier systems, identification of the PCT can require a greater level of interpretation that may result in the method being perceived as subjective in its approach. Although Cogley and McIntyre (2003) made attempts to quell such concerns through experiments designed to assess the extent to which map-reader error occurs with the approach, the work conducted here includes a much wider variety of glacier types than those used in Cogley's experiment. Accordingly, resolving the planform curvature transition to a single point or vector for more complicated glacier systems can be difficult (figure 8.5). With the increasing frequency of publications which present automated methods for extracting glacier information from remotely sensed data (Le Bris and Paul, 2013; Leprince et al., 2007; Paul et al., 2013; Racoviteanu et al., 2010; Raup et al., 2007), one could suggest that the scientific community may be more willing to accept new approaches for glacier health monitoring when researcher

interpretation is kept to a minimum and the automation of work-flows formulate the foundation of the approach. Perhaps this is due to the perception that automated methods are more accurate than human interpretations. However, it is also important to consider that these automated methods are still based upon rules and boundaries imposed by the investigator based upon their own interpretations. Nevertheless, this observation suggests that an important next step for the work presented here may be to develop and implement an automated method for PCT delineation. Such an approach would remove concerns of investigator subjectivity and perhaps even increase the speed at which new measurements can be collected.

Another issue that requires consideration concerns the availability of suitable DEMs required for PCT identification. As has been asserted throughout this study, interpretations concerning glacier flow state that are drawn from PCT_p observations are made with the greatest level of confidence when one has knowledge of how PCT_a and PCT_p have changed over time. In order to gain such knowledge one requires multiple epoch DEMs that enable PCT identification. However, such elevation data are relatively uncommon and the errors associated with the data that are available can be problematic when monitoring PCT change overtime. Owing to the relatively slow rate of PCT_x change observed in this study, it is important that the resolution of the DEMs being used is high enough to enable one to record significant changes in PCT_x during the observation period when changes in PCT_x position are small. The errors associated with PCT_x change observations upon Kesselwandferner highlight that this issue of measurement uncertainty is likely to be greatest when measuring changes in PCT_x over relatively short time periods using medium to coarse resolution DEMs. Accordingly, coarse resolution DEMs are only suitable when PCT_x change is considerably greater than the DEM grid size plus the planimetric errors identified during co-registration of the multiple epoch DEMs. Similarly, when recording PCT_a change over time it is important that one is aware of the absolute and relative elevation errors associated with the DEMs being compared.

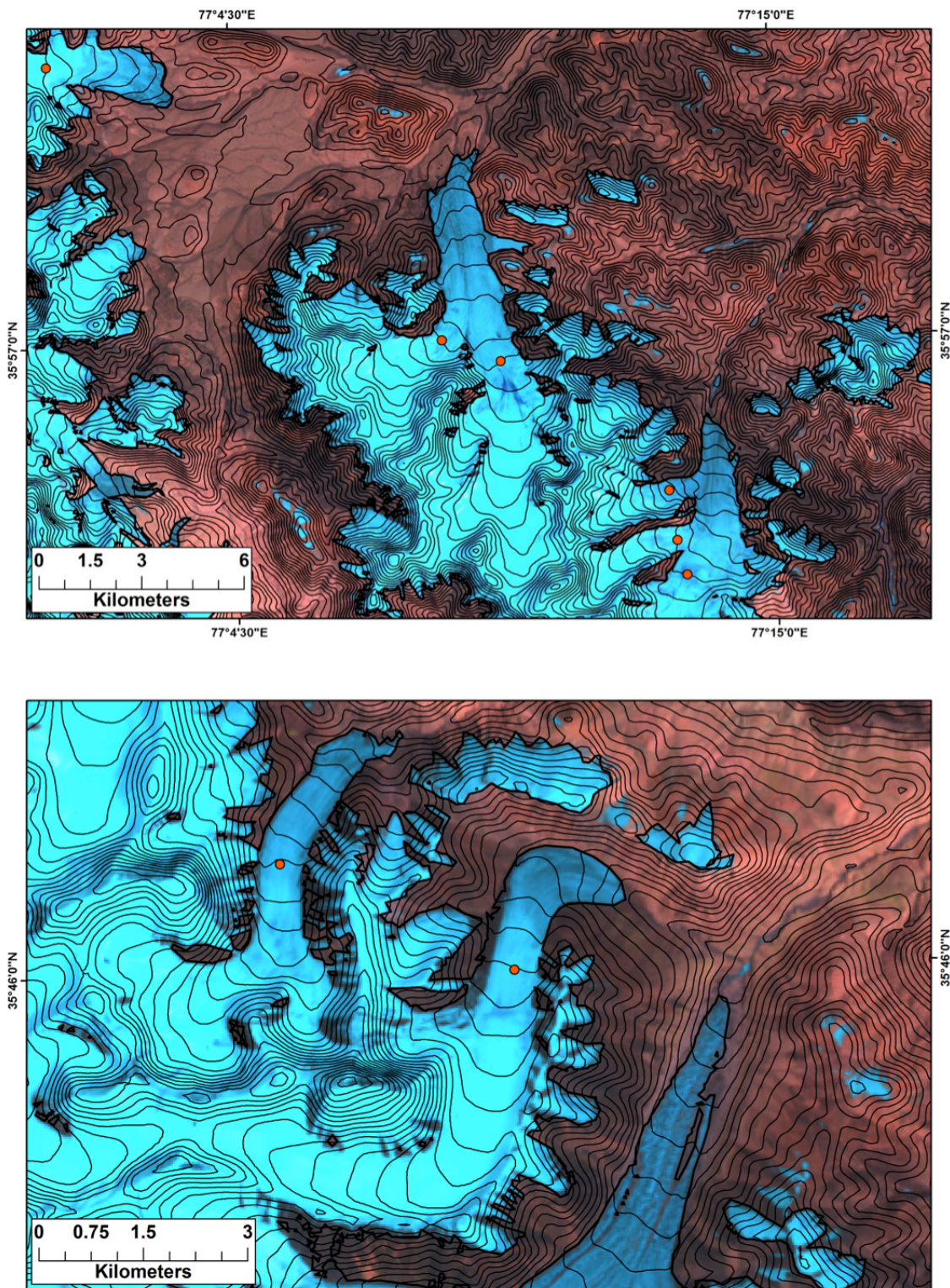


FIGURE 8.4 – SIMPLE PCT DELINIATION

Ice surface geometries for two glaciers in the Karakoram display a clear transition from a concave to convex transverse surface profile as evidenced by the 50m SRTM derived contours overlain upon an FCC Landsat ETM+ image. PCT contour indicated by the red points.

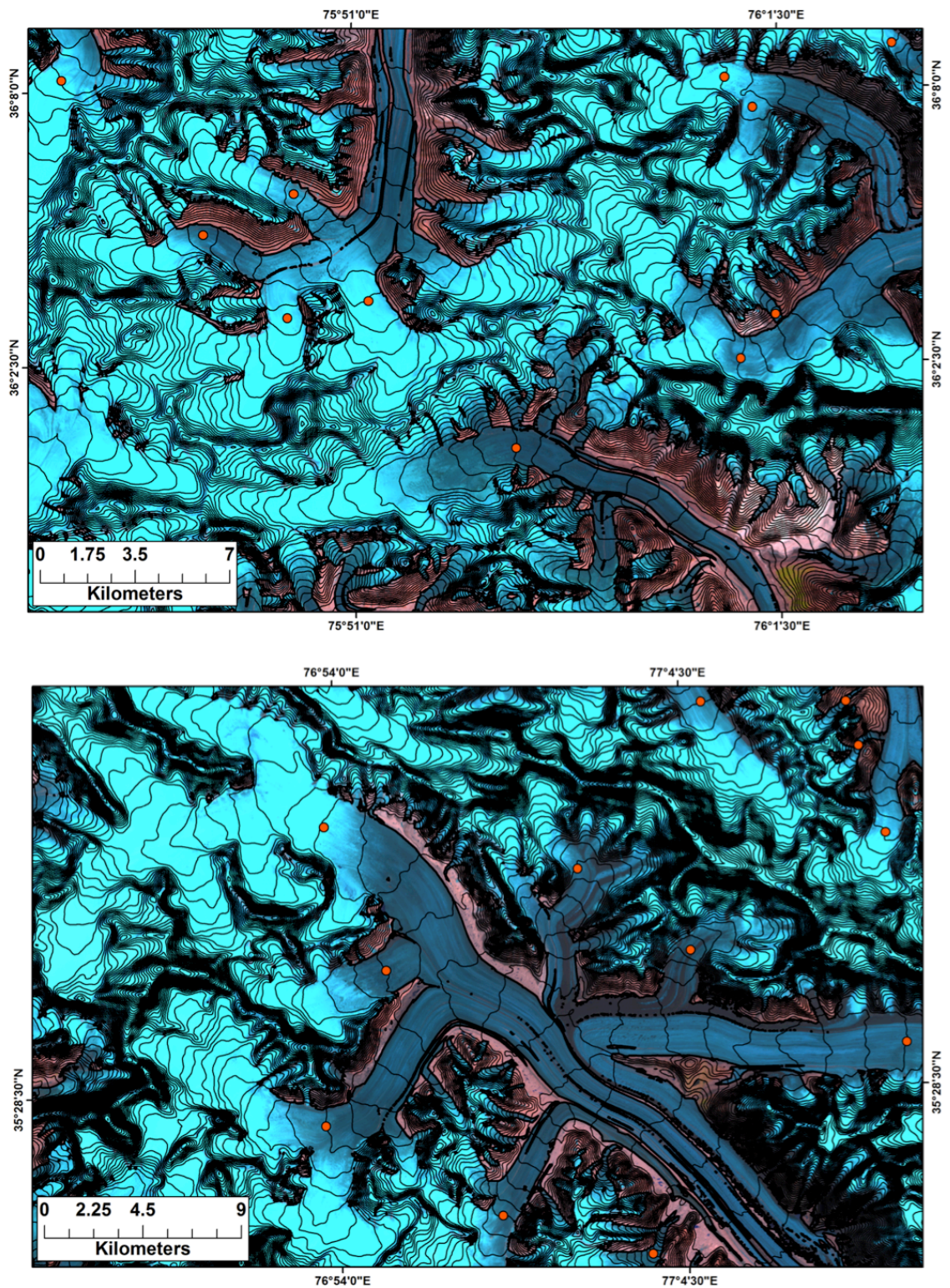


FIGURE 8.5 – COMPLEX PCT DELINEATION

The above examples demonstrate the more complex surface topography of large, compound basins type glacier systems and the associated difficulty in identifying the PCT (red points). In such situations, consideration of the continued ice surface slope down glacier of the proposed PCT is extremely important. I.e the need for surface contours to appear flat or convex down-glacier of the PCT.

Perhaps one of the key limitations concerning the PCT is that in its current form, its use is limited to the role of indicator. Unlike direct mass balance measurements (Andreassen et al., 2005; Braithwaite, 2009; Dyurgerov, 2005; Dyurgerov and Meier, 1997; Fountain and Vecchia, 1999; Hodgkins et al., 1999), geodetic studies (Bolch et al., 2008; Cogley, 2009; Fischer 2011; Gardelle et al., 2012a; Gardelle et al., 2012b; Gardelle et al. 2013; Kääb et al., 2012) and gravimetric indices (Gardner et al., 2011; Gardner et al., 2013; Matsuo and Heki, 2010), observations of PCT variation cannot be used to extract quantitative estimates of volume change or mass balance and so neither can it be used to estimate contributions to sea level. However, this should not prevent the establishment of the PCT as an important tool in glacier monitoring efforts, particularly when one considers that ELA records alone are incapable of providing quantitative estimates of glacier fluctuations, yet it remains one of the fundamental conceptual tools used to understand and monitor glacier health and climate change. Furthermore, although geodetic methods and GRACE data can be used to provide quantitative estimates of mass balance and mass loss, these estimates can often come with high uncertainty. For example, Jacob et al. (2012) produced estimates of glacier mass loss in High Mountain Asia between 2003 and 2010 of $4 \pm 20 \text{ Gt Yr}^{-1}$ using GRACE data.

Despite its limitations, the results from the modelling and empirical observations suggest that the PCT is indeed an observable signal of climate and can provide information concerning glacier health, particularly when observations of PCT change over a period of time are available. This is encouraging considering the minimal time, money and resources that are required to measure PCT. Furthermore, the speed and geographical scale for which the PCT can be utilised far exceeds that of the vastly more time and effort consuming measures such as geodetic and direct mass balance. This is not to say that the PCT should replace such measures but that they should be used in conjunction with one another. Additionally, the fundamentally dynamic nature of the *kinematic partition* means the PCT should not be categorised amongst the more general “Glacier Elevation Indices” (GEIs) such as THAR, maximum elevation of lateral moraines, TSAM or mid range elevation (Benn and Lehmkuhl, 2000) as the insight it provides is much greater than a simple estimation of glaciation levels.

Accordingly, despite the PCT's inability to provide quantitative estimates of glacier volume change, the indicative nature of the PCT and the ease with which it can be utilised on very large geographical scales provides the opportunity to pin point areas exhibiting anomalous glacier dynamics such as locally high PCT_a or extremes in PCT_p values. Accordingly, this provides us with an extremely powerful tool that can be used to direct attention to regions that require further investigation using more costly and time consuming methods.

Chapter 9 Conclusions

The need for an alternative method of assessing glacier health was driven by the fact that currently employed techniques either lacked the necessary spatial resolution to account for local variations in glacier state, or were unsuitable for performing global scale analyses. Accordingly, this need provided the potential for the rejuvenation of an old idea based upon very early observations of glacier – climate interactions by Herman Hess concerning the three-dimensional shape of glacier surfaces. This then set up the aim of the thesis that was to identify whether climate signals could be observed in the three-dimensional surface shape of mountain glaciers and to assess whether these manifestations were suitable for use as a measure of glacier health implementable on a global scale.

The idea that all glaciers tend towards a distinct surface geometry as a result of their surface mass balance regime was introduced in chapter two. The chapter then progressed by developing our theoretical understanding of how this idealised glacier surface geometry related to climate forcing by demonstrating the clear links to mechanical ice flow processes that account for the distinct three-dimensional surface geometries that characterise the accumulation and ablation areas. This understanding was then developed further by proposing how changes to the idealised/steady-state ice surface geometry may relate to changes in glacier mass balance and thus climate forcing; and therefore, how changes in the latter could be inferred from observations of the former. However, before using observations of ice surface geometry to assess glacier health, it was necessary to ensure that the theoretical link between climate forcing, flow dynamics, ice surface geometry and thus glacier health could be observed through real world empirical data.

In order to achieve this, the PCT was compared to other glacier health measures such as ELA and mass balance and the relationships between the variables were assessed geographically (chapter three) and over time (chapter four). The statistically strong relationship between PCT_a and ELA_0 in chapter three provided convincing evidence that the PCT was indeed a function of glacier mass balance and thus climate. This belief was supported by the observations in chapter four that displayed changes in PCT position over time that were

interpreted as a consequence of the respective glaciers' recent mass balance regime. The interpretations drawn from these observations were then tested through ice flow simulations under differing climate forcing mechanisms using David Egholm's iSOSIA ice flow model (Egholm et al., 2011). The results highlighted the close relationship between glacier surface mass balance and PCT behaviour where fluctuations in precipitation, temperature and ultimately mass balance drove observable changes in PCT position. Furthermore, the observations of mean PCT_p recorded in chapters three, four, six and seven revealed that there was little variation in PCT_p across all observations despite significant variations in thermal regimes, elevation distributions, glacier area, longitudinal slope gradients, valley geometries, climate forcing, flow mechanisms, velocities and so on. Thus it is rational to assume then that the PCT and its positioning is a function of a higher order control that overrides glacier specific variations. With a reinforced confidence that the PCT was indeed a measure of glacier health and provider of climate information, the PCT was then used to assess the state of glaciation in High Mountain Asia by recording PCT_a and PCT_p upon 2409 glaciers spanning the entirety of the HKKH region and accounting for ~50% of the region's glaciated area.

This body of work raises a number of implications that impact how we understand the complex relationship between climate and three-dimensional glacier shape. As far as the author is aware, this is the first time a manifestation of the complex interaction between climate, flow dynamics and mass balance has been identified and recorded on such a wide sample of glaciers in the form of a single indice. Previous measures, often described as "Glacier Elevation Indices", such as mean glacier elevation, mid range elevation, median glacier elevation, maximum altitude of lateral moraines, toe-headwall-altitude-ratio and others (Benn and Lehmkuhl, 2000; Braithwaite and Raper, 2010; Carrivick and Brewer, 2004) have been used to infer glacier-climatic information. However, none of these have successfully integrated ice flow dynamics as part of the indices' capabilities. Thus irrespective of the PCT's use as an indicator of glacier health or climate signal, an important outcome of this work is the discovery that the *Kinematic Partition*, as a stand-alone phenomenon, provides evidence of the complex, self-equilibrating organisation of mountain glacier systems. The *Kinematic Partition* provides observable evidence that glaciers tend

towards dynamic balance whilst allowing for variations in the characteristics of the constraining topography, the variation in mass distributions at differing elevations, two dimensional areal geometry, flow mechanism, thermal regime, aspect, climatic regime and so on, with the result of this process being the common ice surface geometry first observed by Hess (1904).

This thesis has also generated new insight into how observations of three-dimensional ice surface geometry may be used to glean information concerning glacier behaviour in response to climate forcing. Firstly, chapters four and six revealed that observations of PCT position over time can be used to gain information concerning glacier mass balance regime. Specifically that observation of PCT_x advance down-glacier is indicative of at least a former positive mass balance regime, whilst observations of PCT_x retreat up glacier are indicative of a long-term negative mass balance regime. Furthermore, owing to the close relationship observed between PCT_a and ELA₀, and the results from the abrupt ELA forcing experiments conducted in chapter six, the evidence suggests that the PCT has the potential to inform us of the relative extent to which flow dynamics are out of sync with current climate forcing by comparing PCT_a to modern day ELA records.

The results from this study also provide the basis for the development of the “*flow balance*” concept. Akin to “dynamic health” (Harrison et al., 2009), PCT_p observations have the potential to inform us of how different components of mountain glacier systems are responding heterogeneously to common forcing, and thus provide information relating to the glacier’s “health” and “flow state”. This is because the observation that glaciers tend towards a surface geometry that produces a PCT_p value in the region of 0.38 suggests that significant insight can be extracted from those glaciers that reveal PCT_p values that deviate substantially from the norm. Specifically that departure from the normal PCT_p range can be used as an indication of a non-equilibrium glacier response to climate forcing (Harrison et al., 2009). Such observations highlight the interpretation that the PCT_p can be used to identify glaciers that are *flow-balanced* or *flow-unbalanced*. It is stated here that flow balanced glaciers exhibit a normal PCT_p, indicative of a flow-state capable of maintaining a constant area-mass distributions. Accordingly, these glaciers are considered to be

demonstrating a gradual, balanced response to current climate forcing. Conversely, glaciers with extreme PCT_p , or those that display large variations in PCT_p over time are *flow-unbalanced*. As a result they possess a flow field structure incapable of maintaining a steady hypsometry and are thus considered to be adjusting to climate perturbations in a non-equilibrium fashion.

These interpretations have enabled glacier health to be assessed for the entire HKKH region. The results reveal that glaciers across the HKKH are displaying heterogeneous responses to current climate trends. Furthermore, observations of geographical clustering of extreme PCT_p values is interpreted to be evidence of glaciers undergoing non-equilibrium responses to climate forcing in large regions of the northern Hindu-Kush, the Eastern, Western and Central Himalayas. These findings are supported by the observation that high frequencies of glaciers with disproportionately high or low PCT_p values were located in regions across the HKKH where recent rapid glacier retreat has been observed (Gardelle et al., 2013). On the other hand, regions where glaciers have been observed to be stable or advancing (Gardelle et al., 2012b) displayed PCT_p values that were deemed to be indicative of “*flow-balanced*” conditions.

However, it is important to reiterate that more thought is needed concerning how one decides upon the PCT_p boundary values that seemingly differentiate between dynamically balanced and unbalanced glaciers. Similarly, an important direction for future work is the creation and application of an automated method for PCT identification and extraction. Not only would this increase the speed in which PCT data could be recorded, it would also reduce the level of investigator interpretation that is required for the approach in its current form.

Nevertheless, this work provides solid grounding for the justification of the PCT to be included in future remotely sensed glacier monitoring campaigns as an additional glacier inventory variable. Although, the PCT cannot provide quantitative estimates of glacier mass loss, it has potential as an indicator of glacier state change, particularly when employed over extended monitoring periods. The speed and logistical ease with which the PCT can be located and recorded means that a global assessment of the state of each individual PCT

forming glacier upon the earth's surface is now a viable option. A global PCT recording campaign, envisaged to be similar to the work conducted here for the HKKH, would identify regions characterised by dynamically unbalanced glaciers and thus point the glaciological community in the direction of areas that require closer attention. This would ultimately lead to us developing a greater understanding of how glaciers are responding, and are likely to respond, to the world's changing climate.

Climate change remains one of the fundamental concerns for public, political and scientific domains in the twenty-first century, yet there is a dearth of information pertaining to how glaciers in many of the world's regions are faring in today's climate. However with our newly acquired understanding of the *kinematic partition*, this gap in our knowledge can be filled. Accordingly, the next logical step in glacier monitoring should be to use the PCT to record and assess the state of each and every PCT forming glacier on the Earth's surface.

References

- Adhikari, S. and Huybrechts, P. (2009). Numerical modelling of historical front variations and the 21st-century evolution of glacier AX010, Nepal Himalaya. *Annals of Glaciology*, 50(52), pp.27–34.
- Adhikari, S., Marshall, S. J., & Huybrechts, P. (2009). A comparison of different methods of evaluating glacier response characteristics: application to glacier AX010, Nepal Himalaya. *The Cryosphere Discussions*, 3(3), 765-804.
- Anderson, R. S. (2000). A model of ablation-dominated medial moraines and the generation of debris-mantled glacier snouts. *Journal of Glaciology*, 46(154), pp.459–469.
- Andreassen, L. M., Elvehoy, H., Kjollmoen, B., Engeset, R. V., & Haakensen, N. (2005). Glacier mass-balance and length variation in Norway. *Annals of Glaciology*, 42(1), 317-325.
- Archer, D.R. and Fowler, H.J. (2004). Spatial and temporal variations in precipitation in the Upper Indus Basin, global teleconnections and hydrological implications. *Hydrology and Earth System Sciences Discussions*, 8(1), 47-61.
- Arendt, A., Luthcke, S., Gardner, A., O'neel, S., Hill, D., Moholdt, G., & Abdalati, W. (2013). Analysis of a GRACE global mascon solution for Gulf of Alaska glaciers. *Journal of Glaciology*, 59(217), pp.913–924.
- Arendt, A. A., Luthcke, S. B., Larsen, C. F., Abdalati, W., Krabill, W. B., & Beedle, M. J. (2008). Validation of high-resolution GRACE mascon estimates of glacier mass changes in the St Elias Mountains, Alaska, USA, using aircraft laser altimetry. *Journal of Glaciology*, 54(188), pp.778–787.
- Armstrong, R. L. (2010). *The glaciers of the Hindu Kush-Himalayan region: a summary of the science regarding glacier melt/retreat in the Himalayan, Hindu Kush, Karakoram, Pamir, and Tien Shan mountain ranges*. International Centre for Integrated Mountain Development (ICIMOD).
- Baral, D. R., Hutter, K., & Greve, R. (2001). Asymptotic theories of large-scale motion, temperature, and moisture distribution in land-based polythermal ice sheets: a critical review and new developments. *Applied Mechanics Reviews*, 54(3), 215-256.

- Kohler, J., James, T. D., Murray, T., Nuth, C., Brandt, O., Barrand, N. E., Aas, H. F. & Luckman, A. (2007). Acceleration in thinning rate on western Svalbard glaciers. *Geophysical Research Letters*, 34(18).
- Kuhn, M. (1981). Begleitworte zur Karte des Hintereisferners 1979,1:10,000. *Zeitschrift für Gletscherkunde und Glazialgeologie*, Vol. 16 (1), p, 117-124.
- Larsen, C. F., Motyka, R. J., Arendt, A. A., Echelmeyer, K. A., & Geissler, P. E. (2007). Glacier changes in southeast Alaska and northwest British Columbia and contribution to sea level rise. *Journal of Geophysical Research: Earth Surface* (2003–2012), 112(F1).
- Le Bris, R. and Paul, F. (2013). An automatic method to create flow lines for determination of glacier length: A pilot study with Alaskan glaciers. *Computers and Geosciences*, 52(C), pp.234–245.
- Leonard, K.C. and Fountain, A.G. (2003). Map-based methods for estimating glacier equilibrium-line altitudes. *Journal of Glaciology*, 49(166), pp.329–336.
- Leprince, S., Barbot, S., Ayoub, F., & Avouac, J. P. (2007). Automatic and precise orthorectification, coregistration, and subpixel correlation of satellite images, application to ground deformation measurements. *IEEE Transactions on Geoscience and Remote Sensing*, 45(6), pp.1529–1558.
- Liu, S., Ding, Y., Shangguan, D., Zhang, Y., Li, J., Han, H., Wang, J. & Xie, C. (2006). Glacier retreat as a result of climate warming and increased precipitation in the Tarim river basin, northwest China. *Annals of Glaciology*, 43(1), 91-96.
- Luckman, A., Quincey, D., & Bevan, S. (2007). The potential of satellite radar interferometry and feature tracking for monitoring flow rates of Himalayan glaciers. *Remote Sensing of Environment*, 111(2), 172-181.
- Luthcke, S. B., Arendt, A. A., Rowlands, D. D., McCarthy, J. J., & Larsen, C. F. (2008). Recent glacier mass changes in the Gulf of Alaska region from GRACE mascon solutions. *Journal of Glaciology*, 54(188), 767-777..
- Matsuo, K. and Heki, K. (2010). Time-variable ice loss in Asian high mountains from satellite gravimetry. *Earth and Planetary Science Letters*, 290(1-2), pp.30–36.
- Meier, M. F., Dyurgerov, M. B., Rick, U. K., O'Neel, S., Pfeffer, W. T., Anderson, R. S., Anderson, S. P. & Glazovsky, A. F. (2007). Glaciers dominate eustatic sea-level rise in the 21st century. *Science*, 317(5841), 1064-1067.

- Meier, M.F., Dyurgerov, M.B. & McCabe, G.J. (2003). The health of glaciers: Recent changes in glacier regime. *Climatic change*, 59(1), pp.123–135.
- Mihalcea, C., Mayer, C., Diolaiuti, G., Lambrecht, A., Smiraglia, C., & Tartari, G. (2006). Ice ablation and meteorological conditions on the debris-covered area of Baltoro glacier, Karakoram, Pakistan. *Annals of Glaciology*, 43(1), pp.292–300.
- Miller, J., Rees, G., Warnars, T., Young, G., Collins D. & Shrestha, A. (2013). What is the evidence for glacial shrinkage across the Himalayas? CEE review10-008. Collaboration for Environmental Evidence: www.environmentalevidence.org/SR10008.html.
- Moholdt, G. (2013). Interactive comment on “Density assumptions for converting geodetic glacier volume change to mass change” by M. Huss. *The Cryosphere Discuss.* 7, C148–C154.
- Moholdt, G., Nuth, C., Hagen, J. O., & Kohler, J. (2010). Recent elevation changes of Svalbard glaciers derived from ICESat laser altimetry. *Remote Sensing of Environment*, 114(11), pp.2756–2767.
- Nakawo, M., & Rana, B. (1999). Estimate of ablation rate of glacier ice under a supraglacial debris layer. *Geografiska Annaler: Series A, Physical Geography*, 81(4), 695-701.
- Narama, C., Käab, A., Duishonakunov, M., & Abdrakhmatov, K. (2010). Spatial variability of recent glacier area changes in the Tien Shan Mountains, Central Asia, using Corona (~ 1970), Landsat (~ 2000), and ALOS (~ 2007) satellite data. *Global and Planetary Change*, 71(1), 42-54.
- Nuimura, T., Fujita, K., Yamaguchi, S., & Sharma, R. R. (2012). Elevation changes of glaciers revealed by multitemporal digital elevation models calibrated by GPS survey in the Khumbu region, Nepal Himalaya, 1992–2008. *Journal of Glaciology*, 58(210), pp.648–656.
- Nuth, C. and Käab, A. (2011). Co-registration and bias corrections of satellite elevation data sets for quantifying glacier thickness change. *The Cryosphere*, 5(1), pp.271–290.
- Nuth, C., Kohler, J., Aas, H. F., Brandt, O., & Hagen, J. O. (2007). Glacier geometry and elevation changes on Svalbard (1936-90): a baseline dataset. *Annals of Glaciology*, 46(1), 106-116.

- Nuth, C., Moholdt, G., Kohler, J., Hagen, J. O., & Kääb, A. (2010). Svalbard glacier elevation changes and contribution to sea level rise. *Journal of Geophysical Research: Earth Surface* (2003–2012), 115(F1).
- Nye, J.F. (1952). The mechanics of glacier flow. *Journal of Glaciology*, 2(12), pp.82–93.
- Oerlemans, J. (2012). Linear modelling of glacier length fluctuations. *Geografiska Annaler: Series A, Physical Geography*, 94(2), 183-194.
- Oerlemans, J. (2005). Extracting a Climate Signal from 169 Glacier Records. *Science*, 308(5722), pp.675–677.
- Oerlemans, J. and Fortuin, J.P.F. (1992). Sensitivity of Glaciers and Small Ice Caps to Greenhouse Warming. *Science*, 258(5079), pp.115–117.
- Oerlemans, J., Anderson, B., Hubbard, A., Huybrechts, P., Johannesson, T., Knap, W. H., Schmeits, M., Stroeven, A. P., van de Wal, R. S. W., Wallinga, J. & Zuo, Z. (1998). Modelling the response of glaciers to climate warming. *Climate dynamics*, 14(4), 267-274.
- Osmaston, H. (2005). Estimates of glacier equilibrium line altitudes by the Area× Altitude, the Area× Altitude Balance Ratio and the Area× Altitude Balance Index methods and their validation. *Quaternary International*, 138, pp.22–31.
- Østrem, G. (1966). The height of the glaciation limit in southern British Columbia and Alberta. *Geografiska Annaler: Series A, Physical Geography*, pp.126–138.
- Paul, F. (2008). Calculation of glacier elevation changes with SRTM: is there an elevation-dependent bias? *Journal of Glaciology*, 54(188), pp.945–946.
- Paul, F. and Haeberli, W., (2008). Spatial variability of glacier elevation changes in the Swiss Alps obtained from two digital elevation models. *Geophysical Research Letters*, 35(21), p.L21502.
- Paul, F., Kaab, A., Maisch, M., Kellenberger, T., & Haeberli, W. (2002). The new remote-sensing-derived Swiss glacier inventory: I. Methods. *Annals of Glaciology*, 34(1), 355-361.
- Paul, F., Kääb, A., Maisch, M., Kellenberger, T., & Haeberli, W. (2004). Rapid disintegration of Alpine glaciers observed with satellite data. *Geophysical Research Letters*, 31(21).

- Paul, F., Kääb, A. & Haeberli, W. (2007). Recent glacier changes in the Alps observed by satellite: Consequences for future monitoring strategies. *Global and Planetary Change*, 56(1-2), pp.111–122.
- Paul, F., Barry, R. G., Cogley, J. G., Frey, H., Haeberli, W., Ohmura, A., Ommanney, C.S.L., Raup, B., Rivera, A. & Zemp, M. (2010). Recommendations for the compilation of glacier inventory data from digital sources. *Annals of Glaciology*, 50(53), 119-126.
- Paul, F., Bolch, T., Kääb, A., Nagler, T., Nuth, C., Scharrer, K., ... & Van Niel, T. (2013). The glaciers climate change initiative: Methods for creating glacier area, elevation change and velocity products. *Remote Sensing of Environment*. (in press)
- Pedersen, V.K. and Egholm, D.L. (2013). Glaciations in response to climate variations preconditioned by evolving topography. *Nature*, 493(7431), pp.206–210.
- Pelto, M. S., McGee, S. R., Adema, G. W., Beedle, M. J., Miller, M. M., Sprenke, K. F., & Lang, M. (2008). The equilibrium flow and mass balance of the Taku Glacier, Alaska 1950–2006. *The Cryosphere Discussions*, 2(3), 275-298..
- Permanent Service on the Fluctuations of Glaciers (PSFG). 1973. Fluctuations of glaciers 1965–1970 (Vol. II), ed. Kasser, P. Paris, International Commission on Snow and Ice of the International Association of Scientific Hydrology/UNESCO.
- PSFG. (1977). Fluctuations of glaciers 1970–1975 (Vol. III), ed. Müller, F. Paris, International Commission on Snow and Ice of the International Association of Scientific Hydrology/UNESCO.
- PSFG. (1985). Fluctuations of glaciers 1975–1980 (Vol. IV), ed. Haeberli, W. Paris, International Commission on Snow and Ice of the International Association of Scientific Hydrology/UNESCO.
- Pu, J., Yao, T., Yang, M., Tian, L., Wang, N., Ageta, Y., & Fujita, K. (2008). Rapid decrease of mass balance observed in the Xiao (Lesser) Dongkemadi Glacier, in the central Tibetan Plateau. *Hydrological Processes*, 22(16), 2953-2958.
- Quincey, D.J. and Luckman, A. (2013). On the magnitude and frequency of Karakoram Glacier surges. *The Cryosphere Discussions*, 7(5), pp.5177–5187.
- Quincey, D. J., Braun, M., Glasser, N. F., Bishop, M. P., Hewitt, K., & Luckman, A. (2011). Karakoram glacier surge dynamics. *Geophysical Research Letters*, 38(18).

- Quincey, D.J., Luckman, A. & Benn, D. (2009). Quantification of Everest region glacier velocities between 1992 and 2002, using satellite radar interferometry and feature tracking. *Journal of Glaciology*, 55(192), pp.596–606.
- Rabus, B., Eineder, M., Roth, A., & Bamler, R. (2003). The shuttle radar topography mission—a new class of digital elevation models acquired by spaceborne radar. *ISPRS Journal of Photogrammetry and Remote Sensing*, 57(4), 241-262.
- Rabus, B. T., & Echelmeyer, K. A. (1998). The mass balance of McCall Glacier, Brooks Range, Alaska, USA; its regional relevance and implications for climate change in the Arctic. *Journal of Glaciology*, 44, 333-351.
- Racoviteanu, A. E., Paul, F., Raup, B., Khalsa, S. J. S., & Armstrong, R. (2010). Challenges and recommendations in mapping of glacier parameters from space: results of the 2008 Global Land Ice Measurements from Space (GLIMS) workshop, Boulder, Colorado, USA. *Annals of Glaciology*, 50(53), 53-69.
- Radić, V. and Hock, R. (2010). Regional and global volumes of glaciers derived from statistical upscaling of glacier inventory data. *Journal of Geophysical Research: Earth Surface* (2003–2012), 115(F1).
- Raper, S.C.B. and Braithwaite, R.J. (2009). Glacier volume response time and its links to climate and topography based on a conceptual model of glacier hypsometry. *The Cryosphere*, 3(2), pp.183–194.
- Raper, S.C.B. and Braithwaite, R.J. (2006). Low sea level rise projections from mountain glaciers and icecaps under global warming. *Nature*, 439(7074), pp.311–313.
- Rasmussen, L. A. (2013). Meteorological controls on glacier mass balance in High Asia. *Annals of Glaciology*, 54(63), 352-359.
- Rau, F., Mauz, F., Vogt, S., Khalsa, S. J. S., & Raup, B. (2005). *Illustrated GLIMS glacier classification manual*. Institut für Physische Geographie Freiburg, NSIDC.
- Raup, B., Kääb, A., Kargel, J. S., Bishop, M. P., Hamilton, G., Lee, E., ... & Helm, C. (2007). Remote sensing and GIS technology in the Global Land Ice Measurements from Space (GLIMS) project. *Computers & Geosciences*, 33(1), 104-125.
- Raymond, C. F. (1969). *Flow in a transverse section of Athabasca Glacier, Alberta, Canada* (Doctoral dissertation, California Institute of Technology).

- Rea, B.R. (2009). Defining modern day Area-Altitude Balance Ratios (AABRs) and their use in glacier-climate reconstructions. *Quaternary Science Reviews*, 28(3), pp.237–248.
- Rees, W. G., & Arnold, N. S. (2007). Mass balance and dynamics of a valley glacier measured by high-resolution LiDAR. *Polar Record*, 43(04), 311-319.
- Ren, J., Jing, Z., Pu, J., & Qin, X. (2006). Glacier variations and climate change in the central Himalaya over the past few decades. *Annals of Glaciology*, 43(1), 218-222.
- Reuter, H.I., Nelson, A. & Jarvis, A. (2007). An evaluation of void-filling interpolation methods for SRTM data. *International Journal of Geographical Information Science*, 21(9), pp.983–1008.
- Rivera, A., & Casassa, G. (2004). Ice elevation, areal, and frontal changes of glaciers from national park Torres del Paine, Southern Patagonia Icefield. *Arctic, Antarctic, and Alpine Research*, 36(4), 379-389.
- Robinson, P.H. (1984). Ice dynamics and thermal regime of Taylor Glacier, south Victoria Land, Antarctica. *Journal of Glaciology*, 30(105), pp.153–160.
- Rodell, M., Velicogna, I., & Famiglietti, J. S. (2009). Satellite-based estimates of groundwater depletion in India. *Nature*, 460(7258), 999-1002.
- Scherler, D., Bookhagen, B. & Strecker, M.R., (2011a). Hillslope-glacier coupling: The interplay of topography and glacial dynamics in High Asia. *Journal of Geophysical Research*, 116(F2), p.F02019.
- Scherler, D., Bookhagen, B. & Strecker, M.R., (2011b). Spatially variable response of Himalayan glaciers to climate change affected by debris cover. *Nature*, 4(1), pp.1–4.
- Schiefer, E., Menounos, B., & Wheate, R. (2007). Recent volume loss of British Columbian glaciers, Canada. *Geophysical Research Letters*, 34(16).
- Schneider, H. (1976). *Die Karte des Kesselwandferners 1971 und die Grundlagen der Vermessungen, Zeitschrift für Gletscherkunde und Glazial geologie*, BD XI/2 (1975), p.229-44.
- Schoof, C. (2005). The effect of cavitation on glacier sliding. *Proceedings of the Royal Society A: Mathematical, Physical and Engineering Sciences*, 461(2055), pp.609–627.

- Shekhar, M. S., Chand, H., Kumar, S., Srinivasan, K., & Ganju, A. (2010). Climate-change studies in the western Himalaya. *Annals of Glaciology*, 51(54), 105-112.
- Shrestha, A.B., Wake, C.P., Dibb, J.E. and Mayweski, P.A.,(2000). Precipitation fluctuations in the Nepal Himalaya and its vicinity and relationship with some large scale climatological parameters. *International. Journal of Climatology*. 20, pp. 317-327.
- Sørbel, L. Tolgensbakk, J., Hagen, J.O. & Høgvard, K. (2001). *Geomorphological and Quaternary geological map, Svalbard 1:100,000, sheet C9Q Adventdalen. With explanatory text, p. 57–78.* Norsk Polarinstittutt Temakart Nr. 31/32.
- Stokes, C. R., Gurney, S. D., Shahgedanova, M., & Popovnin, V. (2006). Late-20th-century changes in glacier extent in the Caucasus Mountains, Russia/Georgia. *Journal of Glaciology*, 52(176), 99-109.
- Stokes, C. R., Popovnin, V., Aleynikov, A., Gurney, S. D., & Shahgedanova, M. (2007). Recent glacier retreat in the Caucasus Mountains, Russia, and associated increase in supraglacial debris cover and supra-/proglacial lake development. *Annals of Glaciology*, 46(1), 195-203.
- Sund, M., Eiken, T., Hagen, J. O., & Käab, A. (2009). Svalbard surge dynamics derived from geometric changes. *Annals of Glaciology*, 50(52), 50-60.
- Surazakov, A. B., & Aizen, V. B. (2006). Estimating volume change of mountain glaciers using SRTM and map-based topographic data. *IEEE Transactions on Geoscience and Remote Sensing*, 44(10), 2991-2995.
- Svoboda, F. and Paul, F. (2010). A new glacier inventory on southern Baffin Island, Canada, from ASTER data: I. Applied methods, challenges and solutions. *Annals of Glaciology*, 50(53), pp.11–21.
- Tamisiea, M.E. (2005). Constraining hydrological and cryospheric mass flux in southeastern Alaska using space-based gravity measurements. *Geophysical Research Letters*, 32(20), p.L20501.
- Taylor, J. R. (2005). *Classical mechanics*. University Science Books. Sausalito.
- Tiwari, V.M., Wahr, J. & Swenson, S. (2009). Dwindling groundwater resources in northern India, from satellite gravity observations. *Geophysical Research Letters*, 36(18), p.L18401.
- Torsnes, I., Rye, N. & Nesje, A. (1993). Modern and Little Ice Age equilibrium-line altitudes on outlet valley glaciers from Jostedalbreen, western Norway:

- an evaluation of different approaches to their calculation. *Arctic and Alpine Research*, pp.106–116.
- Toutin, T. (2008). ASTER DEMs for geomatic and geoscientific applications: a review. *International Journal of Remote Sensing*, 29(7), 1855-1875.
- Van de Wal, R. S. W., & Wild, M. (2001). Modelling the response of glaciers to climate change by applying volume-area scaling in combination with a high resolution GCM. *Climate Dynamics*, 18(3-4), 359-366.
- Vieli, G. J. I., & Gudmundsson, G. H. (2004). On estimating length fluctuations of glaciers caused by changes in climatic forcing. *Journal of Geophysical Research: Earth Surface* (2003–2012), 109(F1).
- Vuille, M., Kaser, G., & Juen, I. (2008). Glacier mass balance variability in the Cordillera Blanca, Peru and its relationship with climate and the large-scale circulation. *Global and Planetary Change*, 62(1), 14-28.
- Wagnon, P., Linda, A., Arnaud, Y., Kumar, R., Sharma, P., Vincent, C., Pottakkal, J. G., Bethier, E., Ramanathan, A., Hasnain, S. I. & Chevallier, P. (2007). Four years of mass balance on Chhota Shigri Glacier, Himachal Pradesh, India, a new benchmark glacier in the western Himalaya. *Journal of Glaciology*, 53(183), 603-611.
- Wahr, J. (2004). Time-variable gravity from GRACE: First results. *Geophysical Research Letters*, 31(11).
- Wang, Y., Hou, S., Hong, S., Do Hur, S., & Liu, Y. (2008). Glacier extent and volume change (1966~ 2000) on the Su-lo Mountain in northeastern Tibetan Plateau, China. *Journal of Mountain Science*, 5(4), 299-309.
- Wang, P., Li, Z., Li, H., Wang, W., & Yao, H. (2014). Comparison of glaciological and geodetic mass balance at Urumqi Glacier No. 1, Tian Shan, Central Asia. *Global and Planetary Change*, 114, 14-22.
- World Glacier Monitoring Service (WGMS). (1988). Fluctuations of glaciers 1980–1985 (Vol. V), ed. Haeberli, W. and P. Muller. IAHS/UNEP/UNESCO, World Glacier Monitoring Service, Zurich.
- WGMS. (1993). Fluctuations of glaciers 1985–1990 (Vol. VI), ed. Haeberli, W. and P. Muller. IAHS/UNEP/UNESCO, World Glacier Monitoring Service, Zurich.

- WGMS. (1996). Glacier Mass Balance Bulletin No. 4 (1994–1995), ed. Haeberli, W., M Hoelzle and S. Suter. IAHS/UNEP/ UNESCO, World Glacier Monitoring Service, Zurich.
- WGMS. (1998). Fluctuations of glaciers 1990–1995 with addendas from earlier years (Vol. VII), ed. Haeberli, W., M. Hoelzle, S. Suter and R. Frauenfelder. IAHS/UNEP/UNESCO, World Glacier Monitoring Service, Zurich.
- WGMS. (2005). Fluctuations of glaciers 1995–2000 (Vol. VIII), ed. Haeberli, W. Zemp M., Frauenfelder R., Hoelzle M., and Käab A. IAHS/UNEP/UNESCO, World Glacier Monitoring Service, Zurich.
- WGMS, (2008). Fluctuations of Glaciers 2000–2005, (Volume IX), ed. Haeberli, W., Zemp, M., Käab, A., Paul, F. and Hoelzle, M. ICSU(FAGS)/IUGG(IACS)/UNEP/UNESCO/ WMO, World Glacier Monitoring Service, Zurich, Switzerland.
- WGMS, (2012). Fluctuations of Glaciers 2005–2010, Volume X. Zemp, M., Frey, H., Gärtner-Roer, I., Nussbaumer, S.U., Hoelzle, M., Paul, F., and Haeberli, W. (eds.), ICSU(WDS)/ IUGG(IACS)/UNEP/UNESCO/WMO, World Glacier Monitoring Service, Zurich, Switzerland: 336 pp.
- WGMS (2013). Glacier Mass Balance Bulletin No. 12 (2010–2011). Zemp, M., Nussbaumer, S. U., Naegeli, K., Gärtner-Roer, I., Paul, F., Hoelzle, M., and Haeberli, W. (eds.), ICSU(WDS)/IUGG(IACS)/UNEP/ UNESCO/WMO, World Glacier Monitoring Service, Zurich, Switzerland, 106 pp
- Wiltshire, A.J. (2013). Climate change implications for the glaciers of the Hindu-Kush, Karakoram and Himalayan region. *The Cryosphere Discussions*, 7(4), pp.3717–3748.
- Yao, T., Thompson, L., Yang, W., Yu, W., Gao, Y., Guo, X., ... & Joswiak, D. (2012). Different glacier status with atmospheric circulations in Tibetan Plateau and surroundings. *Nature Climate Change*, 2(9), 663-667.
- Zemp, M. and van Woerden, J. (2008). Global glacier changes: facts and figures. Roer, I. (2008). Global glacier changes: facts and figures. UNEP/Earthprint.
- Zemp, M., Haeberli, W., Hoelzle, M., & Paul, F. (2006). Alpine glaciers to disappear within decades? *Geophysical Research Letters*, 33(13). L13504.
- Zemp, M., Hoelzle, M. & Haeberli, W. (2007). Distributed modelling of the regional climatic equilibrium line altitude of glaciers in the European Alps. *Global and Planetary Change*, 56(1-2), pp.83–100.

Zemp, M., Hoelzle, M., & Haeberli, W. (2009). Six decades of glacier mass-balance observations: a review of the worldwide monitoring network. *Annals of Glaciology*, 50(50), 101-111.

Zhang, G., Yao, T., Xie, H., Kang, S., & Lei, Y. (2013). Increased mass over the Tibetan Plateau: from lakes or glaciers?. *Geophysical Research Letters*, 40(10), 2125-2130.

Appendix

The following pages contain figures and supporting material supplementary to the main body of work.

Appendix A

<i>Glacier</i>	<i>Country</i>	<i>Latitude</i>	<i>Area in 1995 km²</i>
Peyto	Canada	51.40° N	13.35
White	Canada	79.27° N	38.9
Gulkana	U.S.A.	63.15° N	19.3
South Cascade	U.S.A.	48.22° N	2.5
Blue	U.S.A.	47.49° N	5.5
Wolverine	U.S.A.	60.24° N	17.24
Rabots glaciär	Sweden	67.54° N	3.9
Storglaciären	Sweden	67.54° N	3.1
Hansbreen	Norway	77.05° N	1.84
Hellstugbreen	Norway	61.34° N	3.13
Ålfotbreen	Norway	61.45° N	4.82
Nigardsbreen	Norway	61.43° N	48.2
Hintereisferner	Austria	46.48° N	8.72
Langtalferner	Austria	46.48° N	3.52
Kesselwandferner	Austria	46.50° N	4.29
Sonnblickkees	Austria	47.08° N	1.5
Vernagtferner	Austria	46.53° N	9.18
Limmern	Switzerland	46.49° N	2.62
Plattalva	Switzerland	46.50° N	0.81
Gries	Switzerland	46.26° N	6.25
Silvretta	Switzerland	46.51° N	3.25
Ürümqi No. 1	China	43.05° N	1.84
Hofsjökull ice cap			
north: Sátujökull	Iceland	64.57° N	90.6
east: Þjórsárjökull	Iceland	64.48° N	250
southwest: Blágnjúkjökull	Iceland	64.43° N	51
Lewis	Kenya	0.09° S	0.24
Abramov	CIS/U.S.S.R.	39.38° N	26.21
Davidov	CIS/U.S.S.R.		11.43
Golubina	CIS/U.S.S.R.	42.28° N	5.75
Igly/Tuyuksu	CIS/U.S.S.R.	43.0° N	1.72
Karabatkak	CIS/U.S.S.R.	42.06° N	4.19
Mametova	CIS/U.S.S.R.	43.0° N	0.35
Mayakovskogo	CIS/U.S.S.R.	43.0° N	0.18
Molodezhniy	CIS/U.S.S.R.	43.0° N	1.43
Ordzhonikidze	CIS/U.S.S.R.	43.0° N	0.31
Sary-Tör	CIS/U.S.S.R.		3.61
Shumskiy	CIS/U.S.S.R.	45.05° N	2.81
Suyok-Zapadniy	CIS/U.S.S.R.	41.47° N	1.25
Tuyuksu	CIS/U.S.S.R.	43.03° N	2.72
Visyachiy 1	CIS/U.S.S.R.	43.0° N	0.29

TABLE I - GLACIERS OBSERVED BY LEONARD AND FOUNTAIN (2003)

Appendix B

Name	Path/Row	Acq. Date
Blue Glacier	047/27	22/09/2002
Hintereisferner	193/27	13/09/1999
	193/27	13/09/2006
Kesselwandferner	193/27	13/09/1999
	193/27	13/09/2006

TABLE II LANDSAT TILES USED FOR MULTI-DATE COMPARISON

Mountain Glacier Health Signatures Stored in Their Three-Dimensional Ice Surface Geometry

Glacier Name/No.	Glacier Length (km)	Glacier Area km ²	PCT _A masl	Max Glacier Elev masl	Min Glacier Elev masl	PCT _p	Glacier length (km)	Glacier Area km ²	PCT _A masl	Max Glacier Elev masl	Min Glacier Elev masl	PCT _p	PCT _x Change (m)	Terminus change (m)	PCT _A Change (m)	PCT _p Change	Scenario
June 1936							July 1995						1936 – 1995				
1	2.12	1.04	600±50	800	325	0.58	1.89	0.99	600±50	800	350	0.56	69±52	-41	0±70	-0.02	2
Brandtbreen	3.94	2.51	350±50	900	200	0.21	3.75	1.73	450±50	700	200	0.50	-231±52	-139	100±70	0.29	7
Blackbreen	3.80	3.92	450±50	850	275	0.30	3.47	2.64	450±50	850	325	0.24	-334±52	-298	0±70	-0.07	6
Tellbreen	4.70	5.45	475±50	900	280	0.31	4.37	4.61	375±50	900	300	0.13	100±52	-225	-100±70	-0.19	3
Altbreen	3.81	2.49	525±50	850	380	0.31	3.10	2.15	500±50	800	350	0.33	-378±52	-427	-25±70	0.02	5
6	2.84	1.45	575±50	1050	425	0.24	2.44	1.14	700±50	1050	475	0.39	-339±52	-321	125±70	0.15	7
Malarbreen	4.04	3.84	475±50	950	350	0.21	3.87	2.62	475±50	800	325	0.32	-279±52	0	0±70	0.11	6
Arctowskibreen	3.81	3.38	575±50	973	325	0.39	3.47	2.74	575±50	850	350	0.45	-290±52	-137	-25±70	0.06	5
Arnicabreen	2.46	1.97	550±50	850	425	0.29	2.40	1.80	525±50	850	400	0.28	-42±52	0	-25±70	-0.02	5
Duboisbreen	4.00	3.87	500±50	800	250	0.45	3.74	3.17	450±50	800	250	0.36	0±52	-225	-50±70	-0.09	4
Flowerbreen	3.70	2.63	500±50	900	350	0.27	3.41	2.02	575±50	900	300	0.46	-663±52	-196	75±70	0.19	7
12	2.09	1.40	700±50	1000	550	0.33	2.06	1.14	675±50	1000	550	0.28	-53±52	0	-25±70	-0.06	5
Longyearbreen	4.46	3.59	500±50	1000	275	0.31	4.39	2.81	500±50	1050	250	0.31	-249±52	-68	0±70	0.00	6
Larsbreen	3.60	4.10	600±50	850	300	0.55	3.48	3.07	600±50	800	300	0.60	-131±52	-114	0±70	0.05	6
Grumantbreen	2.58	2.69	600±50	925	350	0.43	2.44	2.01	575±50	950	400	0.32	0±52	-66	-25±70	-0.12	4
Dryadbreen	3.07	2.34	475±50	1000	325	0.22	2.63	1.82	425±50	1030	350	0.11	0±52	-436	-50±70	-0.11	4
Bogerbreen	4.22	4.56	550±50	950	350	0.33	4.09	3.62	525±50	950	350	0.29	0±52	0	-25±70	-0.04	4
18	2.27	1.60	600±50	925	350	0.43	2.25	1.21	550±50	900	400	0.30	-150±52	-19	-50±70	-0.13	5
19	2.35	2.18	650±50	1000	500	0.30	1.82	1.47	625±50	1000	450	0.32	-220±52	-439	-25±70	0.02	5
Svendsenbreen	3.33	2.54	600±50	950	425	0.33	2.87	2.15	575±50	850	450	0.31	-126±52	-87	-25±70	-0.02	5
21	1.64	0.61	450±50	750	350	0.25	1.43	0.54	450±50	700	350	0.29	-156±52	-195	0±70	0.04	6
Tillbergfonna	3.98	4.29	525±50	875	300	0.39	3.54	3.76	475±50	800	300	0.35	0±52	-294	-50±70	-0.04	4
Tufsbreen	3.83	3.63	550±50	1000	300	0.36	3.51	2.72	525±50	850	325	0.38	-124±52	-302	-25±70	0.02	5
Brombreen	2.41	2.28	500±50	850	350	0.30	2.30	1.71	475±50	750	300	0.39	-132±52	-209	-25±70	0.09	5

Mountain Glacier Health Signatures Stored in Their Three-Dimensional Ice Surface Geometry

Medalsbreen	2.95	4.67	450±50	900	325	0.22	2.69	2.24	400±50	900	300	0.17	0±52	-280	-50±70	-0.05	4
Gibsonbreen	3.11	3.35	475±50	900	250	0.35	2.71	2.72	425±50	900	300	0.21	0±52	-450	-50±70	-0.14	4
Ayerbreen	4.46	3.53	600±50	950	300	0.46	4.17	3.10	525±50	900	350	0.32	805±52	-252	-75±70	-0.14	3
Scott Turnerbreen	5.18	4.90	525±50	970	250	0.38	4.91	4.43	425±50	950	250	0.25	891±52	-242	-100±70	-0.13	3
Rieperbreen	4.53	5.32	400±50	900	200	0.29	3.84	4.64	500±50	900	250	0.38	-1103±52	-442	100±70	0.10	4
Foxbreen	3.77	6.01	450±50	900	250	0.31	2.66	4.81	550±50	800	300	0.50	-960±52	-1079	100±70	0.19	7
Fleinisen	4.09	4.87	575±50	1000	325	0.37	4.12	4.28	550±50	950	300	0.38	-96±52	130	-25±70	0.01	5
32	2.46	1.28	500±50	750	300	0.44	2.13	1.01	500±50	700	350	0.43	-358±52	-301	0±70	-0.02	6
Skoltbreen	5.75	4.36	550±50	937	350	0.34	5.89	4.00	550±50	950	250	0.43	518±52	135	0±70	0.09	2
Kokbreen	9.50	22.69	450±50	1000	150	0.35	7.92	19.19	550±50	850	200	0.54	-2029±52	-1401	100±70	0.19	7
Bergmesterbreen	6.09	9.78	500±50	955	225	0.38	4.86	8.45	525±50	950	250	0.39	-176±52	-1123	25±70	0.02	7
Fleksurbreen	3.36	2.63	550±50	990	425	0.22	3.16	2.35	500±50	850	350	0.30	264±52	-88	-50±70	0.08	3
Dronbreen	11.20	26.78	550±50	850	200	0.54	10.21	23.15	600±50	900	200	0.57	-657±52	-977	50±70	0.03	7
Tronisen	4.51	5.49	525±50	900	400	0.25	4.24	4.99	500±50	950	400	0.18	-231±52	-254	-25±70	-0.07	5
Slotsbreen	4.96	5.54	475±50	868	250	0.36	4.39	2.95	500±50	800	250	0.45	-506±52	-469	25±70	0.09	7
40	3.10	3.10	700±50	938	275	0.64	2.72	2.40	700±50	900	325	0.65	-108±52	-311	0±70	0.01	6
41	2.37	1.65	500±50	750	350	0.38	2.18	0.89	450±50	750	325	0.29	-88±52	-220	-50±70	-0.08	5
42	1.45	0.64	575±50	750	425	0.46	1.34	0.58	600±50	750	450	0.50	-248±52	-143	25±70	0.04	7
43	1.89	1.05	450±50	750	275	0.37	1.96	0.81	325±50	700	250	0.17	503±52	291	-125±70	-0.20	3
Dalburgbreen	3.04	3.78	600±50	800	500	0.33	3.19	3.40	600±50	750	425	0.54	0±52	228	0±70	0.05	4
Plogbreen	3.44	3.58	575±50	1005	375	0.32	3.61	2.54	525±50	950	350	0.29	107±52	190	-50±70	-0.03	3
Moysalbreen	5.24	6.30	550±50	900	375	0.33	5.54	5.76	475±50	950	300	0.27	290±52	362	-75±70	-0.06	3
47	2.26	1.61	500±50	750	300	0.44	2.26	1.56	550±50	750	275	0.58	-334±52	0	50±70	0.13	7

TABLE III – GLACIER AND PCT CHANGE IN LONGYEARBYEN BETWEEN 1936 AND 1995

Appendix C

Landsat path/row	Scene date
137/41	28.12.2000
138/40	19.12.2000
138/41	19.12.2000
139/41	08.11.2000
140/40	05.01.2002
140/41	05.01.2002
141/40	22.11.2000
142/40	15.12.2000
143/39	03.10.2000
143/40	09.12.2001
144/39	13.10.2001
145/38	02.11.2000
145/39	01.08.2001
146/37	21.08.2000
146/38	09.09.2001
146/39	05.08.2000
147/35	02.08.2002
147/36	02.08.2002
147/37	02.08.2002
147/38	02.08.2002
148/35	21.07.2001
148/36	04.09.2000
148/37	17.08.1999
149/34	30.09.2001
149/35	30.09.2001
149/36	30.09.2001
150/34	02.09.2000
150/35	16.09.1999
151/34	30.08.2002
151/35	30.08.2002

TABLE IV – LANDSAT IMAGES USED FOR THE HKKH ANALYSIS